STRUCTURAL, ECONOMIC AND ENVIRONMENTAL FEASIBILITY OF PLASTIC LOAD-BEARING WALLING AND ROOFING SYSTEMS FOR LOW-INCOME HOUSING

by

Franel le Roux

Thesis presented in partial fulfilment of the requirements for the degree Master of Science in Engineering at Stellenbosch University

Supervisor: Me. W.I. de Villiers

Faculty of Engineering

December 2014

DECLARATION

By submitting this thesis electronically, I declare that the entirety of the work contained therein is my own original work, that I am the authorship owner thereof (unless to the extent explicitly otherwise stated) and that I have not previously in its entirety or in part submitted it for obtaining any qualification.

Signature:

Date:

ABSTRACT

The lack of adequate housing becomes an increasing concern as the human population increases, which is not only restricted to Africa, but worldwide. With the world becoming more environmentally aware, the aim towards more sustainable development has become more essential. This results in alternative building technologies (ABT's) being investigated to address the backlog in housing.

This study investigates plastic materials as structural elements in low-income housing to address the housing backlog in a structurally stable, cost efficient and environmentally sustainable manner. The viable plastic materials that were identified are FFC (foam-fibre composite) and WPC (wood-plastic composite) as structural elements and EPS (expanded polystyrene) as a core infill panel.

Material parameters were obtained experimentally which were used in a numerical analysis to validate the structural stability of a modular WPC housing unit. The experimental work includes a direct compression, direct tension, compressive creep and a four-point bending test for the WPC. With the sandwich panels a push-though shear and four-point bending test were done. The compressive strength of the EPS as well as a relative bond strength of the selected adhesives was also tested. Furthermore, a comparative study was conducted on the fire performance (fire rating), cost efficiency as well as the environmental sustainability of three housing units constructed of FFC, WPC and block and mortar, respectively. In terms of structural stability, a modular plastic housing unit was devised and validated by both experimental work and plastic material investigations which showed that WPC can be used for load-bearing walling (with EPS as core infill panel), roofing and flooring systems.

From the comparative study, it was found that the fire rating of the block and mortar housing unit met the requirements of 20 and 30 minutes for the internal and external walls, respectively, prescribed by SANS 10400-T (2011). The fire rating of the block and mortar housing unit was met in terms of integrity, insulation and stability. The two modular plastic housing units, however, only met the fire rating in terms of integrity and insulation, but failed to meet the requirements in terms of stability. The approach used to determine the fire behaviour of a housing unit is not as accurate as the physical fire test, since assumptions are made in terms of the fire properties. However, the approach gives an indication of the fire performance of a housing unit.

FFC and WPC are laminated with PVC (polyvinyl chloride) which emits hydrochloride acid (HCl), when burning. Hydrochloride acid is a toxic gas. Thus, according to one of the minimum norms, stipulated by the NHBRC Home Building Manual and Agrément, an adequate housing unit should not emit harmful gasses. Although these regulations are not mandatory, in terms of this, WPC and FFC are not viable building materials for an adequate housing unit, especially when human behaviour and smoke control are considered. However, this aspect can be improved by adding additives to control, and in some cases prevent, smoke production.

The comparative study also indicated that the cost efficiency of the FFC housing unit is comparable to that of the block and mortar design. The modular WPC housing unit has a cost which is substantially greater than that of the FFC as well as the block and mortar housing units. The modular plastic housing units, FFC as well as WPC, typically utilise unskilled labour to construct a housing unit, which can lead to the socio-economic conditions of a community being improved by means of job creation. Due to the relative ease of construction of a modular plastic housing unit as well as a construction period of approximately three days, the demand for housing can be reached at a more rapid pace than by using conventional methods.

In terms of the environmental sustainability, the plastic materials showed less negative environmental impacts as well as improved energy efficiency compared to the block and mortar unit.

OPSOMMING

Die tekort aan voldoende behuising raak ’n kommerwekkende probleem in die huidige samelewing soos die wêreld populasie aan hou toeneem, waar hierdie probleem nie net tot Afrika beperk is nie. Soos die wêreld meer omgewingsbewus raak, word daar gestrewe na meer volhoubare ontwikkeling in die boubedryf wat aanleiding gee tot die ontwikkeling van alternatiewe bou tegnologieë (ABT’e) om die behuisingsagterstand op te los.

Plastiese materiale word ondersoek vir hul gebruik as strukturele elemente in lae-inkomste behuising om die behuisingsagterstand in ’n struktureel stabiele-, koste effektiewe- en omgewingsvolhoubare manier op te los. Geskikte plastiese materiale is geïdentifiseer as SVS (skuim-vesel samestelling) en HPS (hout-plastiek samestelling) vir gebruik as strukturele elemente en uitgesette polistireen is gebruik as ’n invul paneel.

Materiële eienskappe was eksperimenteel bepaal, wat in ’n numeriese analise gebruik was om die strukturele stabiliteit van ’n modulêre HPS behuisingseenheid te verifieer. Die eksperimentele werk sluit ’n direkte druk, direkte trek, druk kruip en ’n vier-punt buig toets in, wat uitgevoer is met HPS. Vir die saamgestelde paneel was daar ’n druk-deur skuif en ’n vier-punt buig toets gedoen. ’n Druk toets met die uitgesette polistireen en ’n relatiewe verband sterkte vir die geselekteerde gomme was ook getoets. Verder, is ’n vergelykende studie gedoen op die vuur uitvoering (vuurbestand waardering), koste effektiwiteit en die omgewingsvolhoubaarheid van ’n SVS-, HPS- en blok-en-mortel behuisingseenheid. ’n Ontwerp is bepaal en geverifieer deur beide eksperimentele werk en analitiese ondersoeke, wat gewys het dat HPS gebruik kan word as ’n lasdraende muurpaneel (met uitgesette polistireen invul), so wel as ’n dak- en vloer sisteem.

Daar is gevind, vanaf die vergelykende studie, dat die vuur uitvoering van die blok-en-mortel behuisingseenheid voldoen aan die vereiste van 20 en 30 minute onderskeidelik vir die interne en eksterne mure, soos voorgeskryf deur die SANS 10400-T (2011). Die vuur waardering van die blok-en-mortel behuisingseenheid het in terme van integriteit, insolasie en stabiliteit voldoen. Die twee modulêre plastiek behuisingseenhede het erger aan die vuur waardering slegs in trems van integriteit en insolasie voldoen. Hul het misluk in die voldoening in terme van stabiliteit. Die benadering wat gebruik was om die vuur gedrag van ’n behuisingseenheid te bepaal, is nie so akkuraat soos ’n fisiese vuur toets nie. Dit is omdat vir die benadering aannames in terme van die vuur eienskappe gemaak is. Die benadering gee egter ’n indikasie van die vuur uitvoering van ’n behuisingseenheid.

SVS en HPS is gelamineer met PVC (poliviniel chloried) wat hidrochloried suur (HCl) afgee wanneer dit brand. Hidrochloried suur is ŉ giftige gas. Volgens een van die minimum norms, gestipuleer deur die NHBRC Home Building Manual en Agrément, moet ŉ voldoende behuisingseenheid nie giftige gasse afgee nie. Al is die regulasies nie verpligtend nie, in terme hiervan, is SVS en HPS nie ŉ uitvoerbare boumateriaal vir ŉ voldoende behuisingseenheid nie, veral wanneer menslike gedrag en rook beheer aangespreek word nie. Nietemin, die aspek kan verbeter word deur die byvoeging van bymiddels om die rook produsering te verminder en in sommige omstandighede te voorkom.

Die vergelykende studie het ook gewys, dat die koste effektiwiteit van die SVS-behuisingseenheid vergelykbaar is met die van ŉ blok-en-mortel behuisingseenheid. Die HPS-behuisingseenheid se koste is aansienlik hoër as die van SVS-en die blok-en-mortel behuisingseenheid. Die modulêre plastiese, SVS en HPS, behuisingseenheid maak tipies gebruik van ongeskoolde werkers om die behuisingseenhuid op te rug, wat tot ŉ verbetering in die sosio-ekonomiese toestande in ŉ gemeenskap kan lei, deur dat dit werk skep. Aangesien die modulêre plastiese behuisingseenheid met relatiewe gemak en in ongeveer drie dae opgerig kan word, kan die aanvraag tot behuising vinniger bereik word, as wanner die konvensionele boumetodes gebruik word.

In terme van omgewingsvolhoubaarheid, het die plastiese materiale minder negatiewe omgewingsimpakte en is meer energie-doeltreffend in vergelyking met die blok-en-mortel onwerp.

ACKNOWLEDGEMENTS

The following persons are thanked for their valued contributions. They never hesitate to assist me with any queries I had and was willing to share their knowledge with me:

Me. W.I de Villiers (study leader) for sharing her willingness to educate, her knowledge, her leadership, her time and effort as well as assistance in completing the my thesis. Thank you for your guidance and interest in my research as well as your patience with me. This thesis would not have been completed without your valid input. I have gain so much knowledge working with you.

Prof. W.P. Boshoff for his open-door policy and helping me with my thought process regarding experiments. Especially, thank you for coming in on a Saturday helping me to understand the creep set-up. Thank you for always being prepared to assist me with any queries.

Jacques Bothma and Tom van der Kolf for their encouragement and support throughout my thesis. Jacques Bothma, thank you for assisting me in the lab and helping me with my experiments. Tom van der Kolf, thank you for sharing your knowledge of ABAQUS™ and willingness to assist me in it. I thank both of you for your motivation and positive energy, especially late at night and early mornings.

My family (André (Father), Elma (Mother) and Loré (Sister) le Roux) for being there for me during my Master's degree. They were always willing to listen to my thought process and gave me advice.

Lab Staff for their assistance with lab related work.

Engineering Faculty (Strategic Fund) for giving me the opportunity to do my Master's degree. Throughout my Master's degree, I gain a great deal of knowledge which sharpened my skills as an Engineer.

Ecowood for supplying the WPC, used for the experiments, at no cost.

TABLE OF CONTENTS

LIST OF FIGURES

LIST OF TABLES

LIST OF SYMBOLS AND ABBREVIATIONS

Symbol/Abbreviation	Description	Unit
a	The thermal conductances of n separate airspaces incorporated in the structure	[W/m^2°C]
A	Area	[mm],[m]
ABS	Acrylonitrile butadiene styrene	
ABT's	Alternative building technologies	
A_f	Net floor area of the room or compartment	[m^2]
ASTM	American Society for Testing and Materials	
A_t	Total enclosed area of room or compartment (include the area of the floor, walls and ceiling.)	[m^2]
A_v	Total area of vertical openings on all the walls	[m^2]
b	Thermal inertia	[J/m^2°Cs$^{1/2}$]
BIS	British Standards Institution	
BNG	Breaking New Ground initiative	
c	Specific heat	[J/kg°C]
CF	Carbon Footprint	
CHP	Comprehensive Housing Plan	
ci	Weighting factor related to EI_i	
CR- value	Total thermal resistance and thermal capacity	[hour]
C_s	Thermal capacity	[J/m^2°C]
CSIR	Council of Scientific and Industrial Research	
d	Thickness/ depth of the material	[m], [mm]
D	Deflection	[mm], [m]
E	Modulus of elasticity, Young modulus, E-modulus	[GPa]
EDIP	Environmental Design of Industrial Products	
e_f	Fire load density (net floor area)	[MJ/m^2]
e_i	Emission factor of the material	
E_i	Quantity of emission emitted	[kg]
EI_1	Carbon footprint (CF)	[kgCO_{2e}]

EIA	Environmental Impact Assessment	
EI*i*	Environmental impact *ith*	
EII	Environmental impact index	
EI_i	Environmental impact	
$EI_{i,ref}$	Normalised reference factor	
EN	European Standards	
EP	Eutrophication potential	
EPS	Expanded polystyrene	
e_t	Fire load density (total enclosed area)	[MJ/m^2]
FFC	Foam Fibre Composite	
fi	Acidification potential factor	
g	Gravity	[m/s^2]
GFRP	Glass fibre-reinforced plastic	
GHG	Greenhouse Gasses	
gi	Eutrophication factor	
G_k	Own weight	[N]
GWPi	Global warming potential	
h_0	Co-efficient of heat transfer for outer surface wall	[W/m^2°C]
h_1	Co-efficient of heat transfer for inner surface wall	[W/m^2°C]
HDPE	High density Polyethylene	
h_{eq}	Weighted average of window heights on all the walls	[m]
HRR	Heat release rate	[MW]
ISO	International Organisation for Standardisation	
k	Thermal conductivity	[W/m°C]
L	Span length, original length	[mm], [m]
LCA	Lifecycle Analysis	
LCIA	Life Cycle Impact Assessment	
LDPE	Low density Polyethylene	
LL	Live load	[Pa]
LSFB	Light Steel Frame Building	
LVD	Linear Variable Displacement Transducer	
M	Mass	[kg]
MAPP	Maleated polypropylene	
MgO	Magnesium oxide	

m_i	Mass or flow of the material	[kg]
$\dot{m}_i$	Burning rate	[kg/s]
NBR	National Building Regulations	
NHBRC	National Home Builders' Registration Council	
O	Opening factor	[$m^{1/2}$]
P	Applied load	[kN], [N]
PC	Polycarbonates	
PE	Polyethylene	
PET	Polyester	
PP	Polypropylene	
PS	Polystyrene	
PTFCE	Polytrifluorochloroethylene	
PTFE	Polytetrafluoroethylene	
PUF	Glass fibre reinforced rigid polyurethane	
PVC	Polyvinyl chloride	
PVC (rigid)	Rigid polyvinyl chloride	
q	Fire load	[MJ]
R	The rate of crosshead motion	[mm/min]
r	Strain of outer fibres	[mm/mm]
R-value	Thermal resistance value	[m^2°C/W]
SABS	South African Bureau of Standards	
SANS	South African National Standards	
s_i	Material layer *i* thickness	[m], [mm]
$s_{lim,1}$	Limiting thickness	[m], [mm]
t	Time	[second], [hour],[minute]
T	Temperature	[°C]
t^*	Fictitious time	[hour]
T_g	Glass transition temperature	[°C]
T_i	Initial temperature	[°C]
T_m	Melt temperature	[°C]
USA	United states of America	
UV	Ultra violet	
U-value	Thermal transmittance	[W/m^2°C]

V	Volume per square meter or thickness	[m], [mm]
V	Shear force	[N], [kN]
υ	Poisson ratio	
VAT	Value-Added Tax	
$v_{b,0}$	Basic wind speed	[m/s]
w	Width of specimen	[mm]
WL	Wind load	[Pa]
WPC	Wood-plastic composite	
XPS	Extruded polystyrene	
y	Conversion factor of 0.2778	
Z	Rate of straining of outer fibres	[mm/mm/s]
ZnSt	Zinc Stearate (Fatty acid metal soap used for lubricant of composite plastic materials)	
Γ	Fictitious time factor	
$\Delta H_{c,n}$	Calorific value or the chemical heat of combustion	[MJ/kg]
ΔL	Change in length	[mm]
ε	Strain	[mm/mm]
ρ	Density	[kg/m^3]
σ	Stress	[MPa]
τ	Shear stress	[MPa]

CHAPTER 1: INTRODUCTION

As the human population increases, the lack of adequate housing becomes an increasing problem that is not only restricted to Africa, but worldwide. This increase in worldwide urbanisation has led to an increase in informal settlements. According to Sexwhale (2010), South Africa planned to build 220 000 new low-income houses per year from 2010 to 2014, but the current backlog is estimated at 2.1 million houses. With the world becoming more environmentally aware, the aim towards more sustainable development has become more essential which results in alternative building technologies (ABT's) being investigated to address the backlog in housing.

The current building methods and materials (such as steel and concrete) used in the construction of low-income housing have large negative environmental impacts such as the emissions of greenhouse gases (Brewis, 2011; Brits, 2011). When considering that South Africa is planning to construct a large number of houses, the potential to develop sustainable low-income houses with less negative environmental impacts and the reduction in the cost per house becomes noticeable.

Plastic materials, which are mostly produced from by-products of the petroleum and oil industry, are investigated as alternative building materials for low-income housing to address the current backlog. Currently, plastics are used as structural members in applications such as decking.

The aim of the study is to determine whether plastic materials could be used as alternative building material in low-income housing, to address the housing backlog. This study has three main objectives. These objectives are to determine the structural feasibility, cost efficiency and environmental sustainability of plastic material if used for low-income housing. This is done by identifying viable plastic materials as well as designing a load-bearing walling, flooring and roofing system (excluding the design of connections) for the application in a low-income housing unit. The most viable plastic materials as well as the building envelope (load-bearing walling, flooring and roofing system) are used to quantify the three objectives for this design.

The research methodology used includes a literature review as well as both experimental and analytical investigations. An extensive literature review of plastic materials and their properties is conducted to determine the most viable plastic materials for the modular plastic housing unit. Experimental investigations are conducted to determine the mechanical properties of the viable plastic materials. The numerical analyses are performed to validate the building envelope by comparing the structural- (structural stability, fire

performance and durability), economic- (cost) and environmental feasibility (environmental impacts and energy efficiency) to a conventional block and mortar design. The results of the experimental investigation are used to perform a numerical analysis, to validate the structural stability of the modular plastic housing unit.

A brief chapter overview includes the following. In Chapter 2, the housing regulations, legislations and policies are discussed as well as the alternative building technologies (ABT's) currently used in South Africa. The current use of plastic materials as structural members worldwide is also discussed. In Chapter 3, the nature of polymers and plastic are described. Chapter 4 investigates the properties of unreinforced plastics, whereas Chapter 5 covers plastic composites and foams. In Chapter 6, the building envelope (design) of a modular plastic housing unit is described and the most viable plastic materials and adhesives are selected. In Chapter 7, experimental work is reported. Chapter 8 discusses the structural feasibility in terms of a numerical analysis, fire performance and durability. In Chapter 9, a cost comparison between two modular housing units and a conventional block and mortar design, is done. Chapter 10 includes an investigation into the environmental feasibility, which is compared for the three housing units, in terms of an environmental impact assessment and energy efficiency. Lastly, conclusions and recommendations are provided for this study in Chapter 11.

CHAPTER 2: LOW-INCOME HOUSING AND ALTERNATIVE BUILDING TECHNOLOGIES

In South Africa, over three million government subsidised houses have been delivered between 1994 and 2010, but the demand for adequate low-income houses in South Africa continues to grow (South African Yearbook, 2012, p. 294). To address the demand for housing in South Africa, the Department of Human Settlements, as well as the Government, has implemented new housing regulations, legislations and policies while promoting the use of alternative building technologies (ABT's).

These South African housing regulations, legislations and policies as well as alternative building technologies available in South Africa are discussed in this chapter. The manner, in which plastic materials are used as an alternative building material, worldwide, is also discussed.

2.1. Housing regulations, legislation and policies in South Africa

In the Constitution of South Africa, in Act 108 of 1996, Section 26 Chapter 2 states that:

(1) "All South Africans have the basic right to have access to adequate housing.
(2) The State is compelled to take reasonable measures within the limits of its available resources, including the introduction of legislation, to work towards ensuring that all South Africans enjoy this right" (Department of Human Settlements, 2012).

After 1994, several policies and strategies have been implemented in South Africa to support the housing sector. The New Housing Policy and Strategy for South Africa: *White Paper 1994* and the Comprehensive Plan for the Development of Sustainable Human Settlement*: Breaking New Grounds 2004* are two documents that constitute the directives of the National Department of Human Settlements (Department of Human Settlements, 2012).

2.1.1. New Housing Policy and Strategy for South Africa, 1994

The vision of the New Housing Policy and Strategy is to establish social, feasible and economic integration of communities, who are situated in areas that are close to work, economic opportunities, education, health and social conveniences. Each South African will have access to the following (New Housing Policy and Strategy for South Africa, 1994):

- "A permanent residential structure with secure tenure, ensuring privacy and providing adequate protection against the elements, and
- Potable water, adequate sanitary facilities including waste disposal and domestic electricity supply."

The goal of the New Housing Policy and Strategy is mainly to increase the housing delivery of South Africa in a sustainable matter. To reach the Government of National Unity's target of delivering one million houses in a five year period, approximately 200 000 housing units should be delivered annually (New Housing Policy and Strategy for South Africa, 1994). However, the human population is still increasing which leads to an increase in the demand of adequate housing. One solution to the increase demand for adequate housing is to deliver houses quicker.

2.1.2. Breaking New Ground: Comprehensive Housing Plan for the Development of Sustainable Human Settlements, 2004

To accelerate the delivery of housing, the National Housing Department introduced the *Breaking New Ground* (BNG) initiative in 2004. The Comprehensive Housing Plan (CHP) was approved by the Cabinet for the Development of Integrated Sustainable Human Settlements (BNG) and is based on the principles of the Housing White Paper of 1994 (South African Yearbook, 2012, p. 294). The main objective of the BNG and the CHP is to eradicate all informal settlements in the shortest time possible, within South Africa (United Nations, 2010).

The BNG focuses on the integration of society and sustainable human settlements by refining the housing environment's quality (Department of Human Settlements, 2012, p. 8). The Upgrade of Informal Settlements Program was developed as part of *Breaking New Ground: Comprehensive Plan for the Development of Sustainable Human Settlement, 2004* (Marais & Ntema, 2013, p. 87). It is another principal point, which aims to improve the life of people living in slums and is aligned with the United Nations Millennium Goals (Marais & Ntema, 2013, p. 87).

The CHP concentrates on the following (South African Yearbook, 2012, p. 294):

- To accelerate the delivery of housing as a strategy to reduce poverty.
- To use the housing delivery as a way to create work.
- To increase the growth in the economy, to promote social cohesion and to combat crime.
- To develop sustainable human settlements by means of housing.
- To use the housing development to overcome the residential barriers.

2.1.3. National Building Regulations, Agrément and National Home Builders' Registration Council

South Africa has building regulations as well as bodies or boards to implement the building regulations. Entities, such as the National Building Regulations, Agrément and National Home Builders' Registration Council are discussed in this section.

The aim of the National Building Regulations (NBR), 1990, is to ensure that structures provide acceptable levels of safety, health, welfare and convenience for both inhabitants and community in which the structure is located (SANS 10400-A, 2010). These objectives are achieved by means of managing the control of the design, construction and operation of a structure (Tonkin, 2008, p. 404). The NBR make provision for local authorities, who enforce the regulations, to obtain an evaluation certificate or a test report for a building system or product. This is issued by the South African Bureau of Standards (SABS), Agrément Board of South Africa or the Council of Scientific and Industrial Research (CSIR). The Agrément Board of South Africa and the CSIR, which comply with the NBR, release certificates, which report on the sufficiency or safety of a system, a material, a method or a product used in or during the construction process (Tonkin, 2008, p. 404). However, non-standard or innovative building products, systems or components, such as alternative building technologies (ABT's) can only gain entry to the South African market through Agrément Certification (SANS 10400-A, 2010).

The NBR and Standards Act, 1977 defines Agrément as follows: "Agrément certificate means a certificate that confirms fitness-for-purpose of a non-standardised product, material or component or the acceptability of the related non-standardised design and the conditions pertaining thereto (or both) issued by the Board of Agrément South Africa." (SANS 10400-A, 2010). Agrément South Africa is funded and mandated by the Department of Public Works to encourage innovative building systems and products, and to protect users against unacceptable ones (Agrément South Africa, 2013). This is accomplished by determining the fit-for-purpose of an innovative or non-standard system or product by means of testing this system or product against performance-based criteria. Some of the aspects, that Agrément South Africa considers to determine

the fit-for-purpose of an innovative or non-standard building system or product, include stability and structural strength, water penetration, fire behaviour, thermal performance, maintenance required and durability (Agrément South Africa, 2013).

The NBR are performance-based regulations for systems and products, whereas the National Home Builders' Registration Council (NHBRC) acts as a guideline to adequate housing rather than the performance of a product (Tonkin, 2008, p. 406). The NHBRC was created as a Section 21 Company in 1995. It is now considered as a statutory body. All the new houses that are built should be registered under the Defect Warranty Scheme and the builders that construct houses must be registered at this statutory body. The Product Defect Warranty Scheme ensures that housing consumers can claim to pay for repairs and structural defects within five years of the completion date (Tonkin, 2008, p. 406). The NHBRC created the Code of Conduct for Home Builders, which protects housing consumers from dishonest builders, developers and contractors. The requirements and norms can be found in the Home Builders Manual (NHBRC, 1999). The factors to be considered for adequate housing (minimum norms) are defined by the Home Builders Manual as well as by Agrément South Africa and are as follows (NHBRC, 1999, p. 5 (Part 1)):

- Structural strength and stability
- Weather tightness
- Behaviour of fire
- Thermal condensation and performance
- Protection against harmful substances
- Provision for natural lighting and ventilation.

2.2. Alternative building technologies used in South Africa for low-income housing

With the background of the housing regulations, legislation and policies in South Africa, the different types of low-income housing are discussed. South Africa exhibits a wide variety of design types for low-income housing. Generally, the economic consideration plays the most important role, followed by social acceptance, in the choice of low-income housing design type.

The conventional design used in South Africa is the block and mortar design and is shown in Figure 2.1. Most contractors, builders and developers use this design, since they are more familiar with the design and it complies with the NHBRC and the NBR. The conventional construction method is time consuming, costly

and inadequate to meet the growing demand for the delivering of low-income housing, therefore the government has introduced programs to encourage the use of ABT's (South African Yearbook, 2012).

Three popular alternative building technologies in South Africa are discussed in the following sections (Brewis, 2011, p. 15). These ABT's could provide a faster way to deliver houses when compared to the block and mortar houses. Thus, they could be more economical construction methods than the conventional construction methods.

Figure 2.1: Conventional design for low-income houses (Brewis, 2011, p. 14)

2.2.1. Light Steel Frame Building

The Light Steel Frame Building (LSFB) method has been used for decades in Europe, United States of America and Australia, but is a relatively new method in South Africa (SASFA, [S.a]). LSFB is the technique that offers some advantages, such as cost efficiency, quality products, durability, minimum energy and product wastage, low wall panel mass and ease of construction, thus reducing construction time. The LSFB fulfil the requirement of the National Building Regulation in terms of quality. An example of the LSFB is shown in Figure 2.2 (SASFA, [S.a]).

LSFB are comprised of structural roof trusses and wall frames (SASFA, [S.a]). These frames and trusses are produced within a factory from steel sections that are cold-formed light gauge galvanised steel. The wall frames are fixed with an exterior cladding that consists of fibre cement boards or a single, thin layer of brick wall. Gypsum boards are usually used as interior walls and ceilings, which are fixed to the frame (SASFA, [S.a]). The gypsum boards also provide fire resistance to the building that comply with the 30 minutes minimum fire rating (NHBRC, 1999). An insulation material is placed in the wall cavity, that is created by the steel frames and services are usually installed in this insulation material (SASFA, [S.a]).

Figure 2.2: Light Steel Frame Building (SASFA, [S.a]).

2.2.2. Imison™ 3 building system

The Imison™ 3 Building System is to some extent similar to the LSFB (Agrément South Africa, 2009-a). It is similar in the sense that it is also comprised of cold-formed light gauge galvanised steel sections. These to building techniques differ, in terms of; the panels used to construct the Imison™ 3 Building System includes of an infill whereas the LSFB uses cladding.

The foundations are adequately thick and function as footings for the system. The columns are comprised of either square, round or back-to-back lip channel steel sections that are cold-formed light gauge galvanised steel. The columns are anchored to the foundation by means of galvanised steel brackets. The ring-beams consist of either rectangular hollow, lipped channels of Z-profile steel sections that are cold-formed light gauge galvanised steel. These ring-beams are connected to the top of the columns and to the roof trusses by means of galvanised steel straps. The core infill panels are made up of expanded polystyrene (EPS) which is plastered with a fire reinforced plaster (Agrément certificate 2007/338: Fibrecote Fibre Reinforced Plaster). Lastly, the roof trusses are either comprised of timber or cold-formed light gauge galvanised steel sections (Agrément South Africa, 2009-a). A section through the foundation, external walls and roof is shown in Figure 2.3.

The main benefit of this building system is that it is time efficient during construction and thus creates a solution for the increased low-income housing demand, which is required in South Africa.

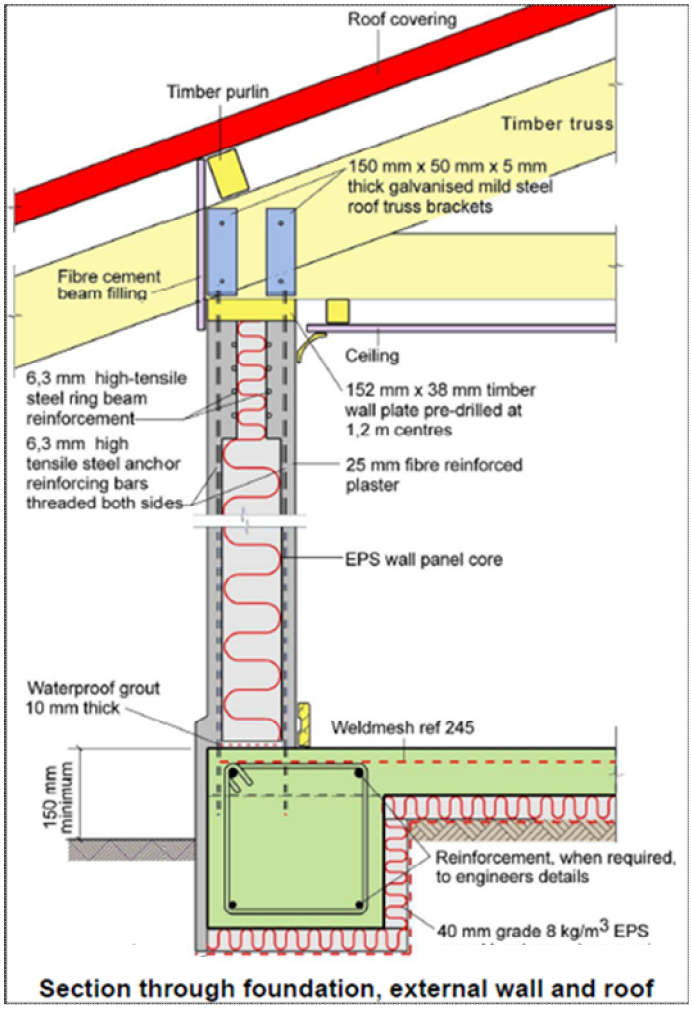

Figure 2.3: Section through the foundation, external walls and roof of an Imison™ building (Agrément South Africa, 2009-a)

2.2.3. Moladi© building system

This system consists of the use of lightweight, reusable, recyclable and removable plastic moulds, which are filled with standard approved concrete to produce a wall structure (Moladi, [S.a]). The system is shown in Figure 2.4.

The Moladi Building System offers a variety of benefits such as rapid production rate, cost efficient, consistent quality, unskilled operators, minimum wastage and it is a transferable construction technology (Moladi, [S.a]). This rapid production makes this design type suitable for mass housing production, without compromising the quality of the system. The plastic formwork panels can be reused up to fifty times, which results in a reduction of construction and transport cost. The Moladi construction process is shown in Figure 2.5 (Moladi, [S.a]).

Figure 2.4: Moladi© Building System (Moladi, [S.a]).

Day 1 (Six hours)	
Step 1:	• Moladi formwork is delivered to the site • The formwork panels are constructed to form the mould panels of the desired house by unskilled labourers
Step 2	• Internal formwork panels are erected • Within the cavity walls, block-outs and window frames are positioned • Within the cavity, reinforcing bars are positioned to the engineer's specifications
Step 3:	• Within the cavity walls, block-outs and door frames are positioned • External formwork panels are erected, thus closing off the wall cavity
Step 4:	• Wall cavities are filled with standard approved concrete to produce a wall structure
Day 2 (Six hours)	
Step 1:	• Moladi formwork panels are removed by unskilled labourers
Step 2:	• Walls are painted with cementitious water based paint • Oil or acrylic based paint can be applied after 28 days
Step 3:	• Installation of engineer certified roof • Installation of windows and door • Final finishes are made
Structure is now ready for occupation	

Figure 2.5: Moladi construction process (Moladi, [S.a])

2.3. Plastic materials as alternative building material

Some plastic materials are considered more environmentally friendly than other building materials (Hauschild & Wenzel, 1998). In the building industry, plastics are generally used as non-structural applications such as cladding, siding or lamination of walling system as well as an insulative material and for piping (PVC pipes). Other non-structural applications include Moladi© Building System plastic formwork. It is also used as fibre reinforcement in concrete. However, plastic can also be used for structural applications such as decking. The structural application of plastic in the building industry is currently limited and is discussed in this section.

2.3.1. Dome construction

In 1966, dome shaped buildings were erected in Lafayette Indiana as an R&D project (Rosato, 1997, p. 455). These domes were constructed using polystyrene foam boards. The buildings were self-supporting which required no support during or after production. They provided insulation and openings were cut out to create windows and doors. The outside of the domes were covered with concrete and steel mesh, whereas the inside walls were covered with plaster (Rosato, 1997, p. 455). These domes are shown in Figure 2.6.

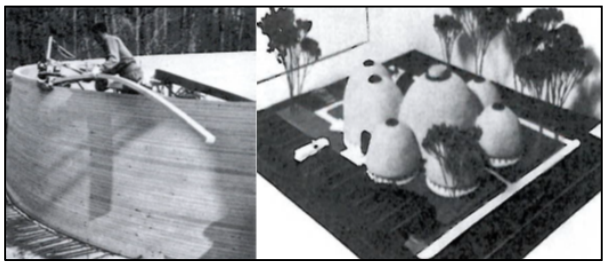

Figure 2.6: Polystyrene foamed boards, dome-shaped houses (Rosato, 1997, pp. 456-457, Figure 9.5).

2.3.2. Reinforced plastic

In 1957, one of the first houses constructed of reinforced plastic was the Monsanto House of the Future, which was erected in Disneyland, USA (Rosato & Rosato, 2004, p. 487). The main components of this house are 4.9 meter U-shape cantilevered “wings” (Rosato, 1997, p. 547). This house consists of different plastic sandwich panels, where different types of plastics were used for the different panels (Rosato & Rosato, 2004, p. 487). After approximately twenty years, the structure displayed insignificant deflection changes, with loads subjected to the house. These loads include earthquakes, wind loads as well as people passing through it (Rosato & Rosato, 2004, p. 488). This house is shown in Figure 2.7.

Figure 2.7: Reinforced plastic house, Monsanto House of the Future (Rosato & Rosato, 2004, p. 488)

2.3.3. Plastic bottle construction

In the village of Sabon Yelwa in Nigeria, plastic PET (thermoplastic polyester) bottles were used to construct a house, the first of its kind (Olukoya, 2011). This construction method was believed to be the answer to the backlog of housing in Nigeria and to the polluted environment. The construction method consists of capped, sand filled PET bottles that weight approximately three kilograms each. The bottles were stacked and bounded by an intricate network of strings that were connected by the neck of the bottles. After the bottles were bonded, mud and cement were used to provide support and serve as plaster (Olukoya, 2011). This plastic bottle construction is shown in Figure 2.8.

In Nigeria, it is estimated that approximately 3 million plastic bottles are thrown out daily (Olukoya, 2011). To construct a 58m^2 house approximately 20 000 bottles are required. This bottle construction house is cheaper in terms of construction and material when compared to the conventional construction method. It costs a quarter of a conventional house. Other advantages, except cost efficiency, include resistance to fire, bullets and earthquakes. The interior of the house remains at a constant temperature of 18 degree celsius, which is considered a comfortable temperature for a tropical climate (Olukoya, 2011).

Figure 2.8: Plastic bottle house construction (Olukoya, 2011)

2.3.4. Wood-plastic composite structural elements

Wood-plastic composite (WPC) is a fabricated product that contains a wood component, such as wood fibres or wood-flour and a plastic component, such as a thermosetting plastic material or thermoplastic (Leu, et al., 2012). In the building industry, WPC is generally used as non-structural and structural elements such as cladding and decking, respectively. The properties of WPC depend on the type of wood and plastic, the ratio of wood to plastic as well as if wood-flour or wood fibre is used. If WPC consists largely of wood, the appearance of the product is similar to wood, but with a far higher durability (Tech-Wood, [S.a]). WPC differs between manufacturers depending on the ratio of wood to plastic and type of wood and plastic used to produce WPC. For example:

- The British Company, Tech-Wood International, developed a product named Tech-Wood (Stewart, 2010). This product consists of 30% polypropylene and 70% pinewood fibre (Tech-Wood, [S.a]).
- Eva-Last is a South African company that produce a product, mainly use for decking, called Eva-Tech. Eva-tech contains 40% recycled high density polyethylene and 60% reclaimed hard wood fibres (Eva-Last, [S.a]).

2.3.5. Structural plastic lumber

Plastic lumber is a product that is manufactured from post-user plastic waste, thus it is produced form recycled plastic and additives (Breslin, et al., 1998). Unlike WPC, plastic lumber usually contains no wood component. An example of a plastic lumber product is Polyforce™ (Tangent, 2009). Polyforce™ is a structural plastic lumber that is manufactured by an American company named Tangent Technologies, LLC. It is made up of recycled high density polyethylene, proprietary strengthening additives, anti-oxidant processing aids, UV-inhibited pigments and a foaming agent. The applications of Polyforce™ include marine structures, docks and boardwalks (Tangent, 2009).

Vertech and Struxure are also plastic lumber products. Struxure Composite is an American-made product by Axion (Axion, [S.a]). This product is produced by a patented formula, which includes 100% recycled materials such as plastic bottles. Both of these products are suited for a variety of structural applications, which include bridges, commercial decking, boardwalks, some marine systems and also beams, boards and piling, and is shown in Figure 2.9 (Axion, [S.a]; Vertech, [S.a]). Vertech and Struxure are light weight products that will not rust, rot, absorb moisture or leach toxic chemicals into the environment (Vertech, [S.a]; Axion, [S.a]). Vertech material was used to construct the first recycled plastic road bridge in the UK (Vertech, [S.a]). This road bridge is shown in Figure 2.10.

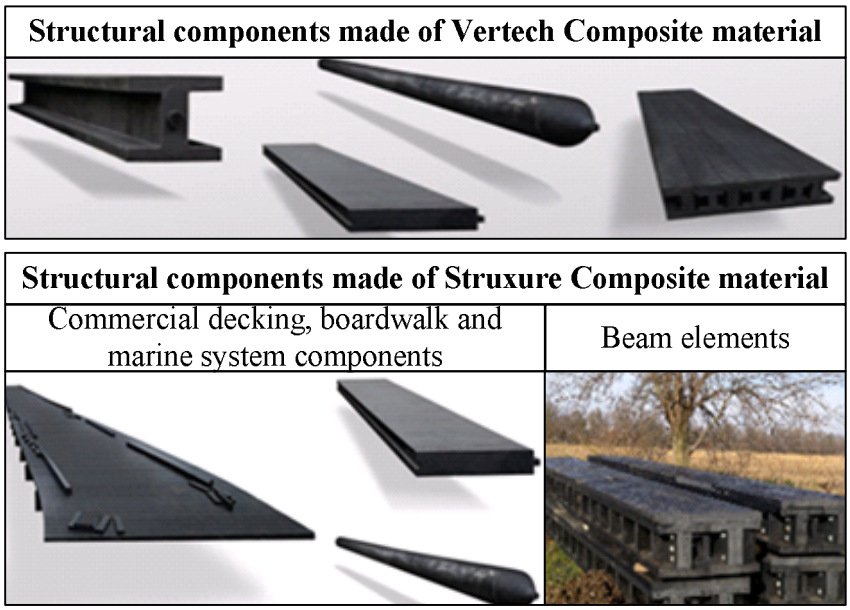

Figure 2.9: Structural components of Struxure and Vertech composite materials (Axion, [S.a]; Vertech, [S.a]).

Figure 2.10: Vertech material bridge. First thermoplastic bridge in the UK (Vertech, [S.a])

2.3.6. FFC^{tm} technology by Friul Filiere Spa

FFC (Foam Fibre Composite) is an ultra-light foam composite material that consists of 50% thermoplastic material and 50% vegetal fibres as well as other materials (Friul Filiere Spa, [S.a]). The applications of this product include decking, windows, doors, skirting, fences and wall panelling. FFC is a flexible, light weight product that acts as a thermal and acoustic insulation. This product is dimensionally stable and can resistant humidity. FFC is fully recyclable and self-extinguishing (Friul Filiere Spa, [S.a]).

2.3.7. Prefabricated composite wall system made from rigid polyurethane and magnesium oxide board

A prefabricated wall system that consists of glass fibre reinforced rigid polyurethane (PUF) and magnesium oxide (MgO) board was investigated in Queensland in Australia (Manalo, 2013, p. 642). This walling system is shown in Figure 2.11. The full scale composite wall was tested for compression, shear and transverse bending (Manalo, 2013, p. 642). The test results show that the strength behaviour of this wall system is controlled by the strength of the MgO board. This walling system can be used as a modular construction for housing, but if high strength is required, the stiffness and strength of the composite wall must be improved (Manalo, 2013, p. 653).

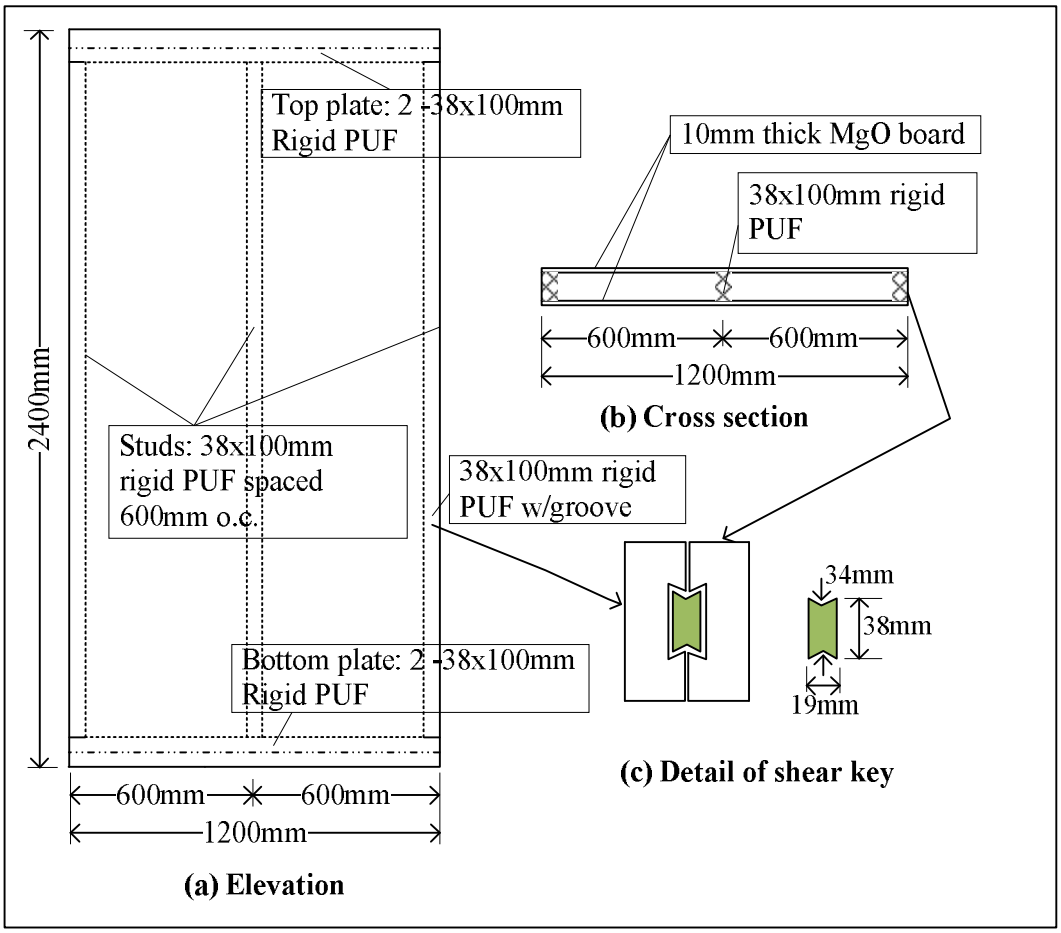

Figure 2.11: Details of prefabricated composite wall system made from rigid polyurethane and magnesium oxide board (Manalo, 2013, p. 644)

2.3.8. InnoVida building system

InnoVida Building System is certified by Agrément for building single-storey structures (Agrément South Africa, 2009-b). A cross-section of the external wall is shown in Figure 2.12. This system is comprised of 2500x6000x64mm thick superstructure wall panels. These wall panels consist of two sheets of saturated glass fibre composite that encapsulate a core created from expanded polyurethane. Surface bed panels, that are exactly the same as the wall panels, are placed on a well compacted fill with a 700x700x650mm high InnoVida corner footing. The roof sheets are also exactly the same as the wall panels and the roof is finished with paint on the exterior. For this system, the door and window frames are made from timber and the services are conventional (Agrément South Africa, 2009-b).

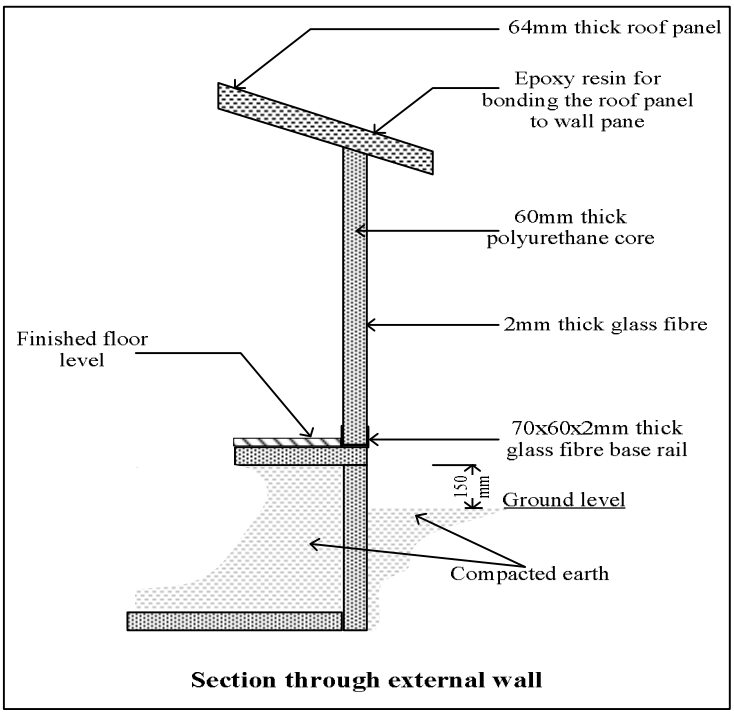

Figure 2.12: A cross-section of the external wall of the InnoVida Building System (Agrément South Africa, 2009-b)

2.4. Summary

As the human population increases, the housing backlog increases (New Housing Policy and Strategy for South Africa, 1994). Therefore, the solution to meet the demand of adequate housing is to deliver houses quicker by means of ABT's. These ABT's need to comply with the South African building regulations, legislation and policies. The ABT's can only gain entry to the South African market through an Agrément Certification (SANS 10400-A, 2010).

The current ABT's used in South Africa provide a faster way to deliver adequate housing, compared to the conventional building design of block and mortar. These ATB's are also accepted by society, which are one of the main problems with innovative building systems and products.

Plastic materials can be a way to address the housing backlog problem in South Africa. There are numerous plastic products available for structural and non-structural applications. Although, structural applications of plastic products are limited, the structural plastic industry is developing at a rapid rate. Some plastic materials are considered more environmentally friendly than other building materials (Hauschild & Wenzel, 1998).

CHAPTER 3: NATURE OF POLYMERS AND PLASTICS

In the previous chapter, the South African building regulations, legislation and policies, the alternative building technologies (ABT's) used in South Africa as well as the manner in which plastic materials are currently used as structural ABT's worldwide, were discussed. To succeed in using plastic material as an alternative building material, the nature of polymers and plastics must be understood. This is summarised in Figure 3.1. In this chapter, the difference between plastic and polymers are discussed. The different types of plastic materials as well as polymer structures are discussed. These aspects which are discussed in this chapter greatly influence the properties of a plastic material (Chapter 4).

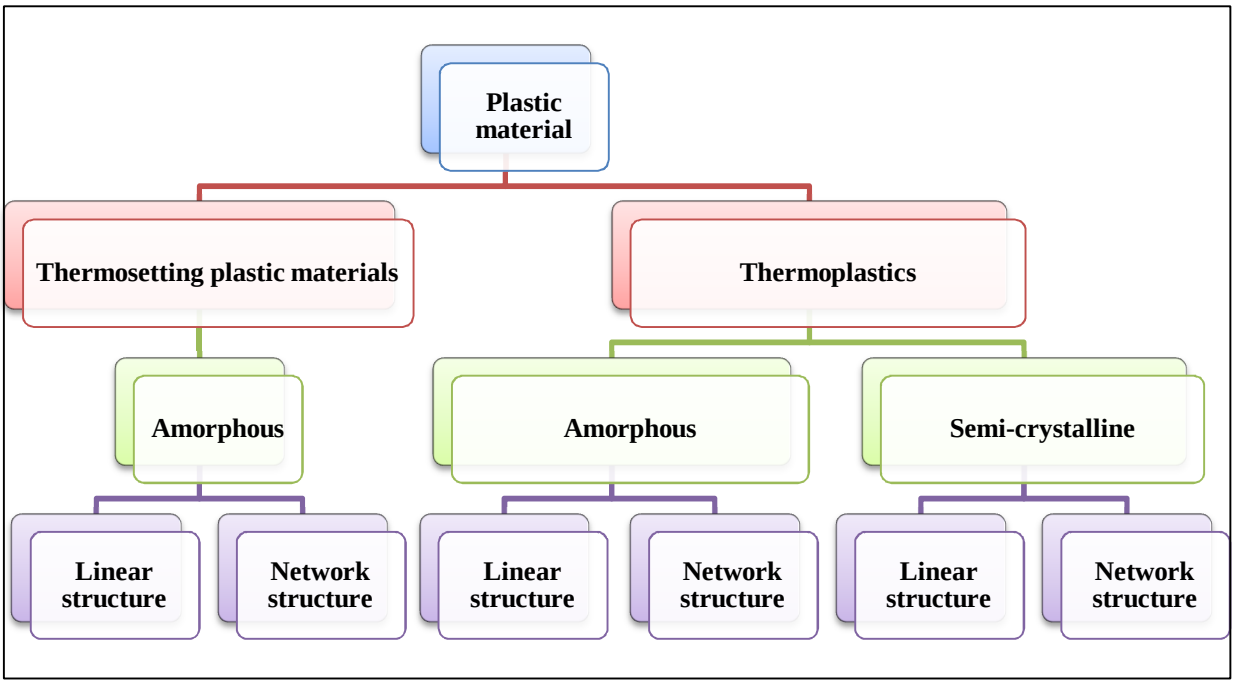

Figure 3.1: Summary of the nature of plastics versus polymers

3.1. Polymers and plastics

The term "polymer" is often used as the synonym for "plastic" (Crawford, 1981, p. 8), but this is not true as these terms refer to different states of a product (Cantor & Watts , 2011, p. 3). The term "plastic" originated from the Greek term which means "mouldable" (Cantor & Watts , 2011, p. 3). Since this meaning of plastic is unclear and can cause misinterpretation (Hiatt & Winding, 1961, p. 4), plastics can be defined as organic or synthetic solid components with a high molecular weight (Rosato, 1997, p. 49), also known as

macromolecular, that is capable of being moulded by moderate temperature or by chemical reaction (Hiatt & Winding, 1961, p. 4). The term plastics is used to describe the final product, made from plastic materials (Hiatt & Winding, 1961, p. 4) and is constructed mostly of polymers, but also contains substances like colorant and other additives (Cantor & Watts , 2011, p. 4).

Polymer, on the other hand, means "many parts" (Cantor & Watts , 2011, p. 3). Polymers consist of larger chain-like molecules that are constructed by connecting monomers, where monomers refer to hundreds of smaller molecular units that are connected (Crawford, 1981, p. 8). The process of connecting the monomers is termed polymerisation, whereas the degree of polymerisation is the amount of components in the long molecule (Crawford, 1981, p. 8). Polymers can be divided into classes according to their state, namely amorphous or semi-crystalline (Cantor & Watts , 2011, p. 3). Semi-crystalline polymers exhibit an ordered region. Chains align themselves in this region. These chains are termed crystals. However, some regions remain disordered and these regions are termed amorphous. Amorphous polymers have chains that are disordered which remain in a random pattern as shown in Figure 3.2 (Cantor & Watts , 2011, p. 3).

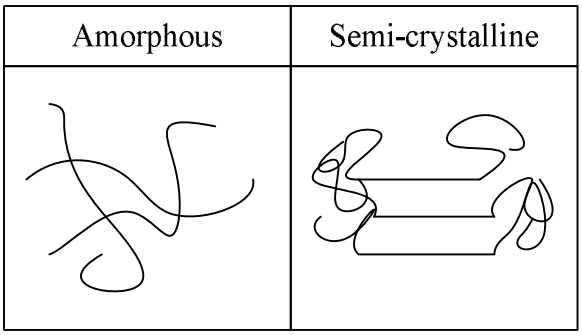

Figure 3.2: Amorphous versus Semi-crystalline (Cantor & Watts , 2011, pp. 3, Figure 1.2)

3.2. Thermosetting and thermoplastic materials

The two most important types of plastic materials are thermosetting and thermoplastic materials (Kinney, 1967, p. 3). The schematic illustration of the structure of thermosets compared to thermoplastics is shown in Figure 3.3. An example of the plastic materials that are classified as thermosets and thermoplastics is shown in Table 3.1. Thermoplastic materials retain the ability to be formed (Hiatt & Winding, 1961, p. 3) by becoming soft when exposed to sufficient heat and/or pressure and solidify when cooled (Rosato, 1997, p. 56). Thermoplastics also experience no permanent changes when heated (Palin, 1967, p. 10). For example, thermoplastics can be compared to a block of ice, that can become soft or turn into liquid when heated, poured into a mould or any shape and when cooled, solidifies again, while no

permanent changes are experienced (Rosato, 1997, p. 55). They are constructed from linear molecules (Palin, 1967, p. 10) and are composed of individual polymer chains (Cantor & Watts , 2011, p. 3).

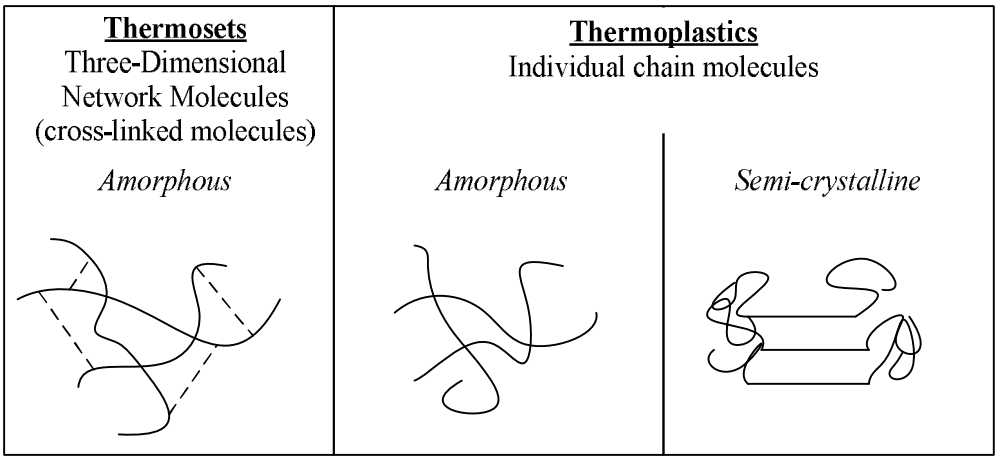

Figure 3.3: Schematic illustration of the structure of thermosets versus thermoplastic materials (Braun, 1999, pp. 12, Figure 1)

Table 3.1: Example of thermosets and thermoplastics (Rosato, 1997, p. 61)

Thermosets	**Thermoplastics**	
Amorphous	*Amorphous*	*Semi-crystalline*
Epoxy (EP)	Acrylonitrile butadiene styrene (ABS)	High density Polyethylene (HDPE)
Melamine formaldehyde (MF)	Polycarbonates (PC)	Low density Polyethylene (LDPE)
Phenol formaldehyde (PH)	Polystyrene (PS)	Polyamide (Nylon 6)
Polyester (unsaturated) (UP)	Polyvinyl chloride (PVC)	Polyamide (Nylon 6.6)
		Polyester (PET)
		Polypropylene (PP)
		Polytetrafluoroethylene (PTFE)
		Polytrifluorochloroethylene (PTFCE)

Thermosetting materials, on the other hand, are created by a chemical reaction that contains two stages (Crawford, 1981, p. 9). The first stage results in a partly polymerised moulded shape and the material can flow when heated (Palin, 1967, p. 10). The second stage occurs during the process of moulding, where extra polymerisation occurs, which results in a highly cross-linked polymeric structure (Palin, 1967, pp. 10-11).

The material loses the ability to be softened, when reheated, after the material has been cooled or moulded (Rosato, 1997, p. 56). For example, thermosets can be compared to a yolk of an egg, when heated the yolk changes form a liquid to a solid and cannot change back to a liquid (Rosato, 1997, p. 57). Partly polymerised shapes are known as resins (Palin, 1967, p. 11). The change to the final shape is termed curing. Most thermosets are cured by mean of applying heat and pressure (Palin, 1967, p. 11). Thermosetting materials are preferred to thermoplastic materials where high heat resistance and/or strength are required (Cantor & Watts , 2011, p. 3).

3.3. Basic structure of polymers

The structures of polymers can be extremely complex, but some generalisations are possible which assist significantly in the understanding of the close relationship between polymeric materials. These generalisations also aid in the understanding of the behaviour of high molecular weight polymers (Hiatt & Winding, 1961, p. 7). The two main structural types of polymers are discussed in the following sections.

3.3.1. Linear polymers

A linear or chain polymer structure is the simplest kind of polymer molecule (Palin, 1967, p. 1) and refers to recurring units which form larger numbers of monomers (Hiatt & Winding, 1961, p. 7). These monomers construct a typical structure (Hiatt & Winding, 1961, p. 7), as shown in Figure 3.4 (Palin, 1967, p. 1) . This figure shows the recurring atom (in most plastic materials this recurring atom refers to carbon atoms), where each carbon atom forms bonds with simple groups or two other atoms and two carbon atoms. There is free rotation about these simple groups or single carbon to carbon bonds and therefore the system has the ability to change (Palin, 1967, p. 1).

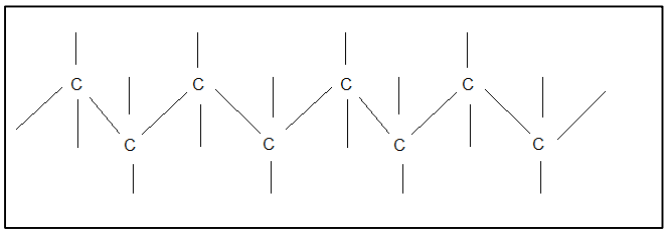

Figure 3.4: Schematic illustration of a linear polymer (Palin, 1967, p. 1)

A linear polymeric structure does not refer to the physical structure but only to the chemical structure of the polymer (Palin, 1967, p. 1). It describes a structure with a considerable polymer length relative to its

thickness (Hiatt & Winding, 1961, p. 8). The physical structure of a linear polymer is extremely rarely straight and changes with time (Palin, 1967, p. 1).

In a linear structure, there are no major forces holding the adjoining chains together. Thermoplastic material is usually associated with this type of polymer structure as shown in Figure 3.3. Most thermoplastic materials are relatively soluble due to their polymer structure, although excessive length of chains or chemical groups connected to the chain results in low solubility (Hiatt & Winding, 1961, pp. 8-9).

3.3.2. Network polymers

A network polymer is the result of a large amount of carbon atoms which form three or four bonds with other carbon atoms, different to those of simple groups (Palin, 1967, p. 2). This type of structure is complex and the chains of this structure type are connected by primary valences (Hiatt & Winding, 1961, pp. 9-10). These network polymers are created in two steps (Palin, 1967, p. 3). Firstly, small molecules, mainly linear of structure are produced. Secondly, these molecules are then affected to react in such a manner that chemical bonds are formed between the molecules, thus resulting in the build-up of a network, termed cross-linking. Polymers can be lightly to highly cross-linked depending on the amount of linear molecules in a network polymer. If no linear molecules are present, the polymer is termed a highly cross-linked polymer, whereas a large amount of linear molecules in a network polymer refers to a lightly cross-linked polymer. The more cross-linked a polymer is, the more restricted is the movement of molecules (Palin, 1967, p. 3).

A highly cross-linked structure is a characteristic of thermosetting polymers and the network is referred to as “tight” due to the repeated occurrence of cross-linkage in the network. This results in extremely low mobility of polymeric molecules. Insolubility, strength, low extensibility of thermosetting materials and infusibility are attributed to the large amounts of cross-linkage in the network (Hiatt & Winding, 1961, pp. 10-11).

3.4. Summary

The terms “plastics” and “polymers” are often used as synonyms. This is due to the unclear meaning of plastics. Plastics can be defined as organic or synthetic solid components with a macromolecular state, whereas, the term “polymers” refers to “many parts”. The relationship between plastics and the state as well as the structure of the polymers can be summarised as shown in Figure 3.1.

Plastics consist mainly of polymers, but also contain substances like colorant and other additives. The two most important types of plastic materials are thermosetting and thermoplastic materials (Figure 3.3). Thermosetting plastic materials only exhibit an amorphous polymeric state, whereas thermoplastic materials can exhibit an amorphous or semi-crystalline polymeric state. Depending on the type of plastic material (both thermosets and thermoplastics), the polymeric structure (linear or network structure) differs. This is illustrated in Figure 3.1.

Polymers are constructed by connecting monomers, which result in large chain-like structures. Polymerisation describes the process used to connect monomers. Polymers can be divided into amorphous and semi-crystalline states (Figure 3.2). However, these states can exhibit a linear or network polymer structure.

The structure of the polymers (linear or network structure) as well as the type of plastic material (thermosets or thermoplastics) greatly influence the properties of a plastic material. This will be discussed in the following chapter.

CHAPTER 4: UNREINFORCED PLASTICS

Unreinforced plastic, also known as a neat or unfilled plastic, contains only polymeric matter. The nature of polymers and plastic, the difference between polymers and plastic and the molecular structures of polymers were discussed in the previous chapter (Chapter 3). The molecular structure of a polymer has an influence on the properties of unreinforced plastics and the influence on the properties is discussed in this chapter. The mechanical, thermal and chemical properties of thermosetting plastics, thermoplastics and common construction materials are compared in this chapter. The various moulding techniques to fabricate unreinforced plastics are also discussed.

4.1. Mechanical properties

Plastic materials exhibit a range of advantages, such as high strength-to-weight ratio, no corrosion, toughness, low friction and ease of manufacture (Crawford, 1981, p. 31). However, mechanical behaviour of plastic materials might be limited by the molecular structures of the material as described in Chapter 3, temperature changes, rate of loading as well as the moulding technique (Hollaway, 1990).

The change in mechanical properties due to the change in temperature for amorphous and crystalline plastic is shown in Figure 4.1. This figure illustrates that mechanical properties of plastics reduce with the increase in temperature. However, crystalline plastics exhibit higher mechanical properties than amorphous plastics, up to the point of the material becoming a liquid. The mechanical properties of both amorphous and crystalline plastics reduce significantly, when the temperature is reached that liquefies the material. The figure also illustrates that only crystalline plastic has a glass transition temperature (this is discussed in Section 4.2.2).

The mechanical properties of the most common unreinforced plastics for engineering applications are discussed in this chapter. The summary table of the mechanical properties of unreinforced plastic is shown in Table A.1 in Appendix A.

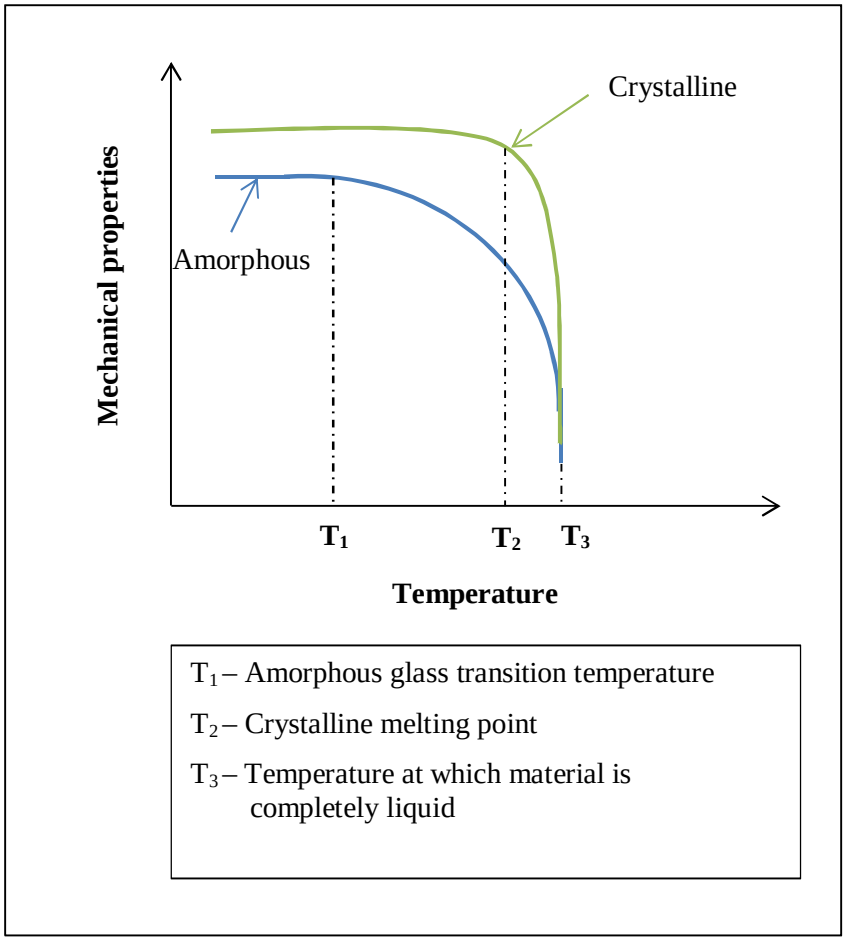

Figure 4.1: Change in mechanical properties due to the change in temperature for amorphous and crystalline plastic (Rosato & Rosato, 2004, pp. 196, Figure 3.7)

4.1.1. Specific gravity

Specific gravity, also known as relative density, is the ratio of the density of a material to the density of water. Low density can be an advantage of plastic materials, however when the weight of plastics is considered as an important factor, for example in the case of floods or extreme uplift wind loading, this low density can be a disadvantage (Kinney, 1967, pp. 1-2). Figure 4.2 illustrates the comparison of the average specific gravity of thermoplastics to thermosetting plastic materials as well as to common construction materials.

According to Rosato (1997, p. 63), polymers with a semi-crystalline structure exhibit a higher specific gravity compared to polymers with an amorphous structure. This is true for most polymers with a semi-crystalline structure, as shown in Figure 4.2. This figure is compiled from various sources (Braun, 1999; Crawford, 1981; Hiatt & Winding, 1961; Ogorkiewicz, 1977; Palin, 1967; Kinney, 1967; Rubin, 1990;

Southern Africa Steel Construction, 2010). This figure elucidates that thermosets as well as thermoplastics have higher specific gravity than typical construction wood, but still relatively low specific gravities. Since typical construction wood is commonly used as a housing construction material, these plastics are plausible housing construction materials in terms of specific gravity. Plastic materials such as polypropylene and all types of polyethylene have a specific gravity of less than one, therefore these plastics have a density less than water hence it will float on water.

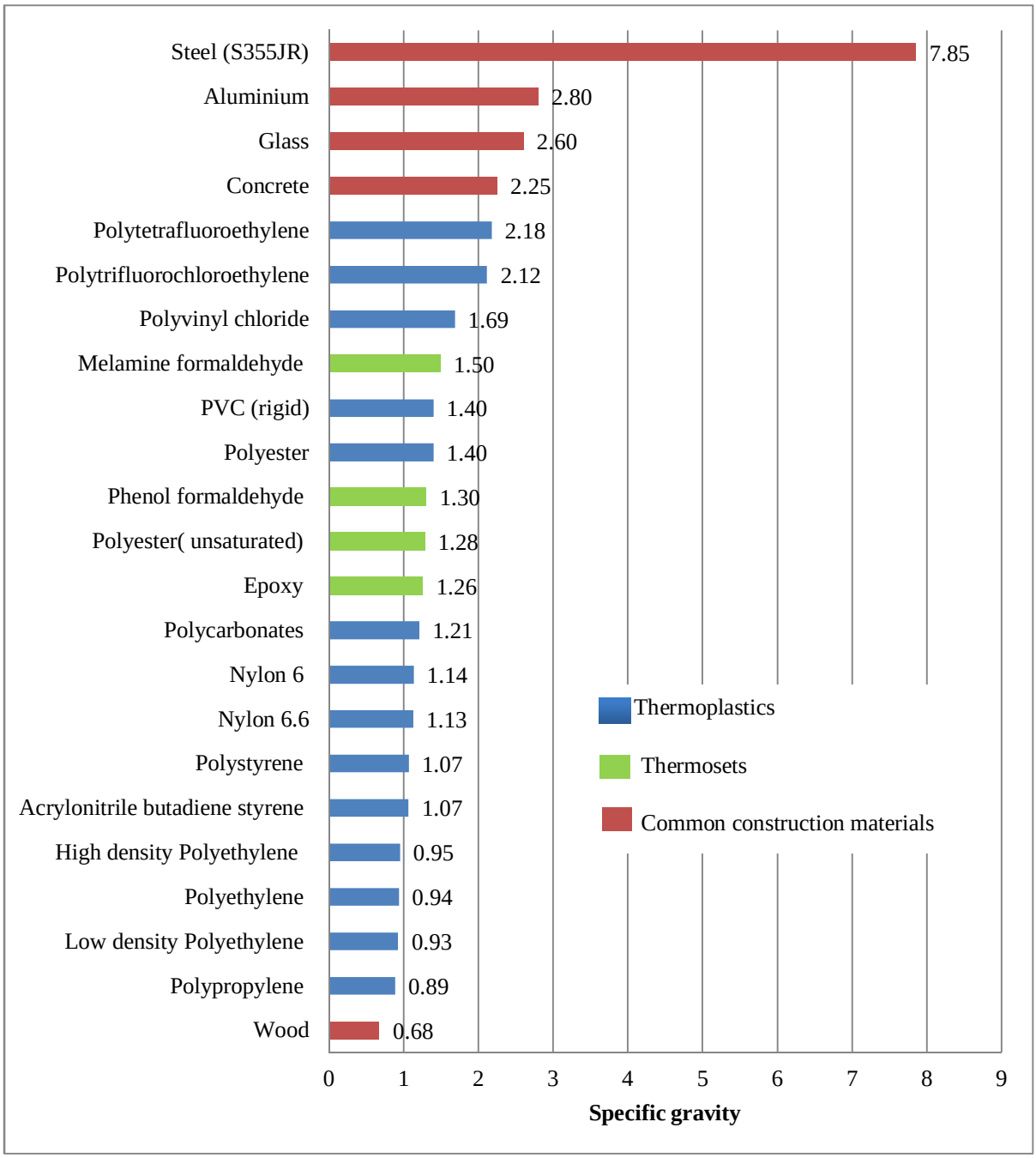

Figure 4.2: Average specific gravity of thermoplastics, thermosets and common construction materials

4.1.2. Deformational characteristics

Stress-strain curves

The relationship between stresses and strains, expressed as a stress-strain curve, is generally used to identify the deformational behaviour of an engineering material (Ogorkiewicz, 1970, p. 26). A general stress-strain curve obtained from a load-deformation test is shown in Figure 4.3. Some types of plastics, such as thermoplastics, follow the path of the curve (shown in Figure 4.3) rather closely (Kinney, 1967, p. 181). Whereas most thermosets might only follow a portion of this curve, due to intermolecular slippage which usually occurs at low strains (Kinney, 1967, p. 181). In general, plastic materials exhibit viscoelastic properties. Thus, the stress-strain curves for plastic materials are non-linear up to the yield point, but in some cases, rupture occurs without any indication of yielding (Benjamin, 1969, pp. 3-5). Different materials, including different plastics, will differ from the curve (shown in Figure 4.3) in two respects; firstly, how far the path of the curve will be followed before failure occurs and secondly, the numerical values obtained from this curve (Kinney, 1967, p. 181).

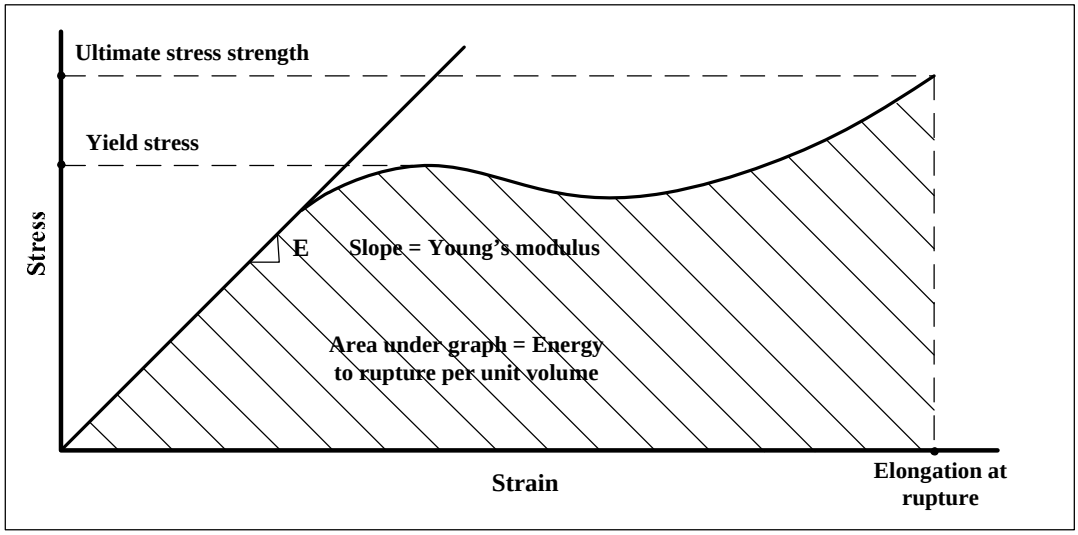

Figure 4.3: Typical stress-strain curve for a plastic during tensile test (Hiatt & Winding, 1961, pp. 66, Figure 3-1)

Five parameters are generally obtained from a stress-strain curve:

(1) The initial part of the curve shown in Figure 4.3 is approximately linear. At this linear portion of the curve, the slope (stress/strain) defines the Modulus of elasticity or Young's modulus (E-modulus) of the material which indicates the stiffness of a material (Hiatt & Winding, 1961, pp. 65-67).

(2) The yield stress is located where the first sign of non-elastic deformation (first knee) on the curve occurs (Palin, 1967, p. 26). This point indicates the resistance of the material to permanent loading and the strength of the material (Hiatt & Winding, 1961, pp. 65-67).

(3) The ultimate stress strength is located at the end of the curve and it indicates the extent of the possible plastic deformation before rupture occurs (Hiatt & Winding, 1961, pp. 65-67).

(4) Toughness of a material is measured as the strain energy at rupture which is determined by means of the area under the stress-strain curve (Kinney, 1967, p. 182).

(5) The ultimate strain refers to the elongation at rupture and is usually a percentage of the original length (Palin, 1967, p. 26).

Generalised stress-strain curves for various types of materials are shown in Figure 4.4 (Palin, 1967, p. 27) and the following characteristics are used to define the properties of plastic materials (Hiatt & Winding, 1961, p. 67; Palin, 1967, p. 27):

- Hard and soft refers to high and low values for E-modulus, respectively.
- Strong and weak refers to high and low values of the yield stresses, respectively.
- Brittle refers to a material that ruptures without yielding.
- Tough refers to a material that is ductile, thus a material which has a high strain energy at rupture per unit volume.

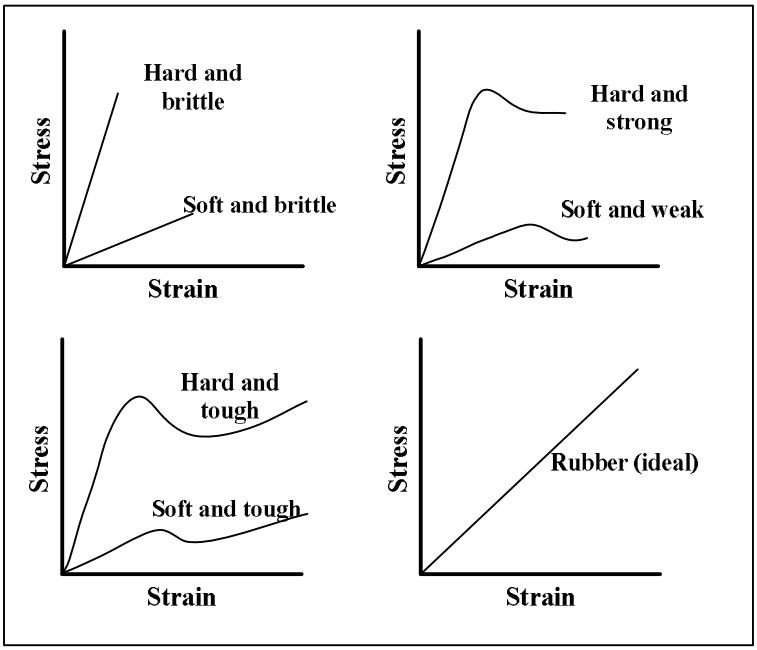

Figure 4.4: Generalised stress-strain curve for a variety of plastics (Rosato & Rosato, 2004, pp. 668, Figure 7.19)

As mentioned before, temperature changes have major effects on the mechanical properties (Hollaway, 1990). An increase in temperature results in a decrease in the modulus of elasticity, the yield stress and the ultimate strength of plastic material, whereas the elongation of the material increases (Hiatt & Winding, 1961, p. 68).

Tensile properties

The tensile properties of a plastic material are obtained from a tensile load-deformation test (Hiatt & Winding, 1961, pp. 65-66). A tensile load-deformation test results in a typical stress-strain curve as illustrated in Figure 4.3. The comparison of the average tensile strength of a variety of plastic materials to common construction materials is shown in Figure 4.5. This figure is compiled from various sources (Hollaway, 1990; Palin, 1967; Rubin, 1990; Craig, 2000; Domone & Illston, 2001; Ogorkiewicz, 1977; Kinney, 1967; Bon, 2003; Southern Africa Steel Construction, 2010).

Note in Figure 4.5 that the tensile strengths of glass and concrete are not included. This is due to glass having a much higher tensile strength compared to the other materials, but it is present in Appendix A, Table A. 1. The tensile strength of glass is 7000MPa (Bon, 2003). Typical conventional concrete, on the other hand, is only used as a compressive member. Most of the plastic materials exhibit a higher tensile strength than typical construction wood, but appear to be weaker in comparison to the other construction materials. A polymer with an amorphous structure has a lower strength when compared to a polymer with a semi-crystalline structure (Rosato, 1997, p. 60). Therefore, most thermoplastic materials with a semi-crystalline structure have higher strength than thermosets, as illustrated in Figure 4.5.

The comparison of the average tensile Young's modulus of a variety of plastic materials to common construction materials is shown in Figure 4.6. Figure 4.6 is compiled from various sources (Hollaway, 1990; Palin, 1967; Rubin, 1990; Craig, 2000; Ogorkiewicz, 1977; Kinney, 1967). Note in Figure 4.6, that not all the construction materials are shown. This is since some construction materials have much greater Young's modulus values compared to the plastic materials, but refer to Appendix A, Table A. 1 for a summary of tensile Young's modulus.

The Young's modulus refers to the stiffness of a material and therefore from Figure 4.6 it is clear that most thermoplastics have a low stiffness when compared to thermosets as well as common construction materials. This low stiffness of thermoplastics results in them being soft materials and can be problematic, especially when used as structural tensile members.

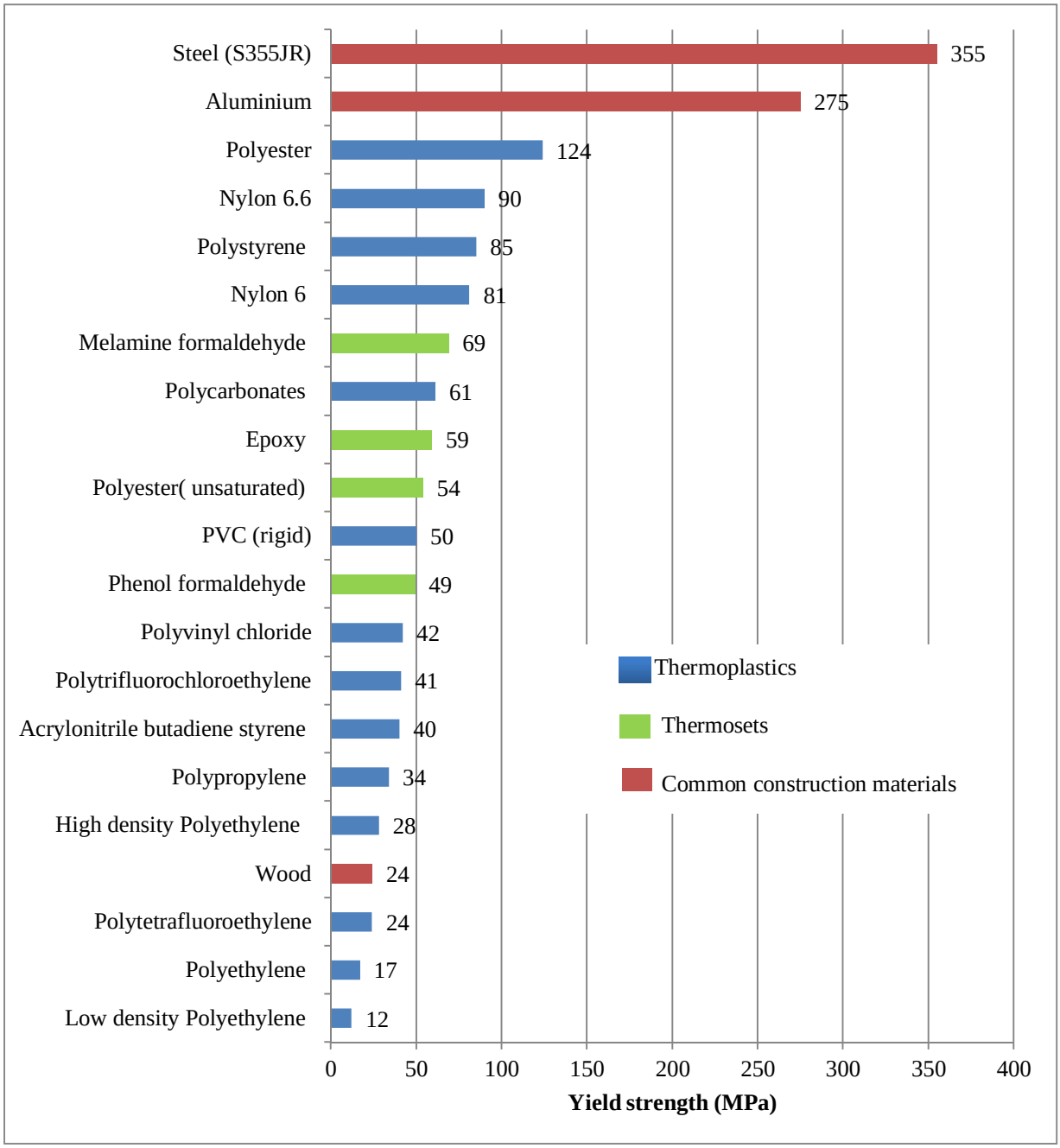

Figure 4.5: Average tensile yield strength of thermoplastics, thermosets and common construction materials

.

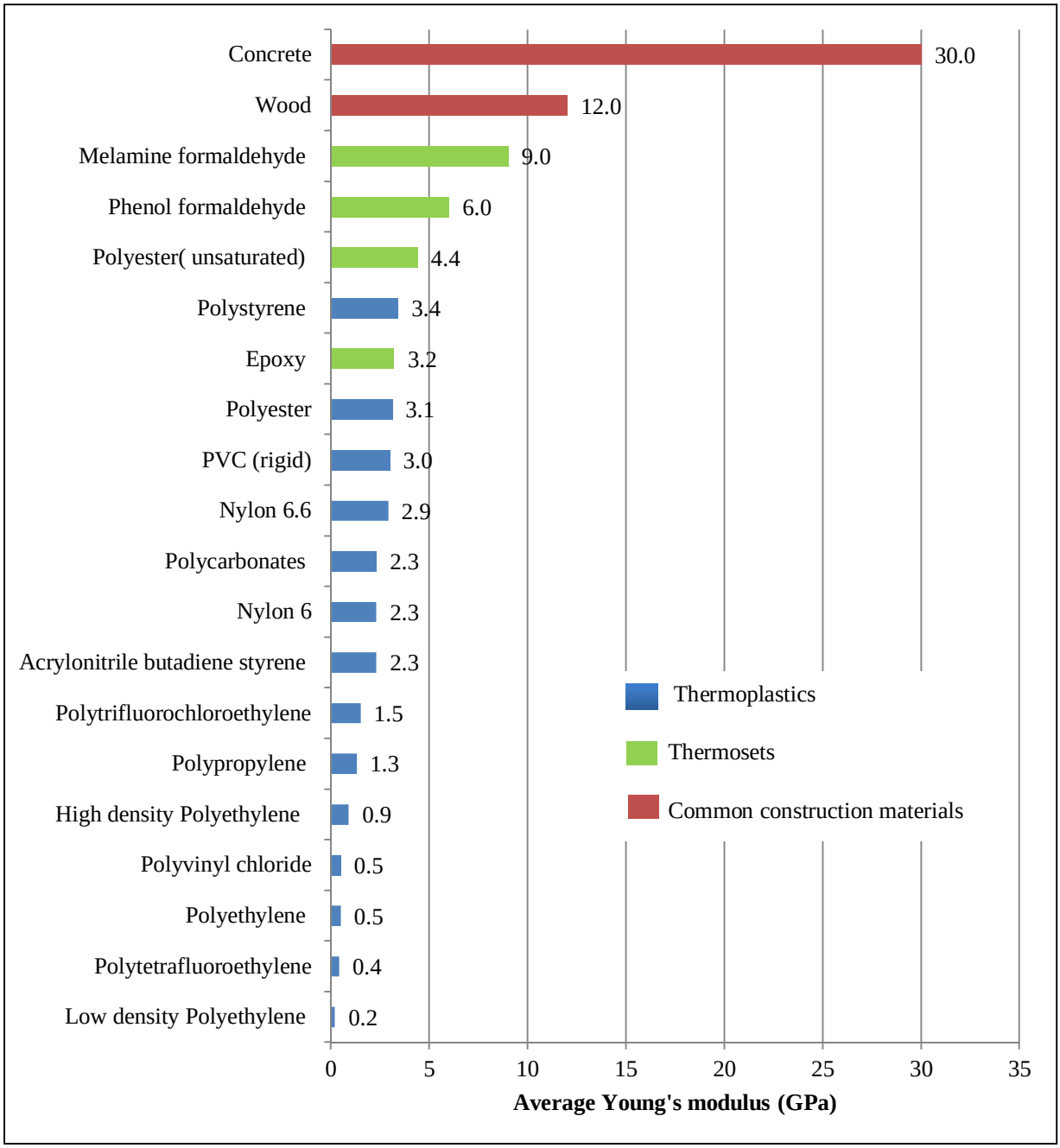

Figure 4.6: Average tensile Young's modulus of thermoplastics, thermosets and common construction materials

Compression properties

The stress-strain curve obtained from a compression load-deformation curve is similar to the one shown in Figure 4.4. The compression test is similarly prepared to the tension test, however only a few plastics exhibit the same deformational characteristics under compression and tension loads (Palin, 1967, p. 30). For example, polystyrene is strong and tough in compression but hard and brittle in tension (Hiatt & Winding, 1961, p. 68). Thus, the Young's modulus might differ in terms of tensile and compressive tests.

Many plastics do not rupture under compression and it can be reduced to a flat disk (Palin, 1967, p. 30). The comparison of the average compressive yield strength of a variety of plastic materials to common construction materials is shown in Figure 4.7. This figure is compiled from various sources (Palin, 1967; Bon, 2003; Domone & Illston, 2001; Kinney, 1967).

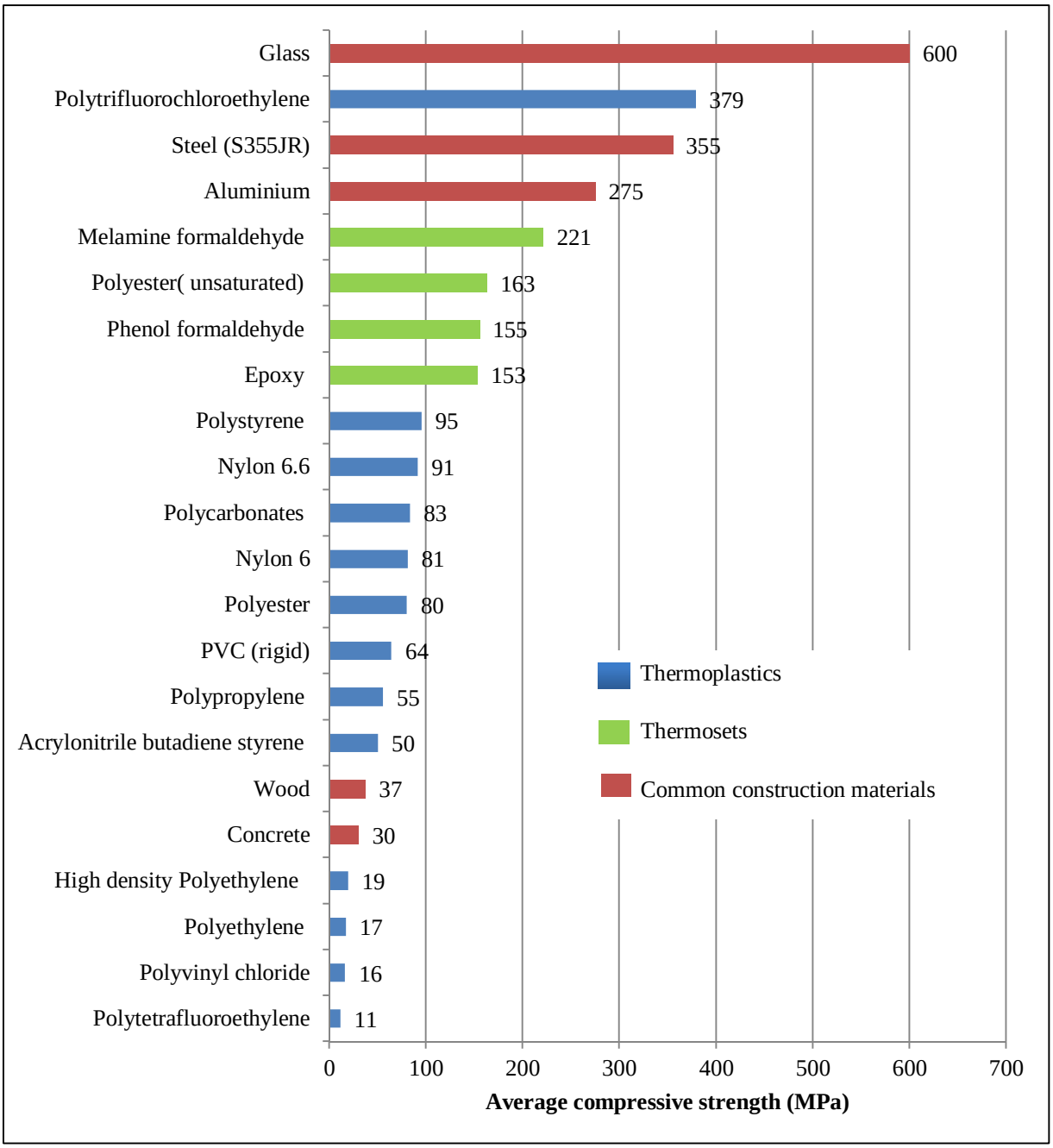

Figure 4.7: Average compressive strength of thermoplastics, thermosets and common construction materials

Figure 4.7 illustrates that the thermosets as well as most thermoplastics exhibit an average compressive strength higher than typical conventional concrete, 30MPa, and typical construction wood, which indicate that these plastic materials are plausible for load bearing applications.

Flexural properties

The flexural properties of plastic materials are influenced by the specimen's dimensions (especially the thickness, since compression and tension moduli of plastics differ (Rudd & Sampson, 1975, pp. 3-8)), rate of loading, temperature and humidity (Palin, 1967, p. 31). These properties are obtained by means of a three-point bending test or a four-point bending test (Rudd & Sampson, 1975, pp. 3-8). The flexural properties measure the distortion of the plastic material (Palin, 1967, p. 31). The flexural strength is also known as the modulus of rupture (Rudd & Sampson, 1975, pp. 3-8) and refers to the bending strength of a material measured as the ultimate tensile stress of the outmost fibres, when subjected to a bending test, at the point of rupture (Harper, 1975). The flexural modulus of a material refers to the slope of a stress-strain curve obtained from a bending test (Harper, 1975). The flexural properties for a variety of plastics and common construction materials are shown in Figure 4.8. Figure 4.8 is compiled from various sources (Rubin, 1990; Palin, 1967; Rudd & Sampson, 1975; Tesser & Scotta, 2012; Bon, 2003; Domone & Illston, 2001).

In Figure 4.8, some materials do not have values for the flexural strength. This is due to the fact that some of the plastics do not rupture and thus do not reveal flexural properties (Palin, 1967). Figure 4.8 shows that thermosetting materials have a relatively larger bending strength when, compared to most thermoplastics. The plastic materials, as expected, can be compared in terms of flexural strength to the metals and exhibit a relatively larger flexural strength than compared to concrete and glass.

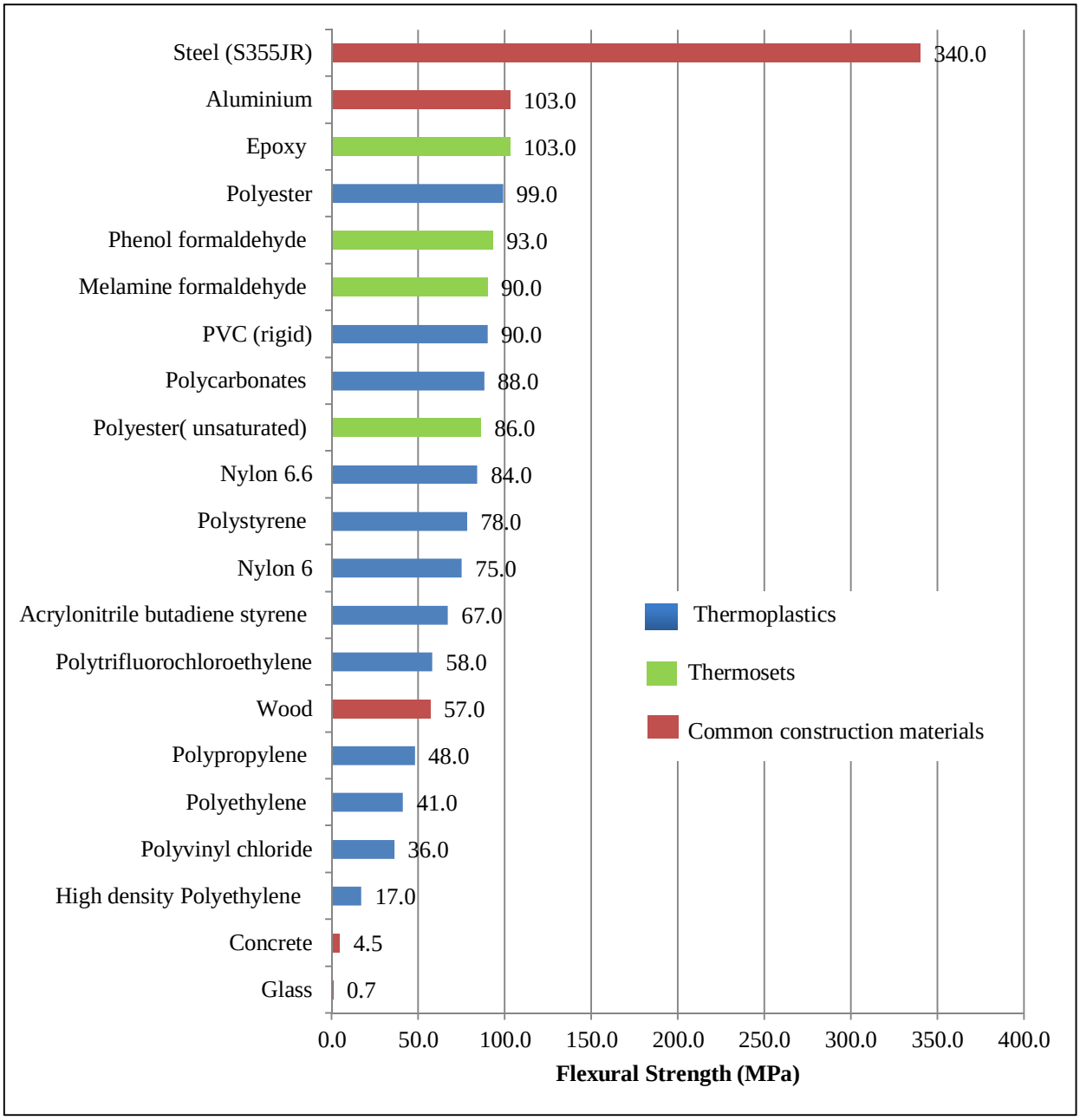

Figure 4.8: Average flexural strength of thermoplastics, thermosets and common construction materials

Elongation at rupture

Elongation of a material refers to the increase in the length of a specimen under a tensile load and it is usually measured as a percentage of the original length of the specimen (Harper, 1975). Elongation at rupture is illustrated in Figure 4.3 and the percentage of elongation of a variety of plastics and common construction materials is shown in Figure 4.9. This figure is compiled from various sources (Craig, 2000; Kinney, 1967; Rubin, 1990).

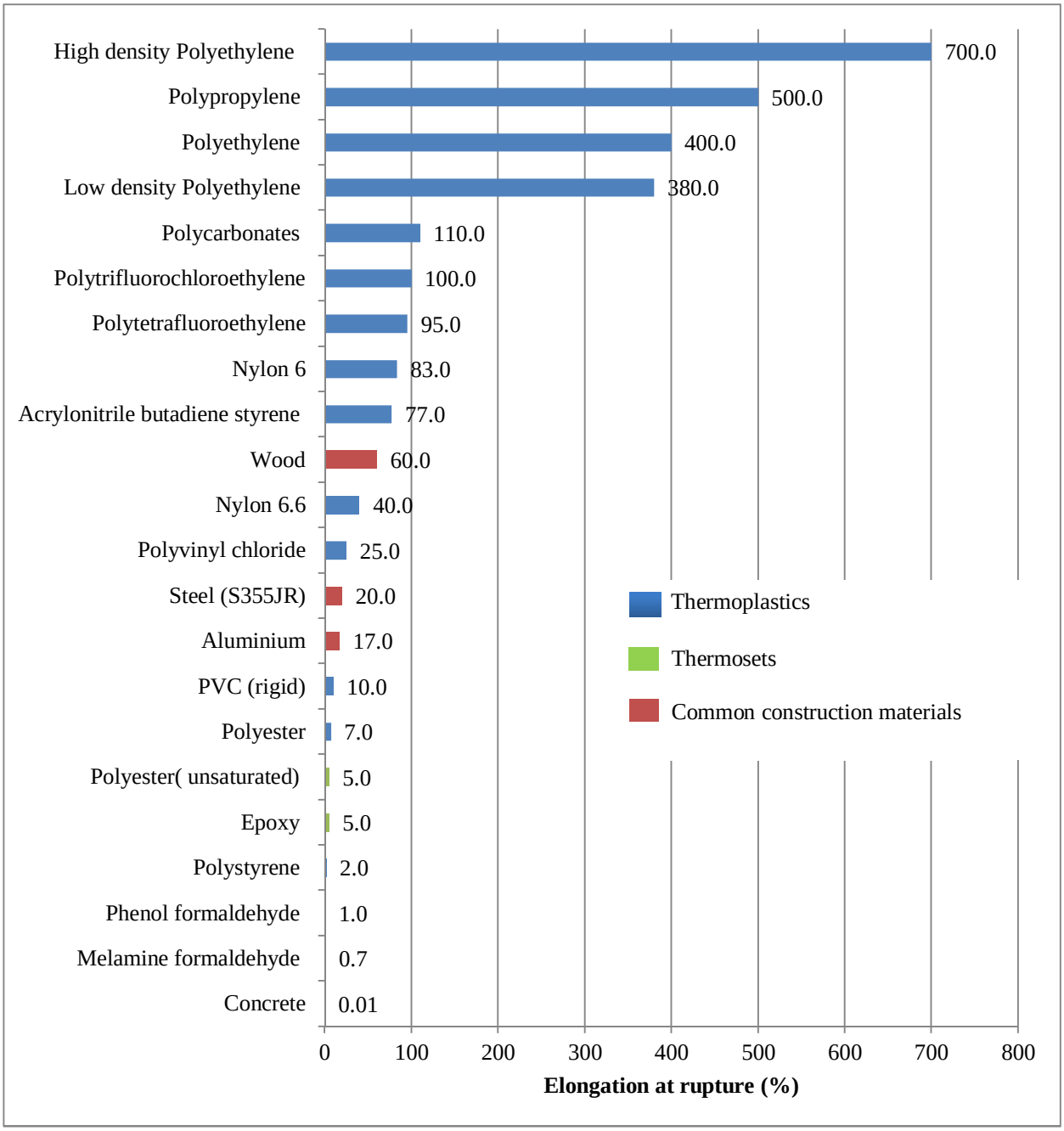

Figure 4.9: Average elongation at rupture of thermoplastics, thermosets and common construction materials

Typical conventional concrete is a brittle material and elongates the least of the materials shown in Figure 4.9. Thermosets elongate less than most of the common construction materials. However, thermoplastics elongate considerably more under a tensile load than thermosets and elongate more than most common construction materials. Due to the large elongation at rupture of most thermoplastic materials, most of them are considered ductile.

4.1.3. Poisson's ratio

The Poisson's ratio is related to the elongation of a material when a uniform axial stress, which is under the proportional limit, is applied to a material (Harper, 1975) and is defined as the "absolute value of the ratio of the transverse strain to the longitudinal strain of the material" (Rudd & Sampson, 1975, pp. 3-8). Poisson's ratio is influenced by the magnitude of strain as well as the nature of the material (Kinney, 1967, p. 184). For plastics that display a more brittle behaviour the Poisson's ratio is assumed to be approximately 0.3, whereas for more ductile plastics the Poisson's ratio is assumed to be in the range of 0.4 to 0.45 (Kinney, 1967, p. 184).

4.1.4. Impact resistance

Impact resistance of a material indicates the toughness of a material (Richardson, 1977) and it is influenced by a wide range of factors such as the geometry of the specimen and striker, temperature, rate of loading, type of material, fabrication conditions and the environmental conditions (Riddell & O'Toole, 1969, pp. 37-40). The impact resistance of a material refers to the energy absorbed of a single high speed blow without rupturing (Hulse, 1965, pp. 163-185). There is a variety of methods to determine the impact resistance of a material and the most common methods include the Izod impact test and the Charpy impact test (Hulse, 1965).

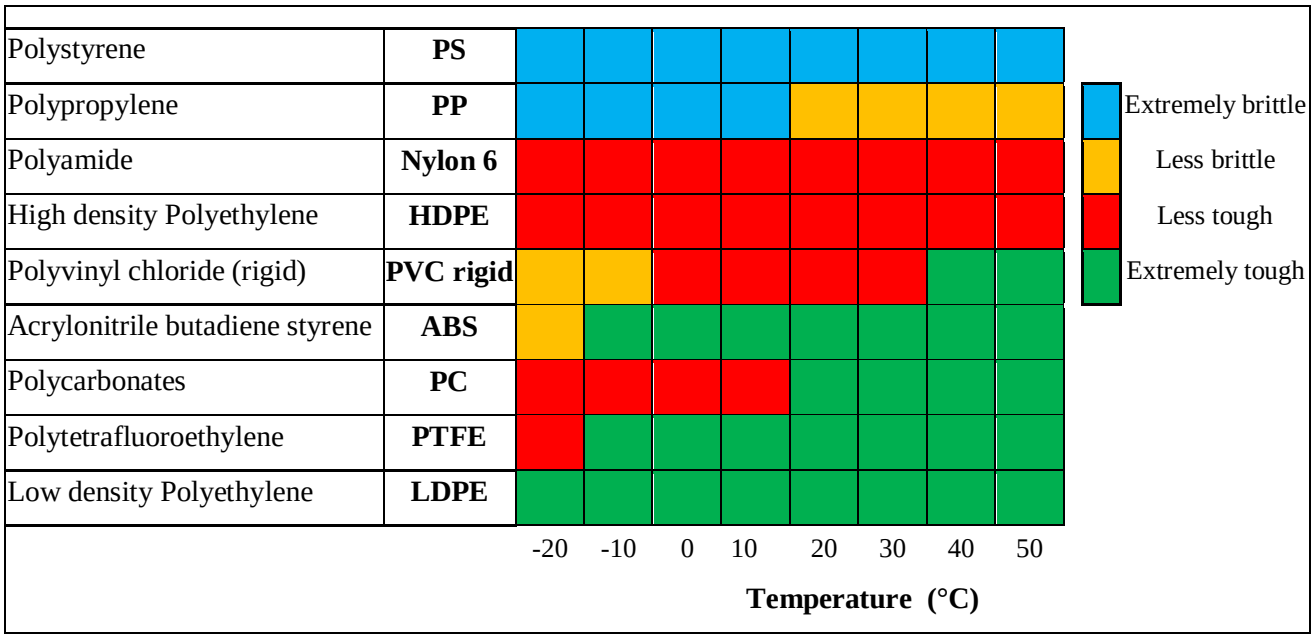

Figure 4.10: Influence of temperature on the impact strength of some thermoplastics

At low temperatures, some ductile plastic materials can behave in a brittle fashion (Ogorkiewicz, 1970, pp. 43-44), whereas an increase in the temperature generally results in a substantial increase in the impact resistance strength (Hiatt & Winding, 1961, p. 70). This influence of temperature on the impact resistance strength is shown in Figure 4.10. Figure 4.10 is compiled from various sources (Birley, et al., 1988; Birley & Scott, 1982).

4.1.5. Creep and shrinkage

Creep and slow flow

Creep can be defined as the increase in strain which is dependent on the time of loading of a material under a constant stress or a constant strain resulting in the relaxation of stress (Addis, 1998, pp. 41-44). Slow deformation such as creep is one of the limiting factors when plastic materials are considered for a load bearing application (Findley & Davis, 2013, p. 3; Palin, 1967, p. 33). Creep behaviour of plastic materials is measured by means of standard methods, where a constant load is applied to a test specimen and the strain is determined as a function of time (Palin, 1967, p. 33). Creep data for plastic materials is usually plotted on logarithmic scales since exceptionally slow deformation of these materials is associated with an exceptionally long time period. (Riddell & O'Toole, 1969, pp. 37-40; Findley & Davis, 2013).

A typical strain-time curve for most plastic materials is shown in Figure 4.11 (Kinney, 1967, p. 192; Findley & Davis, 2013, pp. 2-3). An immediate elastic deformation of the material takes place when the load is initially applied to the specimen (Kinney, 1967, p. 192; Findley & Davis, 2013, p. 2). Primary creep denotes to the increase in slow deformation which occurs at a decreasing rate (Kinney, 1967, p. 192; Findley & Davis, 2013, p. 3). At point X (Figure 4.11), the strain-time curve can either follow an unloading state, which results in permanent set, or it can follow secondary creep. Recovery of the material occurs after removal of the stress and permanent set refers to the state where the material does not return to its original state (Palin, 1967, p. 34; Findley & Davis, 2013, p. 4). Secondary creep denotes to when a continuous stress is applied to the material and the creep rate might tend towards to zero or it might remain at a constant value (Palin, 1967, p. 34; Findley & Davis, 2013, p. 3). Tertiary creep refers to the increasing rate of deformation of the material (Kinney, 1967, p. 192; Findley & Davis, 2013, p. 3).

The creep behaviour of plastic materials is influenced by the type of plastic, temperature, relative humidity and the applied stress (Kinney, 1967, p. 192; Findley & Davis, 2013, pp. 2-4). In general, thermosetting plastic materials exhibit less creep behaviour than thermoplastics, since the greater the freedom of the movement of the molecules, the more significant the creep (Palin, 1967, p. 34). Viscous movement of plastic molecules results in creep behaviour. The effect of applying a small stress to a plastic material for a long time period, is relatable to the effect of applying a greater stress to a plastic material for a short time

period (Palin, 1967, p. 34; Findley & Davis, 2013, p. 15). This is due to the viscoelasticity of plastic materials.

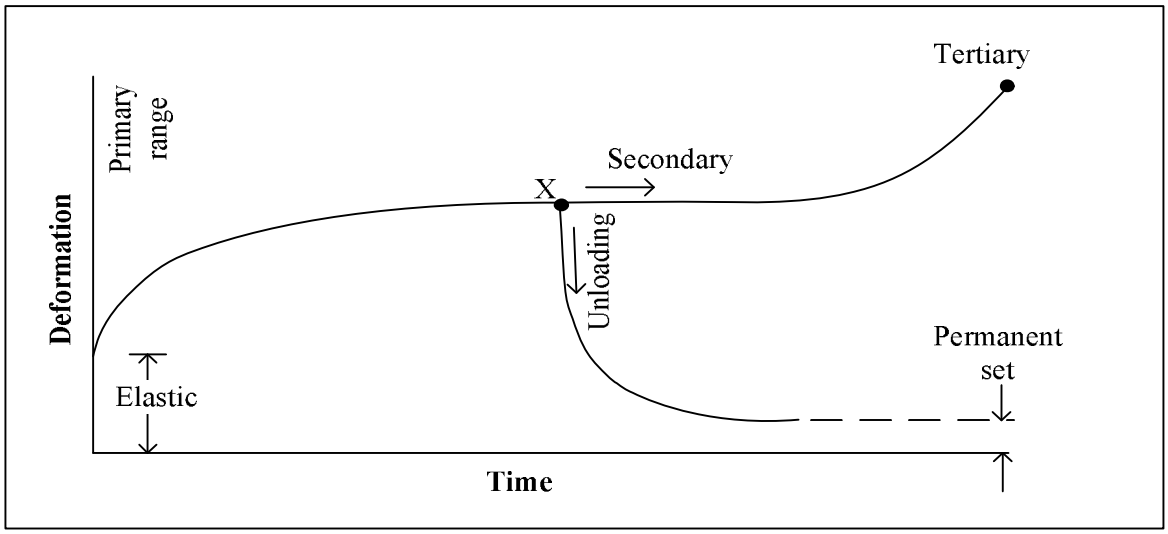

Figure 4.11: Schematic creep diagram (Kinney, 1967, p192, Figure 14-11)

Shrinkage and warping

Creep and shrinkage are similar in terms of molecular movement which cause volume changes (Addis, 1998, p. 47). However, shrinkage due to molecule movement is driven by environmental conditions, whereas creep is driven by stress (Addis, 1998, p. 47). Shrinkage of plastic material is dependent on the environmental conditions as well as the forming or moulding of the plastic material (Kinney, 1967, pp. 193-194). Warping is the internal stresses induced by the moulding processes. It is dependent on temperature changes during curing in the moulding process. Stresses due to shrinkage and warping might exceed the ultimate strength of a plastic material and this might result in cracks and tears in the plastic matrix, which reduce the strength of the plastic material (Kinney, 1967, pp. 193-194).

The occurrence of mould shrinkage is indefinite for some types of plastic materials as shown in Table 4.1. The mould shrinkage of a plastic material is generally measured 12 to 24 hours after fabrication (Rosato, 1997). Total shrinkage is the sum of age shrinkage and mould shrinkage, where age shrinkage is insignificant in comparison to moulding shrinkage (Rubin, 1990). Note in Table 4.1 that the shrinkage is measured for two hours after moulding and this measurement is dependent on the direction of flow of the test specimen (Rubin, 1990).

Table 4.1: Mould shrinkage of various plastic materials (Rubin, 1990)

Materials	Abbreviation	Mould shrinkage			
		In direction of flow		Perpendicular to direction of flow	
		Min (mm)	Max (mm)	Min (mm)	Max (mm)
Thermoplastics					
Acrylonitrile butadiene styrene	ABS [(1)]	0.006	0.009		
High density Polyethylene	HDPE	0.02	0.045		
Low density Polyethylene	LDPE	0.015	0.45		
Polyamide	Nylon 6.6	Insignificant shrinkage			
Polyamide	Nylon 6	Insignificant shrinkage			
Polycarbonates	PC	0.005	0.007	0.005	0.007
Polyester	PET	0.003	0.006	0.003	0.006
Polypropylene	PP [(2)]				
Polystyrene	PS	0.003	0.01	0.003	0.01
Polytetrafluoroethylene	PTFE [(3)]	Insignificant shrinkage			
Polytrifluorochloroethylene	PTFCE	Insignificant shrinkage			
Polyvinyl chloride	PVC	Insignificant shrinkage			
PVC (rigid)	PVC (rigid)	Insignificant shrinkage			
Thermosets					
Epoxy	EP	Insignificant shrinkage			
Melamine formaldehyde	MF	Insignificant shrinkage			
Phenol formaldehyde	PH	Insignificant shrinkage			
Polyester (unsaturated)	UP	Insignificant shrinkage			

NOTE:

(1) –Dependent on the size of the specimen

(2) – Shrinkage effected by too high moulding temperature and too short curing time

(3) *– Increase in total volume up to 10%*

Table 4.1 illustrates that that thermoplastic materials have insignificant or relatively small mould shrinkage, while thermosetting materials have insignificant shrinkage. However, the mould shrinkage of the plastic materials, in Table 4.1, can increase when measured at 12 to 24 hours after fabrication. Pre-fabrication of plastic materials can allow for mould shrinkage, therefore, mould shrinkage has an insignificant effect when plastic materials are pre-fabricated.

4.1.6. Fatigue characteristics

Fatigue refers to the failure of a material under repeated stress cycles, which can occur even if the maximum stress for a cycle is below the yield stress of the material (Palin, 1967, pp. 35-36). The repeated stress cycles result in a gradual weakening of the mechanical properties of a material (Palin, 1967, pp. 35-36; Chanda & Roy, 2012, pp. 3-50) which is caused by the formation of miniature cracks (Kinney, 1967, p. 195; Chanda & Roy, 2012, pp. 3-50). These cracks are unable to bear load and the load is transferred to the surrounding material which leads to spreading of the cracks or an increase in the crack size (Kinney, 1967, p. 195). The degree of fatigue is dependent on the degree of cyclic loading, temperature, amplitude, frequency and frequency mode, which are applied to the material (Palin, 1967, pp. 35-36; Chanda & Roy, 2012, pp. 3-51).

The fatigue data can be represented on an S-N curve, where the S refers to the fatigue strength (apparent strength under cyclic loading (Kinney, 1967, p. 195)) and N refers to the number of cycles essential to produce failure (Hiatt & Winding, 1961, p. 73). As the number of cycles increase, the stress value tends to decrease (Palin, 1967, pp. 35-36). Most plastic materials have a fatigue limit (Palin, 1967, p. 36), which is the stress value below which failure does not occur independently of the number of cycling (Kinney, 1967, p. 195; Chanda & Roy, 2012, pp. 3-50).

4.1.7. Durability

Durability of a plastic material refers to the resistance to change in properties of the material with time and is dependent on physical attacks and chemical attacks (Hiatt & Winding, 1961, p. 74). Degradation of a polymer is caused by both physical and chemical means (Onyon, 1965, pp. 1-23). Under service condition, the main causes of chemical attacks are water, oxygen and ozone, whereas the main causes of physical attacks are environmental conditions such as ultraviolet, heat, mechanical stress and radiation (Chanda & Roy, 2012, pp. 1-70). Due to degradation of polymers, the following types of structural changes of a polymer may come about (Onyon, 1965, pp. 1-23; Chanda & Roy, 2012, pp. 1-74):

- Scission of the main chains which results in a decrease in the molecular weight of the polymer. This may result in decrease in the modulus of elasticity, the mechanical strength of plastic material and the resistance to solvents.
- Chemical change of substituent groups connected to (or in) the main chain, which may increase the mechanical strength of a material.
- The units of the main chain react with one another resulting in cyclisation or generally cross-linking. Cross-linking increase the mechanical strength of a material.
- Any combination of the above.

Environmental conditions lead to weathering of a material (Benjamin, 1969, p. 6). The main factors which cause weathering of a plastic material are the control of fabrication, sunlight especially the ultra-violent component, moisture (water absorption) and heat. The control of fabrication can affect weathering, since nearly all additives affect the weathering of the plastic material (Benjamin, 1969, p. 6; Chanda & Roy, 2012, pp. 1-73).

Water absorption refers to the percentage of the ratio of the weight of water that is absorbed by a material to the dry weight of a material (Harper, 1975). Most plastic materials are not soluble in water, but might absorb water to some degree (Palin, 1967, p. 55). Water absorption may result in a reduction of mechanical strength and dimensional changes. Water that is present before fabrication of plastic material, for example raw materials, can result in problems in the fabrication process and defects in the final product (Palin, 1967, p. 55). The average percentage of water absorption of various plastic materials is shown in Figure 4.12. This figure is compiled from various sources (Harper, 1975; Kinney, 1967; Palin, 1967).

Figure 4.12 illustrates that most thermosetting plastic materials absorb larger amounts of water in comparison to thermoplastic materials, although the percentage of absorption for generally all types of plastics is small. Thus, if correctly manufactured, most plastic materials have a high durability and sufficient resistance to weathering (Hiatt & Winding, 1961, p. 74). Thus, the minimum life expectancy of plastic materials, if correctly manufactured, can increase (Benjamin, 1969, p. 6).

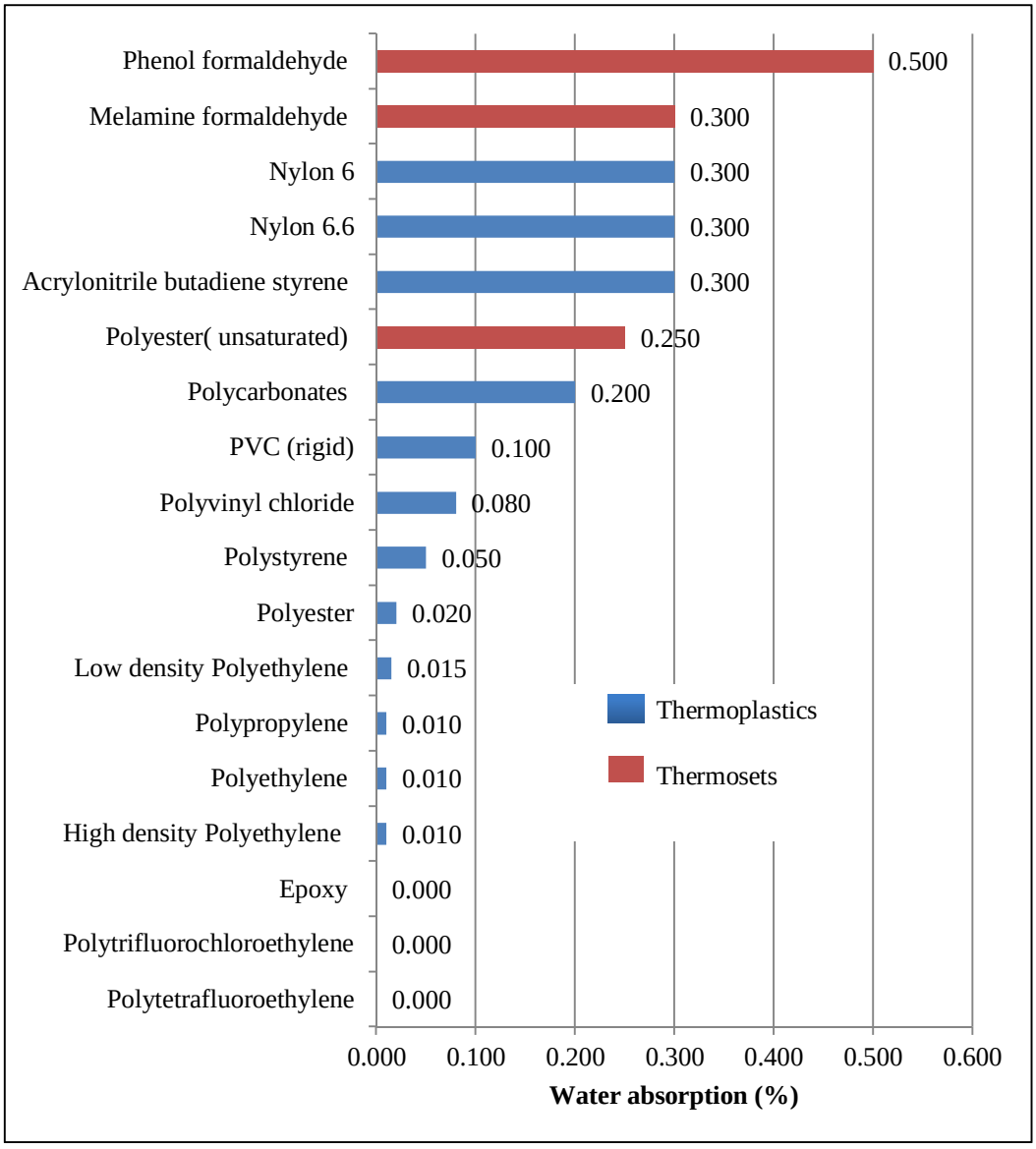

Figure 4.12: Comparison of the average percentage water absorption of thermoplastics and thermosets

4.2. Thermal properties

Thermal properties of plastic materials are important since they influence the mechanical properties of the plastic material. The thermal properties of unreinforced plastic material are mainly dependant on their molecular structure as well as the type of plastic, as shown in Figure 4.13. In Figure 4.13, Point ‘a’ refers to the start of the process, whereas Point ‘b’ represents the temperature and time at which the plastic material melts. The permanent hardening, Point ‘c’, of thermosetting plastics requires higher temperatures. After thermosetting plastics are permanently hardened, they cannot be melted to a liquid state again and are independent on the temperature. For example, thermosets can be compared to the yolk of an egg. When heated, the yolk changes from a liquid to a solid and cannot change back to a liquid (Rosato, 1997, p. 57).

For thermoplastic materials, Point 'c', indicates that the temperature has to decrease in order for the material to harden, but thermoplastics can be re-softened to melt after hardening. For Figure 4.13, thermoplastic require heat to melt, however, curing occurs at extremely low temperatures. The thermal properties of unreinforced plastic materials are summarised in Table A.2 in Appendix A. The most important thermal properties regarding plastic materials are discussed in the following sections.

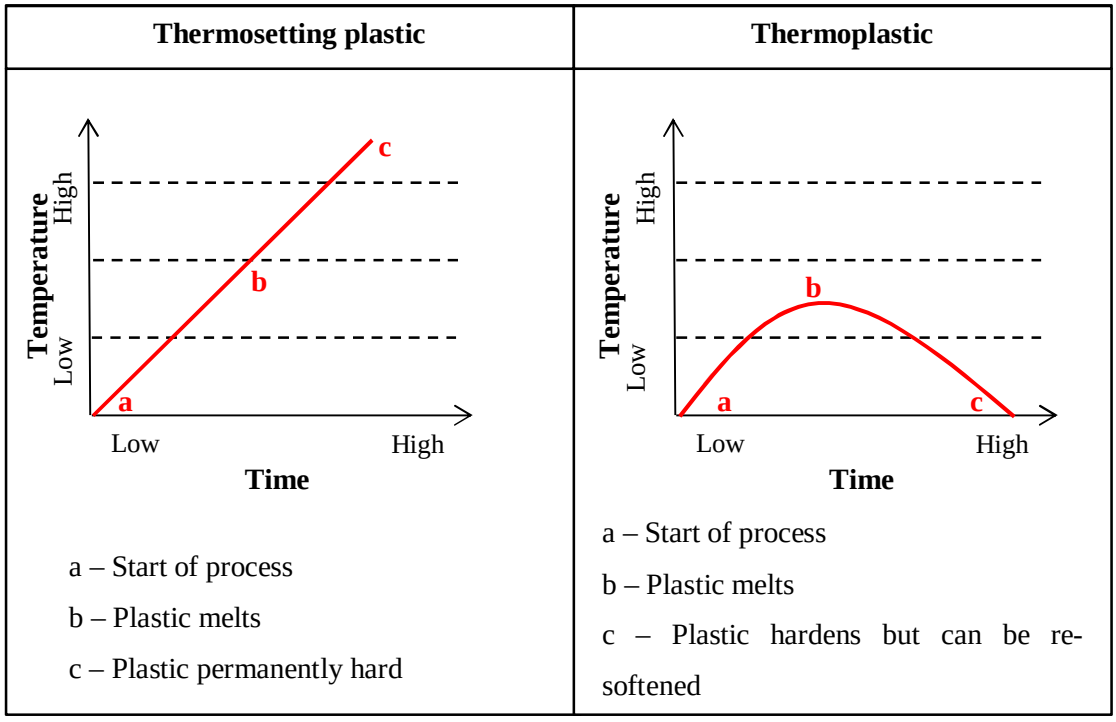

Figure 4.13: Melt characteristics (Processing heat-time profile cycle) of thermoplastic and thermosetting plastics. Processing heat-time profile (Rosato, 1997, p. 29)

4.2.1. Specific heat

The specific heat, also known as heat capacity, of a material indicates the amount of energy needed to increase the temperature of the material's unit mass by 1°C (Engelhardt, 2012). The specific heat of a variety of plastic materials as well as common construction materials is compared in Figure 4.14. Figure 4.14 is compiled from various sources (Engelhardt, 2012; Kinney, 1967; Palin, 1967; Southern Africa Steel Construction, 2010).

Figure 4.14 illustrates that plastic materials require a larger amount of energy to increase the temperature of the material, when compared to common construction materials, except for typical construction wood. For plastic material with an amorphous structure, the specific heat of this material increases with temperature (Rosato, 1997, p. 91). This increase in temperature is in a nearly linear manner, when the temperature is

above or below the glass transition temperature; however a stair like change happens near the glass transition temperature (Rosato, 1997, p. 91).

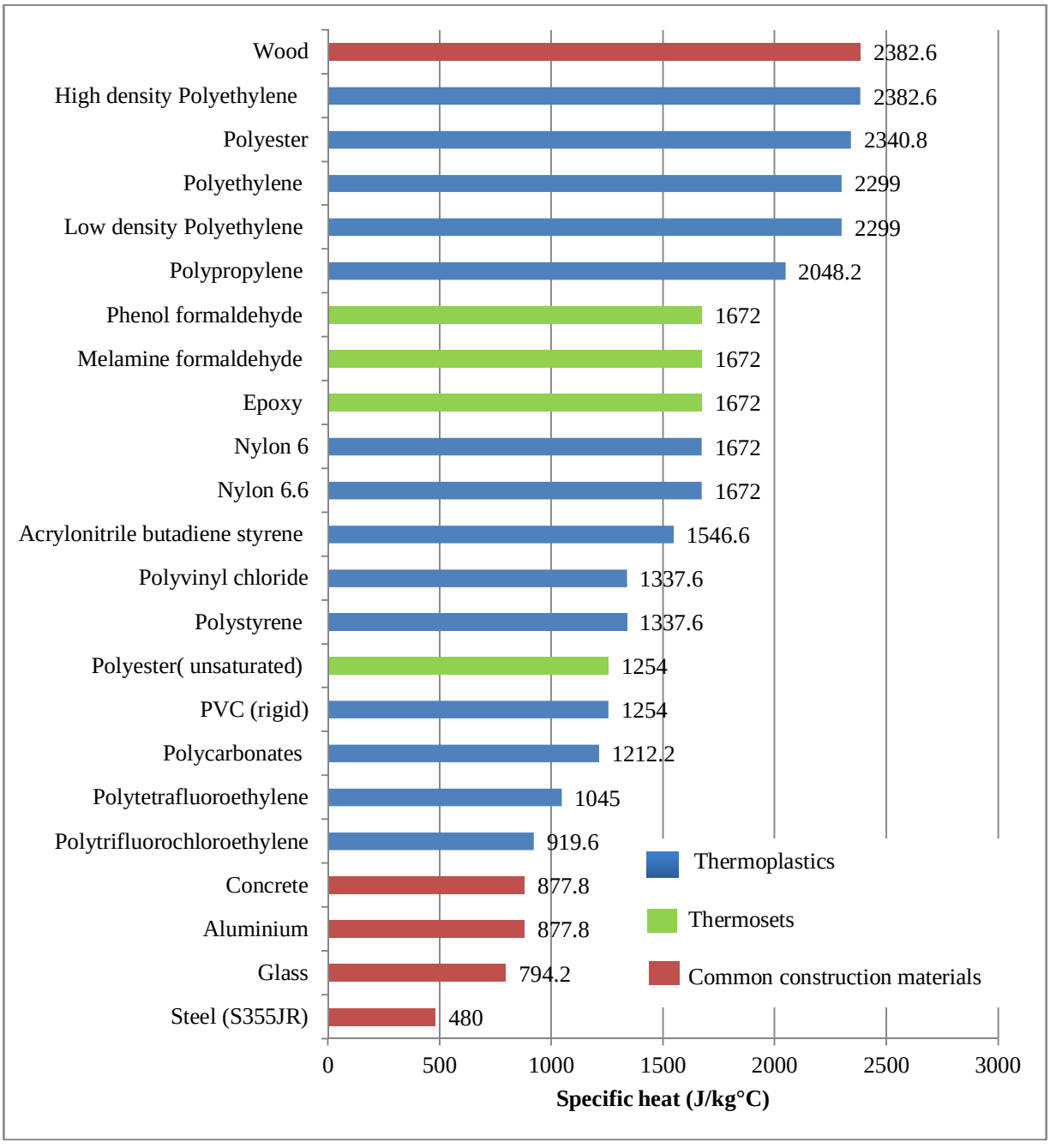

Figure 4.14: Specific heat of thermoplastics, thermosets and common construction materials

4.2.2. Transition temperature

A transition temperature refers to the temperature which causes changes in the properties of the plastic material (Lubin, 1982). There are a number of transition regions, that can be identified when a plastic

material is heated, from absolute zero to the polymers decomposition temperature (Gordon, 1965, pp. 209-247). The two most important transition temperatures, where polymers are concerned, is the glass transition temperature (T_g) and the melt temperature (T_m) (Cantor & Watts , 2011, p. 3). The glass transition temperature is the critical temperature required for the brittle, amorphous regions of plastic materials to have the ability to flow. At the glass transition temperature (T_g), the length or volume of the plastic material can increase as shown in Figure 4.15. Whereas the melt temperature is the temperature required for the crystalline region of plastic materials to have the ability to flow (Cantor & Watts , 2011, p. 3).

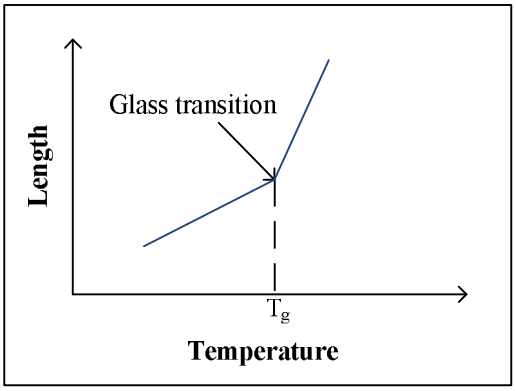

Figure 4.15: Effects of the glass transition temperature (T_g) on the length or volume of a plastic material (Rosato, 1997, pp. 88, Figure 1.32)

Amorphous plastic materials only have a glass transition temperature, whereas semi-crystalline plastic materials have both a glass transition temperature and a melt temperature (Cantor & Watts , 2011, p. 3). The melt temperature is higher than the glass transition temperature. Therefore, semi-crystalline plastic materials may exhibit movement (flow) in the amorphous region, without movement amongst the crystals (Cantor & Watts , 2011, p. 3). The change of volume of amorphous and crystalline plastics at the glass transition temperature (T_g) and the melt temperature (T_m) is shown in Figure 4.16. The melt temperatures and glass transition temperatures of some polymers are shown in Figure 4.17. This figure is compiled from various sources (Rosato & Rosato, 2004; Braun, 1999; Rosato, 1997). Note from this figure, plastic materials with an amorphous polymeric structure do not have melt temperatures. The freezing action is defined as the separation of crystalline plastic material, where the crystalline structure starts to loosen (Rosato & Rosato, 2004, p. 208).

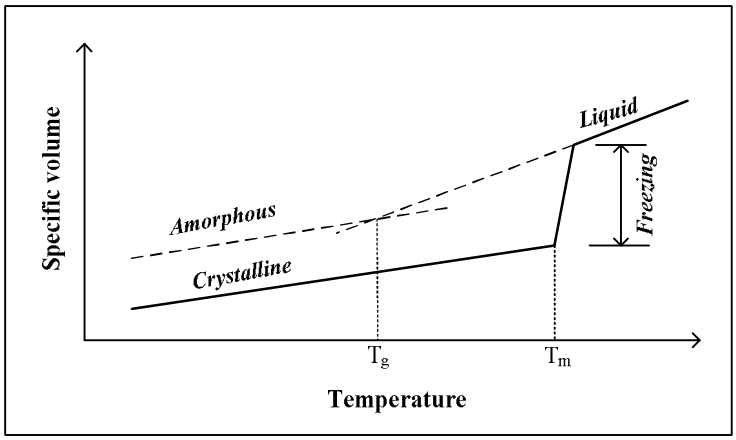

Figure 4.16: Volume change of an amorphous and a crystalline plastic at the glass transition temperature (T_g) and the melt temperature (T_m) (Rosato & Rosato, 2004, pp. 208, Figure 3.14)

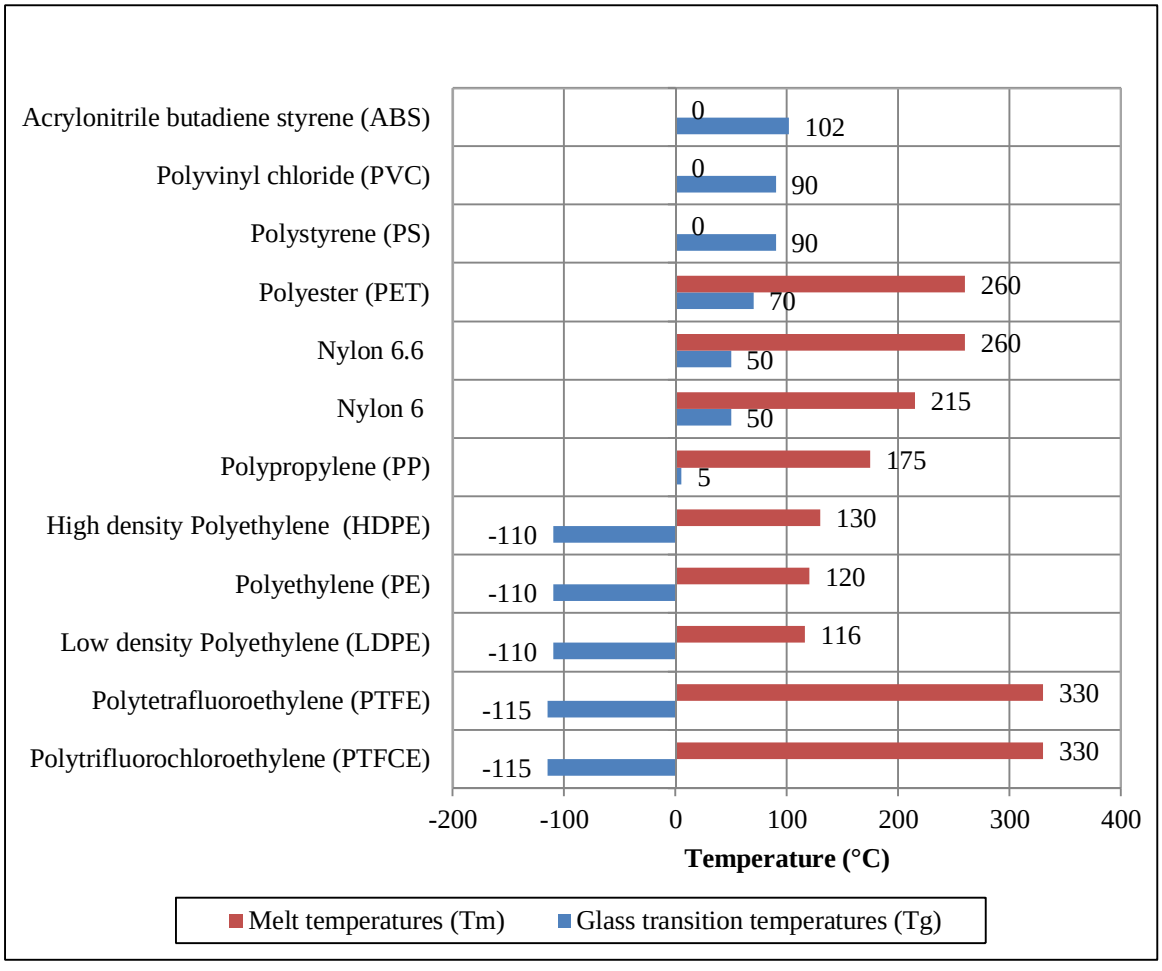

Figure 4.17: Melt temperature and glass transition temperature of various plastic materials

4.2.3. Thermal conductivity

Thermal conductivity is defined as "the ability of a material to conduct heat" (Harper, 1975). Plastic materials exhibit a low thermal conductivity (Palin, 1967, p. 50). Therefore, they are usually used as heat insulators. The thermal conductivity of plastic material is mainly dependant on the structure of the plastic material and the temperature (Rosato, 1982, p. 91). The thermal conductivities of various materials are compared in Figure 4.18. Figure 4.18 is compiled from various sources (Engelhardt, 2012; Harper, 1975; Palin, 1967; Rosato & Rosato, 2004; Kinney, 1967).

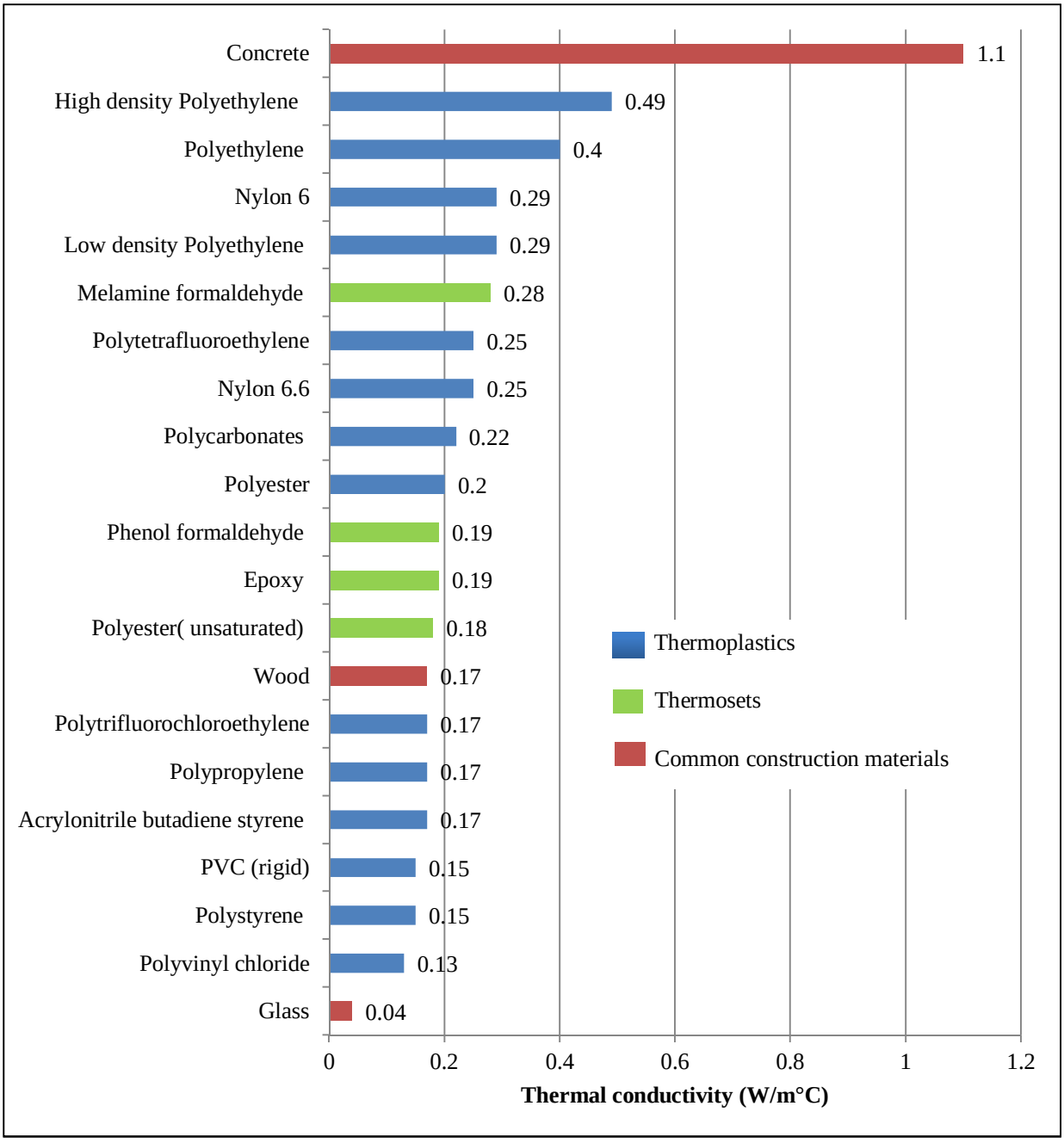

Figure 4.18: Thermal conductivity of thermoplastics, thermosets and common construction materials

Note in Figure 4.18 that steel and aluminium are not shown because they have much larger thermal conductivities when compared to the other materials (the values for the thermal conductivity of all the materials are provided in Appendix A in
Table A. 2). Figure 4.18 illustrates that all the plastic materials have low thermal conductivities, which is expected since plastic materials are used as thermal insulators. Material with a low thermal conductivity exhibits a large temperature gradient (Palin, 1967, p. 51). The temperature gradient of a material is defined as the change of temperature over the thickness of the material. Therefore, isolative materials exhibit a larger surface temperature at the one side (where the heat source is applied) of the material when compared to the other side.

4.2.4. Coefficient of thermal expansion

Coefficient of thermal expansion can be defined as the ratio of "the change of linear dimension to the change in original dimension of a material per unit change in temperature" (Rosato, 1997, p. 91). Plastic materials have a high coefficient of thermal expansion when compared to metals (Palin, 1967, p. 51). This is illustrated in Figure 4.19. This figure is compiled from various sources (Craig, 2000; Palin, 1967; Harper, 1975; Kinney 1967). These large coefficients of thermal expansion result in larger contraction and expansion in the plastic materials (Palin, 1967, p. 51). This can cause problems since the temperature in the mass of the material varies. This indicates that moulded shrinkage is present in some plastic materials and therefore cannot be moulded to such close tolerance as compared to metals (Palin, 1967, p. 51)

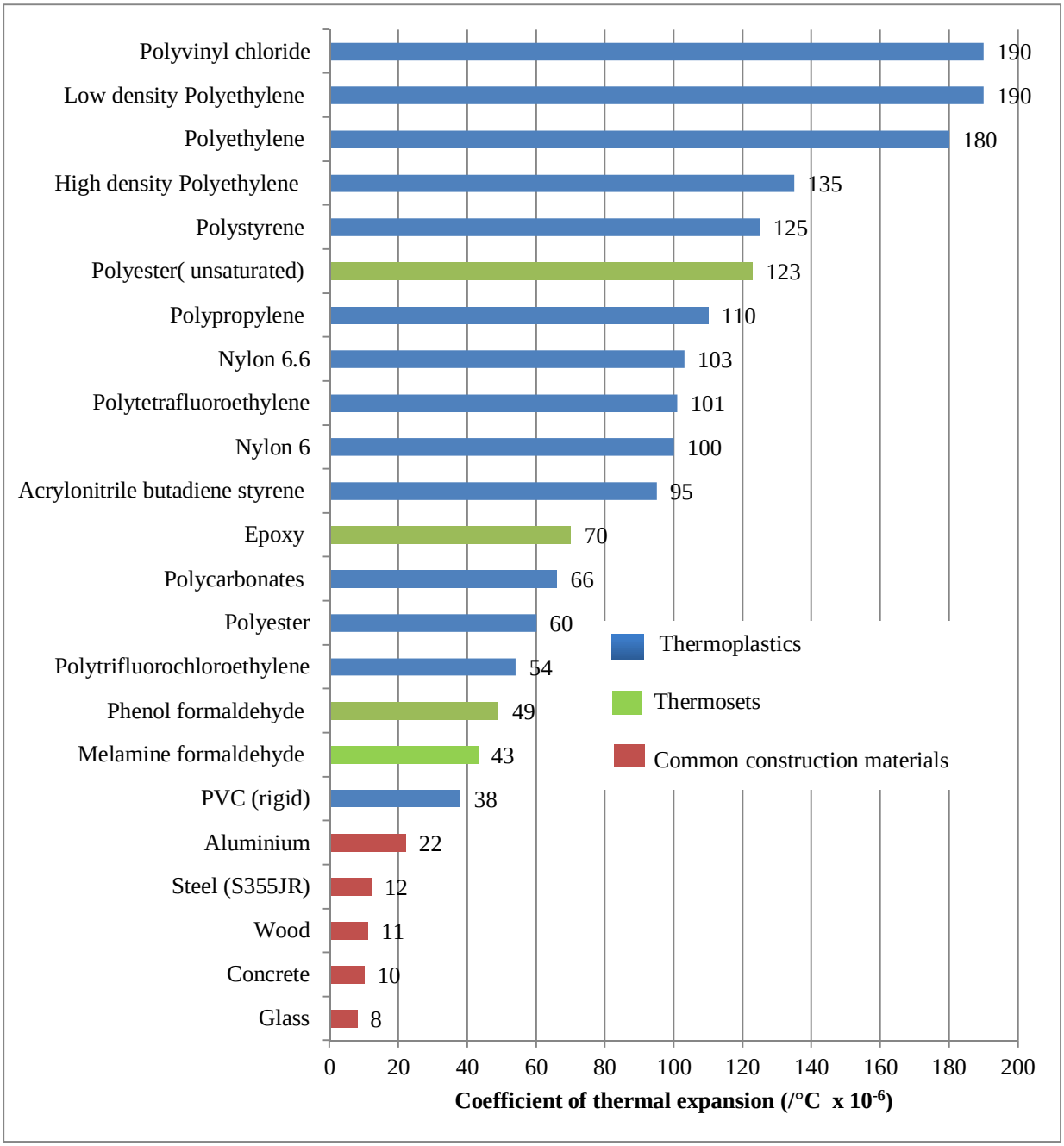

Figure 4.19: Average coefficient of thermal expansion of thermoplastics, thermosets and common construction materials

4.2.5. Flammability

Flammability or burning resistance of plastic materials is of high importance when high temperatures are expected (Palin, 1967, p. 52). The ignition temperature is considered the most important factor, followed by the burning rate, after a material has been ignited, when burning resistance is considered (Palin, 1967, p. 52). Most plastic material exhibits relatively good resistance to burning, especially when compared to typical construction wood and cotton fabrics (Hiatt & Winding, 1961, p. 76) and are difficult to ignited (Palin, 1967, p. 53). For example, thermosetting plastic materials turn into char, rather than burning (Palin, 1967, p. 53). Thus, a large quantity of heat is required to ignite the plastic material (Hiatt & Winding, 1961, p. 76) and it generally burns slowly (Palin, 1967, p. 53). The burning rate however, is different for various plastic materials and depends on a number of factors such as oxygen availability, consumption rate of materials and the ratio of surface exposed to mass (Palin, 1967, p. 53). For example, a thin plastic foil compared to a heavy or thick plastic section will burn more rapidly (Hiatt & Winding, 1961). Most thermoplastic and all the thermosetting plastic materials have the ability to self-extinguish (Rosato & Rosato, 2004, p. 843). The burning characteristics of various plastic materials are shown in Table 4.2. This table is compiled from various sources (Braun, 1982; Palin, 1967). Most plastics emit carbon monoxide (CO), when they burn. Polyvinyl chloride (PVC) emits a toxic gas known as hydrochloric acid (HCl), whereas polycarbonates (PC) and phenol formaldehyde (PH) release a weak acidic gas known as phenol (Klyosov, 2007).

Table 4.2: Burning characteristics of various plastic materials

Material	Abbreviation	Burning characteristic		
		Flammability	**Odor of vapour**	**Other**
Thermoplastics				
High density Polyethylene	HDPE	Burns readily and not self-extinguishing, but extinguish slowly.	Burning paraffin wax	Melts and becomes clear
Low density Polyethylene	LDPE			
Polyethylene	PE			
Polypropylene	PP	Burns readily and not self-extinguishing, but extinguish slowly.	Diesel	Melts and becomes clear
Polyvinyl chloride	PVC	Burns with difficulty and self-extinguishing	Hydrochloric acid (HCl)	White smoke, softens
PVC (rigid)	PVC (rigid)			
Polyamide (Nylon 6.6)	Nylon 6.6	Burns with difficulty and self-extinguishing	Burning vegetation	Melts and froths
Polyamide (Nylon 6)	Nylon 6			
Polycarbonates	PC	Burns with difficulty and self-extinguishing	Phenol (acidic gas)	-
Polytetrafluoroethylene	PTFE	Does not burn	-	-
Polytrifluorochloroethylene	PTFCE			
Polystyrene	PS	Burns readily and continue burning after flame is removed	Marigolds	Softens
Acrylonitrile butadiene styrene	ABS	Burns readily and continue burning after flame is removed	Burning rubber and bitter smell	Softens
Thermosets				
Phenol formaldehyde	PH	Burns with difficulty and often self-extinguishing	Phenol (acidic gas)	Cracks
Melamine formaldehyde	MF	Burns with difficulty and self-extinguishing	Formaldehyde and fish	Cracks
Polyester (unsaturated)	UP	Burns readily and not self-extinguishing, but extinguish slowly.	Sharp	-
Epoxy	EP	Burns readily and not self-extinguishing, but extinguish slowly.	Phenol	-

4.3. Chemical properties

The most important chemical properties of unreinforced plastic materials are discussed in the following sections. Chemical properties can influence the mechanical properties of the plastic material.

4.3.1. Resistance to solvents

In order to dissolve a mass of solute, the molecules of an individual solvent must have the ability to enter the mass of the solute and interfere with the molecules of the solute by overcoming the inter-molecular forces which hold the solute together (Hiatt & Winding, 1961, pp. 81-82). A solid polymer's molecules are bonded by van der Waal's forces, contact of polar groups or hydrogen bonding (Hiatt & Winding, 1961, pp. 81-82). The solubility of plastic materials varies with the type of plastic material, the type of solvent, rigidity of the molecular chains and the manner in which the chains are structured (Palin, 1967, p. 56). Temperature plays an important role in the solubility of plastic materials, since changes in temperature can result in large changes of the molecular structure of a plastic material (Palin, 1967, p. 56)

The manner in which the chains are structured determines the fraction of the maximum amount of secondary bonds which may occur between chains (Hiatt & Winding, 1961, p. 82). Thermoplastic material with a tightly bounded pack and rigid molecular chains are more resistant to solvents when compared to thermoplastic materials which are loosely packed and have flexible molecular chains (Palin, 1967, p. 56). For thermoplastic materials, the inter-molecular forces vary with the length of the molecular chain and therefore the influence of a given solvent on thermoplastic material varies with the molecular weight. The shorter the molecular chain the less the resistance to the solvent (Palin, 1967, p. 56).

Thermosetting polymers with a continuous network or cross-linked molecular structure contain no molecules that can be separated and therefore these plastic materials are insoluble as shown in Table 4.3. Solvents only penetrate the solid polymer (Palin, 1967, p. 56), which results in swelling of the polymer (Hiatt & Winding, 1961, p. 82). The extent of swelling is dependent on the degree of cross-links with in a polymer structure (Palin, 1967, p. 56). For lightly to moderately cross-linked materials swelling can result in as much as fifty per cent increase in volume, whereas highly cross-linked materials might have insignificant swelling (Hiatt & Winding, 1961, p. 82). The effects of various solvents on a variety of plastic materials are summarised in Table 4.3. This table is compiled from various sources (Braun, 1982; Palin, 1967).

Table 4.3: Resistance to solvent of various plastic materials

Material	Abbreviation	Resistance to solvents
Thermoplastics		
Low density Polyethylene	LDPE	Soluble in aromatics above 60°C
Polyethylene	PE	
High density Polyethylene	HDPE	Insoluble below 80°C
Polypropylene	PP	
Polyvinyl chloride	PVC	Swells in aromatic hydrocarbons. Soluble in ketones and esters
PVC (rigid)	PVC (rigid)	
Polyamide (Nylon 6.6)	Nylon 6.6	Not affected by common solvents
Polyamide (Nylon 6)	Nylon 6	
Polycarbonates	PC	Soluble in aromatics and chlorinated hydrocarbons
Polytetrafluoroethylene	PTFE	Insoluble
Polystyrene	PS	Soluble in esters, aromatics, alcohols, hydrocarbons, chlorinates and ketones
Acrylonitrile butadiene styrene	ABS	Soluble in esters, hydrocarbons, chlorinates and ketones
Thermosets		
Phenol formaldehyde	PH	Insoluble
Melamine formaldehyde	MF	
Polyester (unsaturated)	UP	
Epoxy	EP	Slightly affected by chlorinated hydrocarbons and ketones

4.3.2. Resistance to chemicals

Generally, the resistance to chemical attack of plastic material is high (Palin, 1967, p. 57) and is mainly dependent on the type of chemical attack, the type of polymer and also the grade of polymer, especially when plasticisers and fillers are included (Hiatt & Winding, 1961, pp. 82-83). Chemical attacks are experienced by plastic materials by means of (Fenner, 1975, pp. 4.1 - 4.4):

(1) Dissolution
(2) Swelling
(3) Chemical bond breakage by means of hydrolysis, oxidation, pyrolysis and/or radiation
(4) Combination of (1), (2) and (3).

The quantity of water absorption as well as the ability to resistant oxidation is the main properties in forecasting the resistance to chemicals that cause corrosion, which can be associated with the chemical structure of the polymer (Hiatt & Winding, 1961, pp. 82-83). A plastic material that absorbs water is more likely to be attacked by water-soluble chemicals, whereas an unsaturated plastic material is more likely to be attacked by oxidising acid, generally a strong oxidising acid (Palin, 1967, p. 57). The chemical resistances of a variety of plastic materials are summarised in Table 4.4. Table 4.4 is compiled from various sources (Braun, 1999; Palin, 1967).

Table 4.4: Resistance to chemicals of various plastic materials

Material	Abbreviation	Resistance to solvents
Thermoplastics		
Low density Polyethylene	LDPE	Attacked by strong acids
Polyethylene	PE	
High density Polyethylene	HDPE	
Polypropylene	PP	
Polyvinyl chloride	PVC	Not affected
PVC (rigid)	PVC (rigid)	
Polyamide (Nylon 6.6)	Nylon 6.6	Attacked by strong acids
Polyamide (Nylon 6)	Nylon 6	
Polycarbonates	PC	Attacked by alkalis and strong acids
Polytetrafluoroethylene	PTFE	Not affected
Polystyrene	PS	Attacked by strong oxidation acids
Acrylonitrile butadiene styrene	ABS	
Thermosets		
Phenol formaldehyde	PH	Attacked by alkalis and acids. (Degree of attack varies with concentration and filler)
Melamine formaldehyde	MF	Attacked by alkalis and strong acids
Polyester (unsaturated)	UP	Attacked by strong alkalis
Epoxy	EP	Slightly affected by chlorinated hydrocarbons and ketones

4.4. Moulding techniques

The moulding technique used to manufacture a plastic material, mainly affects the mould shrinkage of a plastic material. If a proper moulding technique is selected for the manufacturing of a specific plastic material and the product is properly manufactured, the durability of the product increases. This increase in durability of the product might lead to an increase in the minimum life expectance of the product. Plastic materials are moulded by means of heat and pressure or in a chemical manner. If the heat and pressure or chemical substances are not controlled, changes can occur in the polymeric structure, which can lead to a decrease in mechanical properties.

There are numerous moulding techniques. The type of moulding technique should be selected based on the type of plastic material, the part size and part complexity required (as shown in Figure 4.20) as well as the tolerance required. The moulding techniques to produce a panel (rectangular shaped, with small thickness) as well as the advantages and limitations of each technique are discussed in the following sections.

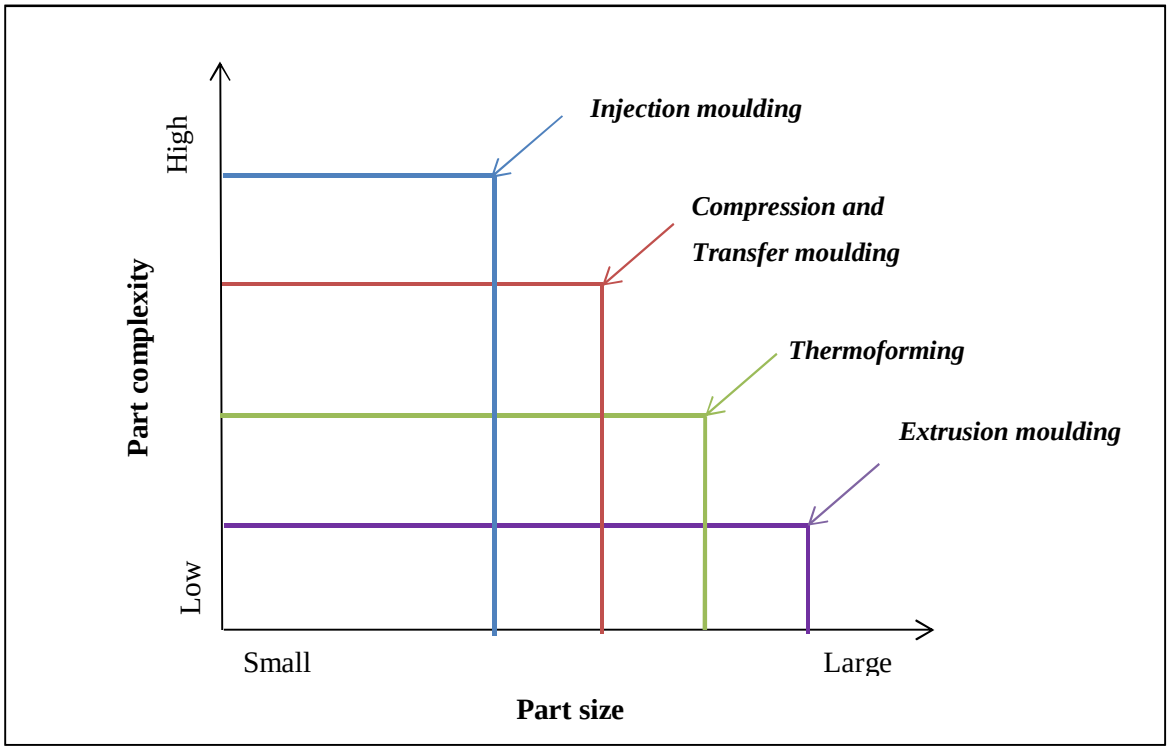

Figure 4.20: Moulding techniques characteristics (Rosato, 1997, p. 6)

4.4.1. Injection moulding

Injection moulding is one of the most commonly used moulding techniques for the fabrication of plastic parts (Grelle, 2006, p. 1). Injection moulding is defined as the process whereby a heat-melted plastic material is forced from a cylinder to a mould or cavity which shapes the material in a desired shape (Harper, 1975). A typical injection moulding machine is shown in Figure 4.21.

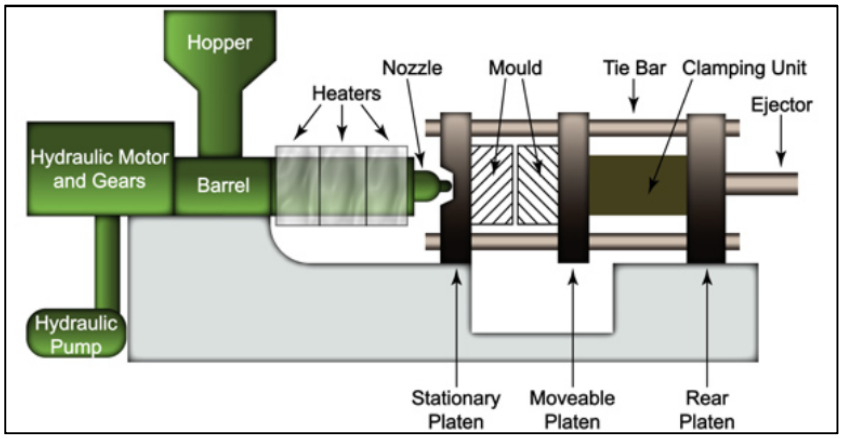

Figure 4.21: Injection moulding machine (Azeez, 2012)

The advantages of using injection moulding are that the temperature, the pressure and the rate of production are controlled (Rosato, 1997, pp. 121-122). Since the rate is controlled, the semi-crystalline plastic material can be allowed to form more crystals when cooling and thus increase the strength of the material (Rosato, 1997, pp. 121-122). Depending on the type of plastic material, injection moulding can mould a material to a close tolerance, thus insignificant mould shrinkage occurs (Rosato, 1997, p. 189). The main advantages and limitations of injection moulding are shown in Table 4.5. This table is compiled from various sources (Rosato, 1997, pp. 18,122; Grelle, 2006).

Table 4.5: Main advantages and limitations of injection moulding

Advantages	Limitations
• Low labour cost • High production rate • Outstanding surface finish • High reproducibility of complex parts	• Uneconomical for small productions • High maintenance cost • High equipment cost

4.4.2. Extrusion moulding

Extrusion moulding is similar to injection moulding, but the main difference is that for extrusion moulding the plastics are produced by a lower pressure, than the pressure used in injection moulding (Rosato, 1997, p. 209). Extrusion moulding is commonly used for continuous production of sheets, films and other profiles (Rosato, 1997, p. 17). The advantages and limitations of extrusion moulding are shown in Table 4.6. Table 4.6 is compiled from various sources (Rosato, 1997, p. 17; Hanson, 2006, pp. 189-288).

Table 4.6: Main advantages and limitations of extrusion moulding

Advantages	Limitations
• Low tool cost • Rapid production rate • Production of complex profile shape is possible	• Producing uniform cross-sections

4.4.3. Thermoforming

Thermoforming is the process where the application of heat and pressure is used to mould thermoplastic sheets into a shape (Crawford, 1981, p. 199). The application of heat results in the flat sheet of plastic to soften and thus distort or deflect into a sagged or draped sheet (MacDonald, 2006, p. 292). When this stage is reached, pressure is applied to force the softened plastic into a male or female mould. Thermoforming generally results in products that are mainly used for packaging (MacDonald, 2006, pp. 292-301). Several variations exist, where the main variation includes vacuum forming, pressure forming and drape forming (Rosato, 1997, p. 20). A schematic diagram of the thermoforming process is shown in Figure 4.22. The main advantages and limitations of thermoforming are shown in Table 4.7. This table is compiled from various sources (Crawford, 1981, pp. 199-200; MacDonald, 2006, pp. 291-302; Rosato, 1997, pp. 19-20).

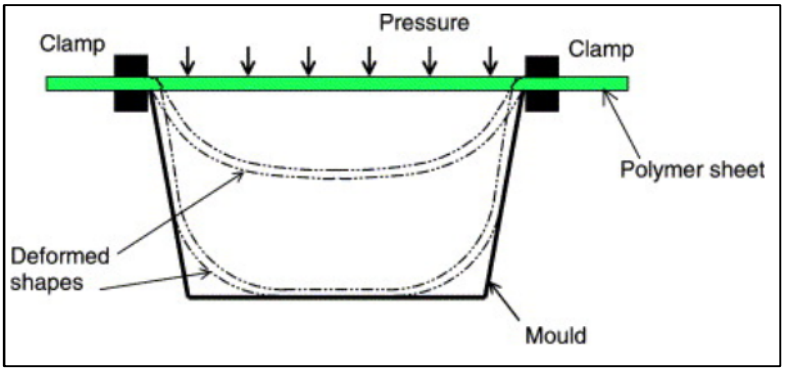

Figure 4.22: Schematic diagram of pressure thermoforming process (Warby, et al., 2003, p. 210)

Table 4.7: Main advantages and limitations of thermoforming

Advantages	Limitations
• Generally tool costs are low • Economical for limited element production • Large element production with thin sections is possible	• Simple configuration elements are limited • Only limited number of materials can be used, namely thermoplastics such as Polycarbonate (PC), Polystyrene (PS), Acrylonitrile butadiene styrene (ABS), Polyvinyl chloride (PVC), Polypropylene (PP), High density Polyethylene (HDPE) and Low density Polyethylene (LDPE)

4.4.4. Compression moulding

Compression moulding is the most commonly used moulding method to produce elements from thermosetting plastics (Crawford, 1981, p. 209). This moulding method can also be used to produce elements from thermoplastics, but are not usually used since cheaper moulding methods exist to produce thermoplastic elements (Palin, 1967, p. 68). A compression mould consists of two halves, one female and one male half (Hull, 2006, p. 455). The female mould or bottom half of the mould contains one or more cavities. The plastic material is placed in these cavities. Both halves of the mould are heated to approximately 150°C, depending on the plastic material being moulded (Hull, 2006, p. 455). The two halves of the mould are then closed, forcing the material to flow and fill the cavities (Rosato, 1997, p. 16). During moulding, thermosetting plastics experience an exothermic and irreversible chemical reaction, which is termed polymerisation (Hull, 2006, p. 455). The polymerisation occurs due to pressure, which is usually between 30MPa and 150MPa, and heat, which is approximately 150°C. After polymerisation of thermosetting plastics, the moulded element retains its chemical, physical and electrical properties when the temperature ranges from approximately -50°C to approximately 150°C (Hull, 2006, p. 455). When thermosetting plastic is moulded, the mould is still hot when opened, whereas when thermoplastic is moulded, the mould must be cooled before it is opened (Palin, 1967, p. 68). The main advantages and limitations of compression moulding are shown in Table 4.8, which is compiled from various sources (Palin, 1967, p. 68; Rosato, 1997, p. 16; Hull, 2006, pp. 455-463).

Table 4.8: Main advantages and limitations of compression moulding

Advantages	Limitations
• Little material waste is possible • Bulky parts can be moulded • Process adaptable to rapid automation	• Close tolerance is difficult to produce • Complicated parts might contain side draws, delicate insets, small holes, undercuts, etc. resulting in a reduction of mechanical properties

4.4.5. Transfer moulding

Transfer moulding is similar to compression moulding and it is also mainly used for thermosetting plastics (Rosato, 1997, p. 20). The process of transfer moulding is described as a plastic material that is transferred from a hopper into a transfer chamber (Rosato, 1997, p. 20), also called transfer pot (Hull, 2006, p. 463). In the transfer pot, the material is heated until soft (Rosato, 1997, p. 20). It is then transferred through gates and runners into a closed mould (Rosato, 1997, p. 20) which contains a cavity or cavities (Hull, 2006, p. 463). In this closed mould, the plastic cures and after curing, the mould opens and the plastic part is ejected (Rosato, 1997, p. 20). The main advantages and limitations of transfer moulding is shown in Table 4.9. This table is compiled from various sources (Rosato, 1997, p. 20; Hull, 2006, pp. 463-473).

Table 4.9: Main advantages and limitations of transfer moulding

Advantages	Limitations
• Good dimensional accuracy • Complicated parts can be produced • Rapid production rate	• High mould cost • A great deal of material waste • Size of parts is somewhat limited

4.4.6. Calendering

Calendering is the process where a dough-consistency thermoplastic mass produces sheets and films (Crawford, 1981, p. 202). The uniform thickness sheets or films are produced by squeezing the dough-consistency material through a gap, also known as a nip, between heated and/or cooled counter-rotating cylinders (Rosato, 1997, p. 15). The main advantages and limitations of calendering are shown in Table 4.10. Table 4.10 is compiled from various sources (Rosato, 1997, p. 20; Hull, 2006, pp. 463-473).

Table 4.10: Main advantages and limitations of calendaring moulding

Advantages	Limitations
• Low cost moulding method • Sheet material has little or no mould-in stresses	• Limited to sheet materials • Production of thin films is impossible

4.4.7. Casting

Casting is the process where a plastic material is melted to a liquid form, cast into a mould without pressure, cured and then removed from the mould (Palin, 1967, p. 77). This method is generally not applicable to plastic materials, since extremely high temperatures are required for plastic materials to become fluid. Decomposition of plastic materials generally occurs before these temperatures are reached (Palin, 1967, p. 77). However, some plastics, generally thermoplastics, can be cast and are known as hot-melt compounds (Rosato, 1997, p. 15). The temperature, the pressure and the rate of production are generally never controlled, which can cause undesirable changes to the mechanical properties, such as creep, decrease in strength, excessive mould shrinkage, which can cause warpage, loss of close tolerance and sink marks (Rosato, 1997, p. 391). The main advantages and limitations of casting are shown in Table 4.11. This table is compiled from various sources (Rosato, 1997, pp. 15,392; Palin, 1967, pp. 77-78).

Table 4.11: Main advantages and limitations of casting moulding

Advantages	Limitations
• Low mould cost • Large parts with thick cross-sections can be produced • Convenient for low-volume production	• Limited to simple shapes • Voids might be present in plastic parts, resulting in a reduction of mechanical properties • Uneconomical at high volume production rate • Limited to hot-melt materials

4.5. Discussion

The mechanical strength of most of the unreinforced plastic material (refer to Figure 4.5, Figure 4.7 and Figure 4.8) is plausible for the use of load bearing applications. In Figure 4.9, it is illustrated that unreinforced plastics are considered ductile under a specific temperature. Some of the mechanical properties of unreinforced plastic are undesirable when a load bearing application is concerned. These mechanical properties include the following:

- Although unreinforced plastic materials have a high strength-to-weight ratio, the Young's modulus is especially low (refer to Figure 4.6). This implies that unreinforced plastics are extremely soft.
- Where long-term loading is concerned, creep and fatigue behaviour of unreinforced plastics limit the plastic material to be of use for structural applications. Creep and cold flow are major limitations of plastics which cause these materials to be dimensionally unstable.
- Durability of unreinforced plastic is another concern. Since unreinforced plastic material may deteriorate when exposed to sunlight (UV).

Where the thermal properties of unreinforced plastics are concerned, unreinforced plastic material is considered rather thermally unstable. Since an increase in temperature can result in a decrease in mechanical properties. This is not desirable in the case of load bearing applications. However, plastic material is used an insulating material. This means that it requires a large amount of energy to increase the temperature of the material and it has low thermal conductivity (Figure 4.18).

The type of moulding technique should be selected based on the type of plastic material, the part size and part complexity required (as shown in Figure 4.20) as well as the tolerance required. For a panel construction, the best moulding techniques are injection moulding and extrusion moulding. The choice between these moulding techniques is made based on the part size, since a panel is not a complicated part.

Since not all the properties of unreinforced plastic material are suitable for a load bearing application, plastic composites and foams are investigated in the next chapter. The moulding techniques used for plastic composites are also investigated.

CHAPTER 5: PLASTIC COMPOSITES AND PLASTIC FOAMS

To improve the properties of unreinforced plastic, the addition of non-polymeric material are investigated. The addition of non-polymeric materials can significantly modify the properties of plastic materials. These non-polymeric materials can be added in the form of a solid, liquid or gas (Palin, 1967, p. 58). In this chapter, these non-polymeric materials that are added to plastic materials as well as the affect they have on the properties of the plastic materials are discussed.

5.1. Plastic foams

Plastic foams, also known as expanded plastics, are due to the addition of gas (Palin, 1967, p. 58). There are several pockets throughout the plastic material, that contain gas and these pockets are known as cells (Palin, 1967, p. 58). There are three types of expanded plastics namely closed-cell, open-cell or a cell structure that contains an open-cell and closed-cell structure (Rosato & Rosato, 2004, p. 364). In closed-cell foam, the cells are totally enclosed by the plastic medium (Palin, 1967, p. 58). Whereas, in an open-cell foam, the cells are unconfined by means of interconnected openings in the plastic medium (Harper, 1975, p. 7.2). The movement of gas in an open-cell foam is unrestricted (Harper, 1975, p. 7.2).

Depending on the plastic material's nature, rigid or flexible plastic foams can be created (Palin, 1967, p. 60). Both thermoplastics and thermosetting plastics can be expanded. Thermoplastic foams are generally produced from a heat softened plastic material by means of an appropriate expansion process. Whereas, thermosetting foams are produced from an uncured plastic resin and the expansion of the plastic material occurs during the curing process (Palin, 1967, pp. 58-59). There are numerous expansion systems, but the most used system is the inclusion of a blowing agent in the plastic material (Rosato & Rosato, 2004, p. 364). This blowing agent is used to produce cells within the plastic material. There are two types of blowing agents, a physical blowing agent and a chemical blowing agent. The type of blowing agent is selected depending on the type of plastic material as well as the process used to create the foams (Rosato & Rosato, 2004, p. 364).

Expanded polystyrene (EPS) and extruded polystyrene (XPS) are foams mostly used as insolative material in construction. XPS has a closed-cell structure and is produced by means of an extrusion process and the use

of a physical blowing agent (Agarwal & Gupta, 2011). Examples of the physical blowing agent used to produce XPS include pentane or hydrochlorofluoro-carbon. EPS, on the other hand, is produced by means of moulding polystyrene beads that are saturated with the blowing agent (Agarwal & Gupta, 2011). These polystyrene beads are heated and the expansion of the blowing agent results in a closed-cell foam structure (Lee, et al., 2006). The blowing agents used to produce EPS include carbon dioxide or pentane (Lee, et al., 2006).

5.2. Plasticisation

A liquid is added to a plastic material in the form of plasticisers (Palin, 1967, p. 60). Plasticisers are included into a plastic material to increase the workability or flexibility of a plastic material, but the addition of plasticisers can also result in a lower transition temperature or elastic modulus of the solidified plastic (Harper, 1975).

5.3. Plastic composites

A composite is defined as a material that is comprised of two or more solid synthetic assembled components (Rosato, 1982, p. 2). For plastic composites, the three main components are generally a selected reinforcing agent or filler, additive(s) and a plastic material (Rosato, 1982, p. 2), as shown in Figure 5.1. Fillers are generally described as finely divided solids, such as wood-flour (Palin, 1967, p. 58). Reinforced plastic refers to a fibrous solid material that is added to a plastic material to enhance the strength of the unreinforced (also known as neat) plastic material. This fibrous solid material ranges from a closely woven mat to a single chopped fibre. Plastics produced from woven mat fibres are often called laminates, whereas plastics produced from single chopped fibres are called fillers. These laminates refer to layers of non-polymeric materials that are joined together by means of layers of plastic materials or it can also refer to plastic sheets comprised of plastic layers that are pressed together (Palin, 1967, p. 58).

Interface constituents of the plastic composites, such as a coupling agent and lubricant, are shown in Figure 5.2. The coupling agent increases the interfacial adhesion and it can cause an increase in mechanical properties (Stark & Rowlands, 2003). The lubricants, on the other hand, enhance wettability and melt temperature during moulding of composites (Simonsen, et al., 2004).

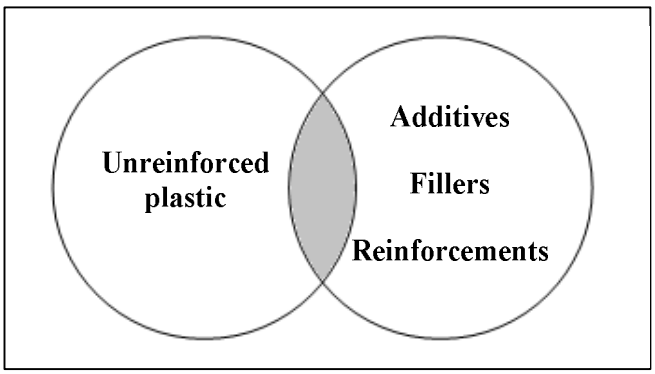

Figure 5.1: Plastic composition (Rosato, 1997, pp. 67, Figure 1.21)

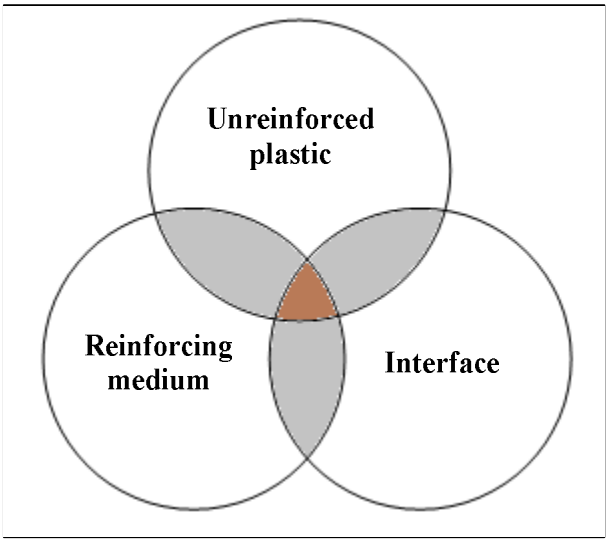

Figure 5.2: The interplay between plastic composite constituents (Rosato, 1997, pp. 67, Figure 1.21)

5.4. Mechanical properties

The mechanical properties of reinforced plastics depend on the following (Rosato & Rosato, 2004, p. 8):

- Mainly on the type of unreinforced plastic material (thermosetting plastics and thermoplastics)
- The interface, thus the type of lubricant and coupling agent used
- The type of reinforcing agent
- The reinforcing agent orientation
- Length and form of the of the reinforcing agent
- The plastic resin to reinforcement ratio

Whereas, the mechanical properties of plastic foams depend mainly on the type of plastic material, the type of blowing agent, the amount of gas in the material medium and whether the foam has a closed-cell or open-cell structure. The mechanical properties of plastic foams are also dependant on the specific gravity of the foam. In this chapter, a medium density is used.

The mechanical properties of plastic composites, such as glass fibre-reinforced plastic (GFRP), FFC (foam fibre composite) (see Chapter 2) and WPC (wood-plastic composite) and plastic foams are compared in general. It is also compared to common construction materials and unreinforced plastics. A summary table of the mechanical properties of plastic composite and plastic foams is shown in Appendix A, Table A.4.

5.4.1. Specific gravity

In Figure 5.3 the average specific gravity of unreinforced plastics, plastic composites, plastic foams and common construction materials is shown. Figure 5.3 is compiled from various sources (Rosato & Rosato, 2004, p. 2; Friul Filiere Spa, [S.a]; Agarwal & Gupta, 2011; Leu, et al., 2012; Fisher, 2013; Eva-Last, [S.a]). Plastic foams have a low specific gravity, since they contain a great amount of gas within the plastic medium, that cause their specific gravity to be much lower compared to the unreinforced plastic. The specific gravity of GFRP and WPC is not significantly more than the specific gravity of the unreinforced plastic. The reinforcing agent of these composites has a smaller specific gravity than the plastic material, thus the unreinforced plastic used to produce GFRP and WPC mainly determines the specific gravity of the composites. FFC, on the other hand, is made up of thermoplastics and vegetal fibres and from Figure 4.2 it can be seen that most thermoplastics have lower specific gravities when compared to thermosetting plastics. The vegetal fibres can also contribute to the low specific gravity of FFC.

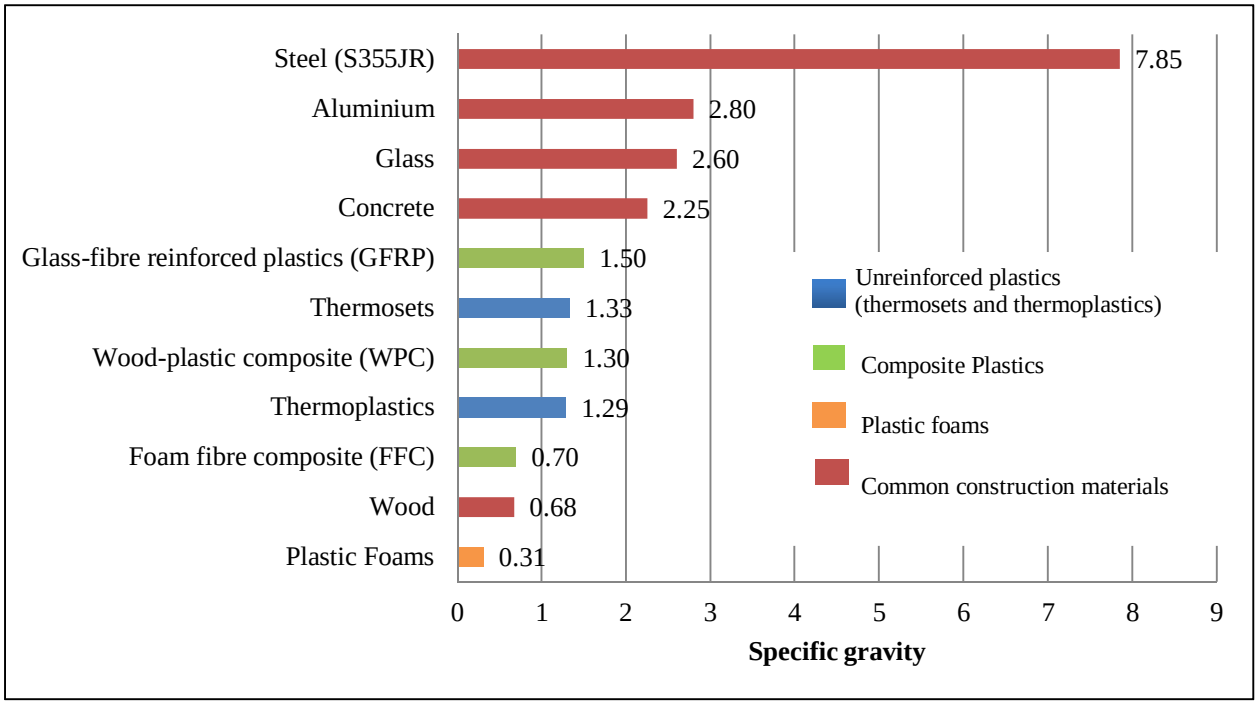

Figure 5.3: Average specific gravity of unreinforced plastics, plastic composites, plastic foams and common construction materials

5.4.2. Deformational characteristics

Stress-strain curves

The stress-strain curves of all the plastics (as shown in Figure 4.3 and Figure 4.4), whether plastic composites or foam plastics, are related to those of unreinforced plastics. The area under the stress-strain curve indicates the toughness of a material. The larger this area is the tougher is the material. However, this is not true for reinforced thermosetting plastics. Some reinforced plastic is extremely strong and tough, but the area under the stress-stain curve is small (Rosato & Rosato, 2004, p. 668). Therefore, the toughness of reinforced plastics, measured as the area under the stress-strain curve, might be misleading. The small area under the stress-strain curve of reinforced plastics might be due to the reinforcing agent (fibres). The reinforced fibres can bridge cracks, thus absorbing some of the applied stress. This leads to a delay in the strain (crack growth), which results in the area under the stress-stain curve being small (Sham Prasad, et al., 2011, p. 1265). The ASTM D5045 can be used to determine the toughness of a reinforced plastic material (ASTM D5045, 1996), where the test set-up is similar to a three-point bending test.

On the other hand, the tensile, compression and flexural properties of composite and foam plastics differ from unreinforced plastics. For example, the elastic limits of various forms of plastic are shown in Figure 5.4.

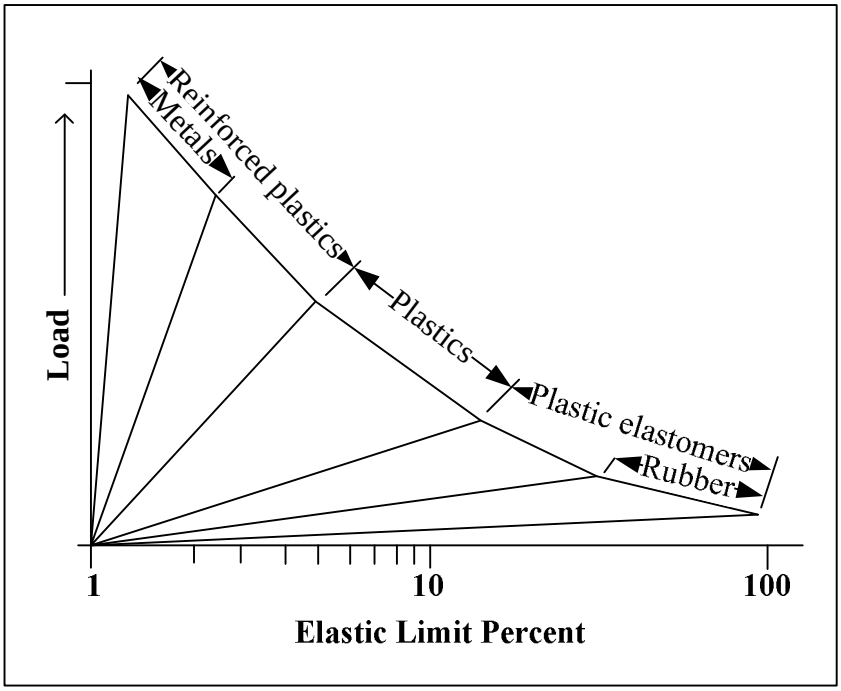

Figure 5.4: Elastic limit of reinforced plastic as well as unreinforced plastic (Rosato & Rosato, 2004, pp. 112, Figure 3.2)

Tensile properties

The plastic foams have an extremely low tensile strength, when compare to the other materials. This is due to gas that exists in the plastic medium. These gas cells cause the plastic foam to crack and rupture under a tensile load, since these gas cells cause weak spots in the plastic medium, as shown Figure 5.5. If the plastic foam has an open-cell structure, the tensile strength would be lower, due to the interconnected opening which results in cracks and thus a lower tensile strength. A closed-cell plastic foam has a larger tensile strength when compared to open-cell foams, since the gas cells are totally enclosed in the plastic medium. The enclosed cells also cause cracks to form when a tensile force is applied to the plastic foam, but the cracks form faster in open-cell plastic foam material. This low tensile strength of plastic foams is shown in Figure 5.6.

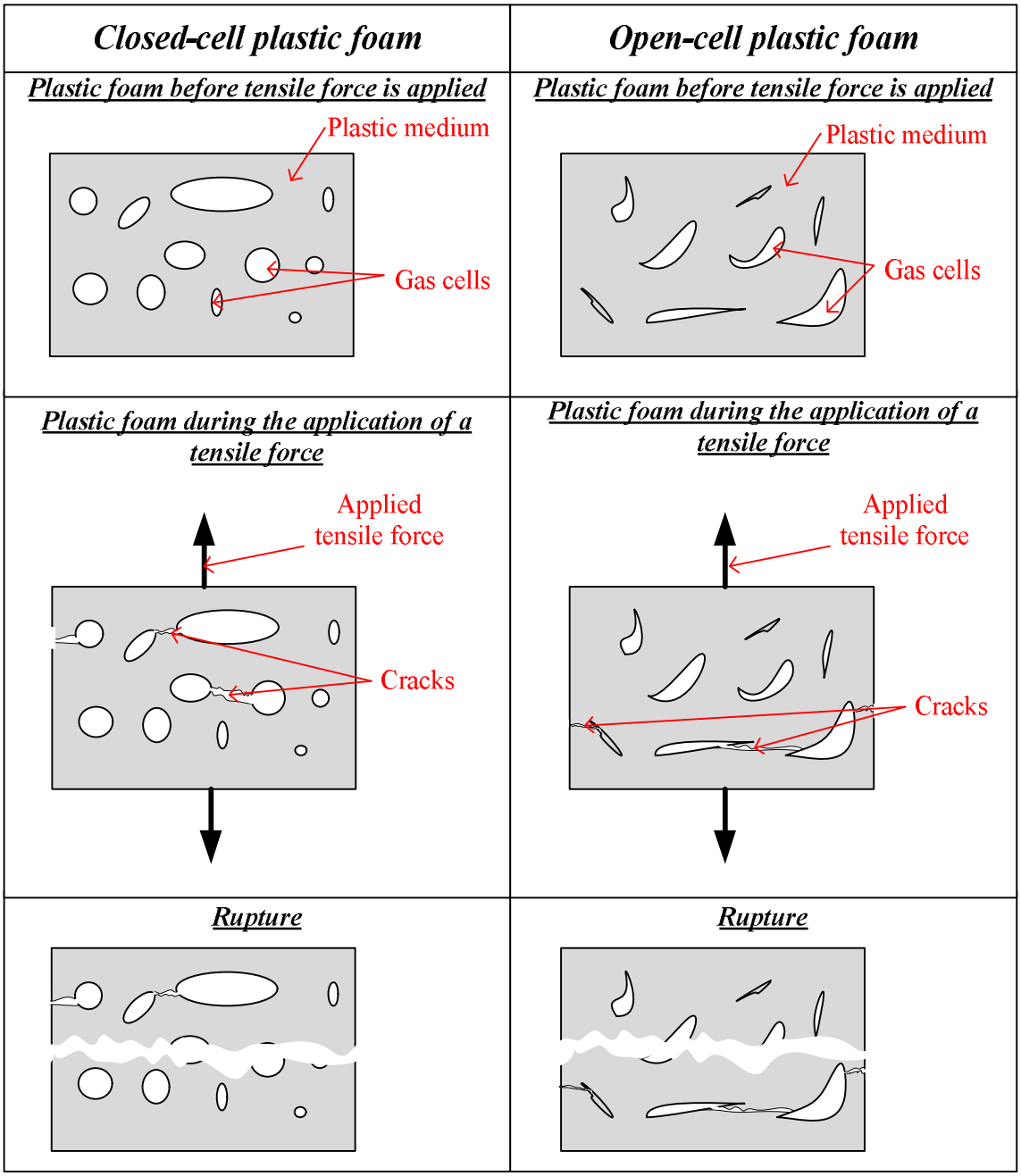

Figure 5.5: Tensile forced applied to closed-cell and open-cell plastic foams

The tensile strength of a reinforced plastic can typically be 550MPa, which is more than the tensile strength of steel (Rosato & Rosato, 2004, p. 2). The tensile strength of plastic composites is affected as follow:

- The larger the tensile strength of the unreinforced plastic material, the larger is the tensile strength of the composite plastic material (Rosato & Rosato, 2004, p. 8).
- The larger the tensile strength of the reinforcing agent, the larger is the tensile strength of the composite plastic material. This is shown in Figure 5.6.

- The form of the reinforcing agent has a significant influence on the tensile strength of the composite. For example, a cloth-reinforced plastic can have a tensile strength of as much as three to four times more than a coarse mat reinforced plastic (Palin, 1967, p. 65).
- An increase in the length of the fibre of the reinforcement results in a larger tensile strength of the composite material (Rosato & Rosato, 2004, p. 8). For example, the tensile strength of WPC is larger when wood fibre is used in comparison to when wood-flour is used as the reinforcing agent.
- An increase in the content of the reinforcing agent will result in an increase in the tensile strength of the composite (Rosato & Rosato, 2004, p. 8). However, too much reinforcing agent can also result in a lower tensile strength.

In Figure 5.6 the average tensile yield strength of unreinforced plastics, plastic composites, plastic foams and common construction materials is shown. This figure is compiled from various sources (Rosato & Rosato, 2004, p. 2; Friul Filiere Spa, [S.a]; Agarwal & Gupta, 2011; Rosato, 1982; Murphy, 1998; Fisher, 2013). The WPC and FFC are produced from thermoplastics, which have a lower tensile strength than thermosetting plastic materials. The reinforcing agent of the WPC, used in Figure 5.6, is wood-flour which also reduces the tensile strength of this material, due to a short fibre length and tensile strength of wood is relatively low.

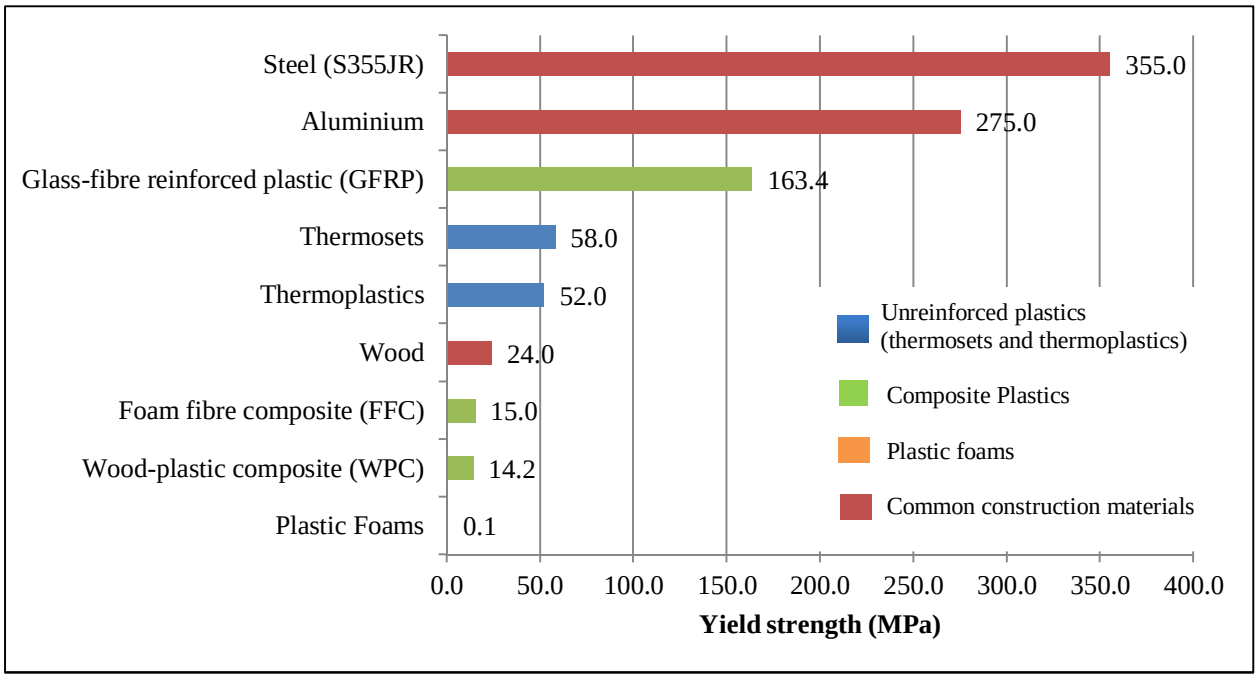

Figure 5.6: Average tensile yield strength of unreinforced plastics, plastic composites, plastic foams and common construction materials

The comparison of the average tensile Young's modulus of unreinforced plastics, plastic composites, plastic foams and common construction materials, is shown in Figure 5.7. This figure is compiled from various sources (Rosato & Rosato, 2004, p. 2; Agarwal & Gupta, 2011; Rosato, 1982; Murphy, 1998; Leu, et al., 2012; Fisher, 2013). This figure is assembled from various sources. Note in Figure 5.7, that not all the construction materials are shown. This is since some construction materials have much larger Young's modulus values compared. No published values for the modulus of elasticity of FFC could be found.

The Young's moduli of the plastic materials, shown in Figure 5.7, are relatively low when compared to the common construction materials. The type of plastic material, thermoplastics or thermosets, used to produce plastic foams or composite materials, plays an important role in the value of the Young's modulus. This is due to thermosets and thermoplastics that differ considerably when Young's modulus is considered.

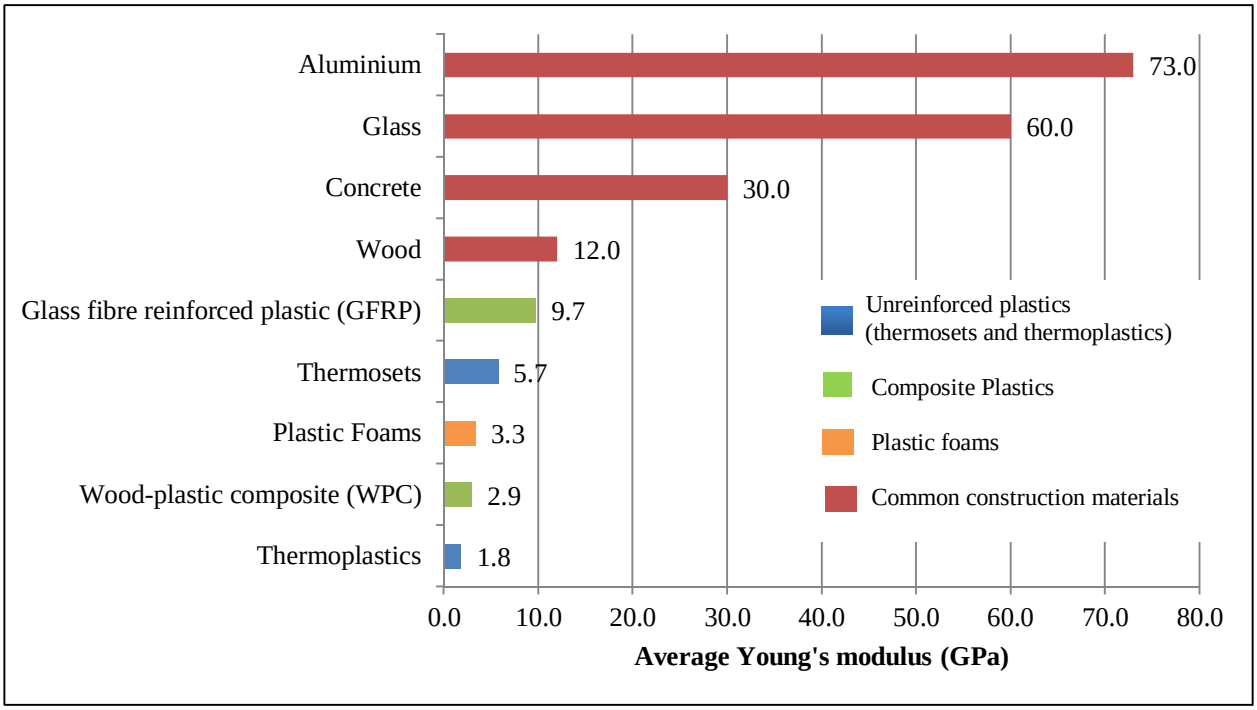

Figure 5.7: Average tensile Young's modulus of unreinforced plastics, plastic composites, plastic foams and common construction materials

The plastic foams exhibit a Young's modulus that is comparable to the Young's modulus of unreinforced plastics. However, the foams exhibit a lower tensile strength and therefore plastic foams are considered soft, brittle materials. The Young's modulus of plastic composites is mainly dependant on the type of reinforcing agent as well as the orientation of the reinforcing agent. For example, in Figure 5.7 the plastic material reinforced with glass fibre exhibits a higher Young's modulus compared to the other composite materials and the unreinforced plastics. WPC, which is reinforced with wood-flour, has a higher Young's modulus than

that of the thermoplastic. This is due to wood having a larger Young's modulus. However, the Young's modulus of a reinforced plastic can typically be 330GPa (Rosato & Rosato, 2004, p. 2).

Compression properties

The comparison of the average compressive strength of unreinforced plastics, plastic composites, plastic foams and common construction materials, is shown in Figure 5.8. This figure is compiled from various sources (Rosato & Rosato, 2004, p. 2; Agarwal & Gupta, 2011; Rosato, 1982; Murphy, 1998; Eva-Last, [S.a]). The composite materials in Figure 5.8 are produced using thermoplastics. Thermoplastics compared to thermosets exhibits a lower compressive strength.

Plastic foams have extremely low compressive strength, as shown in Figure 5.8. This is due to gas cells that are pressurised and reduce to a flat disk. This results in failure in compression. The open-cell plastic foams will have a lower compressive strength than the closed-cell foams. This is due to the interconnected openings in an open-cell foam structure that are pressurised, causes the material crush, and reduce to a flat disk quicker.

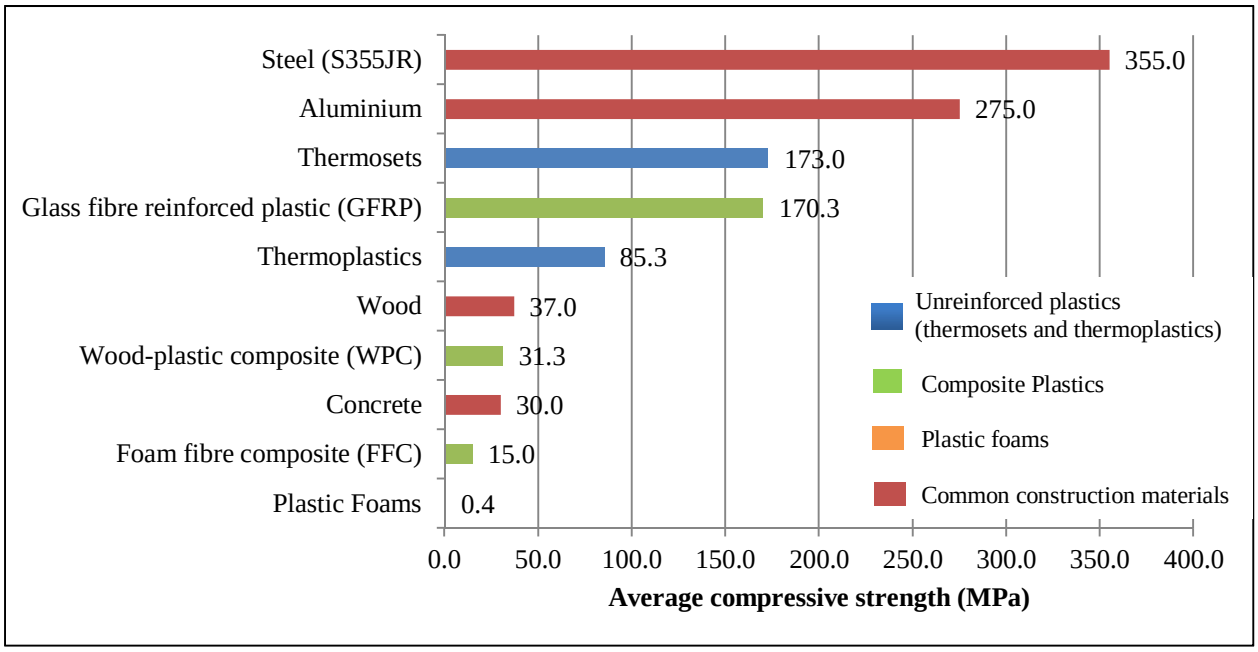

Figure 5.8: Average compressive strength of unreinforced plastics, Plastic composites, plastic foams and common construction materials

The compressive strength of plastic composites depends mainly on the compressive strength of the reinforcing agent. For example, wood-flour used to produce WPC has a lower compressive strength than wood, whereas wood has a lower compressive strength than unreinforced plastics. Therefore, WPC has a

much lower compressive strength than unreinforced plastics. However, when glass fibre is the reinforcing agent, the compressive strength of this plastic composite is higher that the compressive strength of unreinforced plastics. This is due to the high compressive strength of the glass fibre. FFC, on the other hand, has vegetal fibres to reinforce a thermoplastic material. These vegetal fibres have a lower compressive strength than that of unreinforced plastics, which cause this plastic composite to have a lower compressive strength when compared to unreinforced plastics.

Flexural properties

Plastic foams exhibit a low bending strength due to the gas cells that cause cracks. The average flexural strength of unreinforced plastics, plastic composites, plastic foams and common construction materials, is shown in Figure 5.9. Figure 5.9 is compiled from various sources (Rosato & Rosato, 2004, p. 2; Agarwal & Gupta, 2011; Rosato, 1982; Murphy, 1998; Leu, et al., 2012; Fisher, 2013).

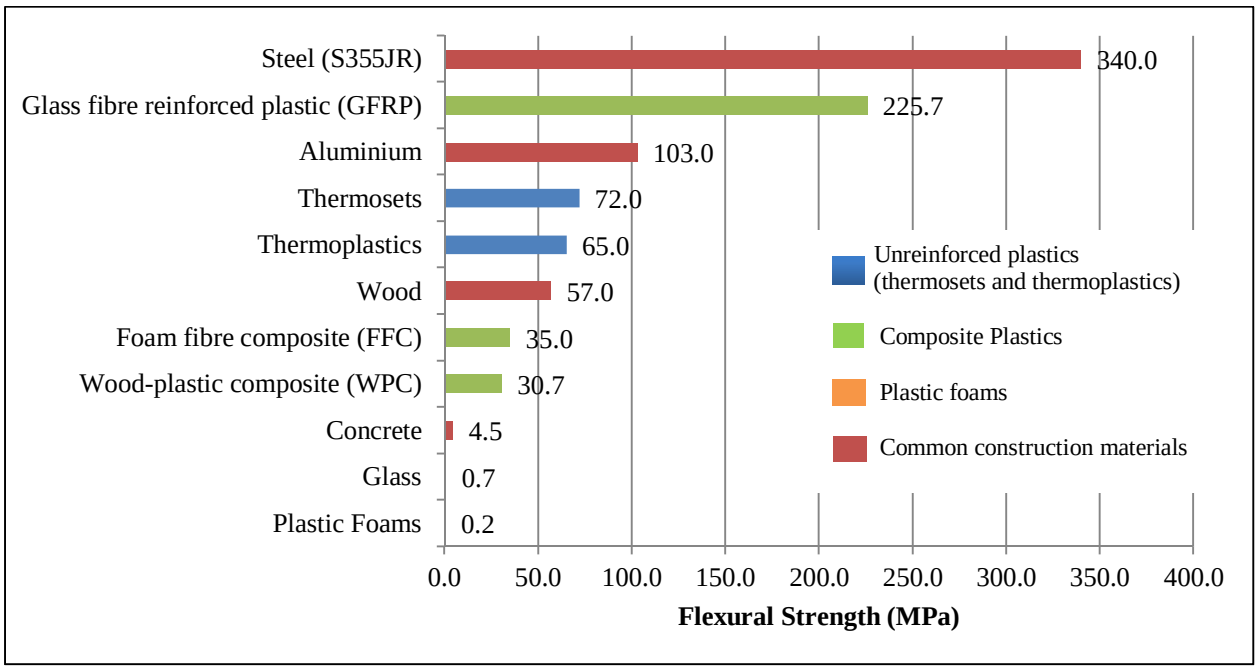

Figure 5.9: Average flexural strength of unreinforced plastics, plastic composites, plastic foams and common construction materials

The bending strength of plastic composites is mainly affected by the type of reinforcing agent, but is also affected as follow:

- The higher the bending strength of the reinforcing agent will result in an increase in the tensile strength of the composite plastic material. For example, wood has a lower bending strength than

unreinforced plastics which results in WPC having a lower bending strength than unreinforced plastics. This is shown in Figure 5.9.

- The flexural properties are influenced by the form of the reinforcing agent. For example, wood-flour, as a reinforcing agent, has a lower bending strength when compared to wood fibres, used as a reinforcing agent (Leu, et al., 2012).
- An increase in the length of the fibre of the reinforcement results in a higher bending strength of the composite material (Rosato & Rosato, 2004, p. 8). For example, the use of wood fibres as the reinforcing agent results in a higher bending strength compared to when wood-flour is used.

Elongation at rupture

Plastic foams are considered a brittle material therefore, this material is not shown in Figure 5.10. However, the elongation at rupture of unreinforced plastics, plastic composites and common construction materials are shown in Figure 5.10. This figure is compiled from various sources (Rosato & Rosato, 2004, p. 2; Agarwal & Gupta, 2011; Rosato, 1982; Murphy, 1998; Fisher, 2013). Thermoplastic materials exhibit the highest elongation at rupture in Figure 5.10, thus the thermoplastic materials are more flexible. Plastic composite materials are dependent on the type of reinforcement, but the reinforcing agent causes the elongation at rupture to be lower.

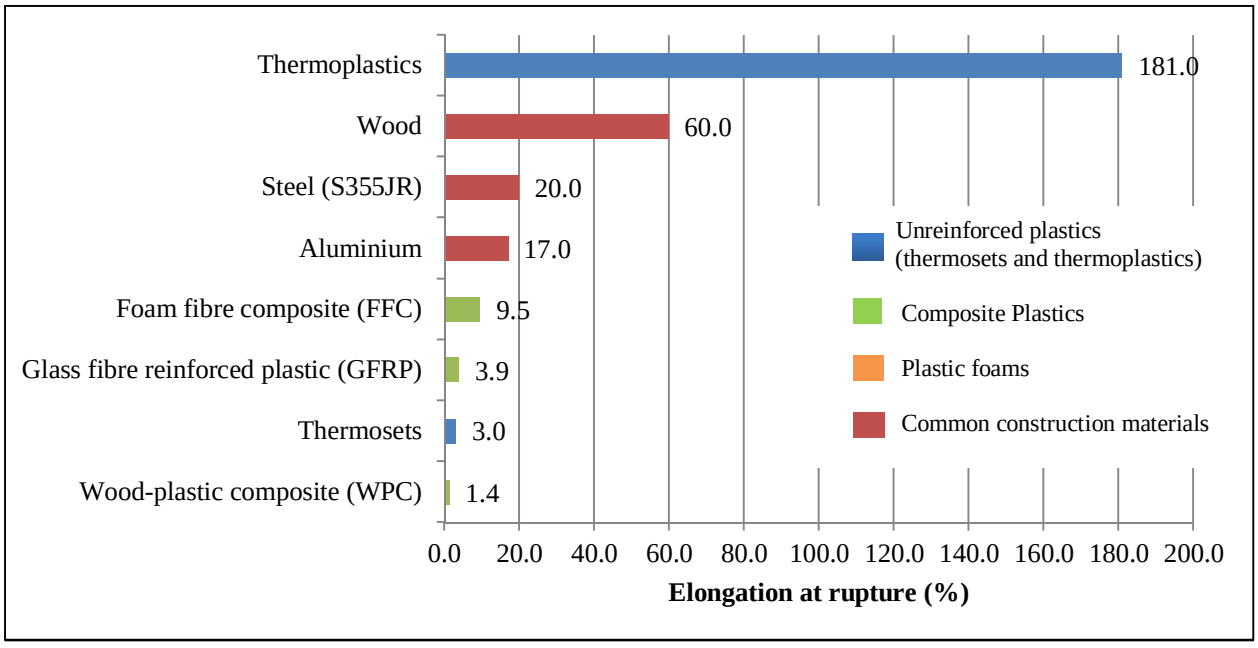

Figure 5.10: Average elongation at rupture of unreinforced plastics, plastic composites, plastic foams and common construction materials

5.4.3. Poisson's ratio

The Poisson's ratio of plastic composites is related to the Poisson's ratio of unreinforced plastics. For example, composites display either a brittle or ductile behaviour. Therefore, Poisson's ratio of a brittle composite is assumed to be approximately 0.3, whereas the Poisson's ratio of a more ductile composite is assumed to be in the range of 0.4 to 0.45 (Kinney, 1967, p. 184). The Poisson's ratio under the initial loading of plastic foams, such as expanded polystyrene (EPS) according to Horvath (1993) is approximately 0.1.

5.4.4. Impact resistance

The impact resistance of a composite is mainly dependant on the choice of plastic matrix, the interface and the reinforcement (Murphy, 1998, p. 181). This high impact resistance of unreinforced plastic material is lowered by the addition of reinforcing agents, especially with the addition of a brittle reinforcement (Staunton, 1982, p. 516). Like the unreinforced plastics, the impact resistance of plastic composites is also influenced by temperature (Murphy, 1998, p. 181), as shown in Figure 4.10. An increase in the stiffness of the composite generally results in a decrease in the impact resistance (Staunton, 1982, p. 517).

5.4.5. Creep and shrinkage

Creep and slow flow

The effect of creep on plastic foams is dependent on the density of the foam. An increase in the density of the plastic foam will result in a decrease in the creep effects (Horvath, 1994). Similar to unreinforced plastics, plastic composites follow the typical strain-time as shown in Figure 4.11. The creep behaviour of unreinforced plastic materials is greatly dependent the on the type of plastic, time and temperature (Rosato & Rosato, 2004, p. 210). Composites are also dependent on these factors, however in a smaller degree (Rosato & Rosato, 2004, p. 210).

Shrinkage and warping

Age shrinkage of unreinforced plastic is insignificant in comparison to moulding shrinkage (Rubin, 1990). However, the mould shrinkage of most of the unreinforced plastics is relatively low. This is also true for plastic foams (Horvath, 1994). The addition of fillers or fibres, to an unreinforced plastic to produce a plastic composite, results in a reduction in volumetric as well as mould shrinkage (Murphy, 1998, p. 97; Young, 1982, p. 398). Mould shrinkage of composite materials is considerably reduced or even negligible by the addition of fibres or fillers to the unreinforced plastic (Rosato & Rosato, 2004, p. 16). Therefore,

insignificant shrinkage occurs with the addition of fillers or fibres, which results in these composites to be moulded to a close tolerance.

5.4.6. Fatigue

Plastic composites have a high resistance to the usual effects of fatigue (Staunton, 1982, p. 515). Most composites have a higher resistance to fatigue when compared to most metals and especially compared to unreinforced plastics (Rosato & Rosato, 2004, pp. 676-687). The resistance of fatigue behaviour of plastic composites is mainly influenced as follows:

- If the unreinforced plastic, that is used to produce the plastic composite, is ductile and has a high resistance to fatigue, the composite will have a better resistance to fatigue.
- If the type reinforcing agent, used in the composite, is stiff and also ductile, the composite will have a better resistance to fatigue.
- The reinforcing agent orientation is important to improve the resistance to fatigue of a plastic composite. Since a random orientation of the reinforcing agent might result in a lower resistance to fatigue of a plastic composite when compared to a reinforcing agent that is positioned perpendicular to the forced applied.
- A reinforcing agent with a long length improves the resistance to fatigue of a composite, especially if the reinforcing agent is positioned perpendicular to the forced applied.
- A reinforcing mat has a better resistance to fatigue than a single fibre, since a single fibre might have a random ordination, whereas a reinforcing mat ensures the alignment of the fibres.

5.4.7. Durability

The durability of plastic composites and plastic foams are dependent on numerous factors, where some include environmental conditions and thermal degradation. Environmental conditions can be subdivided into moisture (water) absorption, ultraviolet radiation and biodegradation. Biodegradation includes degradation caused by fungi and insects. An increase in moisture absorption of the plastic material can increase the biodegradation (Azwa, et al., 2013). All these types of degradation of plastic foams and composites (Figure 5.11) can lead to a decrease of mechanical properties. These degradations of plastic material are discussed below:

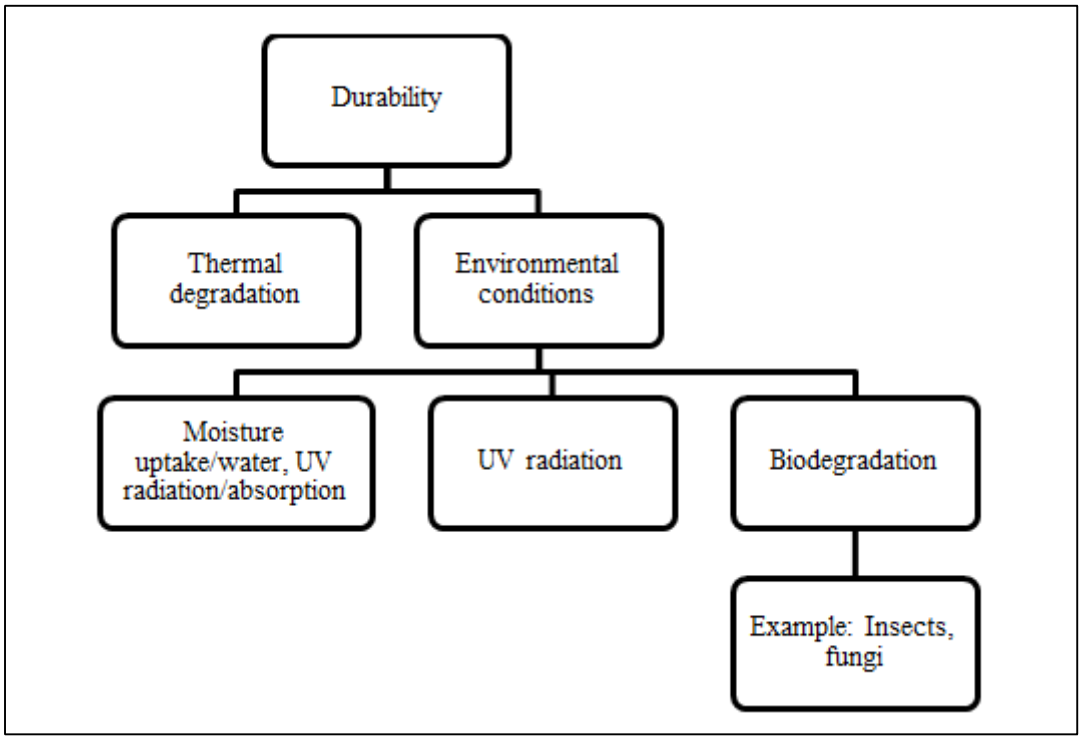

Figure 5.11: Degradations affecting durability of composite and plastic foams

Moisture uptake/ Water absorption:

Moisture (water) absorption by plastic foam is mainly dependent on the type of blowing agent, the type of gas-cell structure (open or closed-cells) as well as the type of plastic matrix (Vo, et al., 2011).

Composites' ability to absorb moisture (water) is mainly influenced by the following factors (Azwa, et al., 2013):

- The type of reinforcing agent: If the reinforcing agent is capable of absorbing water then the composite will exhibit an increase in the ability to absorb water.
- The amount of reinforcing agent that is detectable on the exposed surface of the plastic product: The reinforcing agent can cause an increase in the ability to absorb water of plastic composites.
- The plastic to reinforcing agent ratio: A larger plastic to reinforcing agent ratio results in a reduction of water absorption. This is true for all the plastic composite material.
- The type of plastic used in the composite: From Figure 5.12, it is clear that thermosets absorb more water, therefore if a thermoplastic material is used in the plastic composite the ability to absorb water is lower.
- The type of interface: The addition of some coupling agents can reduce the moisture uptake of composite.

- The time of moisture exposure: An increase of time results in an increase of water absorption, in the case of some composites.
- Temperature: An increase in temperature causes an increase of water absorption for some plastic composites.

The average percentage of water absorption of unreinforced plastics, plastic composites and plastic foams is shown in Figure 5.12. This figure is compiled from various sources (Rosato & Rosato, 2004, p. 2; Agarwal & Gupta, 2011; Rosato, 1982; Murphy, 1998; Fisher, 2013). Plastic foams have higher water absorption than thermoplastics, which might be due to voids at the surface of the material, caused by the manufacturing process. Composite plastics adsorb more water than unreinforced plastics, as shown in Figure 5.12. This is mainly due to the type of reinforcement. For example, wood is prone to water absorption, which cause WPC and FFC to have greater water absorption when compared to the other materials in Figure 5.12. This water absorption can cause an increase in the volume of the product and leads to a reduction in flexural strength (Pilarski & Matuana, 2005).

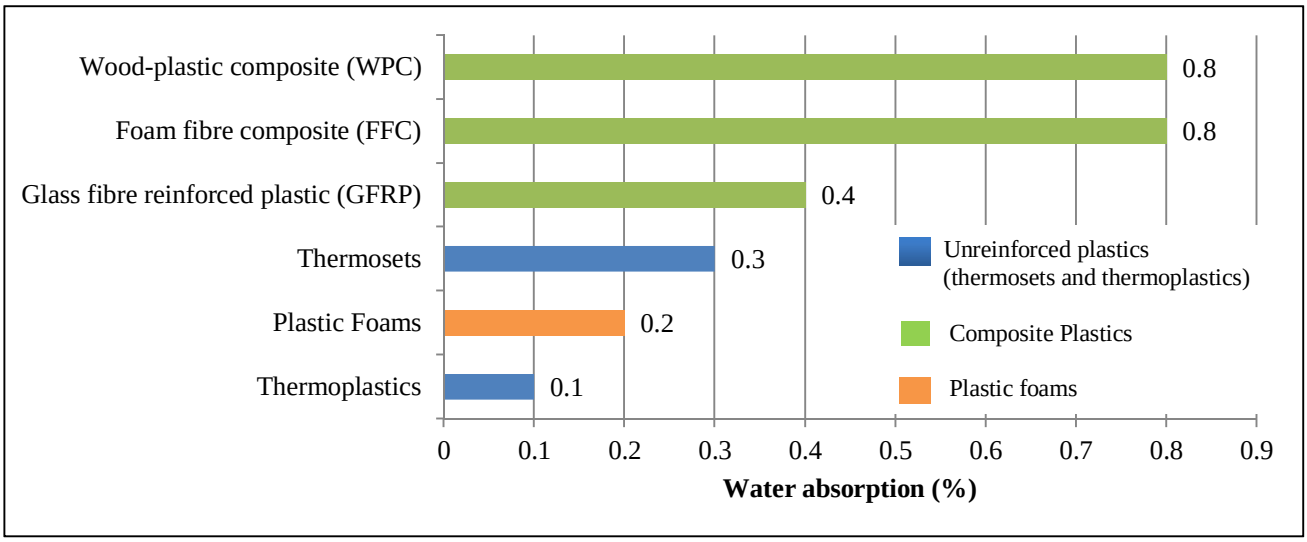

Figure 5.12: Average water absorption of unreinforced plastics, plastic composites and plastic foams

Degradation caused by ultraviolet radiation:

Plastic foams exposed to ultraviolet (UV) radiation mainly depend on the type of plastic, blowing agent and exposure intensity and time. UV radiation of plastic foams results in a continuous discoloration and becoming more brittle, as a function of exposure time and intensity. Thus, UV resistance of plastic foams is poor (Gan & Tan, 2003).

UV radiation absorbed by composites is termed photodegradation. Photodegradation of plastic composites can cause surface oxidation, chain scission, crosslinking and/or the breakdown of tied crystals and molecules. Surface oxidation and chain scission can result in micro cracks that form within the composite. Micro-cracks as well as the breakdown of tied crystals and molecules can result in mechanical properties degrading. Photodegradation can also cause crosslinking of composites, which can cause the material to become more brittle (Azwa, et al., 2013).

Degradation caused by UV radiation is mainly measured by the discoloration of the material as well as the decrease in elongation after exposure (Matuana & Kamdem, 2002). It is mainly influenced by the following (Matuana & Kamdem, 2002; Azwa, et al., 2013):

- Type of reinforcing agent: For example, a reinforcing agent that is more prone to UV absorption can an increase in deterioration of the composite.
- Type of plastic matrix: Different plastic materials respond differently to the absorption of UV radiation.
- The interface material: Some interface materials can reduce photodegradation.
- Manufacturing method: Discussed in Section 4.1.7.
- Climatic conditions: For different climatic condition, the UV radiation is different.
- Time of UV exposure: An increase in the time of UV exposure, can lead to an increase of degradation.

Additives can be added to improve the UV resistance of composite materials, to ensure an UV stable product (Fisher, 2013). However, ultraviolet light can reduce the flexural strength of WPC by approximately 14% (Fisher, 2013). According to Fruil Filiere Spa [S.a], FFC does not deteriorate when exposed to UV radiation. Glass fibre reinforced plastics (GFRP), on the other hand, can become brittle when exposed to UV radiation (Benjamin, 1969).

Biodegradation:

Plastic foams have a high resistance to biodegradation, since no composite within the plastic foams attracts fungi, termites or mildew (Gan & Tan, 2003). Whereas plastic composites, such as WPC and FFC, contain wood-flour, which is attractive for fungal, termites and/or mildew. The biodegradation of plastic composites is mainly dependent on the following (Azwa, et al., 2013):

- Type of reinforcing agent. For example, the addition of wood-flour increases the biodegradation of the composite material, whereas, in the case of GFRP, glassfibre has a high resistance against fungi and termites.

- The plastic to reinforcing ratio: For example, a higher plastic to wood ratio results in a higher resistance to mildew and termites.
- The interface material: Some interface materials can increase the resistance to mildew, termites and fungi.
- Moisture content: The higher the moisture content within the composite the greater is the biodegradation due to fungi.

Thermal degradation

As mentioned before, the mechanical properties of unreinforced plastic material are influenced by temperature. Increase in temperature can cause a decrease in the mechanical properties. Thermal degradation is mainly dependent on the following:

- Type of unreinforced plastic material, its glass transition temperature (Section 5.5.2) and burning characteristics (Section 5.5.6): The lower the glass transition temperature, the greater the thermal degradation.
- The interface material, such as lubricant and coupling agent: Some interface materials can decrease the thermal degradation.
- Type of reinforcing agent: For example, the addition of wood-flour increases the thermal degradation of the composite material, whereas, in the addition of a reinforcing agent with a high thermal conductivity can decrease the thermal degradation.
- Ratio of plastic to reinforcing agent: An increase in this ratio can result an in increase in the thermal degradation.

5.5. Thermal properties

The most important thermal properties of plastic composites and plastic foams are discussed in this section. Most of the thermal properties are governed by the unreinforced plastic material. However, most of the thermal properties improve with the addition of a reinforcing agent. Table A.3 in Appendix A, represent a summary table of thermal properties of plastic composites and plastic foams.

5.5.1. Specific heat

The average specific heat of unreinforced plastics, plastic composites, plastic foams and common construction materials is shown in Figure 5.13. This figure is compiled from various sources (Rosato &

Rosato, 2004, pp. 2,1009; Friul Filiere Spa, [S.a]; Agarwal & Gupta, 2011; Fisher, 2013). The specific heat of the GFRP was not available and therefore it is not shown in Figure 5.13.

Form Figure 5.13, it is clear that addition of fibre or fillers to an unreinforced plastic material can result in an increase in specific heat as in the case of WPC. However, FFC has a lower specific heat than thermoplastics. Thus, the type of reinforcing agent as well as the amount of reinforcing agent on the exterior surface of the product plays the main roles in the specific heat of composite material.

The open and closed-cell plastic foams have insignificant differences when specific heat is concern. This is due to approximately the same amount of energy is needed to heat the open and closed-cell plastic foams to the same temperature. When the specific heat of the plastic foams is compared to the unreinforced plastic, less energy is needed to cause a rise in the temperature of the plastic foams. This is due the gas cells in the plastic foams. The specific heat of the plastic foams is, however higher than most of the common building materials.

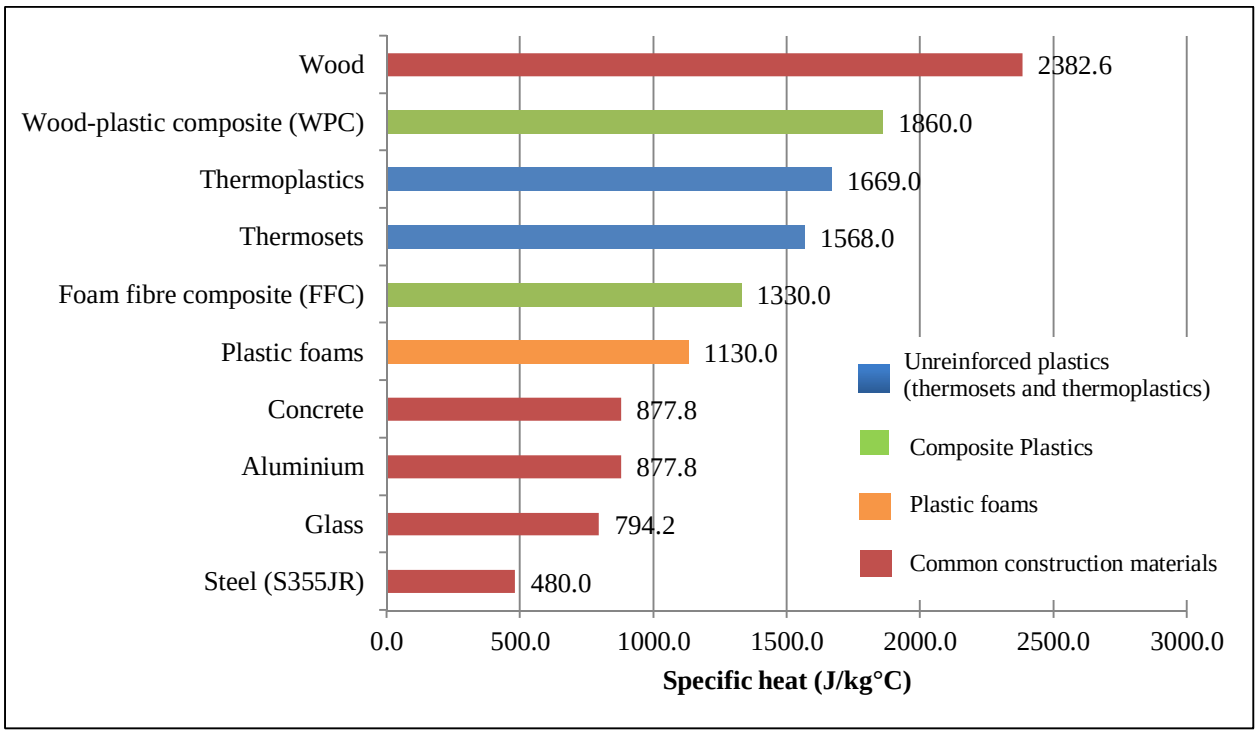

Figure 5.13: Average specific heat of unreinforced plastics, plastic composites, plastic foams and common construction materials

5.5.2. Transition temperature

All plastic materials have a transition temperature. The transition temperature of composites is governed by the unreinforced plastic, as discussed in Section 4.2.2.

5.5.3. Thermal conductivity

The thermal conductivity of unreinforced plastics, plastic composites, plastic foams and common construction materials is shown in Figure 5.14. Figure 5.14 is compiled from various sources (Rosato & Rosato, 2004, pp. 2,1009; Friul Filiere Spa, [S.a]; Agarwal & Gupta, 2011; Fisher, 2013).

In closed-cell plastic foams, the gas is stagnant. This result in a material that is extremely resistance to the transfer of heat, thus plastic foams have a low thermal conductivity (Agarwal & Gupta, 2011). In open-cell plastic foams, the gas has the ability of some movement. Therefore, the thermal conductivity of open-cell foams is higher when compared to a closed-cell foams. However, plastic foams are generally used as insolative materials, hence a low thermal conductivity.

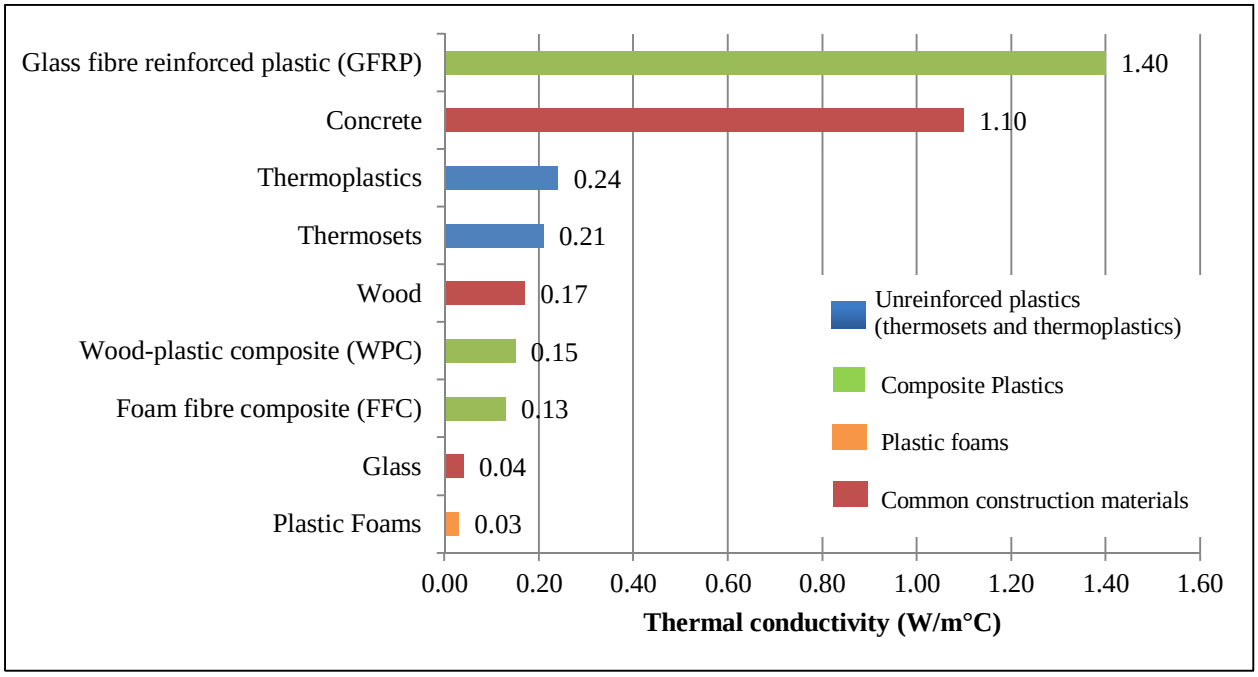

Figure 5.14: Average thermal conductivity of unreinforced plastics, plastic composites, plastic foams and common construction materials

When composite materials are considered, the addition of fibre or fillers to an unreinforced plastic material can result in an increase in the thermal conductivity of the product. This increase in thermal conductivity is influenced mainly by the type of reinforcing agent (Rosato & Rosato, 2004, p. 694). For example, when vegetal fibre is used as a reinforcing agent (as in the case of FFC), the thermal conductivity is lower than when glass fibre is used as a reinforcing agent (as in the case of glass fibre reinforced plastics). Reinforced plastics can exhibit a thermal conductivity as high as 1.25 W/m°C (Rosato & Rosato, 2004, p. 2).

5.5.4. Coefficient of thermal expansion

The average coefficient of thermal expansion of unreinforced plastics, plastic composites, plastic foams and common construction materials is shown in Figure 5.15. This figure is compiled from various sources (Rosato & Rosato, 2004, pp. 2,900; Friul Filiere Spa, [S.a]; Agarwal & Gupta, 2011; Murphy, 1998; Fisher, 2013). The large coefficients of thermal expansion of plastic foams result in larger contraction and expansion in this plastic matrix (Palin, 1967, p. 51). This indicates that moulded shrinkage is present in plastic foam materials and therefore cannot be moulded to such close tolerances (Palin, 1967, p. 51).

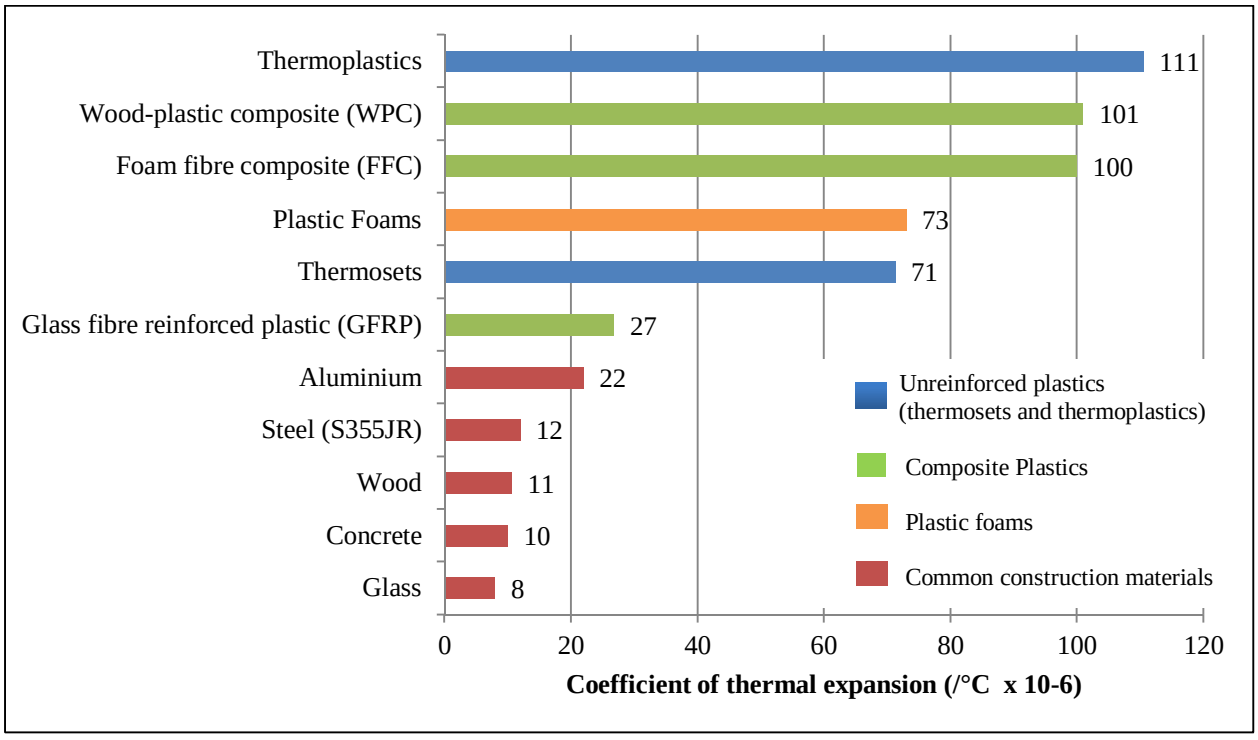

Figure 5.15: Average coefficient of thermal expansion of unreinforced plastics, plastic composites, plastic foams and common construction materials

The composite material exhibits a much larger coefficient of thermal expansion and it can be compared to the coefficient of thermal expansion of common construction materials. However, when compared to thermoplastic materials the coefficient of thermal expansion is lower. Therefore, the addition of a reinforcing agent results in a lower coefficient of thermal expansion. The coefficient of thermal expansion of plastic composites is influenced by the type of unreinforced plastic, the type of reinforcing agent, the form and length of the reinforcing agent and plastic resin to reinforcement ratio.

5.5.5. Heat distortion temperature

The heat distortion temperature is defined as the temperature that causes a specific deflection in a standard test bar under a specified load (Lubin, 1982). The average heat distortion temperature of unreinforced plastics, plastic composites and plastic foams is shown in Table 5.1. This table is compiled from various sources (Friul Filiere Spa, [S.a]; Agarwal & Gupta, 2011; Murphy, 1998; Palin, 1967; Fisher, 2013; Eva-Last, [S.a]). From Table 5.1, FFC requires a much lower temperature to result in a deflection in a standard test bar, when compared to glass fibre reinforced plastics. This might be due to the vegetal fibres and the thermoplastic resin of FFC. Glass fibre reinforced plastics perform better under temperature than unreinforced plastics as well as plastic foams. Thus the heat distortion temperature of composites are mainly dependent on the plastic resin, the type of reinforcing agent as well as the ratio of plastic to reinforcing agent.

Table 5.1: Average heat distortion temperature of unreinforced plastics, plastic foams and plastic composites

	Heat distortion temperature (°C)
Foam fibre composite (FFC)	65
Plastic foams	90
Thermoplastics	98.6
Wood-plastic composite (WPC	100.6
Thermosets	164.5
Glass fibre reinforced plastic (GFRP)	190.5

5.5.6. Flammability

Most plastic foams are self-extinguishing (Barito & Eastman, 1975, p. 7.63). EPS has an ignition temperature range of 350°C to 490°C (Agarwal & Gupta, 2011). However, the flammability of plastic foams as well as plastic composites is controlled by the unreinforced plastic matrix, as shown in Section 4.2.5. The addition of fibres or fillers can improve the flame resistance of the composite material (Rosato & Rosato, 2004, p. 844). This improvement of the flame resistance can be considered minor. Composite materials can be highly resistant to flames, when flame retardant additives are added to the composite material.

5.6. Chemical properties

The chemical properties of composite and plastic foams are mainly governed by unreinforced plastics, as discussed in Section 4.3. The reinforcing agent as well as the amount of reinforcing agent exposed to an exterior surface can influence the chemical properties of a plastic composite.

5.7. Moulding techniques

The moulding techniques of plastic foams, such as EPS and XPS are discussed in Section 5.1. The moulding techniques discussed for unreinforced plastics, in Section 4.4, are applicable for plastic composite materials. However, injection moulding or extrusion moulding are the preferred moulding techniques for plastic composite materials (Rosato, 1997).

5.8. Summary

The properties of composite materials are mainly dependent on the following:

- Type of plastic material
- Type of interface materials
- Reinforcing agent (type, orientation, length and form)
- Ratio of plastic to reinforcing agent

The properties of plastic foams, on the other hand, mainly depend on the following:

- Type of plastic material
- Blowing agent
- Amount of gas within the plastic medium
- Closed- or open-cell structure

Unreinforced plastics have properties which can be a disadvantage when used for structural applications. These properties include Young's modulus, creep, fatigue and durability. With the addition of a reinforcing agent and interface material, these properties can be improved. In the case of WPC and FFC, where the main plastic component is PVC and the reinforcing agent is wood-flour, the tensile- and flexural strengths might be lower compared to unreinforced plastic. However, the addition of a reinforcing agent and interface material improve the other properties of unreinforced plastic materials. Thus, the composite material might exhibit adequate properties for a load bearing system.

The plastic foams exhibit poor properties, especially when emphasis is placed on a structural application. However, they are excellent thermal insulators, since they exhibit relatively high specific heat and a low thermal conductivity.

CHAPTER 6: BUILDING ENVELOPE AND VIABLE MATERIALS

In order to reach the aim and objectives of this study, a design for a load-bearing walling, flooring and roofing system (excluding the design of connections) for the application in a low-income housing unit needs to be determined. The viable materials must also be identified for this building envelope. With knowledge gained from Chapters 4 and 5, the viable materials and adhesives are discussed in this chapter. The viable plastic materials are chosen based on their cost and their material properties.

The design is discussed in terms of the roofing, walling and flooring systems. A plan view of the modular plastic house is shown in Figure 6.1 (see Appendix C, Figure C.1). This is representative of a 41m^2 government subsidised housing unit. Connections are not part of the scope, thus are not designed.

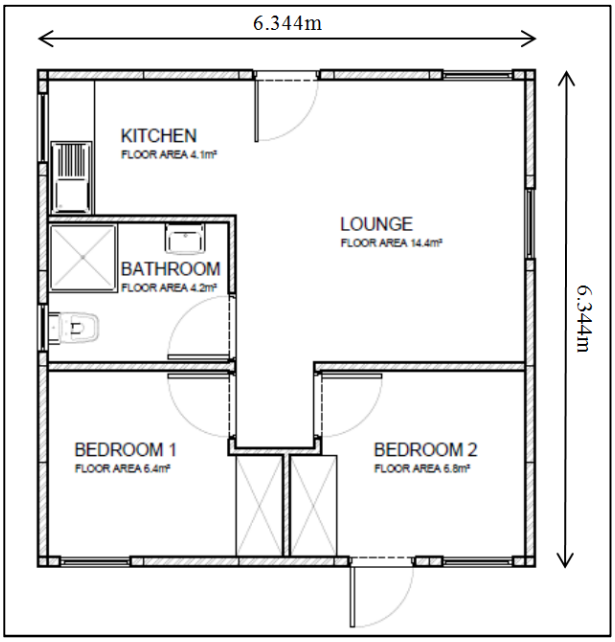

Figure 6.1: Plan view of modular plastic housing unit

6.1. Roofing system

The design of the roofing system is done according to the requirements of SANS 10400-L (2011). It states that for roofing systems the following requirements should be satisfied (SANS 10400-L, 2011, p. Table 1):

- The roof should not have an angle of slope less than 11°
- The minimum overhang of the roof is 250mm

The roofing system consists of a truss system and roof sheeting. Six trusses and three rafters form the truss system. The truss system is made up of wood members with dimensions of 48x73mm and it is shown in Figure 6.2. In this figure, at points a, b and c rafters connect to the roof trusses to provide lateral support to the roof trusses and the walls.

Figure 6.2, only half of the roof truss members have numbering. This is due to symmetry. The truss members' numbers are used to describe the length of each truss, as shown in Table 6.1. Also, note that the angle of the roofing system is 11.2° and the overhang is 300mm. Both the angle of slope and the overhang of the roof meet the requirements stated in SANS10400-L (2011).

The trusses are exposed at two sides of the housing unit. One of these surfaces is shown in Figure 6.2. These surfaces are closed with a 5mm triangular sheet (gable) and it is connected to the roof trusses and to the wall. These gable sheets are made of the structural material used for the walling system. It is typically connected by bolts.

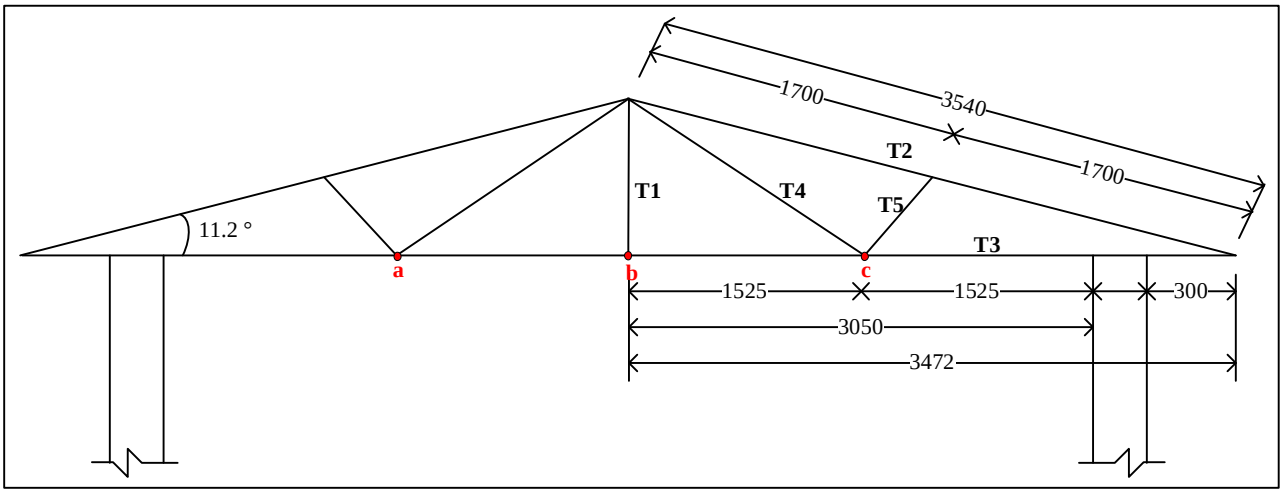

Figure 6.2: Roof trusses

The roof sheeting, on the other hand, is comprised of 1220x3450x25mm material which is the same material as used for the structural elements in the walling system. This sheeting connects the truss system and has corrugated cross-sectional shape (the same as metal sheeting). This ensures that the area on which wind lift-up forces act, is lesser than that of a flat surface is more susceptible to wind up-lift forces. The applied force is carried by two parts of the roof sheeting as explained in Figure 6.3. The roof sheeting is typically connected to roof trusses by using holding down hooks, in the same manner, that metal sheeting is connected

to trusses. The distances and sizes of these hooks are not determined since connections are not part of the scope.

Table 6.1: Lengths of roof trusses

Truss number	Length (mm)
T1	690
T2	3450
T3	3472
T4	1800
T5	403

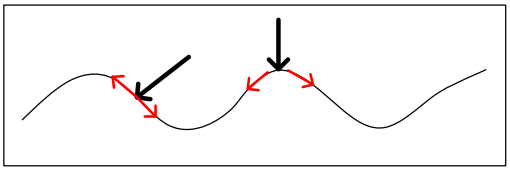

Figure 6.3: Load effects on corrugated shape roof sheeting

6.2. Load bearing walling system

The walling system for the internal and external walls consists of a structural sandwich construction. This consists of three parts, which are shown in Figure 6.4. The three parts are a pair of structural face panels (the interior and exterior structural panel), a core panel and an adhesive. The face (interior and exterior) panels are made from a plastic composite material, whereas the core panel consists of plastic foam. The core material is usually not considered as a load bearing element. The purpose of the core material is to serve as insulation and to house services, where the plastic composite face panels are load bearing elements.

The dimensions of the internal and external sandwich wall panels are 1220x2700x90mm and 1220x2700x122mm respectively. For the internal and external walls, the thicknesses differ, as shown in Table 6.2. The total thickness of the external walls is 122mm, whereas, the total thickness of the internal walls is 90mm. The internal wall thickness is sufficient to ensure the fixing of door frames.

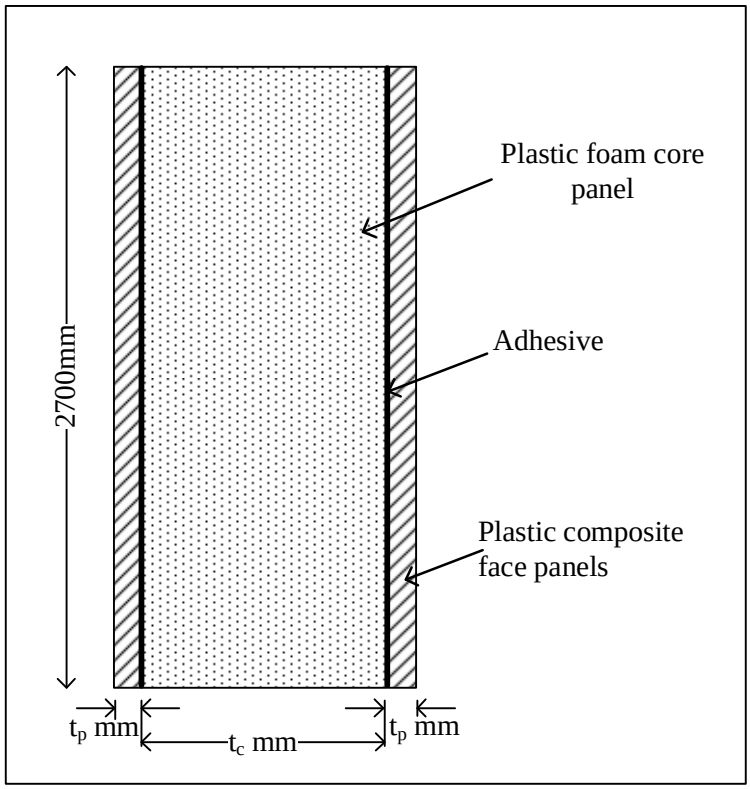

Figure 6.4: Cross-section of a wall panel (sandwich panel)

Table 6.2: Wall panel thicknesses

	External walls	**Internal walls**
t_c - Core panel thickness (refer to Figure 6.4)	100 mm	75 mm
t_p - Structural face panel thickness (refer to Figure 6.4)	11 mm	7.5 mm
Total thickness	122 mm	90 mm

The wall panels are typically connected by an interlocking connection system, which is continuous over the height of the wall. An interlocking connecting part is made from the structural face panel material. The connection is dipped in an adhesive and then inserted in between two panels, where it sets, expands and provides a connection. This interlocking connection is shown in Figure 6.5. The walls are connected by means of strap ties to the roof trusses.

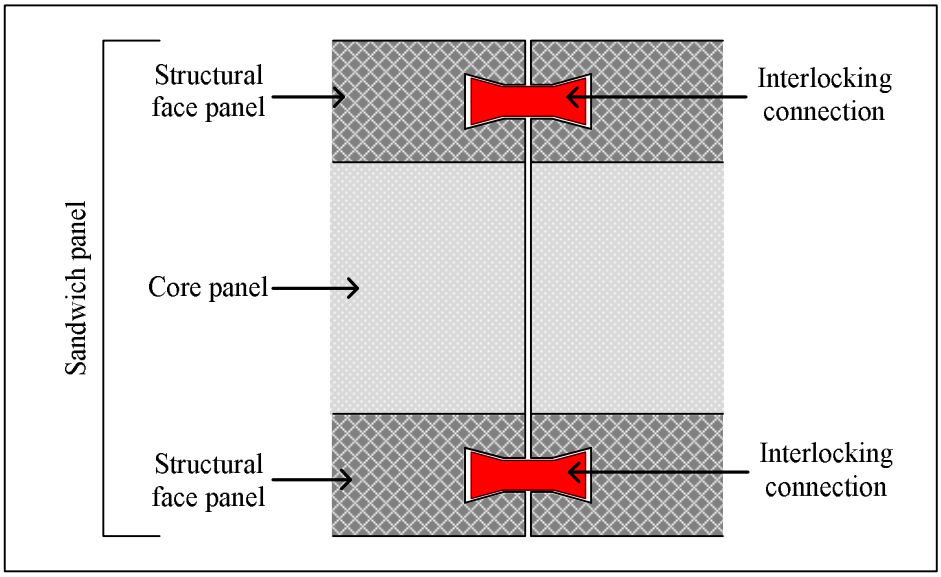

Figure 6.5: Typical wall to wall interlocking connection (Top view)

The sandwich wall panels are supported by a concrete strip footing. A typical connection of the wall panels to the strip footing is shown in Figure 6.6. From this figure, it is clear that the concrete strip footing provides elevation of the housing unit. This is required especially when the housing units are built in such a manner that water can enter the housing unit if no elevation is provided.

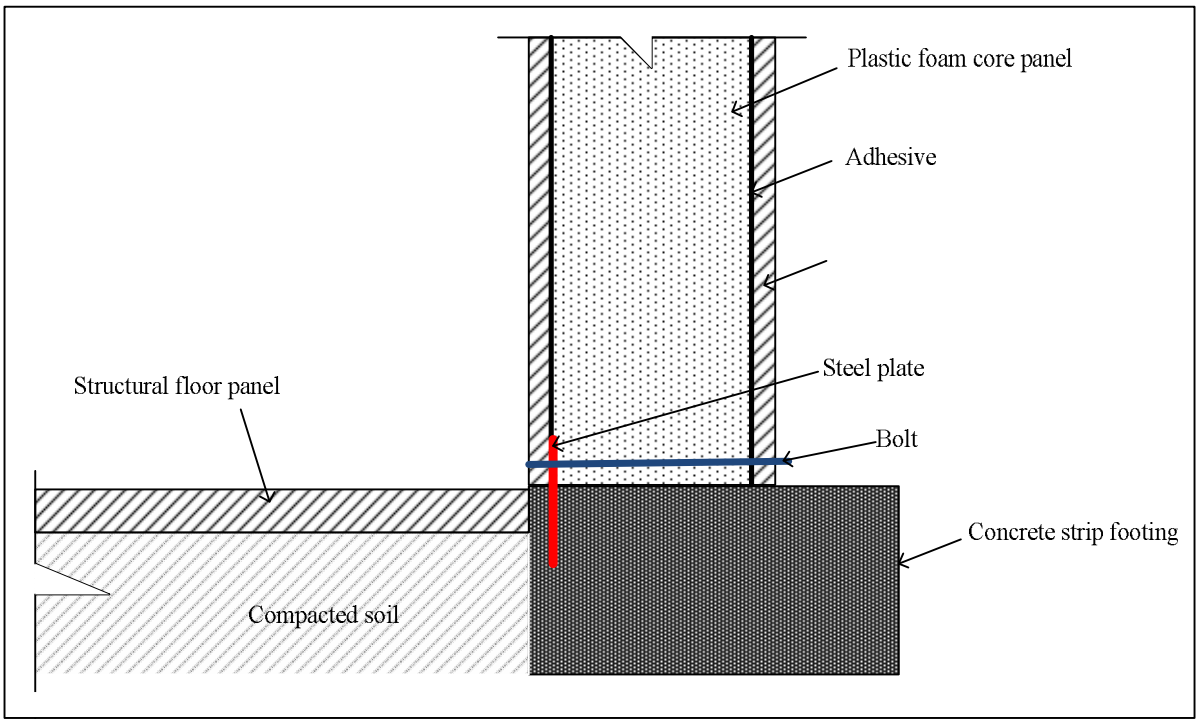

Figure 6.6: Typical walling system to concrete strip footing connection

6.3. Flooring system

The flooring system consists of a single panel with dimensions of 1220x1220x10mm. This panel is comprised of the same material used for the face panel of the walling system as shown in Figure 6.6. The flooring system is supported by compacted soil as shown in Figure 6.6. It is not connected to the concrete strip footing, to enable contraction and expansion of the floor panels. The floor panels would typically be connected similarly to that of the walling systems (Figure 6.5).

6.4. Viable materials

The core panel in the walling system is comprised of plastic foams. Expanded polystyrene (EPS) and extruded polystyrene (XPS) have been considered as viable core materials. EPS and XPS provide adequate insulation and exhibit low weight properties (Agarwal & Gupta, 2011). The structural face panels for the walling system and roofing system consist of a plastic composite material. Glass fibre reinforced plastic (GFRP), wood plastic composite (WPC) and foam fibre composite (FFC) are considered for the face panels. Adhesives that are compatible with EPS and XPS are considered.

6.5. Material properties of viable materials

The mechanical properties of the materials used for the face panels as well as the core materials are compared in this section. Refer to Chapter 5, where properties of plastic composites and plastic foam are discussed.

6.5.1. Materials for structural face panels and roofing panels

When WPC is considered, different manufactures use different types of reinforcing (in this case wood-flour was used rather than wood fibre), type of unreinforced plastic material and plastic to wood ratio. Therefore, the properties of a few manufactures were considered. FFC is produced by Friul Filiere Spa (see Section 2.3.6). GFRP, on the other hand, differs in terms of the form of reinforcing agent (in this case, single fibre was used) and the type of unreinforced plastic material. The optimum glass fibre content was considered for a specific unreinforced plastic to ensure the optimum properties of the composite (Murphy, 1998).

The comparison of mechanical properties of the viable material for the face panels is shown in Table 6.3. As mentioned in Chapter 5, composite material requires an interface, such as a coupling agent as well as a lubricant. MAPP (Maleated polypropylene) is a typical coupling agent and ZnSt (fatty acid metal soap) is a typical lubricant. The percentage of glass fibres is determined by volume of the composite material.

Table 6.3: Mechanical properties of viable materials for face panel for the walling system and panels for roofing system (Friul Filiere Spa, [S.a]; Leu, et al., 2012; Fisher, 2013; Murphy, 1998; Fisher, 2013)

Material	Description	Density (kg/m^3)	Tensile yield strength (MPa)	Compressive yield strength (MPa)	Young's modulus (GPa)	Flexural strength (MPa)	Water absorption (%)
FFC	PVC + vegetal fibres	650 - 750	15	15	-	35	0.8 (1)
WPC	47%PP, 47% wood-flour, 3% MAPP, 3% ZnSt (A)	1120	-	-	2.9	29.5	1.4
	4EVERDECK (PE, PP, wood-flour)	1331	14.2	31.3	0.84 (2)	24.4	0.77
	ECOWOOD (50% PVC, 50% wood-flour)	1331	13	20	-	35	0.8
	EVALAST (40% recycled HDPE, 60% wood-flour)	1390	-	-	-	21.8	0.2
GFRP	EP 80% GF	2080	551.7	310.3	27.6	689.6	0.5
	Nylon 6.6 30% GF	1480	158.6	182.8	8.3	241.4	0.5
	Nylon 6 30% GF	1370	165.5	165.5	7.2	200	1.3
	PET 30% GF	1560	144.8	172.4	9	220.7	0.05
	PP 40% GF	1040	44.8	172.4	3.7	57.2	0.05
	ABS 20% GF	1220	75.9	96.6	6.2	106.9	0.3

Note:

(1) – Water absorption at 50°C for 48hours

(2) – Compressive modulus

(A) – HDPE tensile strength of 20MPa

\- Not available

FFC has the lowest density and is therefore the least heavy of the materials shown in Table 6.3. However, it has relatable properties to WPC. The GFRP has much greater density and strength when compared to FFC and WPC. This is also illustrated in Chapter 5.

6.5.2. Core panel

The core panel is only used in the sandwich panel of the load bearing walling system. The comparison of mechanical properties of viable materials for the core panel is shown in Table 6.4. Refer to Chapter 5 for more information on plastic foams. Table 6.4 shows that XPS has a higher strength than EPS, however XPS also has a greater percentage of water absorption than EPS. Since the core material is sandwiched in between two face panels, insignificant water absorption is expected.

Table 6.4: Mechanical properties of viable core panel materials of the walling system (Agarwal & Gupta, 2011)

Material	Description	Density (kg/m^3)	Tensile yield strength (MPa)	Compressive yield strength (MPa)	Young's modulus (GPa)	Flexural strength (MPa)	Water absorption (%)
EPS	EPS properties depended on the density (1)	12-50	0.11-0.14	0.07-0.5	0.001-0.004	0.14-0.21	0.03-0.1
XPS	XPS properties depended on the density (1)	20-80	-	0.4-1	-	-	0.6

Note:
(1) – Properties for medium density
\- Not available

The core material is mainly used for insolation therefore, the thermal properties of core material are important. The thermal properties of EPS and XPS are shown in Table 6.5. EPS has a slightly higher thermal conductivity than XPS. However, this is an insignificant difference. EPS has a lower minimum and higher maximum service temperatures than XPS. This makes this material more suitable for a structural purpose, such as housing.

Table 6.5: Thermal properties of viable core panel materials of the walling system (Agarwal & Gupta, 2011).

Material	Specific heat (J/kg°C)	Thermal conductivity (W/m°C)	Coefficient of thermal expansion (/°C x10^{-6})	Heat distortion temperature (°C)	Maximum temperature (°C)	Minimum temperature (°C)	Flammability
EPS	1130	0.029-0.041	60-80	90	80	-100	• Same or lesser toxic risk as natural materials (see Section 6.6.2) • EPS is combustible. (ignition temp 350 -490°C)
XPS	-	0.025-0.035	75	-	75	-60	Hydrochlorofluoro-carbon (blowing agent) is harmful and is banned from Europe
Note: Properties for medium density - Not available							

The properties of EPS as well as XPS are sensitive to the density. Only the properties of EPS were available from the manufacturer, in this case Isolite. These are shown in Table 6.6. In this table, the standard densities of EPS are shown. It is clear that a higher density results in improved mechanical properties.

Table 6.6: Material properties of various EPS densities (Rachel, 2013)

		Units	SD	HD	EHD
Mechanical properties	**Density**	kg/m^3	15	20	30
	Tensile strength	MPa	0.2	0.28	0.44
	Compressive strength	MPa	0.08	0.12	0.21
	Shear strength	MPa	0.19	0.27	0.46
	Young's modulus	GPa	0.002	0.006	0.001
Thermal properties	**Thermal conductivity**	W/m°C	0.03	0.038	0.036
	Specific heat	J/kg°C	1500	1500	1500
	Coefficient of thermal expansion	$/°C \times 10^{-6}$	70	70	70
	Maximum temperature	°C	70	70	70
	Minimum temperature	°C	-110	-110	-110

6.6. Material cost of viable materials

In this section, the cost of the structural face panels, core panel materials and adhesives are compared.

6.6.1. Materials for structural face panels

The costs of FFC, WPC and GFRP are compared in terms of cost per square meter and are shown in Table 6.7. This table is based on a thickness of 11mm. Note the WPC and FFC prices were supplied by manufactures, which includes finishing (to ensure a smooth surface), lubricant, and coupling agent costs. The GFRP does not include finishing cost (to ensure a smooth surface), lubricant, and coupling agent cost. This can result in a higher actual cost. The cost of unreinforced plastic used for GFRP can also differ.

For Table 6.7, it is clear that FFC is the least expensive and GFRP is the most expensive. The cost estimation of WPC depends on the manufacturer, where EverJade is a company based in China. This implies that transport cost needs to be added to the cost estimate.

Table 6.7: Cost estimation of viable materials for face panel for the walling system (Friul Filiere Spa, [S.a]; Fisher, 2013; Fisher, 2013; Eva-Last, [S.a]; Murphy, 1998; Harper, 1975)

Material	Description	Price (R/m^2)
FFC	PVC, vegetal fibres and other additives	128.63
WPC	Everjade (WPC)	137.03
	ECOWOOD (50%PVC, 50% Wood flour)	244.22
	4EVERDECK (PE,PP, Wood flour)	278.52
	EVA-LAST (40%recycled HDPE, 60%wood flour)	279.15
GFRP	Acrylonitrile butadiene styrene (ABS) 20% GF	2952.52
	Polyester (unsaturated) (UP) 30% GF	4069.85
	Polypropylene (PP) 40% GF	4094.80
	Polycarbonates (PC) 10% GF	4911.88
	Nylon 6.6 30%GF	5581.08
	Nylon 6 30%GF	5606.96
	Polyester (PET) 30%GF	5941.71
	Epoxy (EP) 80%GF	7481.50
Note: GF = Glass fibre R9.88/ USD R 12.85/EURO		

GFRP is known to be stronger than the rest of the materials in Table 6.7. Thus, as an extreme example, if the GFRP walling system is assumed to have a thickness of 1mm (which will create an extremely slender member) and the rest of the materials have a thickness of 11mm, the cost comparison results are as shown in Table 6.8. The cost of the FFC and WPC products includes surface finishes, whereas the cost of the GFRP products does not include surface finishes. Thus, in all instances except one, the FFC and WPC products are cheaper than the GFRP, however additional cost for surface finishes should be added to the cost of the GFRP products. The cost estimation calculations are shown in Appendix B.

Table 6.8: Cost comparison of a 1mm thick GFRP structural face to an 11mm thick FFC and WPC structural face (Friul Filiere Spa, [S.a]; Fisher, 2013; Fisher, 2013; Eva-Last, [S.a]; Murphy, 1998; Harper, 1975)

Material	Description	Price (R/m^2)
FFC	PVC, vegetal fibres and other additives	128.63
WPC	Everjade (WPC)	137.03
	ECOWOOD (50%PVC, 50% Wood flour)	244.22
	4EVERDECK (PE,PP, Wood flour)	278.52
	EVA-LAST (40%recycled HDPE, 60%wood flour)	279.15
Glass fibre reinforced plastic	ABS 20% GF	268.41
	UP 30% GF	369.99
	PP 40% GF	372.25
	PC 10% GF	446.53
	Nylon 6.6 30%GF	507.37
	Nylon 6 30%GF	509.72
	PET 30%GF	540.16
	EP 80%GF	680.14

6.6.2. Core panel

Expanded polystyrene (EPS) and extruded polystyrene (XPS) differ in terms of their blowing agent and manufacturing processes. EPS uses carbon dioxide or pentane as a blowing agent, whereas the blowing agents used in XPS include pentane and hydrochlorofluoro-carbon. When EPS is burnt, the fumes have the same or lesser toxic risk as natural materials, such as wood or wool (Lee, et al., 2006). Gasses produced by burning EPS are carbon monoxide (CO), which is, to some extent, always emitted by fires (Baker, 2002). The odor when EPS burns can be detected at a concentration of 25 parts per million (ppm), whereas a fatal intake is approximately 10000ppm of CO. The amount of CO released when EPS burns, increases with an increase in temperature. For example, when EPS burns at 30°C a CO concentration of 50ppm is released and at 600°C a CO concentration of 1000ppm is released (Baker, 2002), which is lower than the fatal intake threshold. However, the plastic foam (EPS or XPS) is enclosed in structural face panels (Figure 6.4), which reduce the risk of the emissions of CO in the housing unit (Baker, 2002).

EPS is produced by moulding polystyrene beads saturated with the blowing agent (Agarwal & Gupta, 2011). These polystyrene beads are heated and the expansion of the blowing agent results in a foam-like structure (Lee, et al., 2006). The blowing agent of XPS, hydrochlorofluoro-carbon, is considered a harmful product,

especially when burnt and is thus banned from use in Europe (Chau, et al., 2011). Other blowing agents are currently investigated for XPS, which is produced by a complex extrusion process.

EPS is considered the least expensive core panel material, when EPS and XPS are considered, since EPS is produced by a simpler and less expensive process. According to Stec & Hall (2011), EPS is also considered as the plastic foam material that emits the least toxic fumes when burnt.

6.6.3. Adhesive

Some adhesives were considered for the structural application. The adhesives are limited due to the compatibility of the adhesive with the plastic foams. The costs per square metre as well as cost per litre of the compatible adhesives are shown in Table 6.9. It is clear that epoxy adhesives are the most expensive adhesives. Thus, the least expensive adhesives, The Pekadur A663 polyurethane adhesive and the GB685 spray grade rubber adhesive were selected as the viable adhesives.

Table 6.9: Costs of the adhesives

Adhesive (manufacturer)	Cost	Amount (ml)	Rand/litre	Rand/m^2
Pekadur A663 Polyurethane Adhesive (Pekay)	136.45	5000	27.29	5.46
GB685 Spray grade synthetic rubber adhesive (Pekay)	183.39	5000	36.68	12.23
Stixall (EverBuild)	114	300	380.00	20.73
Polystyrene foam adhesive (Genkem)	105	500	210.00	35.00
Geocell : Flexible Acrylic Fillers (Abe)	40	310	129.03	64.52
MaxTrack (Sika)	70	300	233.33	77.78
Sick2 Rapid Epoxy Syringe Adhesive (EverBuild)	62	24	2583.33	80.73
Rapid Epoxy (Alcolin)	82	24	3416.67	106.77
Spabond 340LV (Amt)	497.21	1000	497.21	248.61

6.7. Summary

As this design is for a low-income house, the cost needs to be as low as possible, but the mechanical properties required for structural use, need to be met. Therefore, the roof trusses as well as the rafters are made from grade 5 Pinewood.

FFC has properties that are relatable to the properties of WPC. However, GFRP exhibits much higher and thus better mechanical properties compared to the WPC and FFC. FFC is the cheapest material of the viable structural materials considered, especially when compared to GFRP. For the roof sheeting, the structural face panels of the walling system and the flooring system, FFC is considered the most viable, with WPC as an alternative material. However, due to logistical problems, FFC was not available. Therefore, WPC was used as the viable material.

EPS and XPS, which were both considered for the core material, exhibit nearly the same mechanical and thermal properties, with insignificant differences. However, the process to produce EPS is less expensive than the process used to produce XPS. Therefore, EPS is considered the least expensive material of the viable core material considered. XPS also uses a blowing agent that is harmful. Therefore, EPS with a density of 15kg/m^3 is considered the most viable core material. This was supplied by Isolite Cape.

The Pekadur A663 polyurethane adhesive and the GB685 spray grade rubber adhesive manufactured by Pekay were considered the two most viable adhesives. The Pekadur A663 polyurethane adhesive is used mainly in the cooling industry, where an adhesive is used to attach steel plates to polystyrene foam. The steel undergoes contraction and expansion, which results in large residual stresses. These stresses are absorbed by the adhesive to ensure no failure in the polystyrene foam. The GB685 spray grade rubber adhesive is mainly used for the bonding of polystyrene foam when used as a contact adhesive. This adhesive creates a soft glue line. The relative bond strength of these two adhesives is compared in Chapter 7.

CHAPTER 7: EXPERIMENTAL WORK

In this chapter, experiments are reported which were conducted to determine the material properties of materials such as WPC (wood-plastic composite), EPS (expanded polystyrene) and the adhesives (Pekadur A663 polyurethane adhesive and GB685 spray grade rubber adhesive). These properties are used to investigate the structural feasibility (Chapter 8) of the building envelope described in Chapter 6. The following experiments are reported in this chapter, where for each of these experiments the test methodology and the result of the experiment are described:

- Relative bond strength of the adhesives
- Direct compression test of WPC
- Direct tension test of WPC
- Four-point bending test of WPC
- Compressive creep test for WPC
- Direct compression test of EPS
- Push-through shear test of composite sandwich panel
- Four-point bending test of Composite sandwich panel

A 15 kg/m^3 EPS supplied by Isolite Cape, is used as the core material. Due to unforeseen circumstances, WPC is used as the structural element for the experiments, instead of FFC (fibre foam composite). The manufacturer of WPC, Ecowood, is the least expensive and therefore this product (WPC: 50%PVC and 50% wood-flour) is chosen. Ecowood only supply decking plank sizes of 110x4000x22mm. The material exhibits cracks throughout the cross-section of the decking planks as shown in Figure 7.1. This could be due to the 50% wood-flour and the extrusion moulding. The extrusion moulding process causes the flour to align in a horizontal direction, due to the pressure and pulling actions associated with this process. This results in bundling of only wood-flour with no interface material. This could causes cracks within the material, since the wood-flour has insufficient dimensions to bridge the larger crack widths. Another explanation for the occurrence of these cracks can be the effects of mould shrinkage.

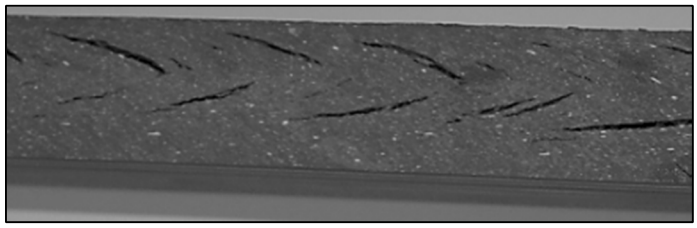

Figure 7.1: Cracks throughout the cross-section of the WPC decking planks

The planks were cut to the specimen size needed for each experiment. The most sufficient adhesive of the two selected (Pekadur A663 polyurethane adhesive and the GB685 spray grade rubber adhesive) for the walling system application is also determined. The failure of a specimen is classified as the event when rupture occurs or when no further load can be sustained.

7.1. Relative bond strength of the adhesives

The aim of this experiment was to give an indication of the behaviour of the adhesives. The Contest (compression machine) was used to perform this experiment. In Sections 7.4 and 7.5, the bond strength of the adhesives is tested when they are applied to the surfaces of the EPS and WPC.

7.1.1. Test methodology

Three steel plates were attached by using the adhesives, as shown in Figure 7.2 (not to scale). Examples of these specimens are shown in Figure 7.3. Stiff steel plates were used to ensure failure occurred in the bonded area to determine the relative bond strength. The surface of the steel plates was cleaned by applying paint thinners and sanded with sandpaper. The adhesives were applied to an area of 50x38mm, as illustrated in Figure 7.2, at a thickness of approximately 1mm. Only one specimen for each adhesive was tested at a rate of 1.5MPa/min (0.25MPa/second), as specified in SANS 5863 (2006). The method of applying each of the adhesives is described in Table 7.1. The specimens were cured for 12h. The load was applied until failure occurred. The way in which the load was applied is illustrated in Figure 7.4.

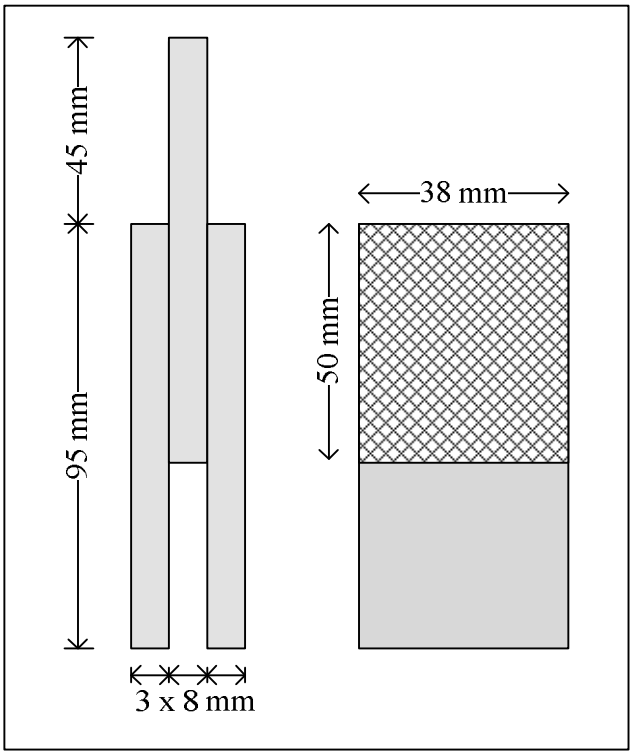

Figure 7.2: Schematic representation of the relative adhesive strength specimens

The Pekadur A663 polyurethane adhesive	GB685 spray grade rubber adhesive
	

Figure 7.3: Examples of relative bond strength specimens

Table 7.1: Method of application of adhesives

The Pekadur A663 polyurethane adhesive	GB685 spray grade rubber adhesive
• The mixing ratio of Part A (soft paste) to Part B (thin liquid) is 5 to 1 by weight • The mixture is mixed thoroughly until the colour is uniform • The adhesive is applied to one surface which is attached to the other surface immediately • Specimen curing time is 12 to 20 hours • Pressure needs to be applied during curing	• Adhesive is applied to both surfaces of the specimen • Before the surfaces are attached, a curing period of 8 to 10 minutes is required • After the curing period, the surfaces can be attached • Pressure needs to be applied during curing

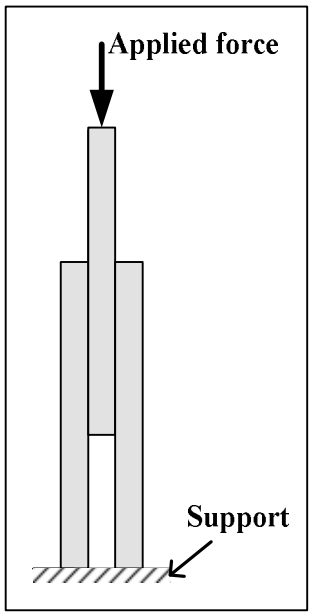

Figure 7.4: Schematic representation of force applied to relative bond strength specimen

7.1.2. Results

The results obtained from this test are in shown in Table 7.2. The bond resistance is calculated by dividing the maximum resisted shear force by the shear area. The GB685 spray grade synthetic rubber adhesive has a relative strength of approximately 18.4% greater than that of the Pekadur A663 polyurethane adhesive. When the Pekadur A663 polyurethane adhesive cures, it becomes extremely hard in texture which resulted in brittle failure of its bond. The GB685 spray grade synthetic rubber adhesive, on the other hand, has a more ductile bond and the top steel plate slid in-between the other two steel plates when a load was applied. Thus, the specimen failed in a ductile manner. Examples of the two adhesives after failure are shown in Figure 7.5.

Table 7.2: Results of the bond strength test

	Pekadur A663 Polyurethane Adhesive	**GB685 Spray Grade Synthetic Rubber Adhesive**
Bond strength (kN)	8.7	10.3
Type of failure	Brittle	Ductile
Shear area (mm^2)	1900	1900
Bond resistance (MPa)	2.29	2.71

The Pekadur A663 polyurethane adhesive	**GB685 spray grade rubber adhesive**

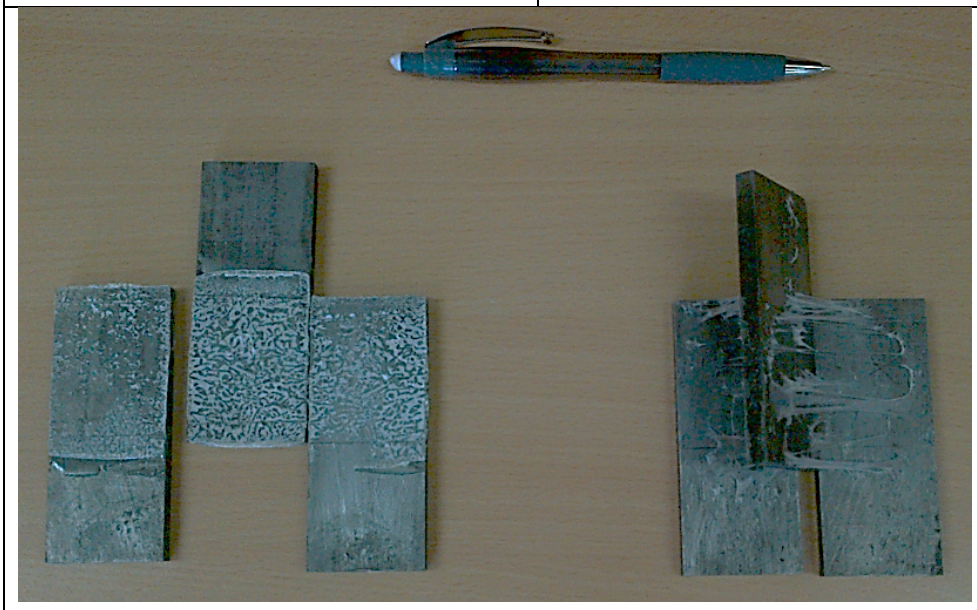

Figure 7.5: Example of test specimens after failure

7.2. Direct compression test of WPC

The aim of the experiment is to determine the compressive properties of WPC, such as the compressive yield strength and compressive modulus of elasticity can be determined. The Zwick Z250 (material testing machine) and LVDTs (Linear variable displacement transducers) was used to conduct this experiment.

7.2.1. Test methodology

The test-setup of the direct compression test was performed according to ASTM D695 (2010). This code specifies the following:

- A prism with a length twice the width.
- A minimum of five test specimens.
- A displacement-rate of 1.3mm/min.
- Constant humidity and temperature.

A specimen size of 22x22x44mm was used to conduct the experiment. The load was applied to a smooth surface to ensure direct compression as shown Figure 7.6. Eight specimens were tested at a temperature of 21.6°C and humidity of 62%.

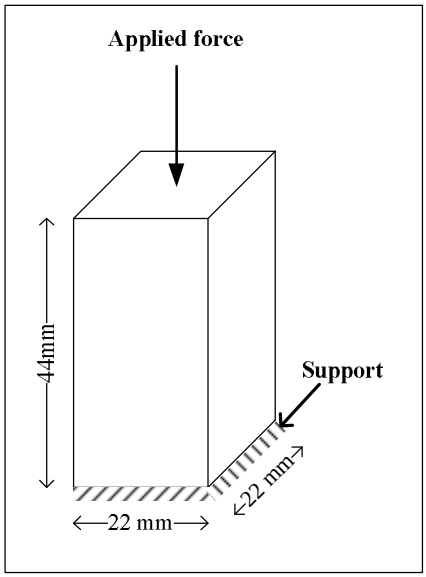

Figure 7.6: Schematic representation of direct compression test-setup

The Zwick Z250 was fitted with a ball-joint. The top surface was free to rotate. The specimen was placed on top of steel spacer to accommodate the LVDTs. This setup is shown in Figure 7.7. An independent frame was used to house the LVDTs to ensure that the true deflection of the specimen is measured.

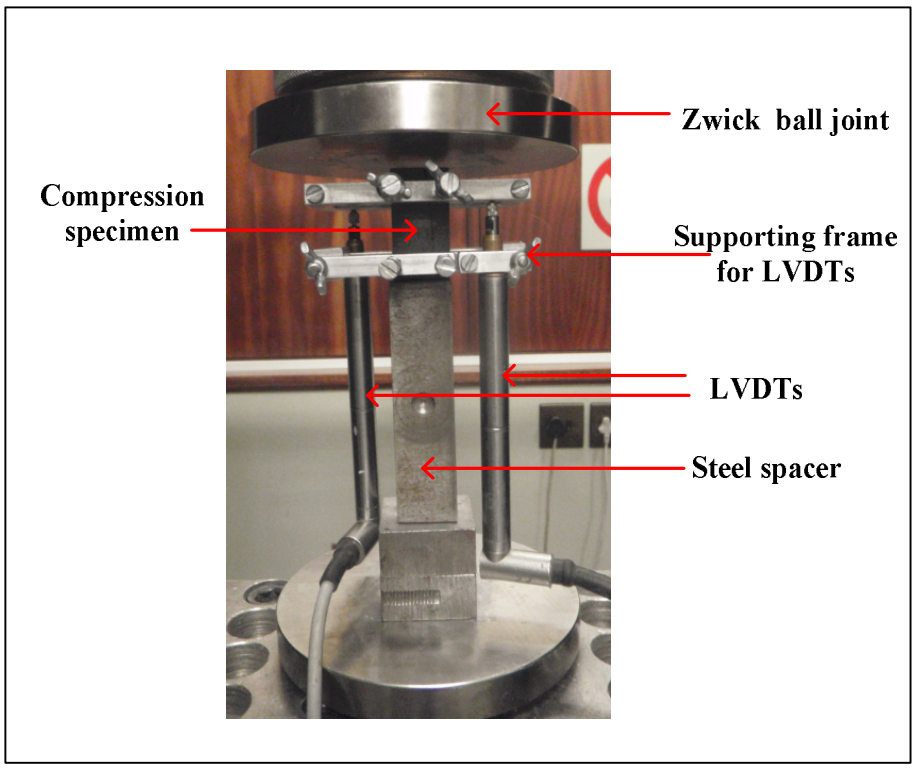

Figure 7.7: WPC compression test-setup

7.2.2. Results

The displacement is measured by the average of the two LVDTs. The average displacement was converted to strain by means of the following expression:

$$\varepsilon = \frac{\Delta L}{L} \qquad \text{(7.1)}$$

where,

ε = Strain (mm/mm)

ΔL = Change in length (mm)

L = Original length (mm)

The applied force measured by the Zwick Z250 was converted to stress by using the following equation:

$$\sigma = \frac{P}{wd} \qquad \text{(7.2)}$$

where,

σ = Stress (MPa)

P = Applied load (N)

w = Width of specimen (mm)

d = Depth of specimen (mm)

The characteristic compressive strength (5%) is obtained by using the following equation:

$$f_{cu} = m - 1.64s \quad \text{..... (7.3)}$$

where,

fcu = Characteristic strength (5% fractile)

m = Average

s = Standard deviation

Figure 7.8 illustrates the compressive stress-strain responses for the eight specimens. In this figure, the compressive yield strength of Specimen 1, 33.8MPa, is an outlier. A 95% confidence interval (Montgonmery & Runger, 2007, p. 261), results in an average compressive yield strength range of 23.184MPa to 32.367MPa. The compressive yield strength of Specimen 1 falls outsides of this range and is therefore not used in further calculation of the results. The specimens failed, illustrated in Figure 7.9, in a brittle manner.

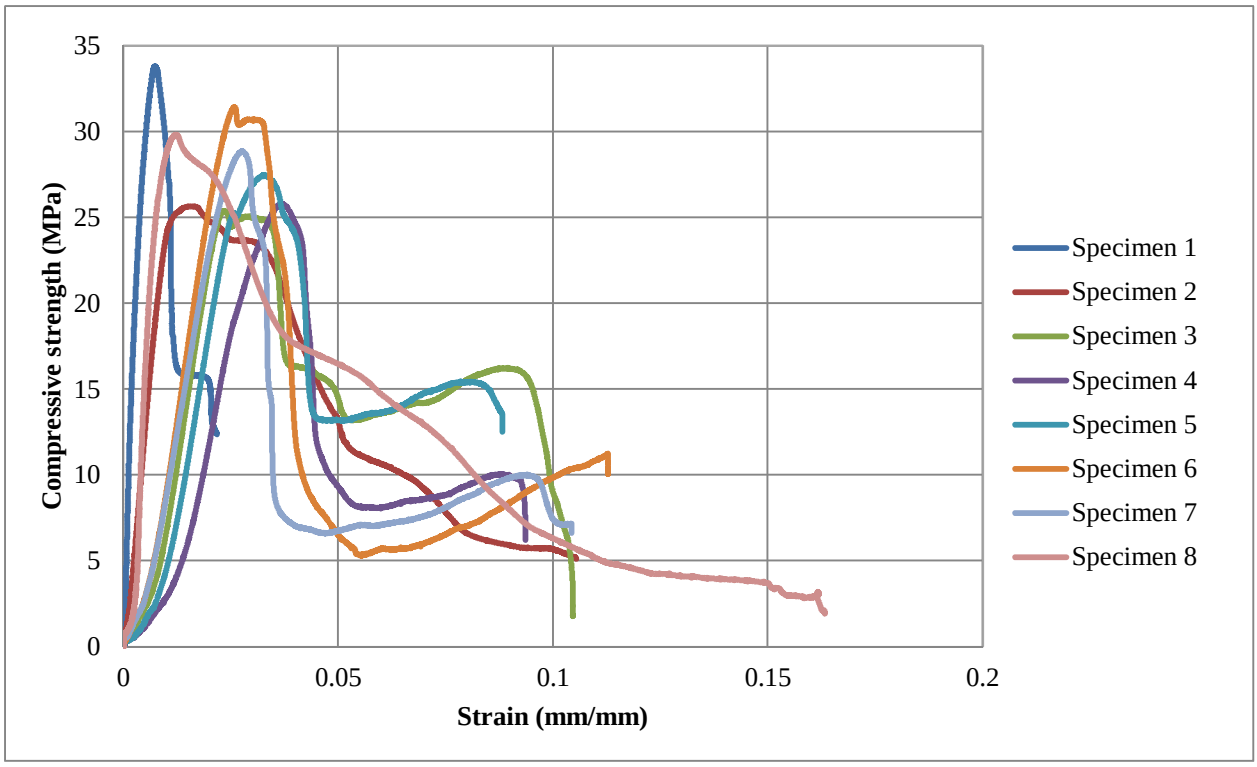

Figure 7.8: Compressive stress-strain responses of the test specimens

Figure 7.9: Before and after compressive failure of WPC test specimen

The results of these seven compression specimens are shown in Table 7.3. All the results were obtained by calculating the specific material property of each of the responses and then determining the average. The coefficient of variation for the compressive yield stress is relatively low, therefore acceptable. The coefficient of variation for the Young's modulus, on the other hand, is relatively high. The Young's modulus was determined according to the guidelines provided in the ASTM 695 (2010) (Annex A1: Toe compensation).

Table 7.3: Results of the compression test of WPC

	Compressive yield stress	Compressive Young's modulus
Average	27.776MPa	1347.780MPa
Standard deviation	2.343MPa	221.459MPa
Coefficient of variation	8.435%	16.431%
Characteristic compressive stress (5%) (Equation 7.3)	23.933MPa	

7.3. Direct tension test of WPC

A direct tension test was performed to determine the tensile properties of WPC. The results from this test are used to determine the tensile yield strength and Young's modulus are determined. The Zwick Z250 was used to conduct the experiment.

7.3.1. Test methodology

The ASTM D638 (2010), is used to specify the test-setup. This code specifies the following:

- Reinforced composites, Type I specimen size, as shown in Figure 7.10. The specimen has a thickness of 7mm.
- A minimum of five test specimens.
- For a Type I, displacement-rate of 5mm/min.
- Constant humidity and temperature.

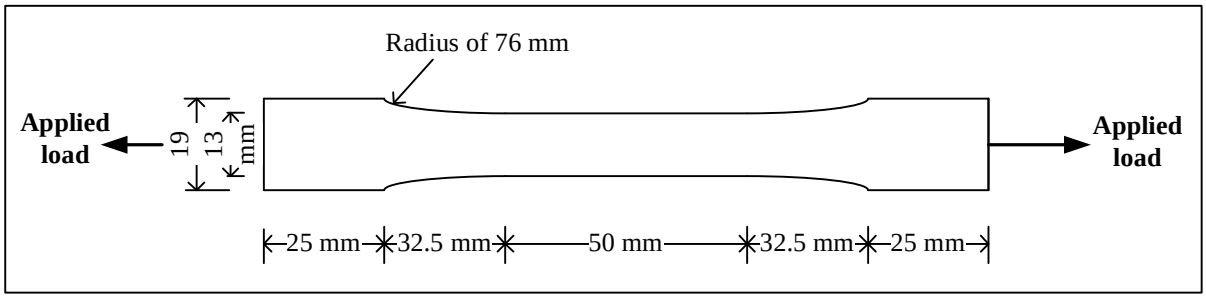

Figure 7.10: Schematic representation of a direct tensile test specimen (dog bone) as well as the applied load

The specimen size as well as the manner in which load were applied as shown in Figure 7.10. Six specimens were tested at a constant temperature of 22.2 °C and humidity of 52%. The displacement-rate for testing as prescribed by ASTM D638 (2010) was used.

The Zwick Z250 was fitted with hydraulic clamps. The clamps can only apply a force to the specimen in multiples of 6kN. Therefore, 6kN were applied which is equal to a compressive strength of 9.8MPa applied to the specimen. This applied stress ensures that no slippage occurs while it is smaller than the compressive yield strength of 23.57MPa. This setup is shown in Figure 7.11.

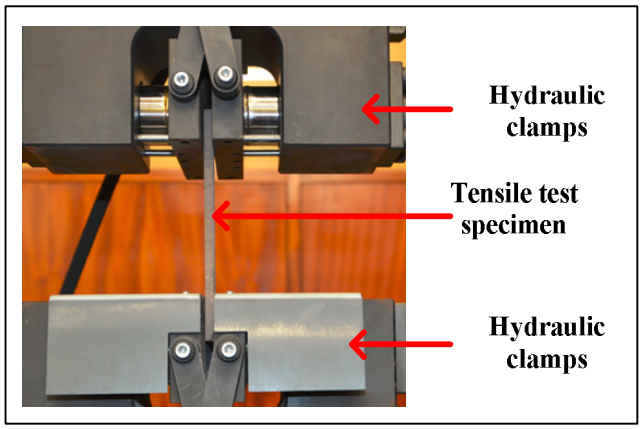

Figure 7.11: WPC tension test-setup

7.3.2. Results

The displacement measured by the standard travel of the Zwick Z250 was converted to strain using the Equation 7.1. The force measured by the Zwick Z250, on the other hand, was converted to stress using Equation 7.2.

The tensile stress-strain responses for the six specimens are shown in Figure 7.12. This figure illustrates a sudden drop in load capacity at an average strain of approximately 0.027mm/mm. This refers to rupture of the specimen. Figure 7.13 illustrates the test specimen before and after rupture occurred.

Table 7.4 illustrates the results of the tensile tests of the six specimens. All the results were obtained by calculating the specific material property of each of the responses and then determining the average. The coefficient of variation of both the tensile yield and tensile Young's modulus are low, which is desirable.

Table 7.4: Results of direct tensile test

	Tensile yield stress	Tensile Young's modulus
Average	21.704MPa	949.395MPa
Standard deviation	2.166MPa	40.894MPa
Coefficient of variation	9.980%	4.307%
Characteristic tensile stress (5%) (Equation 7.3)	18.152MPa	

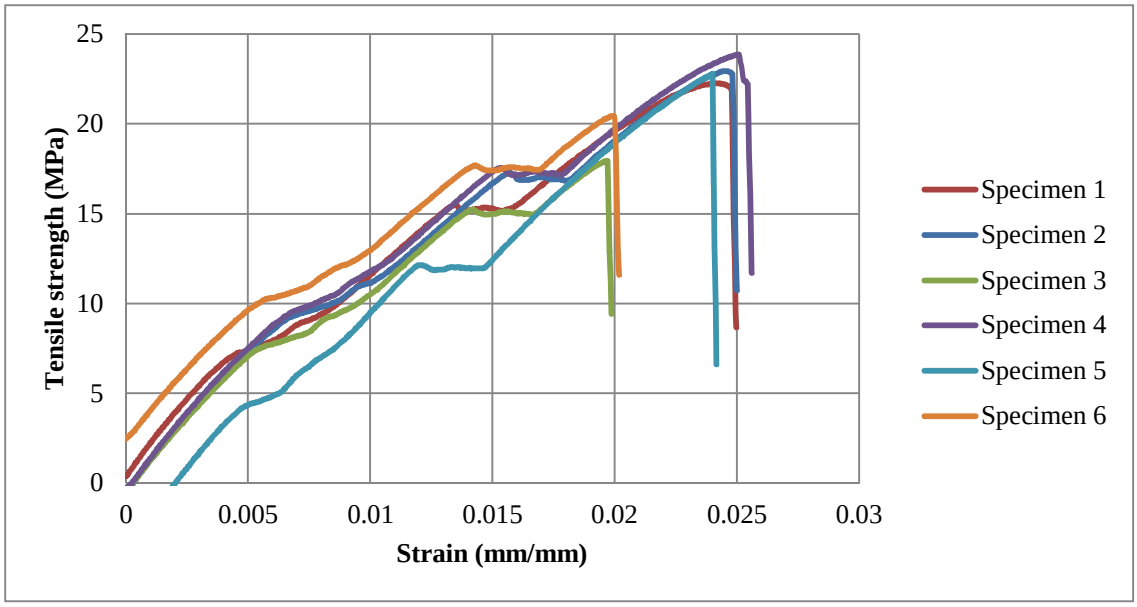

Figure 7.12: Tensile stress-strain responses of the test specimens

Figure 7.13: Before and after tensile rupture of WPC test specimen occur

7.4. Four-point bending test of WPC

The aim of the four-point bending test is to determine the bending properties of WPC. These bending properties include the bending stress, ultimate strain as well as bending moment. The Zwick Z250 and LVDTs were used to conduct the experiment.

The main difference between the four-point- and three-point bending modes is the position where the maximum bending moment occurs. This is shown in Figure 7.14. In this figure, L refers to the span length and P to the applied load. For the three-point bending, the maximum bending moment occurs directly

beneath the point of loading. Thus, this maximum bending moment occurs where the maximum axial fibre stress occurs. For the four-point bending, the maximum bending moment is evenly distributed between the loading points. The four-point bending test has a larger area under the bending moment diagram. Therefore, when fibre reinforced materials are used the four-point bending is a more conservative approach, since more fibre bridging can occur.

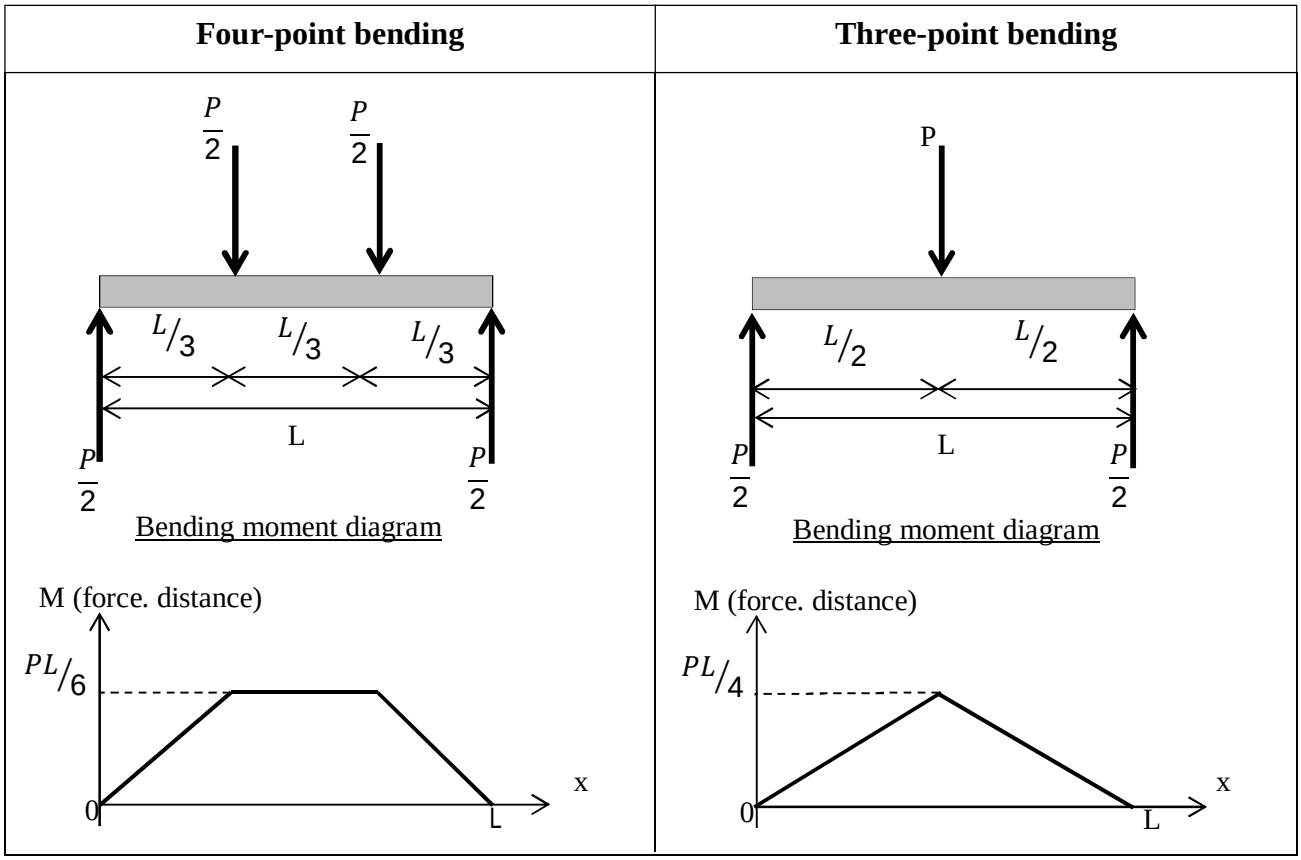

Figure 7.14: Comparison of bending moments, four-point bending versus three-point bending

7.4.1. Test methodology

A four-point bending test, where the load is applied at one third of span length was used. Refer to the four-point bending in Figure 7.14. This experiment was performed according to ASTM D6272 (2010), where procedure B is used. Procedure B is specified for materials that have large deflections. For procedure B, ASTM D6272 (2010) specifies the following requirements:

- The specimen size with span-to-depth ratio of at least 1 to 16
- A minimum of five test specimens.
- Displacement-rate according to Equation 7.4.

- Discontinue the test if the midspan deflection, calculated in Equation 7.5, is reached.
- Constant humidity and temperature.

Five specimens were tested. The specimen size is 22x22x450mm and has a span-to-depth ratio of 1 to 20.5. This satisfies requirements set out by the ASTM D6272 (2010). The displacement-rate used for this test is 17mm/min and is calculated by using the following equation (ASTM D6272, 2010):

$$R = {0.185\,ZL^2}/{w} \qquad \text{(7.4)}$$

where,

R = Rate of crosshead motion (mm/min)

Z = Rate of straining of outer fibres. This is equal to 0.01 mm/mm/s

L = Span length (mm)

w = Width of beam (mm)

The tests were discontinued when failure occurred or when the midspan deflection was approximately 96mm. This was calculated by using the following equation (ASTM D6272, 2010):

$$D = {0.21\,rL^2}/{w} \qquad \text{(7.5)}$$

where,

D = Deflection at midspan (mm)

r = Strain of outer fibres. This is equal to 0.05 mm/mm

L = Span length (mm)

w = Width of beam (mm)

During this experiment the temperature and humidity was 22.2°C and 60%, respectively. The recommended displacement-rate of 17mm/min was used.

Steel plates were attached to the bottom of the specimen. This was done to ensure that the LVDTs measured the outer fibre deflection of the specimen accurately. The test-setup is shown in Figure 7.15. Two rollers were attached to the Zwick Z250 which apply half the force per roller as shown in Figure 7.15.

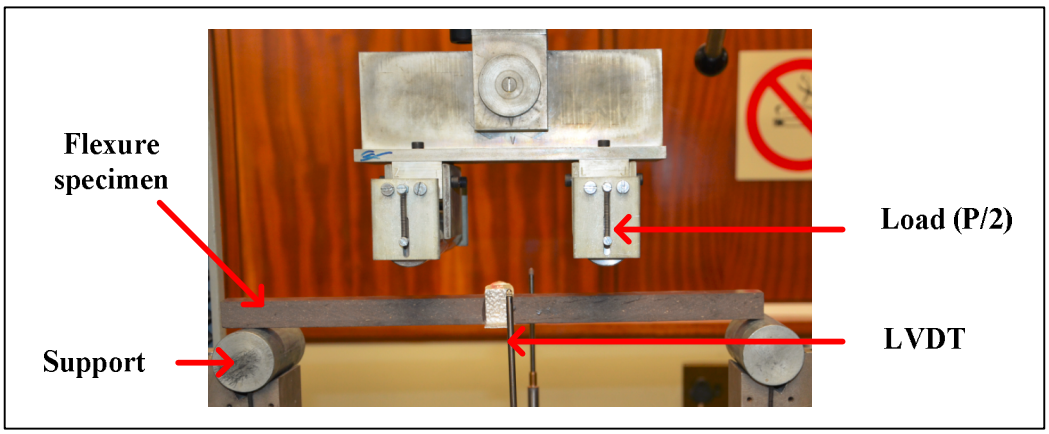

Figure 7.15: WPC bending test-setup

7.4.2. Results

The applied force measured by the Zwick Z250 was converted to stress. This is the stress of the outer fibres of the specimen and is calculated by using the following equation (ASTM D6272, 2010):

$$\sigma = \frac{PL}{wd^2} \quad \text{(7.6)}$$

where,

σ = Bending stress (MPa)

P = Applied load (N)

L = Span length (mm)

w = Width of specimen (mm)

d = Depth of specimen (mm)

The maximum strain is calculated as follows (ASTM D6272, 2010):

$$\varepsilon = \frac{4.7Dd}{L^2} \quad \text{(7.7)}$$

where,

ε = Strain (mm/mm)

D = Deflection (mm)

d = Depth of specimen (mm)

L = Span length (mm)

Five specimens were tested for bending and the stress-deflection responses of these test specimens are shown in Figure 7.16. Specimen 4 exhibited more pre-existing cracks which resulted in a lower ultimate bending stress. Most of the specimens did not have a clear yield point. Table 7.5 illustrates the results of these five bending test specimens.

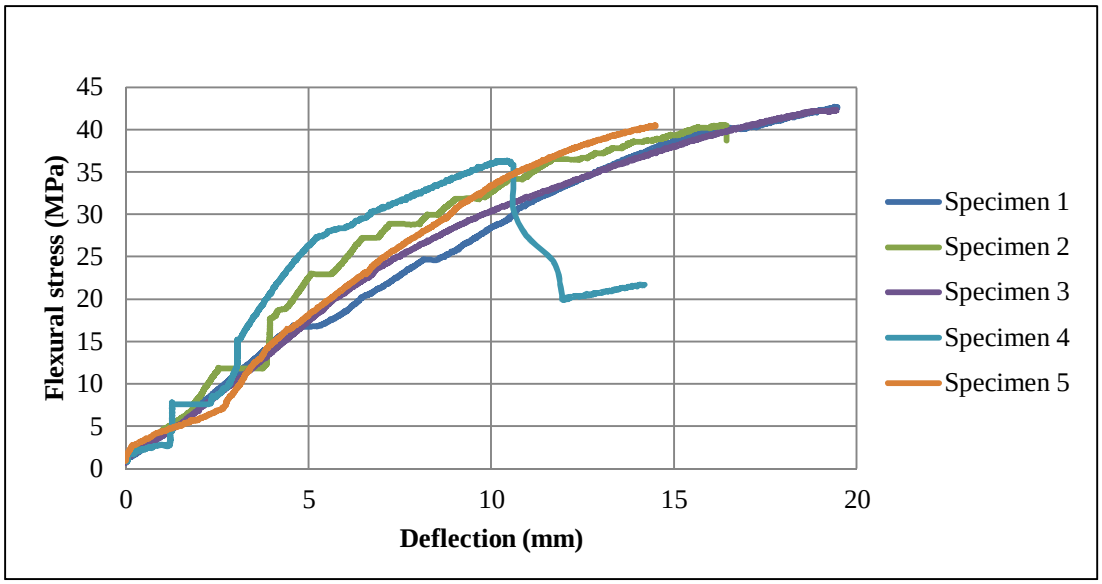

Figure 7.16: Bending stress-deflection responses of WPC test specimens

Table 7.5contains the results of the bending test. All the results were obtained by calculating the specific material property of each of the responses and then determining the average. The bending stress is calculated by using Equation 7.6, whereas the ultimate bending strain is calculated using Equation 7.7. The bending moment is determined by using the Figure 7.14 (PL/6). The coefficient of variation of both the ultimate bending stress and the bending moment is small, which is desired. The coefficient of variation of the ultimate bending strain is high. This could be due to some of the specimens having more profound cracks, which caused the material to fail at different deflections. The maximum deflection to span ratio resulted in 3.56%.

Table 7.5: Results of bending test of WPC

	Ultimate bending stress	Ultimate bending strain	Maximum bending moment
Average	40.511MPa	0.008mm/mm	71.893N.m
Standard deviation	2.517MPa	0.002mm/mm	4.466N.m
Coefficient of variation	6.212%	23.992%	6.212%
Characteristic bending stress (5%) (Equation 7.3)	36.383MPa		

As shown in Figure 7.14, the maximum bending moment occurs between top rollers. Failure of the WPC in bending occurred in this region. Thus, failure of the specimen is due to tension or compression stress. The maximum induced tension- and compression stress are equal. Tensile stresses occur at the bottom of a specimen whereas compression forces occur at the top of a specimen. The governing failure mode of a bending specimen is a tensile failure. This is due to tensile failure occurring first, as shown in Figure 7.17.

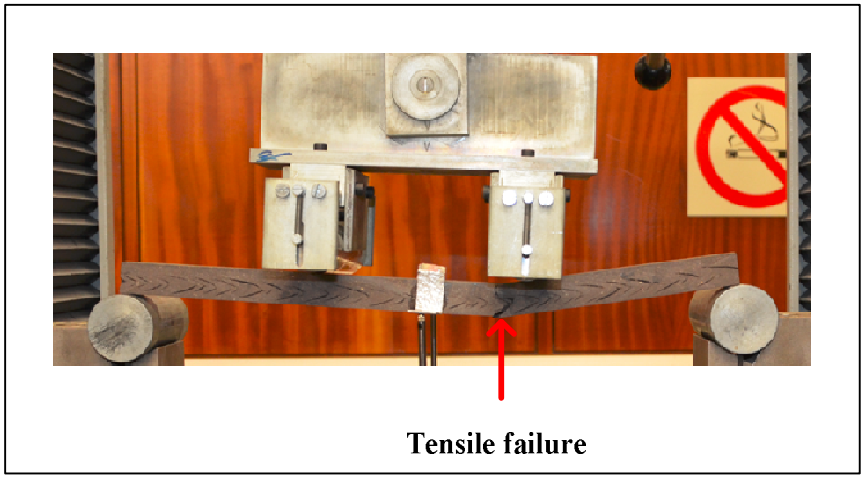

Figure 7.17: Tension failure in bending test of WPC

7.5. Compressive creep test for WPC

A compressive creep test was performed to determine the deformation-time response as well as the creep behaviour for WPC. The deformation-time curve is used to predict the creep-strength and -modulus of the WPC. It is also performed to determine whether creep is a major concern for the use of WPC as a load-bearing element.

7.5.1. Test methodology

The test-setup is performed according to ASTM D2990 (2009). This code specifies the following requirements:

- Temperature, where the test is performed, shall be maintained constant with a tolerance of ± 2°C, since the creep test is sensitive to temperature changes.
- The creep test is also sensitive to the change of relative humidity in the test and it shall be maintained constant with a tolerance of ±5%.

- A minimum of two specimens should be tested.
- The deformation of the specimen is measured by the following time schedule: 0,1,6,12, and 30min; 1,2,5,20,50,100,200,500,700,1000 hours.
- The test specimens should be preconditioned for at least 48 hours prior to the test, to ensure that the specimens are in moisture and temperature equilibrium.
- The total applied load shall be applied (at start of test) and removed (at end of test) rapid and smoothly within 1 to 5 seconds.

Eight specimens with a dimension of 22x 50x150mm were used for this experiment. The applied load is 30% of the compressive yield strength. Thus, a creep load of 8.15MPa is applied.

The test-setup is shown in Figure 7.18. A steel disk is placed on top of a ball-joint to ensure that the ball-joint remains stable at the top of the specimens. The bolt-joint ensures that the load is applied vertically to the top of the specimens. Specimens were placed on top of each other and were separated by a steel plate. A load-cell was used to ensure the correct constant load of 8.97kN was applied. Bolts were used to apply the load. Four bolts were tightened on threaded rod for each pair of specimens. The creep load was applied within 5 seconds.

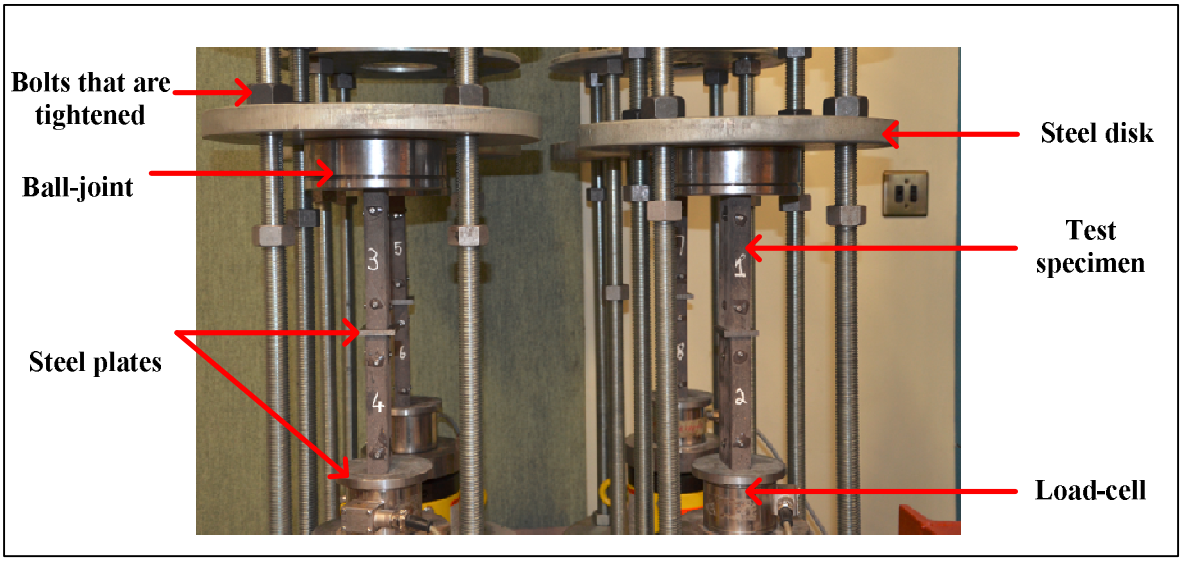

Figure 7.18: Compressive creep of WPC test-setup

The specimens were sanded with sandpaper to ensure clean surfaces where the creep targets were attached. These targets are shown in Figure 7.19. The targets are used to measure the creep and were attached 100mm apart. The creep was measured by using a MarCator 1075R extensometer (also known as a digital indicator)

over a distance of 100mm. This creep measuring device is shown in Figure 7.20. The device is sensitive to temperature changes and is therefore kept in the same controlled room as the creep specimens. The device is zeroed at 100mm before measurements, for each of the measuring times, were taken.

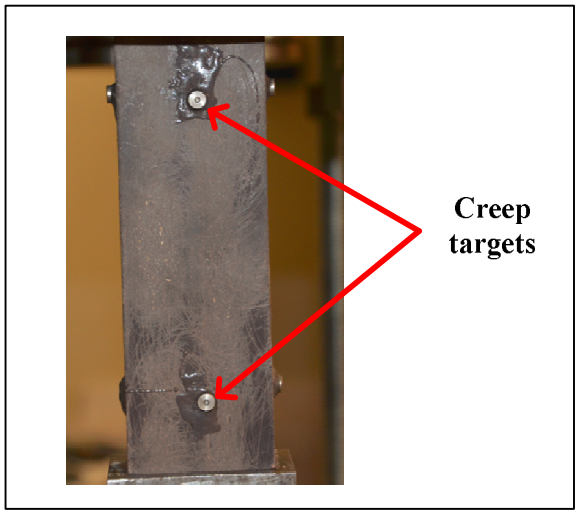

Figure 7.19: Creep targets

Figure 7.20: MarCator 1075R (Creep measuring device)

7.5.2. Results

Eight specimens were tested for creep and the strain-time responses of these test specimens are shown in Figure 7.21 and Figure 7.22. From this figure it can be seen that, Specimens 2 and 5 exhibit a greater creep strain compared to the other specimens. This can be due to Specimens 2 and 5 rotating about their vertical axes, which occurred during the experiment. This resulted in the same compressive force being transferred over a smaller surface area, which caused higher compressive stresses in the specimens. The temperature and

humidity fluctuated during the creep test, as shown in Figure 7.23. From Figure 7.21 it is clear that the large fluctuation in humidity (Figure 7.23) had an insignificant effect on the WPC.

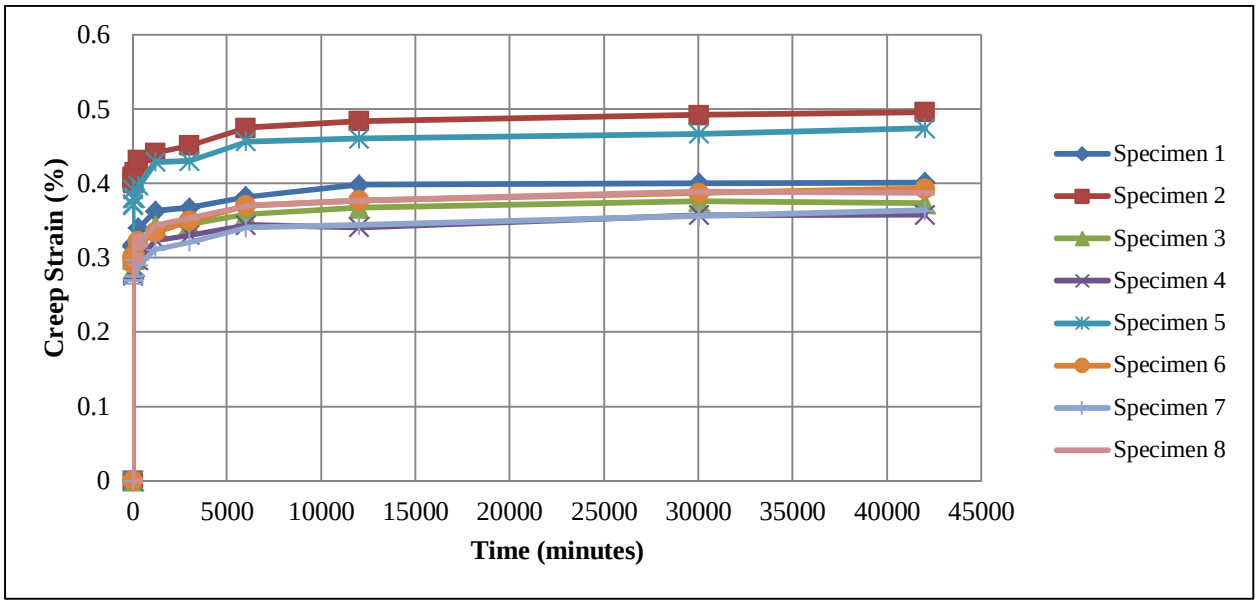

Figure 7.21: Creep strain-time responses for WPC test specimens (at 30% compressive yield stress)

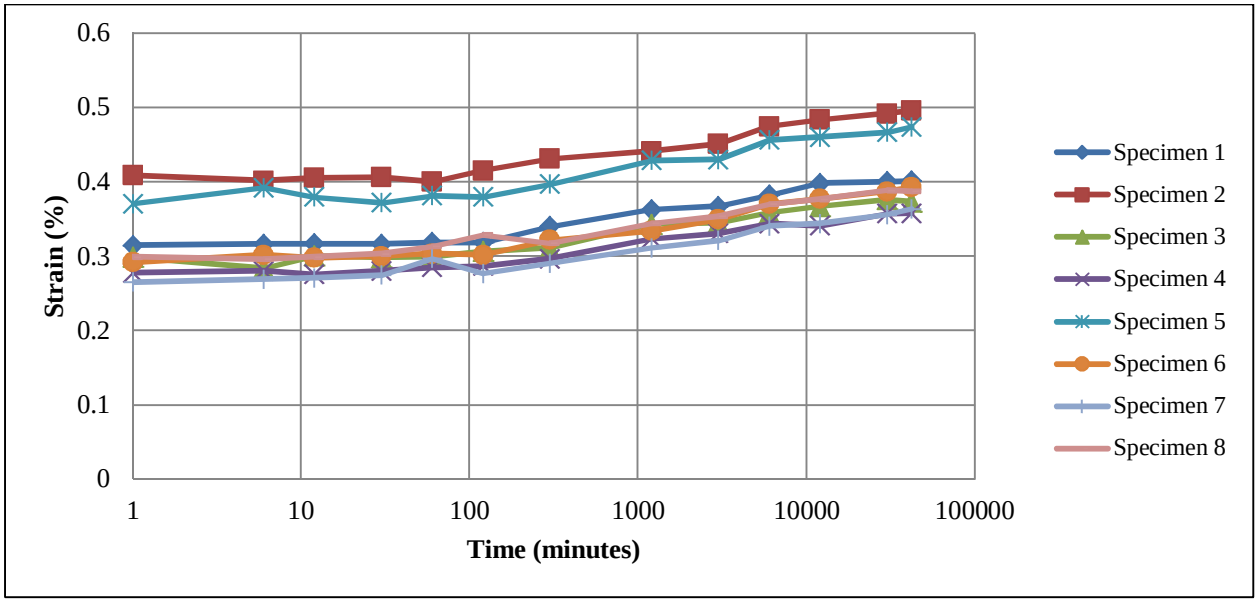

Figure 7.22: Creep strain-time responses for WPC test specimens (at 30% compressive yield stress) represented on a logarithmic scale

The average strains of test specimens in Figure 7.21 and Figure 7.22 were calculated to determine a single creep strain-time response for WPC, which is shown in Figure 7.24 . In this figure, the initial elastic as well as plastic strain is shown. The initial elastic strain was calculated from the results obtained from the direct

compression test (Section 7.2). Primarily creep shows an increase in the strain which occurs at a decreasing rate whereas the secondary creep illustrates an approximately constant strain over time. Refer to Section 4.1.5 for the typical strain-time curve and the description thereof. Tertiary creep might not yet occur, due to the relatively short time period. However, for the time period tested, it seems that the creep strain remains constant over an extended period for 30% of the yield compressive stress. The strain, at the 1000 hour time period, is approximately constant at 0.41%. This indicates that the walling system, which is the critical element when compressive creep is considered, will displace about 11mm (0.41% multiplied with the length of walling unit, 2700mm), if no tertiary creep or unloading occurs.

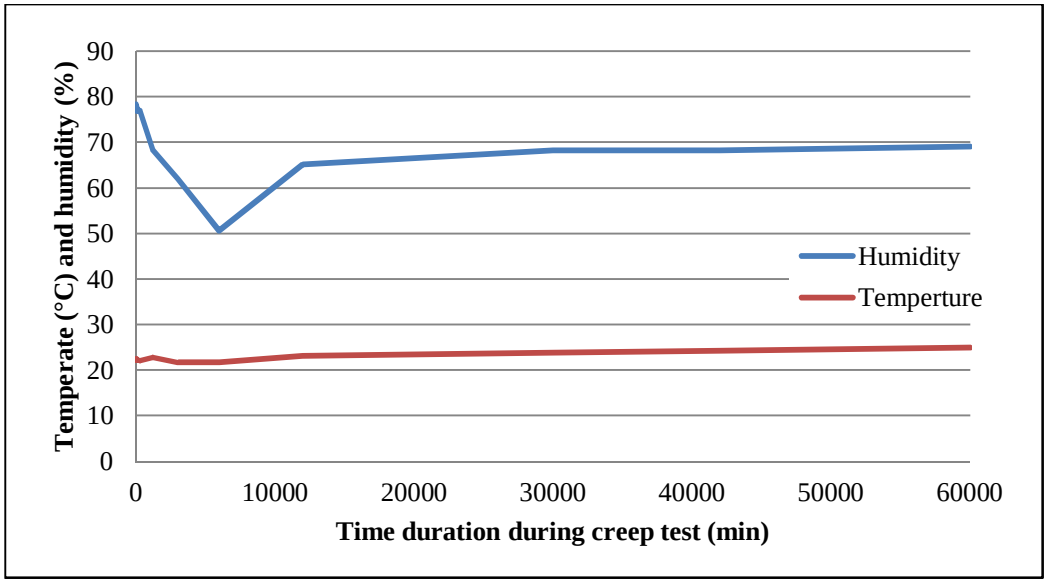

Figure 7.23: Temperature and humidity fluctuation during compressive creep test

The average creep-modulus to time response for WPC was calculated by taking the averages of the creep modulus for each specimen. The creep modulus is determined by dividing the constant stress (8.15MPa) by the strain at each measured time. This response is shown in Figure 7.25. From this curve, it is clear that with time the stiffness of the material to sustain a load decreases. However, the curve flattens out after about 20 hours, after which the modulus remains approximately constant over an extended time.

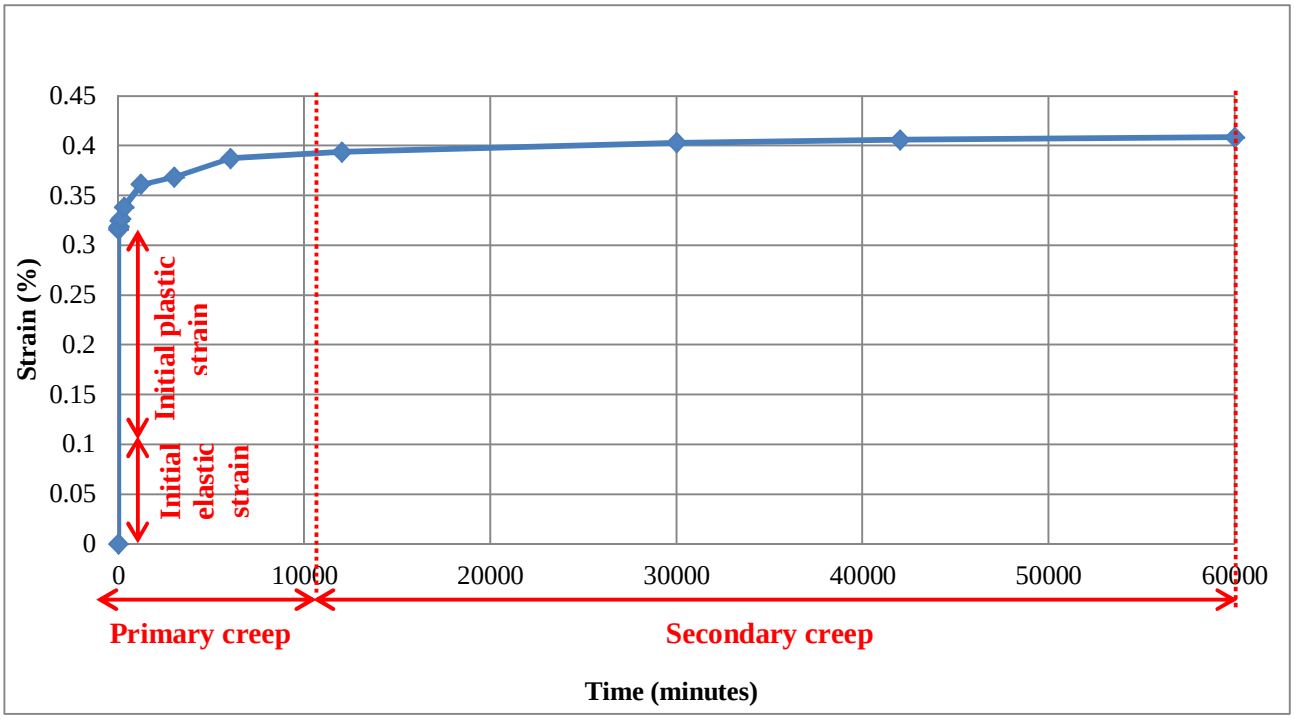

Figure 7.24: Average creep strain-time response of WPC

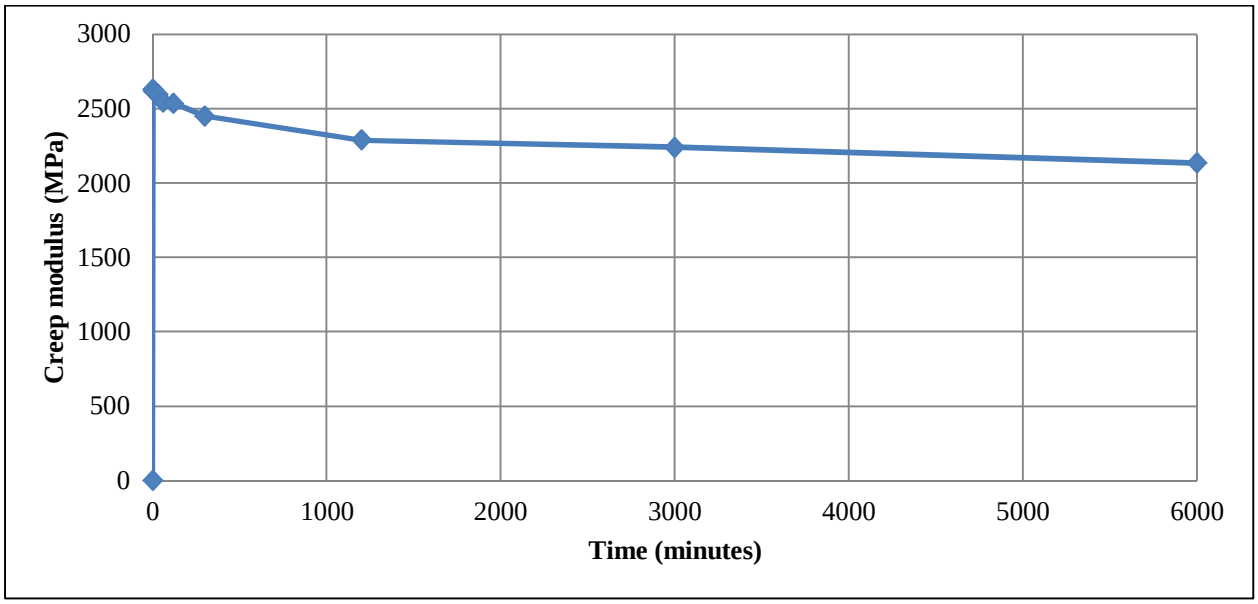

Figure 7.25: Average creep modulus-time response for WPC (30% compressive yield stress)

7.6. Direct compression test of EPS

The aim of the experiment was to determine the compressive properties of EPS (expanded polystyrene). The Zwick Z250 was used to conduct this experiment.

7.6.1. Test methodology

This experiment was conducted in a similar way as the compression test in Section 7.2. A specimen size of 22x22x44mm was used to conduct the experiment. A displacement-rate of 1.3mm/min was applied. Six specimens were tested at a temperature of 21.1°C and humidity of 53%.

No LVDTs were fitted to the test specimen, as deflection was not the critical parameter tested. The standard travel of the Zwick Z250 was used to determine the deflection of the specimen. The upper support was free to rotate, by fitting the Zwick Z250 with a ball-joint. This setup is shown in Figure 7.26. The test was aborted as soon as the deflection of the specimen is equal to 35mm.

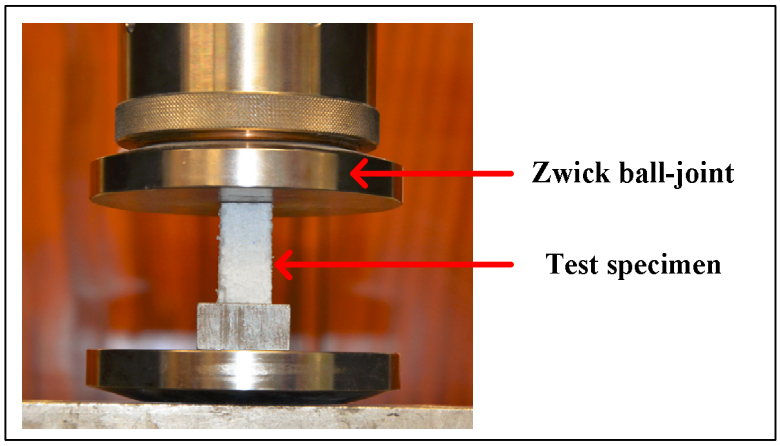

Figure 7.26: EPS compression test-setup

7.6.2. Results

Figure 7.27 illustrates the compressive behaviour of EPS. The strain and stress were obtained by using Equations 7.1 and 7.2, respectively. Since the EPS reduced to a flat disk, as shown in Figure 7.28, the compression strength after yield is of no significance. Thus, only the elastic properties of EPS can be determined.

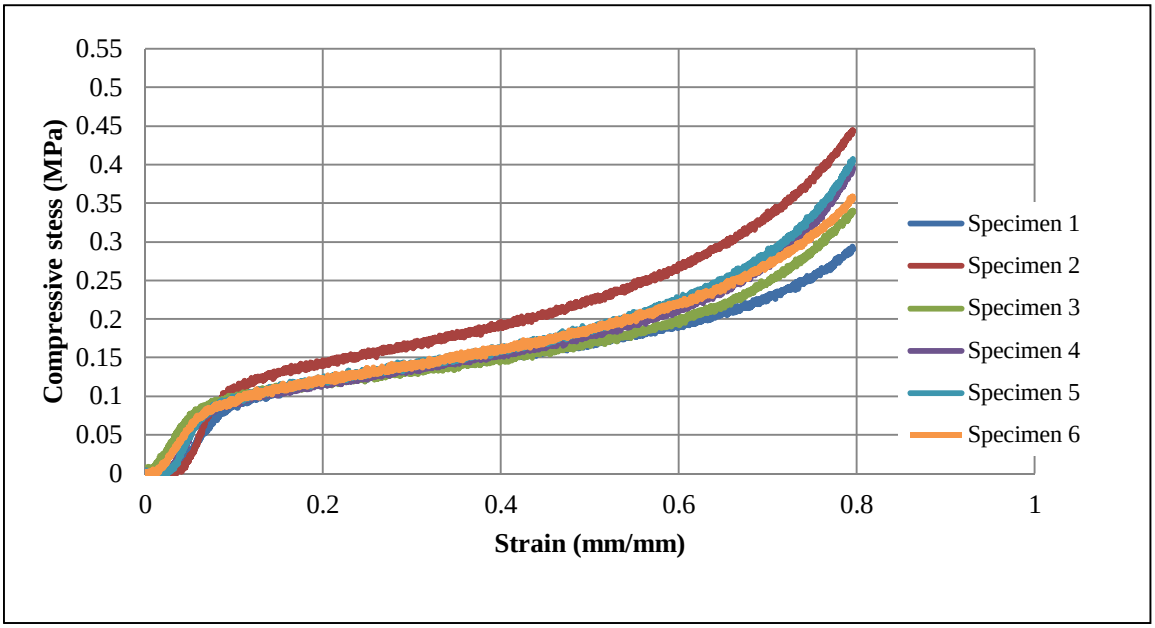

Figure 7.27: Compressive behaviour of EPS

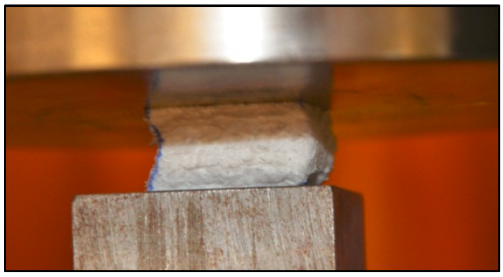

Figure 7.28: EPS reduced to flat disk

Table 7.6 illustrates the result of the six EPS compression specimens. As desired, the results of the experiment exhibit a low standard deviation as well as a coefficient of variation.

Table 7.6: Results of the compression test of EPS

Average compressive yield strength	80.368kPa
Standard deviation	5.656kPa
Coefficient of variation	7.039%
Characteristic compressive stress (5%) (Equation 7.3)	71.091kPa

7.7. Push-through shear test

The push-through shear test was performed to determine the bond-shear strength of the adhesive surface between the EPS and WPC. An adhesive with a high shear strength might cause rupture or cracks in the EPS, whereas a low shear strength might cause cracks or slippage between the EPS and the WPC (in the adhesive layer). However, if the adhesive has insignificant shear strength, the EPS and WPC can separate under load-bearing conditions, which are not desired. The Zwick Z250 was used to conduct this experiment.

7.7.1. Test methodology

This experiment was performed for the two adhesives as discussed in Chapter 6 and Section 7.1. For each adhesive, five specimens were tested at a displacement-rate of 1.3mm/minute. The test specimens have a depth of 100mm. A test specimen as well as the way in which the load was applied is shown in Figure 7.29. The tests were conducted at a temperature of 22.4°C and a humidity of 70.9%. The adhesive was applied as described in Table 7.1. The Pekadur A663 polyurethane adhesive was cured for 20 hours before testing. The test-setups of the Pekadur A663 polyurethane adhesive and the GB685 spray grade rubber adhesive are shown in Figure 7.30 and Figure 7.31, respectively.

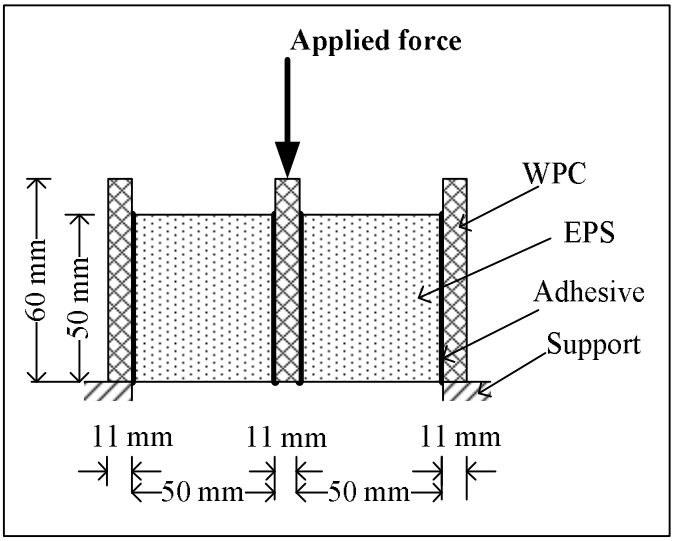

Figure 7.29: Schematic representation of push through shear test specimen with the applied load

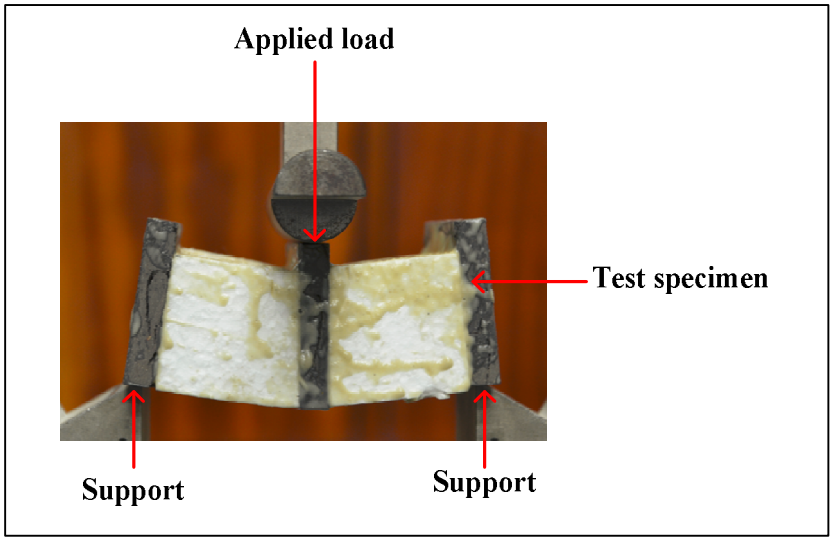

Figure 7.30: Push-through shear test-setup for the Pekadur A663 polyurethane adhesive

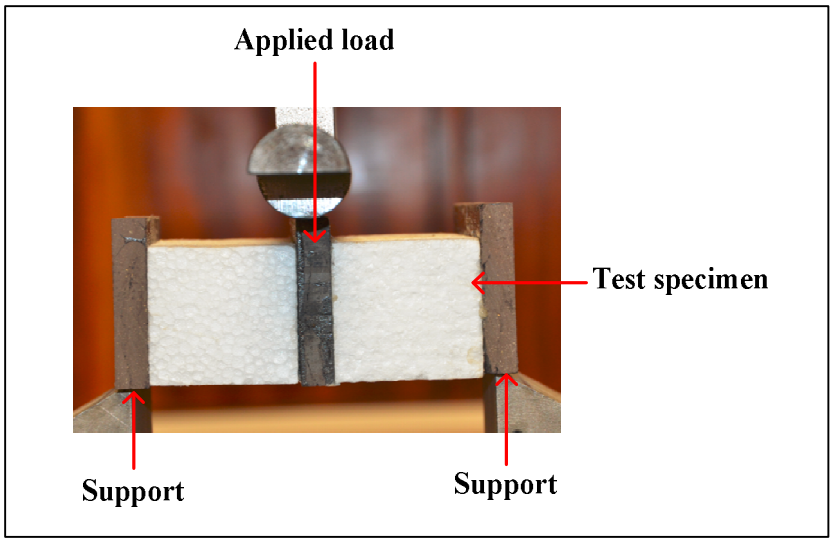

Figure 7.31: Push-through shear test-setup for the GB685 spray grade rubber adhesive

7.7.2. Results

Half the applied load is transferred to each of the supports, which ensues equilibrium of the specimens. Therefore, the shear force that passes through the adhesive at the supports is half of the applied load. The shear stress is calculated by dividing the shear force per bond surface by the shear area. The Zwick Z250 was used to determine the force as well as the deflection of the specimens. The two adhesives are discussed individually and then compared to each other.

The Pekadur A663 polyurethane adhesive

Figure 7.32 illustrates the results of the push-through shear test for the specimens tested with the Pekadur A663 polyurethane adhesive. At the peak shear stress, an initial rupture in the EPS occurred as shown in Figure 7.33. After this rupture, the specimen deforms. This resulted in the EPS of Specimens 1, 2 and 3 to move over the support. Therefore, in Figure 7.32, these specimens have different plastic behaviour in shear. Specimens 4 and 5 represent pure shear, since after deformation of the specimen, the EPS remained unsupported.

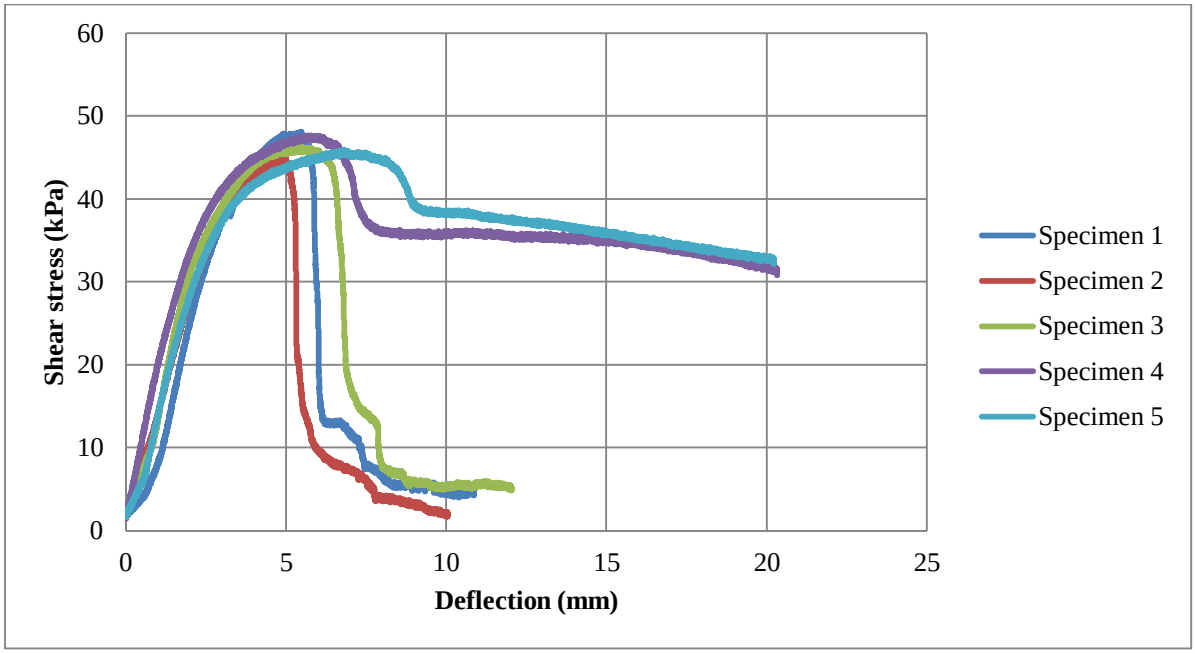

Figure 7.32: Shear stress for Pekadur A663 polyurethane adhesive

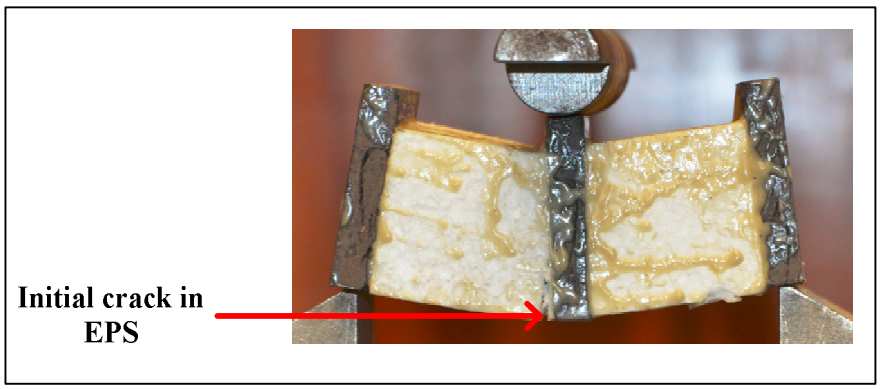

Figure 7.33: Initial rupture in the EPS when Pekadur A663 polyurethane adhesive was used

The results of this test for the five specimens are shown in Table 7.7. The results show a low standard deviation and a low coefficient of variation, which is desired.

Rupture occurred in the EPS, since the adhesive has a greater shear strength. This results in the EPS having an average yield shear stress of 46.662kPa. If Specimens 4 and 5 are considered (pure shear), the force decreases after initial rupture occurs, but some load is still sustained. This is due to the EPS pushing against the WPC after initial rupture has occurred. The initial crack propagates through the depth of the specimen parallel to the plane of the adhesive. This is shown in Figure 7.34.

Table 7.7: Results of the push-through shear test for the Pekadur A663 polyurethane adhesive

Average maximum (yield) shear stress	46.662kPa
Standard deviation	1.186kPa
Coefficient of variation	2.542%
Characteristic shear stress (5%) (Equation 7.3)	44.717kPa

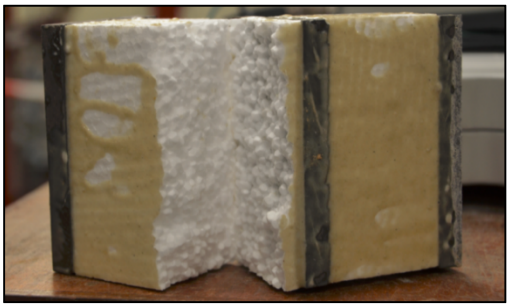

Figure 7.34: Total failure of push-through shear test for Pekadur A663 polyurethane adhesive

GB685 spray grade rubber adhesive

The results of the push-through shear test for the GB685 spray grade rubber adhesive specimens are shown in Figure 7.36. The first neck of the curve illustrates the shear stress yield point. At this point, the EPS and WPC slide over each other in a vertical plane, but is still bonded by the adhesive as shown inFigure 7.35. The specimen remains able to transfer the shear load to the supports, until total failure occurs. Total failure occurs when the applied load cannot be transferred and the specimen fails to transfer the load as shown in Figure 7.37.

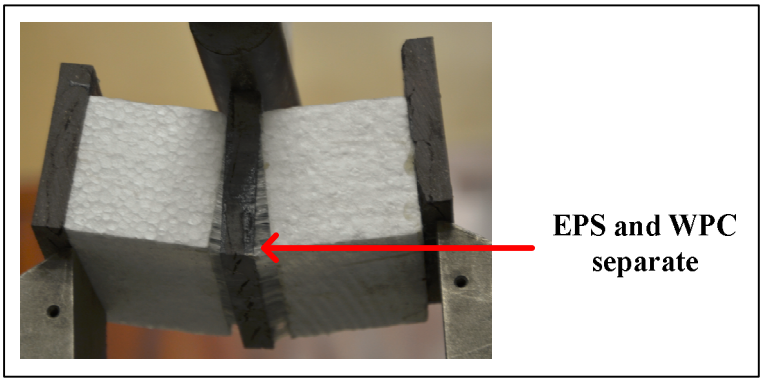

Figure 7.35: EPS and WPC separate (push-through shear test, GB685 spray grade rubber adhesive)

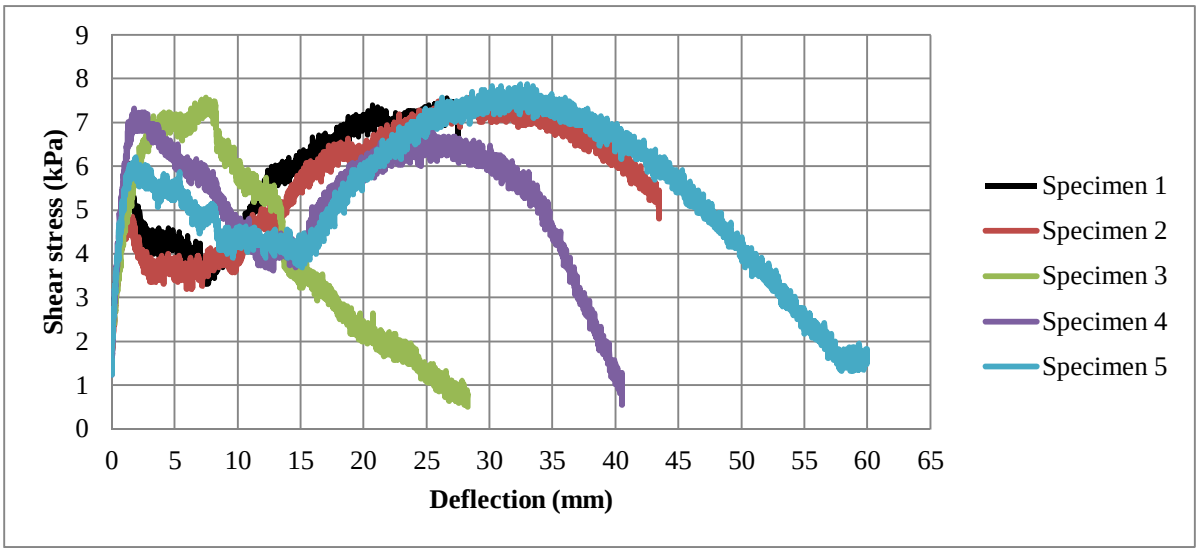

Figure 7.36: Shear stress for the GB685 spray grade rubber adhesive

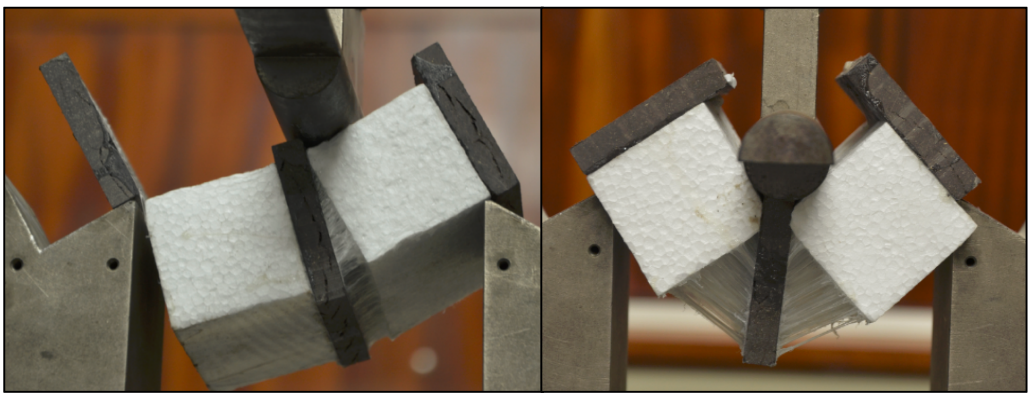

Figure 7.37: Total failure of push through shear test for the GB685 spray grade rubber adhesive

Table 7.8 illustrates the results of the five test specimens. The results display a desired distribution of average maximum shear stress, since the results express a low standard deviation and coefficient of variation. This shear stress of the adhesive is less than the shear stress of EPS (46.662kPa, determined from the push-though shear test of the Pekadur A663 polyurethane adhesive), which results in failure of the adhesive.

Table 7.8: Results of the push through shear test for the GB685 spray grade rubber adhesive

Average shear ultimate stress	7.593kPa
Standard deviation	0.198kPa
Coefficient of variation	2.614%
Average shear yield stress	6.337kPa
Characteristic shear ultimate stress	7.27kPa

Comparison of the two adhesives

The average shear stress obtained by the push-through test for both adhesives is shown in Figure 7.38. From this figure, it is clear that Pekadur A663 polyurethane adhesive can resist more shear stress than that of when the GB685 spray grade rubber adhesive is used. This is due to the failure of the EPS when Pekadur A663 polyurethane adhesive was used. In contrast, the adhesive failed when the GB685 spray grade rubber adhesive was used. Thus, according to these results, Pekadur A663 polyurethane adhesive shows better performance under shear loading.

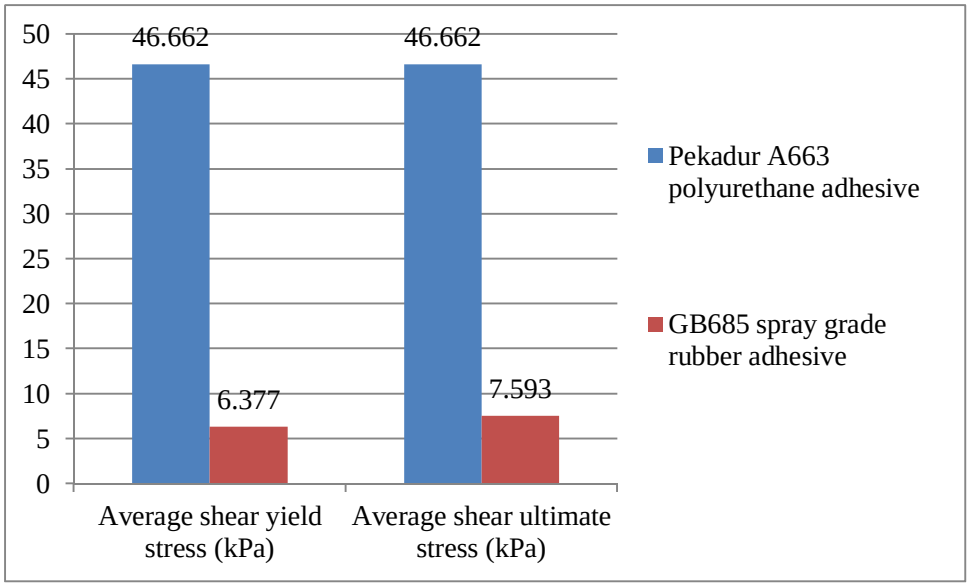

Figure 7.38: Comparison of the average shear stress for both adhesives (push-through shear test)

7.8. Composite sandwich panel four-point bending test

The aim of this experiment is to determine the bending properties of a composite panel of WPC and EPS. The Zwick Z250 and LVDTs was be used to conduct the experiment.

7.8.1. Test methodology

For each adhesive, five specimens were tested. A test specimen as well as the way in which the load is applied is shown in Figure 7.39. The test specimen has a dimension of 95x122x450mm and the displacement-rate of 3mm/minute was used. This was calculated according to Equation 7.3. The temperature and humidity during the test was kept constant at 22.3°C and 55.7%, respectively. Steel plates were attached to the bottom of the specimen. This was done to ensure that the LVDTs measured the outer fibre deflection of the specimen accurately. The test-setup is shown in Figure 7.30 and Figure 7.31.

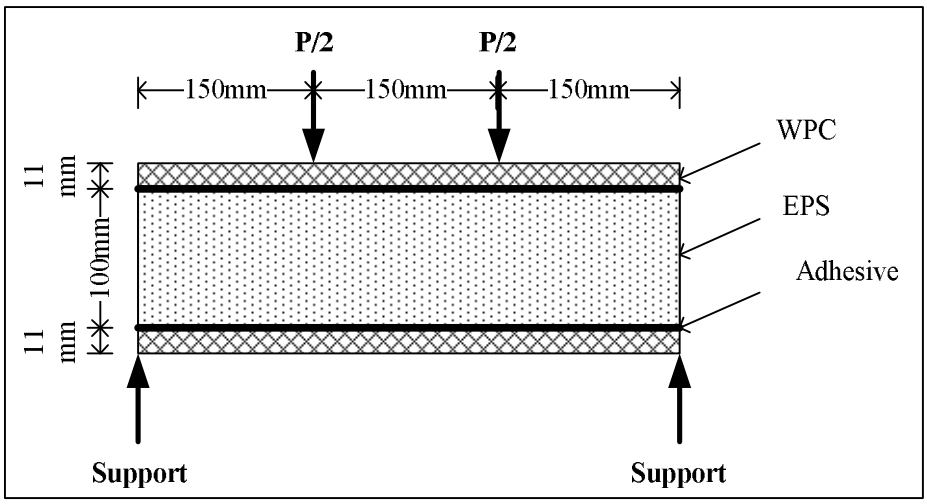

Figure 7.39: Schematic representation of composite sandwich panel four-point bending test-setup

The adhesive was applied as described in Table 7.1. The Pekadur A663 polyurethane adhesive was cured for 20 hours before testing. The test-setups for the bending test of the sandwich panel for the Pekadur A663 polyurethane adhesive and GB685 spray grade rubber adhesive are shown in Figure 7.40 and Figure 7.41 respectively.

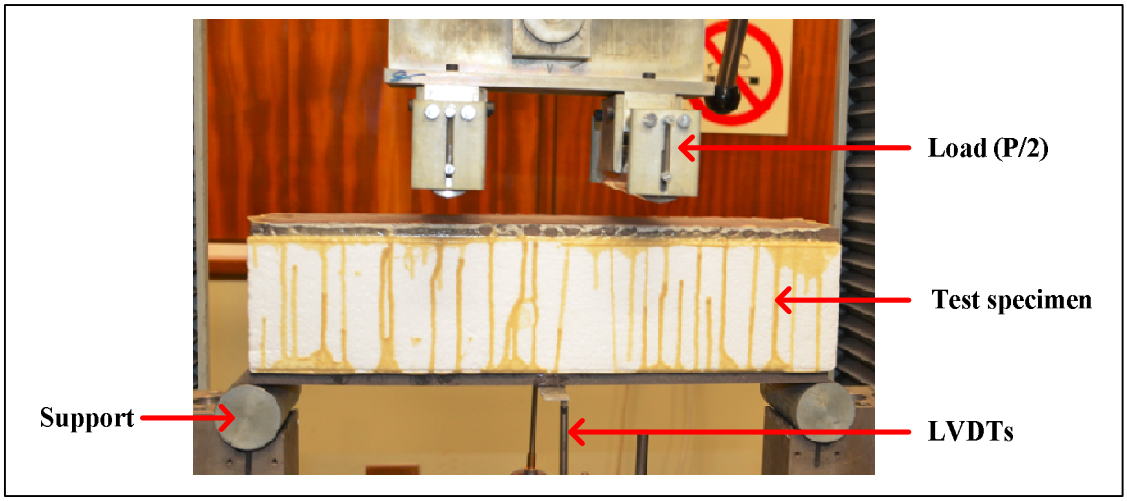

Figure 7.40: Bending test-setup of the sandwich panel for the Pekadur A663 polyurethane adhesive

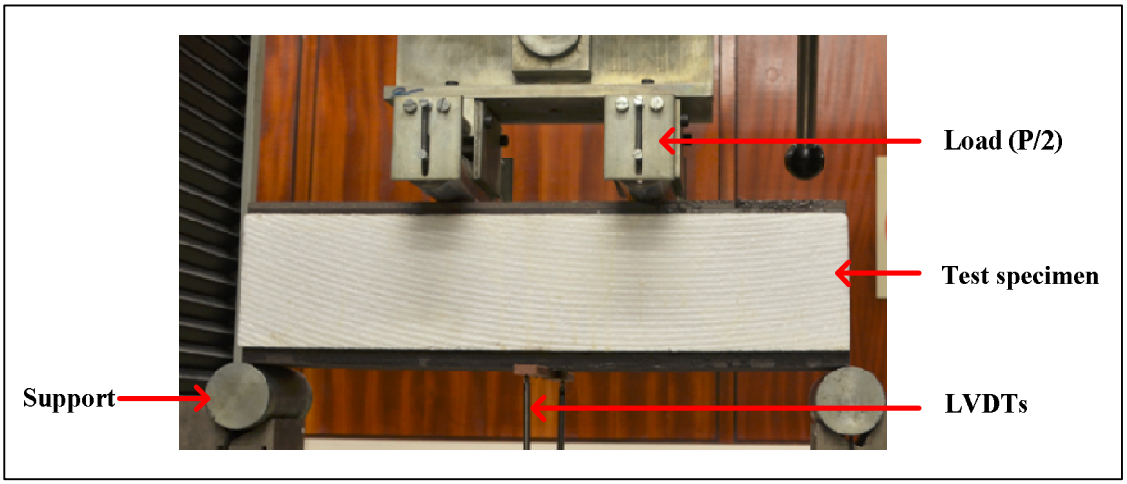

Figure 7.41: Bending test-setup of the sandwich panel for the GB685 spray grade rubber adhesive

7.8.2. Results

The stress of the outer fibres of the specimens is determined by nonhomogeneous beam theories. The stress of the outer fibres of the nonhomogeneous beam is calculated using the following equation (Craig, 2000, p. 362):

$$\sigma = \frac{PLE_f d}{12(EI)_{eq}} \quad \text{.....} \quad \textbf{(7.8)}$$

where,

σ = Stress of the outer fibres of the specimen (Pa)

P = Applied load (N)

L = Span length (m)

E_f = Young's modulus of face panel material, in this case Young's modulus of WPC (Pa)

d = Depth of the specimen (m)

The weighted bending rigidity $(EI)_{eq}$, on the other hand, depends on the ratio of the Young's modulus of the EPS to the WPC (Craig, 2000; Davies, 2008):

$$(EI)_{eq} = {E_f\, w.t.\,(c+t)^2}/{2} \qquad \textbf{For } E_c/E_f \leq 0.01 \quad \textbf{(7.9)}$$

$$(EI)_{eq} = \sum E_i I_i \qquad \textbf{For } E_c/E_f > 0.01 \quad \textbf{(7.10)}$$

where,

$(EI)_{eq}$ =weighted bending rigidity ($N.m^3$)

Ef = Young's modulus of WPC (Pa)

Ec = Young's modulus of EPS (Pa)

w = Width of specimen (m)

t = Thickness of WPC (m)

c = Thickness of EPS (m)

E_i = Young's modulus of layer *i* (Pa)

I_i =Moment of inertia of layer *i* (m^4)

In this case, E_c/E_f is smaller than 0.01, therefore, Equations 7.9 and 7.8 is used to calculate the stress of the outer fibres of the specimen. The two adhesives are discussed individually and then compared to each other.

The Pekadur A663 polyurethane adhesive

Figure 7.42 illustrates the bending stress-deflection responses of the composite beams with use of the Pekadur A663 polyurethane adhesive. These specimens exhibited a lower bending stress when compared to that of the WPC (Figure 7.16). This is due to the lower bending stress resistance of the EPS.

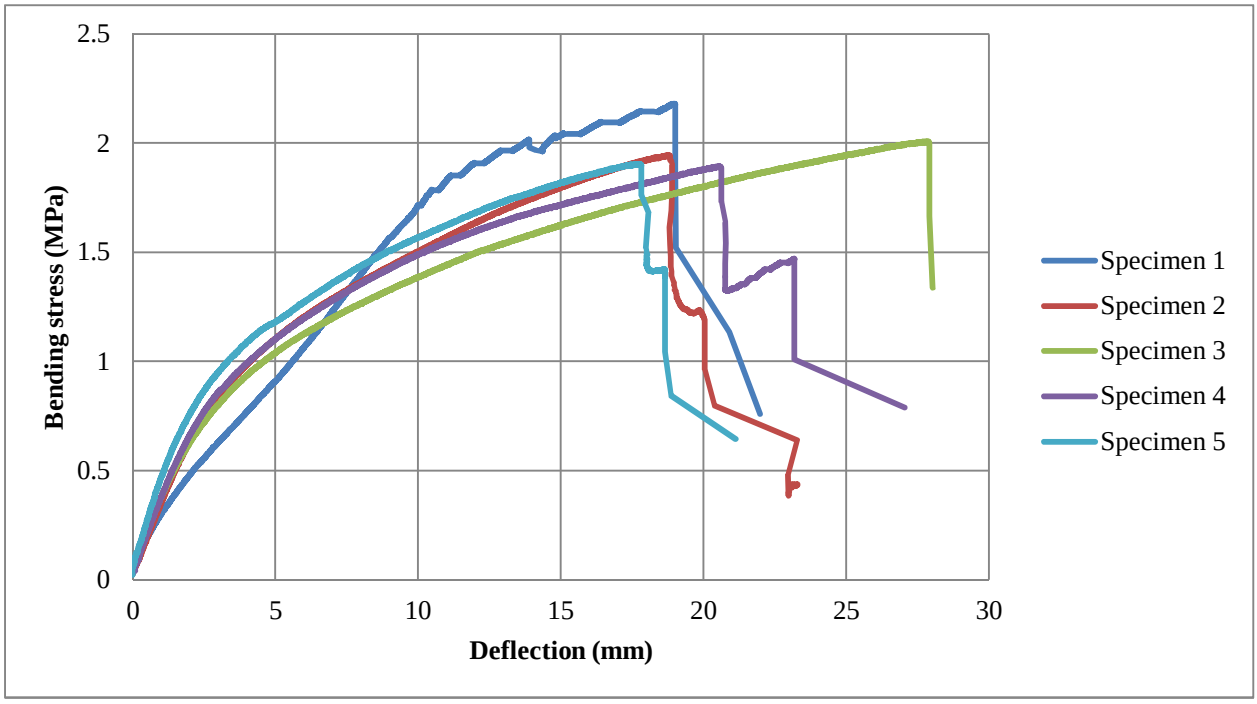

Figure 7.42: Bending stress-deflection responses of composite beam test specimens (Pekadur A663 polyurethane adhesive)

The statistical properties of the results are shown in Table 7.9. This table illustrates an acceptable standard deviation and coefficient of variation. All the results were obtained by calculating the specific material property of each of the responses and then determining the average. The bending stress is calculated by using Equation 7.6, whereas the maximum bending moment is determined by using Figure 7.14 (PL/6). The maximum shear force is determined by dividing the applied force by two (P/2). This shear force results in a shear stress of 59.446kPa, which is resisted by the EPS (calculations shown in Appendix D). The average deflection, where yielding occurs, for this test is 20.788mm. This resulted in a yield-deflection to span ratio of 4.620%.

Table 7.9: Results of the bending test for Pekadur A663 polyurethane adhesive

	Ultimate/ Yield bending stress	Maximum bending moment	Maximum shear force
Average	1.986MPa	209.590Nm	1397.269N
Standard deviation	0.118MPa	12.435Nm	82.834N
Coefficient of variation	5.928%	5.928%	5.928%
Characteristic bending stress (5%) (Equation 7.3)	1.719MPa		

The bending of a composite beam is shown in Figure 7.43. This figure illustrates that the top WPC panel remains horizontal, whereas the bottom WPC panel deflects. This is due to the EPS having weaker mechanical properties when compared to that of the WPC. The applied load causes the EPS to distribute the load evenly as the rigidity of the adhesive causes the beam to act as a unit. This results in the deflection of the bottom WPC panel.

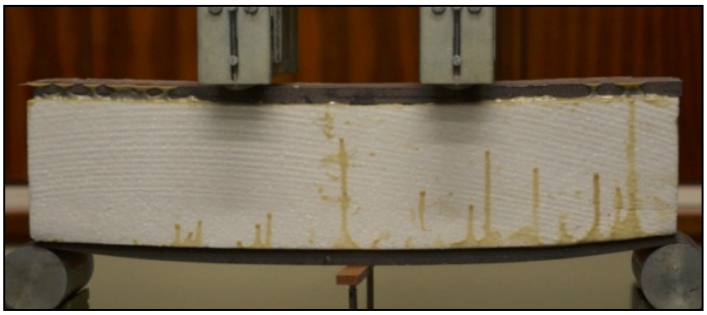

Figure 7.43: Bending in bottom WPC panel (Pekadur A663 polyurethane adhesive)

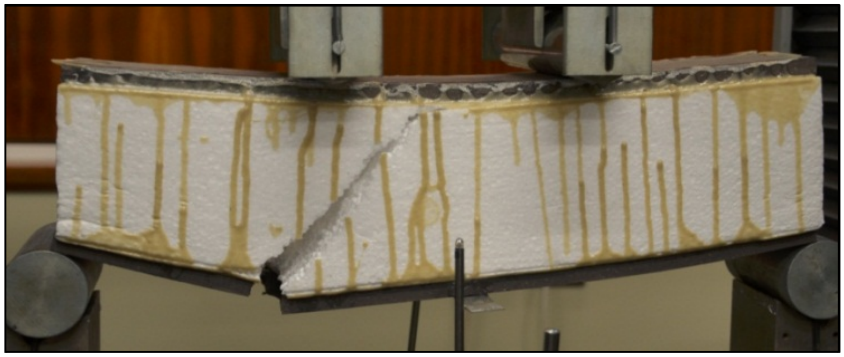

Figure 7.44: Failure of composite beam (Pekadur A663 polyurethane adhesive)

The maximum load occurs just before failure of the bottom WPC panel. After the bottom WPC panel fails, the load decreases after which the load is carried by the EPS and the top WPC panel. In the case of Specimen 3 (see Figure 7.42), the failure of the bottom WPC and EPS occurred simultaneously. Failure of the composite beam is shown in Figure 7.44. For all the specimens, expect Specimen 3, the bottom WPC panel fails first followed by the failure of the EPS. The bottom WPC panel fails in tension, followed by the EPS failing in shear. As shown in Figure 7.44, the EPS failed in the region between the support and the upper rollers, where the shear force is at a maximum. The shear force between the upper rollers is zero. Thus, the shear force is the governing factor, which results in a 45 degree angle shear failure in the EPS. The failure of the WPC also occurred in the region between the support and the upper roller. This is due to the

EPS that transferred most of the load to this area where the largest shear forces occurred. Although the EPS failed in shear, the WPC still failed in tension.

GB685 spray grade rubber adhesive

The bending stress-deflection responses of the composite beams, with use of the GB685 spray grade rubber adhesive, are shown in Figure 7.45. The test specimens displayed a lower bending strength than that of the previous sections (Section 7.4). This is due the specimens not bending as a unit.

Figure 7.46, illustrates the bending of the composite beam attached with GB685 spray grade rubber adhesive. This figure illustrates how the top and bottom WPC panels deflect in a similar shape and magnitude. This is due to the adhesive causing the WPC to slide over the EPS, as shown in Figure 7.47. Thus, this beam acts as three separate parts.

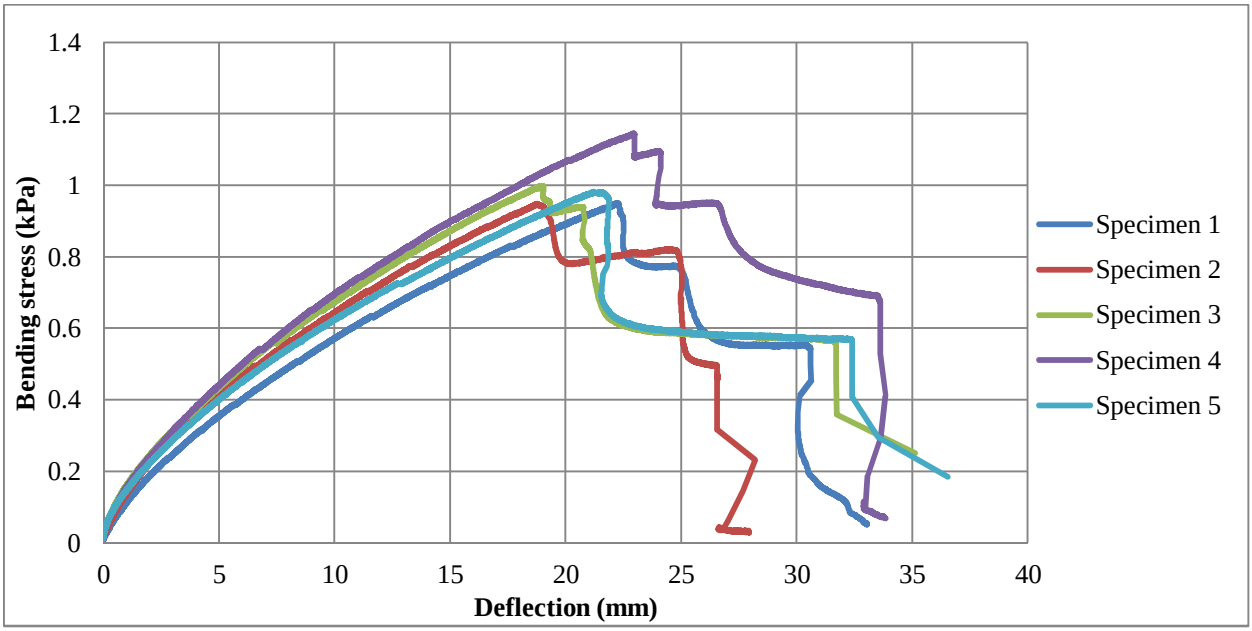

Figure 7.45: Bending stress-deflection responses of composite beam test specimens (GB685 spray grade rubber adhesive)

The results of these tests are shown in Table 7.10. This table shows a standard deviation and coefficient of variation. All the results were obtained by calculating the specific material property of each of the responses and then determining the average. The bending stress is calculated by using Equation 7.6, whereas the maximum bending moment is determined by using Figure 7.14 (PL/6). The maximum shear force is determined by dividing the applied force by two (P/2). This shear force results in a shear stress of 11.761kPa (refer to Appendix D) due to bending, which is resisted by the adhesive on the bonded surface. However, sliding friction caused by the panels sliding over each other also contributes to the shear stress of the

adhesive. The average yield deflection (deflection where yielding occurs) for this test is 20.825mm, which resulted into a yield-deflection to span ratio of 4.628%.

Table 7.10: Results of the bending test for the GB685 spray grade rubber adhesive

	Ultimate/ Yield bending stress	Maximum bending moment	Maximum shear force
Average	1.005MPa	106.058Nm	707.052N
Standard deviation	0.081MPa	8.584Nm	57.229N
Coefficient of variation	8.094%	8.094%	8.094%
Characteristic bending stress (5%) (Equation 7.3)	0.872MPa		

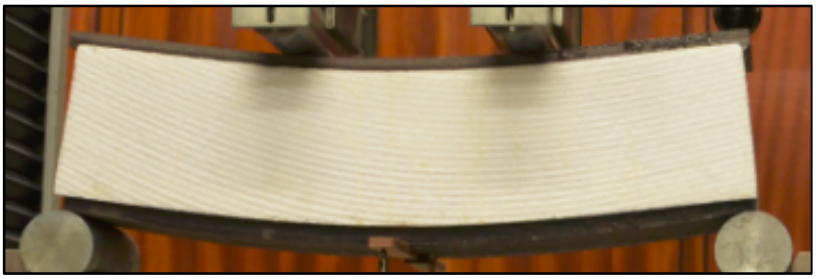

Figure 7.46: Bending of composite beam (GB685 spray grade rubber adhesive)

Figure 7.47: WPC sliding over EPS (GB685 spray grade rubber adhesive)

Failure of a composite beam is shown in Figure 7.48. The top WPC panel failed in tension, followed by the EPS failing in tension and finally total failure of the composite beam occurred when the bottom WPC panel failed. The maximum load was reached shortly before failure of the top WPC panel. The top WPC panel failed first due to greater sliding friction on the top panel, as shown in Figure 7.47. This figure illustrates that

the top WPC slid more over the EPS than that of the bottom WPC panel, thus a greater sliding friction. After the top WPC panel failed, the load decreased after which the load was carried by the EPS and the bottom WPC panel. In the case of Specimen 4 (see Figure 7.45), a higher bending stress was caused by the WPC and the EPS that slid over each other (see Figure 7.47) to a greater degree, causing the top WPC to fail at a later stage compared to the other specimens.

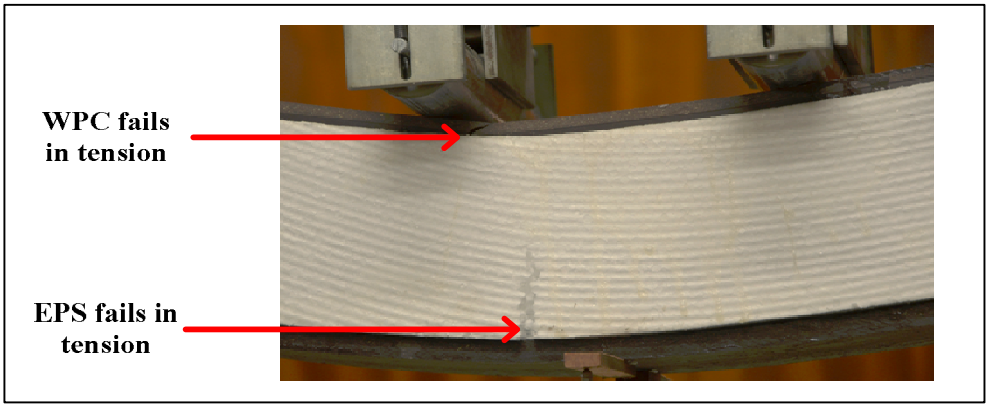

Figure 7.48: Failure of composite beam (GB685 spray grade rubber adhesive)

Comparison of the two adhesives

Figure 7.49 the comparison of the average bending stress for both adhesives used. From this figure, it is clear that when the Pekadur A663 polyurethane adhesive was used the composite beam could resist more bending stress than when the GB685 spray grade rubber adhesive was used.

As mentioned before, the bottom WPC panel failed in tension, followed by shear failure of EPS when the Pekadur A663 polyurethane adhesive was used. For the Pekadur A663 polyurethane adhesive, the maximum bending stress at the outer fibres of the composite is equal to 1.986MPa. The bottom WPC panel failed in tension at, according to calculation in Appendix D, at 1.986MPa.Due to the complexity of load transfer through this composite section, this bending stress does not reflect the true tensile strength of WPC. The calculated bending stress illustrates that the bottom WPC panel fails at a lower tensile stress than that obtained from the direct tensile test (Section 7.3). After the bottom WPC panel ruptured, the EPS ruptured in shear. The shear stress at this point is equal 59.446kPa, which is approximately 27% larger than that of the push-through shear test, Section 7.7 (EPS shear stress is 46.662kPa).

For GB685 spray grade rubber adhesive, the failure occurred at the top WPC panel, followed by tensile failure of the EPS. The maximum bending stress of the outer fibres is 1.005MPa due to the applied load. However, due to the addition of sliding friction, which is greater in the top bonded area (Figure 7.47), the top WPC panel failed in tension. However, no published values for the kinetic and static friction coefficient of

the GB685 spray grade rubber adhesive were found. Therefore, the effect of the sliding friction is unknown. The EPS also failed in tension, as shown in Figure 7.48.

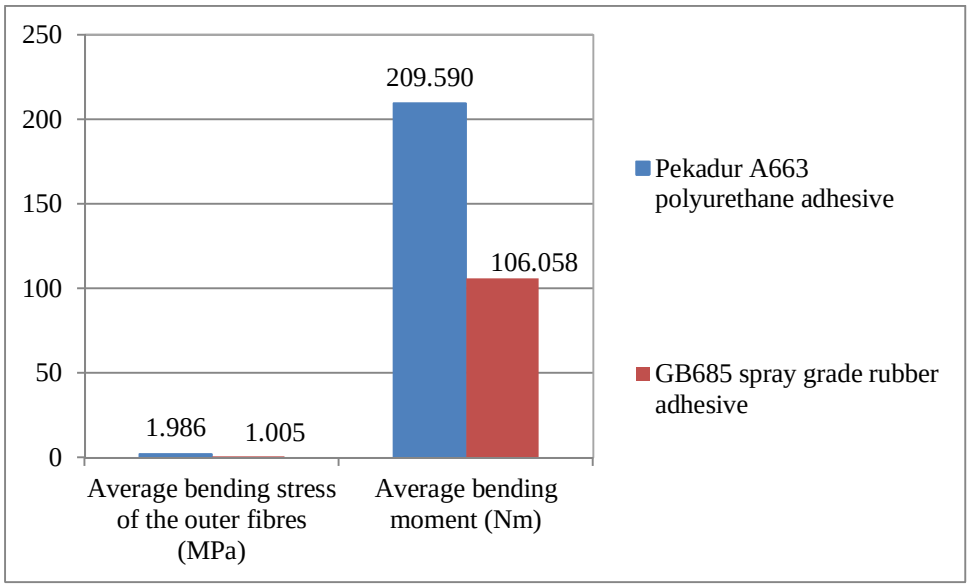

Figure 7.49: Comparison of the average bending stress and average bending moment for adhesives used (composite four-point bending test)

7.9. Summary

WPC is a homogenous and anisotropic material. The Young's modulus of this material differs for tension and compression loading. The Young's modulus in compression (1.347GPa) is greater than the tensile Young's modulus (0.949GPa), however still relatively small. The compressive yield stress (23.933MPa) of WPC is greater than that of the tensile yield stress (18.152MPa). Thus, the material is stronger and stiffer in compression, than in tension.

The average creep strain-time response (for 30% compressive stress) as shown in Figure 7.24 resulted in a displacement of approximately 11mm over the length of the walling system, for the testing period (1000 hours). The average creep-modulus response proved that the the curve stagnates after about 20 hours, for the testing period of 1000 hours. Thus, if no tertiary creep or unloading occurs, the walling unit (length of 2700mm) will result in a displacement of approximately 11mm. However, a longer creep testing period is recommended to investigate whether tertiary creep occurs.

The bending test of the WPC resulted in a bending stress which is greater than the tensile and compressive yield strength of the material. This implies that the material fails in tension since the material is weaker in

tension. Figure 7.17 also illustrates failure of the specimen in tension. The material has a deflection to span length ratio of 3.56% which is relatively high. Thus, the material is ductile up untill the point of failure.

The push-through shear test revealed that the Pekadur A663 polyurethane adhesive can resist larger shear forces (Figure 7.38). The shear-bond formed by this adhesive is stronger than that of the shear force resistance of the EPS. Therefore, failure occurred in the EPS when this adhesive was used. When the GB685 spray grade rubber adhesive was used, shear failure occurred within the bond surface. Thus, this adhesive resists less shear forces than that of EPS (no failure on the EPS). Figure 7.38 illustrates that the Pekadur A663 polyurethane adhesive resulted in a shear bond strength approximately seven times larger than that of the GB685 spray grade rubber adhesive.

The composite bending test, Figure 7.49, illustrates that the Pekadur A663 polyurethane adhesive can resist larger resultant shear stress than the GB685 spray grade rubber adhesive. The rigid bond formed by the Pekadur A663 polyurethane adhesive resulted in less overall deflection than the beams tested with the GB685 spray grade rubber adhesiv However, when the GB685 spray grade rubber adhesive is used, the WPC and EPS slid over each other, which resulted in higher deflections of the specimens before failure occurred.

When the results from the bending test of the material, WPC (Table 7.5) are compared to those of the composite (Figure 7.49), it is clear that the EPS caused the composite to fail at significantly lower bending strengths, but at higher deflections. The adhesive used also plays an important role in the bending strength of the composite. Since the EPS is weaker in bending, compression and tension, the composite is slightly weaker. The larger deflection of the composite when subjected to bending forces can be due to the EPS that can reduce to a flat disk as shown in Section 7.6.

When the two selected adhesive are considered, the Pekadur A663 polyurethane adhesive showed greater shear strength (Section 7.7) and resultant shear strength (from bending test, Section 7.8) compared to that of the GB685 spray grade rubber adhesive. Larger deflections were witnessed when the GB685 spray grade rubber adhesive was used. However, the Pekadur A663 polyurethane adhesive cures to a hard bond surface, whereas the GB685 spray grade rubber adhesive does not harden. Thus, due to the larger endured strengths and the hardened bond surface, the Pekadur A663 polyurethane adhesive is recommended as the most viable adhesive for the walling system of the housing application.

CHAPTER 8: STRUCTURAL FEASIBILITY

In this chapter, a structural feasibility study is discussed by performing a numerical analysis and assessing fire performance and durability of the housing unit described in Chapter 6. The results of the experiments are used in this chapter to perform the numerical analysis. Therefore, the numerical analysis is performed for a modular WPC (wood-plastic composite) housing unit only. The fire performance is discussed in terms of fire rating which is determined for three housing units. These three housing units include the modular WPC and FFC (foam fibre composite) housing units and the block and mortar housing unit. The durability is discussed for the WPC, FFC and EPS (expanded polystyrene). The durability of a block and mortar housing unit is known to industry and it complies with various standards. The plan view of a modular plastic housing unit and a block and mortar housing unit are illustrated in Appendix C.

8.1. Numerical analysis

ABAQUS^{TM}, a finite element modelling software package, is used to perform the numerical analysis for the roof and walling system. For the structural face, WPC (wood-plastic composite) is used. Table 8.1 summarises the properties of the materials used in this analysis. The properties of the WPC were obtained from the results of the experiments (Chapter 7).

Table 8.1: Properties of materials used in numerical analysis (Domone & Illston, 2001; Rachel, 2013)

	Unit	WPC	EPS	Grade 5 Pinewood
Density, ρ	kg/m^3	1331.00	15.000	510.00
Poisson ratio, υ		0.30	0.100	0.20
Characteristic compressive yield stress, σ_{cy}	MPa	23.933	0.071 (Chapter 7)	4.70
Compressive modulus of elasticity, E_c	GPa	1.284	0.002	7.80
Tensile yield stress, σ_{ty}	MPa	18.152	0.200	0.36
Tensile modulus of elasticity, E_t	GPa	0.949	0.002	7.80
Reference		Chapter 7	(Rachel, 2013)	(Domone & Illston, 2001)

The flooring unit is supported by compacted soil (Figure 6.6). The stiffness of the compacted soil should be at least equal to the loading on the flooring system. This stiffness is determined in this section.

8.1.1. Roofing and walling system

A static linear elastic analysis was performed. This was ensured by ABAQUS™ aborting the analysis if any material's yield point was reached. The roof and walling system was analysed simultaneously, since the walling system is tied to the roof and the load deformations on the roof affects the stress and deformation of the walls. A simplified model could not be used since no symmetry exists for the layout of the structure. This is due to the unsymmetrical positioning of the openings in the walling system. The model is illustrated in Figure 8.1. Internal walls were not included, since they are only subjected to their own weight. Thus, the loading on the roof does not affect the internal walls.

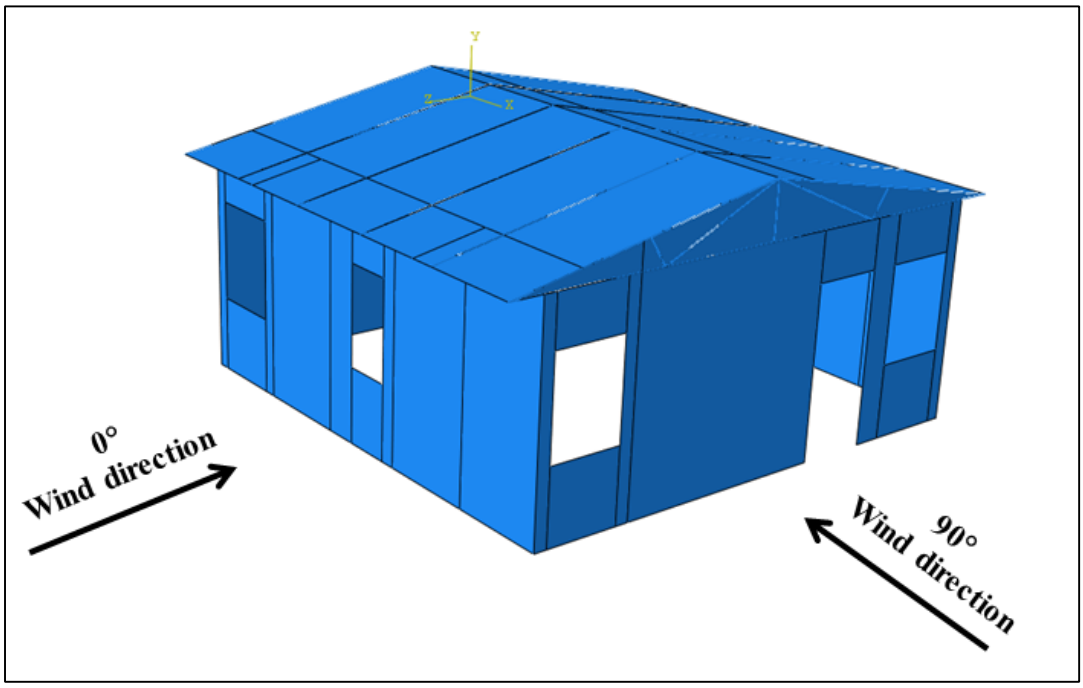

Figure 8.1: Modular WPC housing unit and wind directions

In this section the element type, size, boundary conditions, constraints, loads, load combinations and results of the roof and walling systems that were analysis are discussed.

Element type and mesh size

The roof trusses and rafters are comprised of 73x48mm Grade 5 Pinewood (Figure 6.2 and Table 6.1). Two-noded stress-displacement beam elements are used to analyse the trusses and rafters. The roof sheeting

comprises of 25mm thick WPC panels, which is modelled as four-noded stress-displacement shell elements with a thickness of 25mm. Refer to Section 6.1 for the design of the roofing system.

ABAQUS™ has an element type, termed composite (layered) shell elements, which ensures continuity conditions (for stresses and displacements) between layers. The nodes are shared as shown in Figure 8.2. For the walling system, four-noded stress-displacement composite shell elements are used. The composite shell element has a thickness of 11mm WPC structural face panel, 100mm EPS core panel and 11mm WPC structural face panel (refer to the external wall in Figure 6.4). The WPC shell elements (layers) are placed eccentrically. As illustrated in Chapter 7, when Pekadur A663 polyurethane adhesive was used, the failure of the sandwich panel occurred within the EPS. Thus, this adhesive creates a rigid bond between the WPC and the EPS with a higher strength than that of the EPS (Sections 7.7 and 7.8). Therefore, the adhesive is not included in the analysis of this model. The gable is assumed part of the wall and four-noded stress-displacement shell elements are used with a thickness of 5mm, to model the gable. Refer to Section 6.2 for the design of the walling system. The mesh, on the other hand, is the same for all the elements. A mesh of 100x100mm is selected for all the elements.

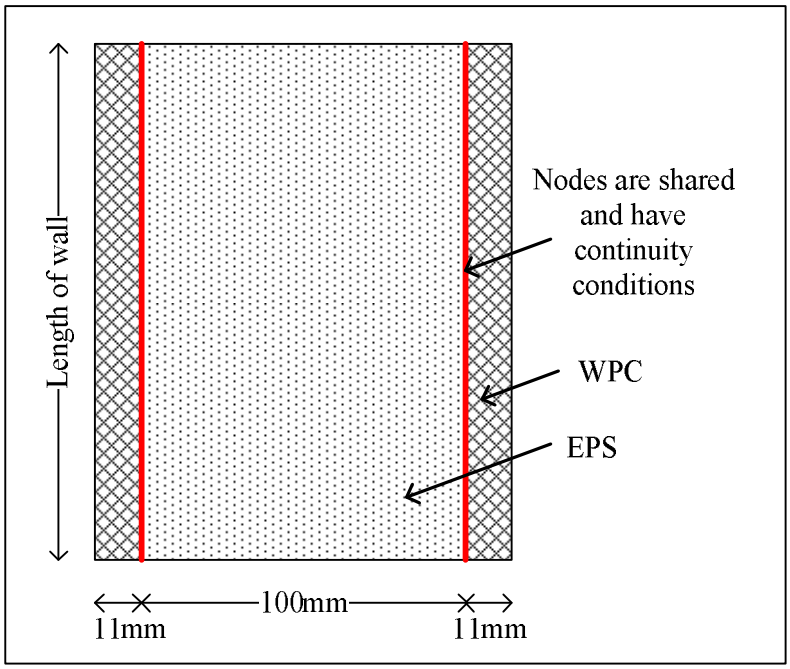

Figure 8.2: Composite (layered) shell element

Boundary conditions and constraints

All the connections are assumed pinned. Therefore, the supported members are only supported in the lateral and axial direction. The members are free to rotate. Some elements are constrained by means of ties, where a

master element and slave(s) elements are identified. Deflection of the master element affects the deflection of the slave element. The following elements are tied, by of pin connection, to each other:

- The roof sheeting (master element) is tied to the roof trusses.
- Trusses (master element) are tied to the rafters.
- The roof trusses (master element) are tied to the gable.
- The roof trusses (master element) are tied to the walling system.
- The rafters (master element) are tied to the walling systems.

The walling system has a boundary condition that is pinned. This pinned connection is located where the walling system is supported by the concrete strip footing (Figure 6.6).

Loads

Two types of loading can be applied to the roof and walling system. These two types of loads include the own weight of the structure (G_k) as well as an imposed load (Q_k). The imposed load is divided into a live load (LL) and wind load (WL). The own weight of the structure is determined by ABAQUS™, based on the material densities, and is applied as a gravity load. SANS 10600-2 (2011) specifies a live load for the roofing system. For a category H2 roof, a live load of 0.25kPa is recommended (SANS 10160-2, 2011, p. Table 5).

For the wind loads, the specified calculations according to SANS 10160-3 were followed. The following assumptions are made to determine the wind peak pressure, q_p (z) (SANS 10160-3, 2011, pp. 12-19).

- The basic wind speed, $v_{b,0}$, is equal to 36m/s (SANS 10160-3, 2011, pp. 14, Figure 1). This is the largest basic wind speed in South Africa according to SANS 10160-3, 2011 (Figure 1) and is therefore the worst case senario for wind loading.
- A terrain category C was chosen, since this terrain decribes typical conditions for low-income housing locations (SANS 10160-3, 2011, pp. 17, Table 2).
- Design working life was assumed to be 25 years (SANS 10160-1, 2011, p. 24).
- A topography factor of 1 is used (SANS 10160-3, 2011, p. 19).
- The air density in terms of the site altitude is assumed to be 1.2kg/m^3 (SANS 10160-3, 2011, pp. 20, Table 4). This is selected, since it results in the worst case scenario for wind.

With these assumptions, the wind peak pressure, q_p (z) was calculated as 509.5Pa. All calculations performed to determine the wind peak pressure, q_p (z), are shown in Appendix E.1.

In SANS10160-3, the wind pressure applied to the walls and roof is divided into different areas. For each area, an external wind pressure coefficient, $c_{pe,}$ is prescribed. The external wind pressure coefficient, $c_{pe,}$ of the roof differs for a 0° or 90° wind direction. These wind directions are illustrated in Figure 8.1. An internal wind pressure coefficient, c_{pi}, is also prescribed for the openings, such as windows and doors. This is obtained from Figure 16 and Equation 16 of SANS10160-3. If it is assumed that the openings are closed, the internal wind pressure coefficient is zero.

A positive coefficient will result in a compressive pressure and a negative coefficient in a tension pressure. The resultant coefficient per area is determined by subtracting or adding the coefficients, depending on whether the coefficients are acting in compression or tension. This resultant wind pressure coefficient is multiplied with the peak wind pressure to obtain the wind pressure per area. The internal and external wind pressure coefficients for the walls and roof, 0° and 90°, are shown in Appendix E.1.

The wind pressure per area for open and closed openings, as well as 0° and 90° for the walls and the roof, are shown in Table 8.2 and Table 8.3 respectively. The calculations are shown in Appendix E.1. For the 0° wind direction for open and closed openings, only the first two sets are selected for the wind pressure on the roofs. This is since Sets 1, 2, 6 and 7 results in the worst case scenarios for wind pressure on the roof. Where Sets 1 and 6 refer to uplift wind pressures on the roof and Sets 2 and 7 have downward and uplift wind pressures.

Table 8.2: Wind pressure per area for open and closed openings as well as 0° or 90° for the walls

	Wind pressure (Pa)			
	Open openings		**Closed openings**	
	0°	***90°***	***0°***	***90°***
A	-586	-408	-611	-611
B	-382	-204	-408	-408
D	382	560	357	357
E	-127	51	-153	-153

Table 8.3: Wind pressure per area for open and closed openings as well as 0° or 90° for the roof

	Wind pressure (Pa)									
	Open openings					**Closed openings**				
	0°				***90°***	***0°***				***90°***
	Set 1	***Set 2***	***Set 3***	***Set 4***	***Set5***	***Set 6***	***Set 7***	***Set 8***	***Set 9***	***Set 10***
F	-596	87	-260	-250	-520	-622	61	-285	-275	-723
G	-464	87	-158	-219	-459	-489	61	-183	-245	-662
H	-189	87	-36	-66	-122	-214	61	-61	-92	-326
I	-219	-97	-97	-219	-71	-245	-122	-122	-245	-275
J	-239	-97	66	-219	0	-265	-122	41	-245	0

Load combinations

The safety of people as well as the structure is immensely important when the walling and roofing system are considered. Therefore, the ultimate limit state design loading combinations are used. The following load combinations are used (SANS 10160-1, 2011, pp. 38, Table 3):

- For uplift (tension, negative) pressure on the roof or part of the roof:
  - $LC = 0.9G_k + 1.3WL$
- For compression pressure on the roof or part of the roof:
  - $LC = 1.2G_k + (1.6\Psi)LL + 1.3WL$
- For pressure on the walls:
  - $LC = 0.9G_k + 1.3WL$

Where LC refers to the load combination, G_k denotes to the own weight of the member, LL is the live load of the roof and WL is the wind pressure on the member. The combination factor, Ψ, is equal to 0.3 (SANS 10160-1, 2011, pp. 34, Table 2). The combination factor is multiplied with the factorised live load since the live load is the less critical imposed load. Wind load is the critical imposed load.

Six loading scenarios are possible and they are shown in Table 8.4. The roof Member X and Y are explained in Figure 8.3. Forces on member of the roof may differ, since one side can be subjected to up-lift wind forces while the other side of the roof is subjected to downward forces.

Table 8.4: Six loading scenarios considered for analysis

				Load combinations		
Scenario	**Openings**	**Wind direction**	**Roof set**	**Wall**	**Roof part x**	**Roof part y**
1	Open	0°	Set 1	$0.9G_k$ +1.3WL	$0.9G_k$ +1.3WL	$0.9G_k$ +1.3WL
2	Open	0°	Set 2	$0.9G_k$ +1.3WL	$1.2G_k$ +0.48LL+1.3WL	$0.9G_k$ +1.3WL
3	Open	90°	Set 5	$0.9G_k$ +1.3WL	$0.9G_k$ +1.3WL	$0.9G_k$ +1.3WL
4	Closed	0°	Set 6	$0.9G_k$ +1.3WL	$0.9G_k$ +1.3WL	$0.9G_k$ +1.3WL
5	Closed	0°	Set 7	$0.9G_k$ +1.3WL	$1.2G_k$ +0.48LL+1.3WL	$0.9G_k$ +1.3WL
6	Closed	90°	Set 10	$0.9G_k$ +1.3WL	$0.9G_k$ +1.3WL	0.9Gk +1.3WL

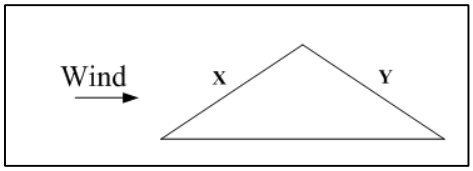

Figure 8.3: Member X and Y of the roof

Results:

Table 8.5 illustrates the maximum stress, -tension, -compression and -deflection of the roof sheeting and walls for each scenario. Figure 8.4 and Figure 8.5 indicate the location where the maximum stress, -tension, -compression and -deflection of the roof sheeting and walls occur. In these figures, the red markers indicate the results of the walling system (Table 8.5) and the blue markers indicate the results of the roof sheeting (Table 8.5).

For the results in Table 8.5, the roof trusses and gable are not included. The reaction of the WPC and/or EPS for applied loads is investigated. The results shown in Table 8.5, illustrate that no yielding occur. All analyses under the described loading conditions, the six scenarios, remained in the elastic range of the materials. Therefore, no member yielded. The yielding stresses of the material are shown in Table 8.1. The results obtained from ABAQUS™ for the housing unit are shown in Appendix E.2. The maximum compressive and tensile stresses of the walling system, shown in Table 8.5, Figure 8.4 and Figure 8.5, occur at the interior WPC panel of the walling system. This area where the maximum stresses occur is shown in Figure 8.6.

Table 8.5: Analysis results of the walling system and roof sheeting for each loading scenario

	WALLING SYSTEM			ROOF SHEETING		
Scenario	**$\sigma_{ci,\ wall}$ (MPa)**	**$\sigma_{ti\ wall}$ (MPa)**	**$D_{i,wall}$ (mm)**	**$\sigma_{ci,\ roof}$ (MPa)**	**$\sigma_{ti\ roof}$ (MPa)**	**$D_{i,roof}$ (mm)**
1	0.62	0.58	13.4	0.53	0.55	6.0
2	0.65	0.75	14.6	0.90	0.69	11.3
3	0.36	0.83	24.7	0.75	0.93	4.4
4	0.72	0.83	13.9	0.58	0.50	7.0
5	0.66	0.71	13.6	0.86	0.65	10.5
6	0.70	0.67	14.6	0.61	0.72	6.7

NOTE:

From experiment results (Chapter 7):

Walling system	*Roofing system:*
• *Compressive and tensile strength = 1.986MPa* • *Allowable maximum deflection (defection/ span ratio = 4.620%) = 124.7mm*	• *Compressive yield of WPC = 23.933MPa* • *Tensile yield of WPC=18.152MPa* • *Allowable maximum deflection (defection/ span ratio =3.560%) = 126.0mm*

$\sigma_{ci,\ wall}$ = Maximum compression stress of the wall for scenario *i*

$\sigma_{ti,\ wall}$ = Maximum tension stress of the wall for scenario *i*

$D_{i,wall}$ = Maximum deflection of the wall for scenario *i*

$\sigma_{ci,\ roof}$ = Maximum compression stress of the roof for scenario *i*

$\sigma_{ti,\ roof}$ = Maximum tension stress of the roof for scenario *i*

$D_{i,roof}$ = Maximum deflection of the roof for scenario *i*

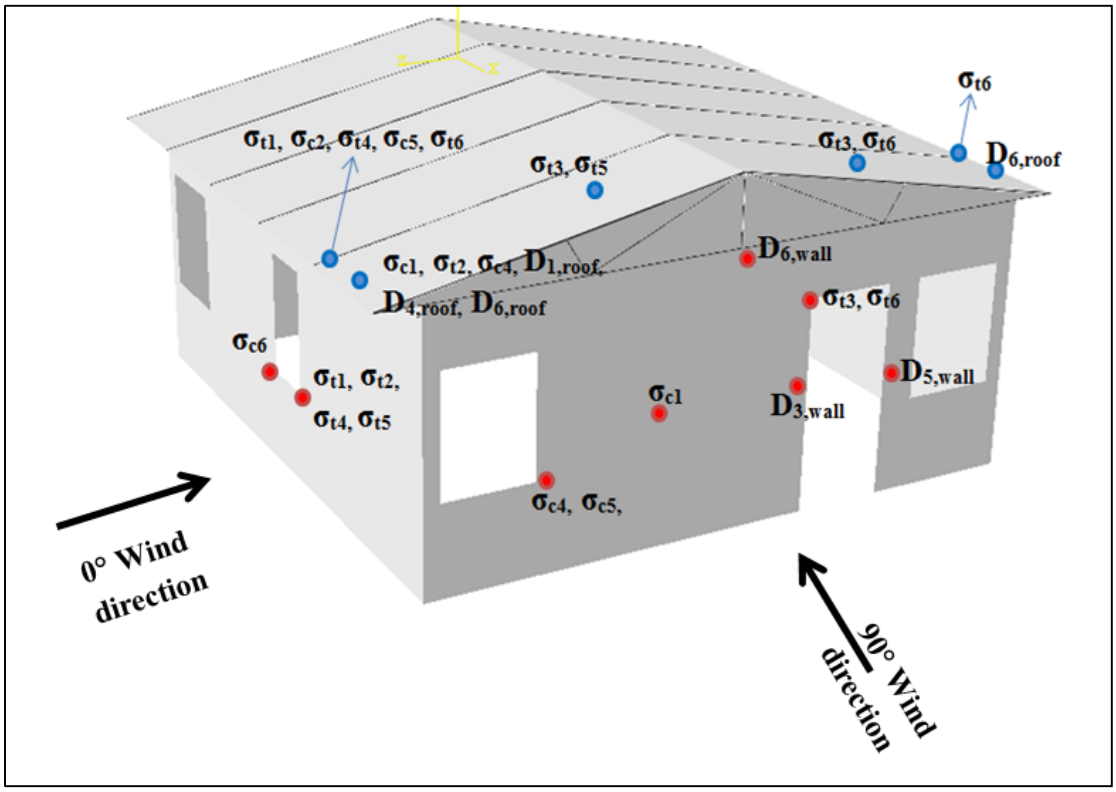

Figure 8.4: The location where the maximum stress, -tension, -compression, and -deflection of the roof sheeting and walls occur (opposite side of housing unit)

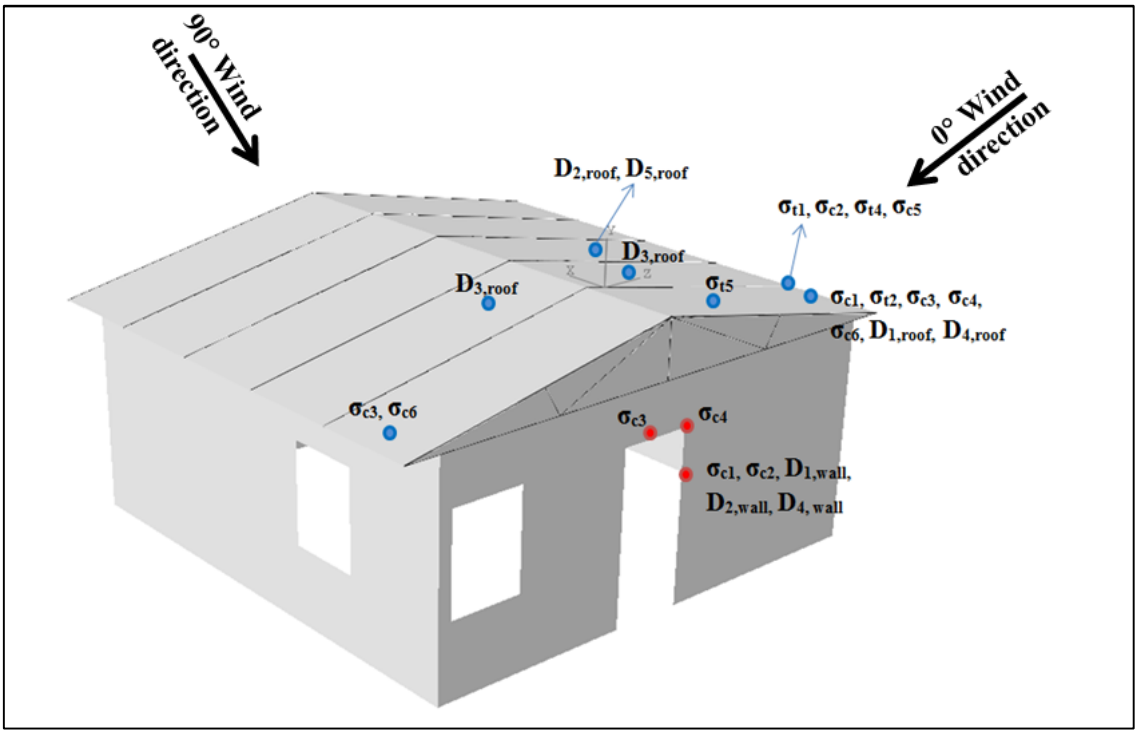

Figure 8.5: The location where the maximum stress, -tension, -compression, and -deflection of the roof sheeting and walls occur (opposite side of housing unit)

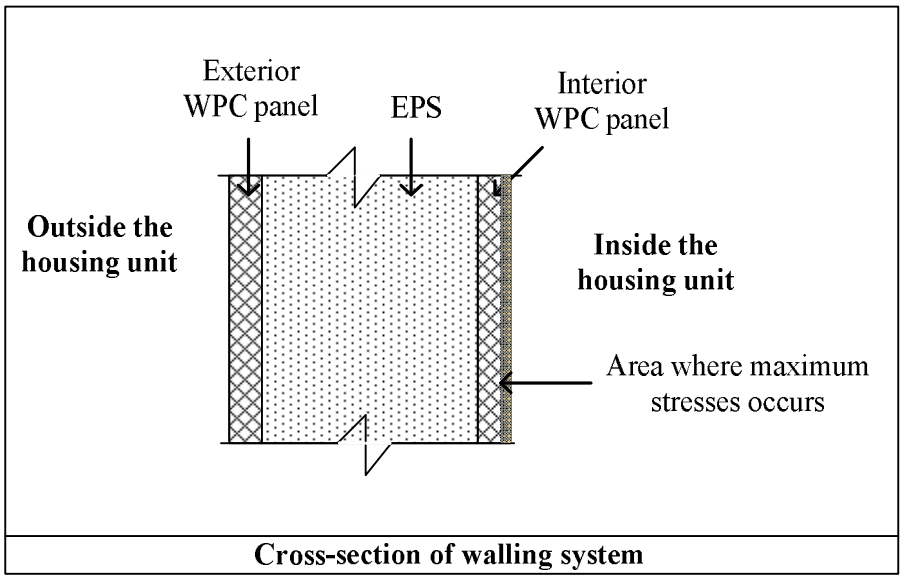

Figure 8.6: Area where the maximum stresses occurs

8.1.2. Verification of composite elements by numerical analysis

In this section, the sandwich panel bending test (Section 7.8) is analysed in ABAQUS™ using composite elements (Figure 8.2). The results of this analysis are compared to that of the sandwich panel bending test, in order to verify the use of composite elements in the numerical analysis of the housing unit (Section 8.1.1).

In this section the element type, size, material properties, boundary conditions, loads and results of the sandwich panel bending test (Figure 7.39), that were analysed, are discussed.

Elements and mesh size:

Four-noded composite shell elements were used to analyse the beam. The composite shell has a thickness of 11mm WPC structural face panel, 100mm EPS core panel and 11mm WPC structural face panel, thus a total thickness of 122mm, which is the same as the total thickness illustrated in Figure 7.39. The thickness of the three layers (WPC, EPS and WPC) does not have a significant effect on the results. A mesh of 75x95mm is selected to analyse the beam, as shown in Figure 8.7.

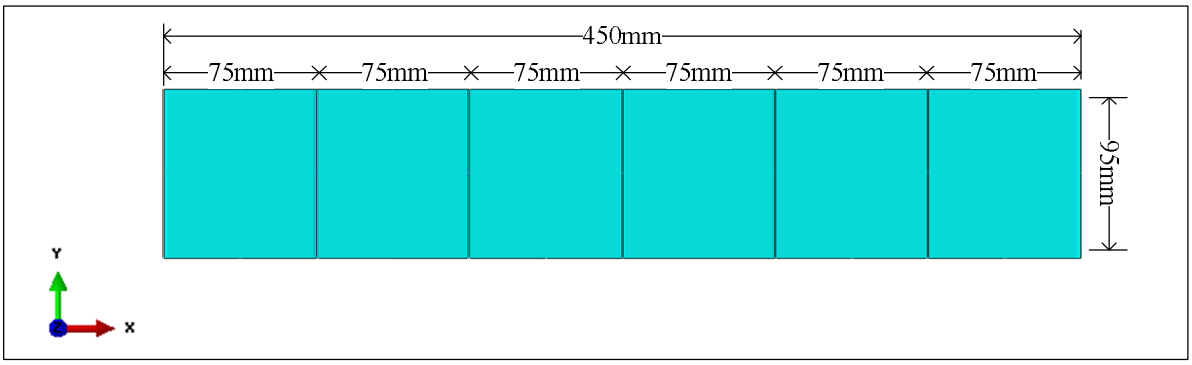

Figure 8.7: Mesh size of sandwich panel beam (Top view)

Material properties:

The material properties of WPC and EPS, specified in Table 8.1, were used to analyse the sandwich panel beam.

Boundary conditions:

The boundary conditions were applied as illustrated in Figure 8.8. Where the pin connection implies that the specimen was free to rotate about the Y-axis and the displacement in the Z-direction, X-direction as well as the rotation about the X-axis is zero (fixed). Whereas, the roller connection is similar to that of the pin connection, expect for that the specimen was allowed to displace in the X-direction.

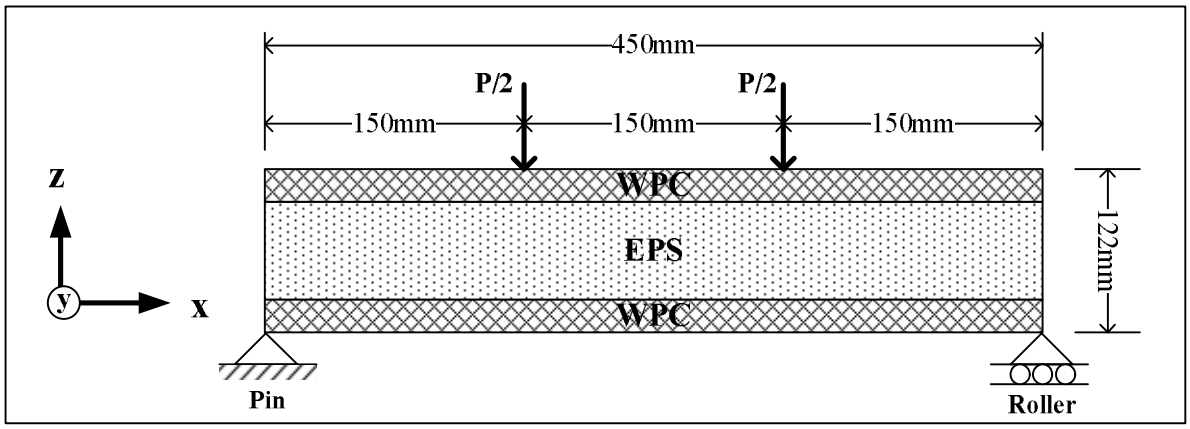

Figure 8.8: Boundary conditions (Verification of composite elements)

Loads:

The loads were applied as line loads. The maximum load applied (P) during the experiment (Section 7.8) was 2 794.537N, thus line loads of 14 708N/m were applied. These line loads were calculated by dividing the

maximum load (P) by 95mm length and two (for each line load). Refer to Figure 7.39 for the manner in which the loads are applied.

Results:

Results of this analysis are shown in Figure 8.9 and Table 8.6. In this table, the comparison of the results of the analysis as well as the experimental work is shown. The comparison of this result indicates a close correlation between the experimental work and the ABAQUS™ analysis. Therefore, the use of composite shell elements in Section 8.1.1 leads to accurate results.

Table 8.6: Comparison of the results of the ABAQUS™ analysis and the experimental work of the sandwich panel beam

	ABAQUS™ analysis of sandwich panel beam (Figure 8.9)	Experimental results of sandwich panel beam (Table 7.9)
Bending stress (MPa)	1.983	1.986
Deflection (mm)	20.360	20.788
Bending moment (N.m)	221.00	209.590

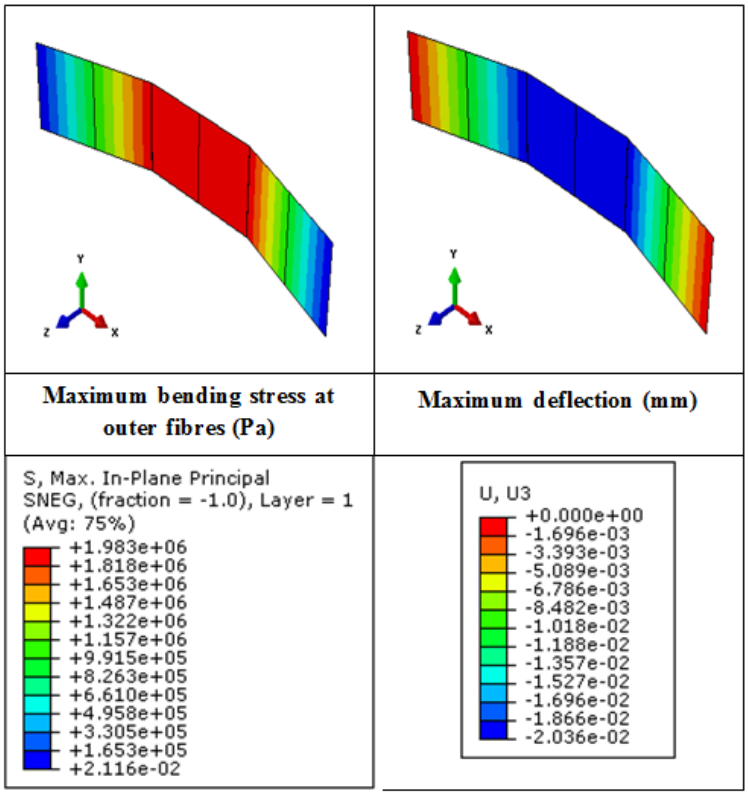

Figure 8.9: Results of ABAQUS™ analysis of the sandwich panel beam

8.1.3. Flooring system

The serviceability limit state design load combination for the flooring system is shown in Equation 8.1 (SANS 10160-1, 2011, pp. 38, Table 3). The imposed load, Q_k, on the flooring system is 1.5kN/m^2 (SANS 10160-2, 2011, pp. 13, Table1).

$$\boldsymbol{LC = 1.0G_k + 1.1Q_k} \quad \text{..... (8.1)}$$

Thus, the required soil stiffness should not be less than 0.017N/mm^3. The calculations are shown in Appendix E.3. The range of stiffness of slightly compacted soil is approximately 0.015 to 0.03N/mm^3 (Technical report No 34, 2003, pp. 34, Table 6.2). Therefore, slightly compacted soil will meet the required stiffness to support the flooring system with a deflection of approximately 0.85mm.

8.2. Fire performance

Fire resistance can be divided into two categories, namely passive and active fire protection. Passive fire protection refers to a material or system that is permanently prepared for a fire, which includes the adequacy of fire escapes and the satisfactory structural performance. Whereas, active fire protection are materials or systems that are activated once a fire is ignited. Active fire protection includes, for example, sprinklers and human actions (Buchanan, 2002, p. 4).

Fire resistance of a building element or building is measured as the shortest period to sustain one or more of the following (Lennon, 2011, p. 25):

- Stability
- Integrity
- Insulation

The stability of a building element refers to the resistance against collapse, thus the ability to maintain the component's load-bearing capacity. This applies for building elements such as walls, columns, floors and beams. The integrity of a building element refers to fire penetration resistance (Lennon, 2011, p. 25). An unexposed surface should not exhibit a temperature that results in combustion of nearby materials (Purkiss, 2007, p. 17). For integrity, elements such as walls and floors are considered. The insulation of a building element refers to its resistance to transfer excessive heat (Lennon, 2011, p. 25).

The most accurate way to determine the fire resistance of a building or building element is to conduct tests. SANS 10177-2 describes such a test. However, in this section the fire resistance is determined by calculating fire curves and then conducting a heat transfer analysis and compare it to the requirements of SANS 10400-T (2011). This analysis is performed for a modular FFC and WPC housing unit as well as a block and mortar housing unit. The approach used in this section to determine the fire behaviour of a housing unit is not as accurate as the fire test, since assumptions are made in terms of the fire properties. The approach gives an indication of the fire performance of a housing unit.

8.2.1. Behaviour of compartment fires

Compartment fires are defined as a fire that is contained within a room or enclosed building. The development of a compartment fire can be divided into four phases. These are shown in Figure 8.10. These four phases include pre-flashover, post-flashover and the decay phase (Drysdale, 1998, p. 291).

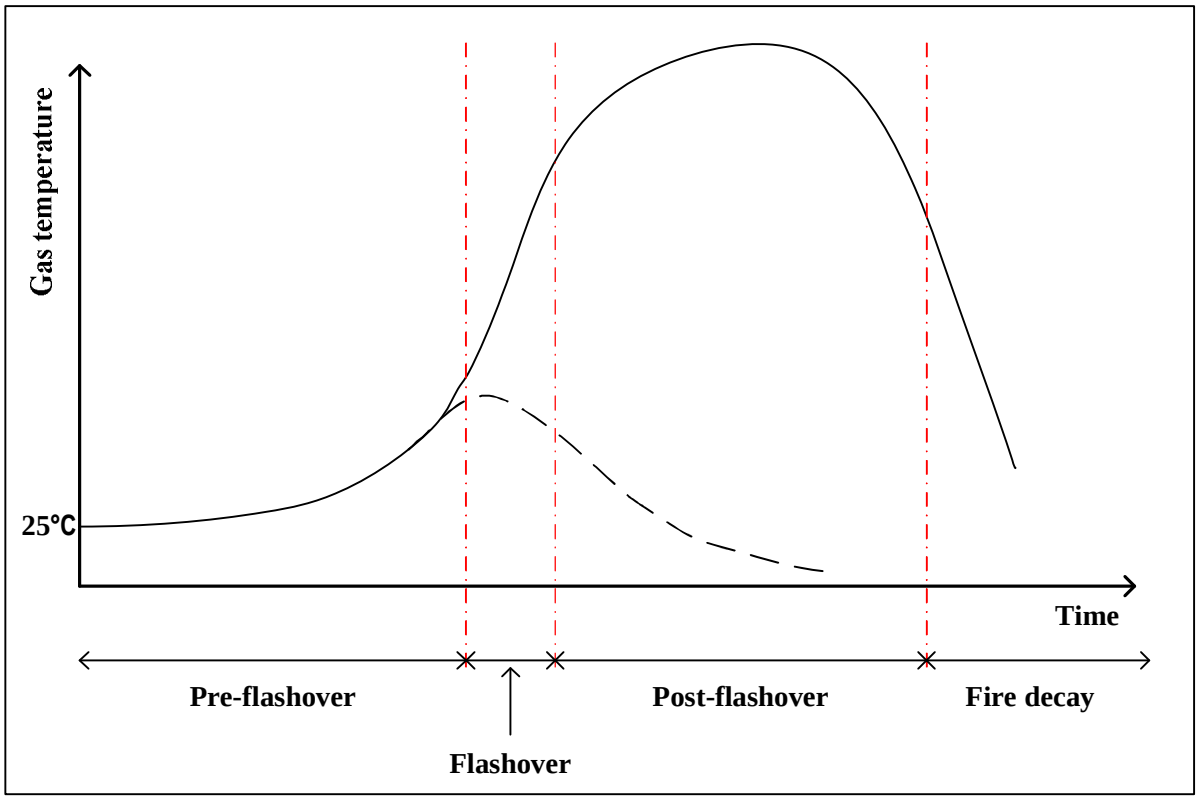

Figure 8.10: The four phases of a compartment fire (Drysdale, 1998, p. 291)

Pre-flashover phase

The pre-flashover phase, also known as the ignition or fire growth phase, are restricted to a small area within the compartment where the fire originated (Purkiss, 2007, p. 43). The fire is mainly fuel controlled. The

term fuel refers to any object (gas, liquid or solid) that can ignite. Most fuels are of organic matter. The broken line curve in Figure 8.10 illustrates the depletion of fuel before flashover occurs (Drysdale, 1998, p. 291). The growth of the fire as well as the rise in temperature mainly depends on sufficient ventilation (oxygen) for combustion as well as the type of, amount, surface area and geometry of the fuel.

The fire growth phase is characterised by flaming or smouldering. It often has a relatively low rise of average temperature within the area where the fire originated. This phase is the most critical for safety since burning fuels produce toxic gases and smoke. The maximum manageable temperatures for humans are reached in this phase (Lennon, 2011, p. 42).

Flashover

Flashover is the transition zone between pre-flashover and post-flashover. The temperature as well as the pressure caused by the smoke that accumulates at the ceiling, also known as the hot gas layer, causes all the available fuel to combust (Lennon, 2011, p. 42).

Post-flashover phase

In the post-flashover phase, also known as the fully developed fire phase, the temperature throughout the compartment rises rapidly and the heat release rate within the room or compartment reaches its peak. This is due to all the available fuels that are combusting. This phase is mainly ventilation controlled. In terms of structural stability and integrity, this is the most critical phase (Purkiss, 2007, p. 44).

Fire decay phase

In this phase, the fuel combustion rate decreases which results in a decrease in the room or compartment temperature over time. This will occur if approximately 70% of all the fuels have been consumed by the fire (Lennon, 2011, p. 42).

8.2.2. Method for calculate fire rating

In Figure 8.11, the method to calculate the fire rating is described. After the fire load and fire load density of the compartment are calculated, the post-flashover fire curves can be determined. Once the fire curves are determined, heat transfer analysis can be performed by using a heat transfer analysis software package, such as ABAQUS™. The time-temperature curves throughout the thickness of the walls obtained from the heat transfer analysis are used to conclude the fire rating of the compartment. This calculated fire rating is compared to the requirements stipulated in SANS 10400-T (2011). If the requirements are not met, the thickness of the wall needs to be increase to meet the requirements.

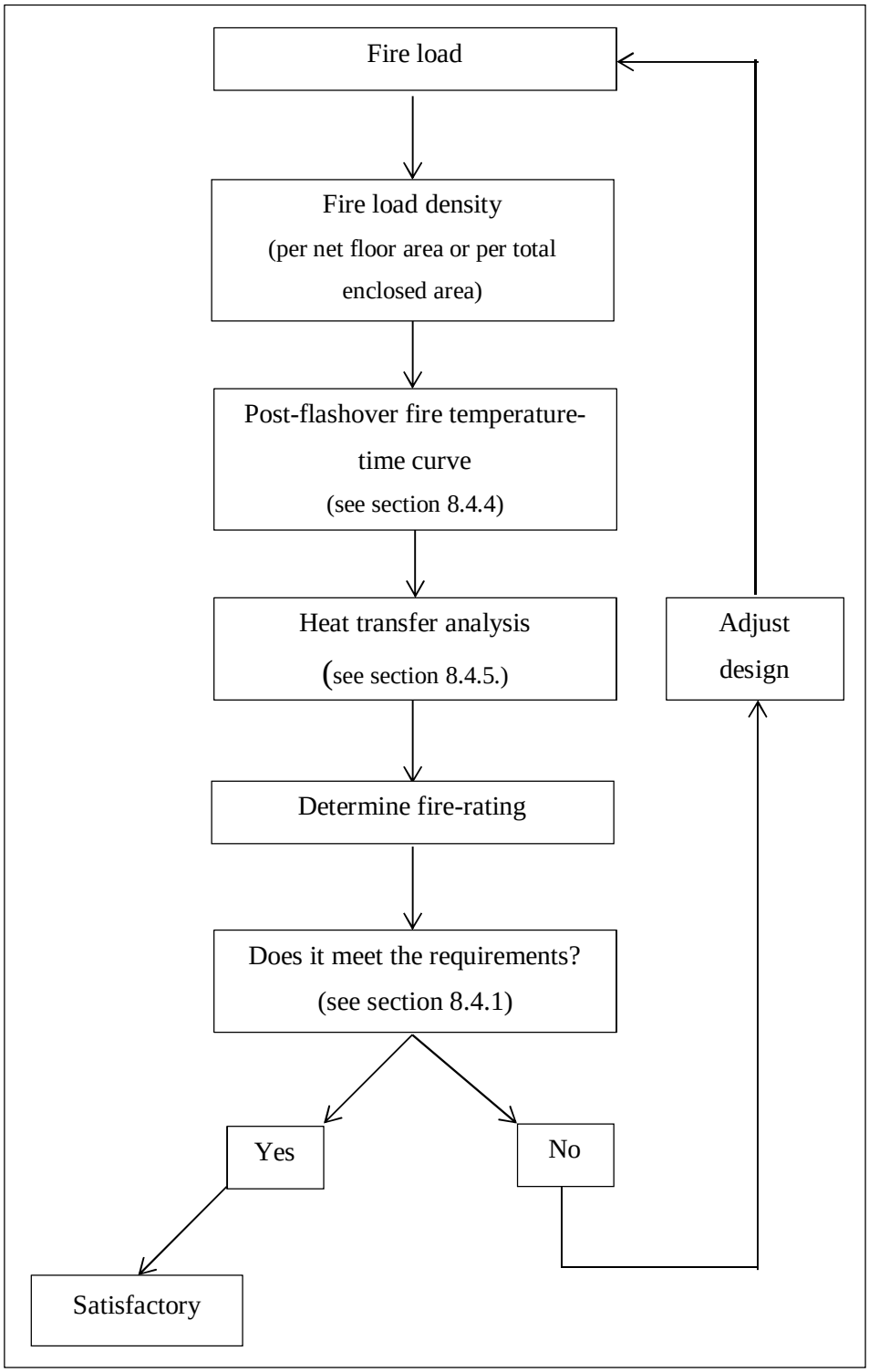

Figure 8.11: Flow diagram describing the method for calculating the fire rating of a housing unit

8.2.3. South African National Standard (SANS) requirements

Requirements regarding the fire rating of internal walls and external walls are prescribes in SANS 10400-T (2011). The minimum safety distance is also stipulated. The safety distance is defined as the minimum distance between the adjacent boundary of the site and any building, to ensure that the effect of radiant heat that results in fire spread is at a minimum.

According to Table 1 of SANS 10400-A (2010) the occupancy classification of a low-income house is H4. For the fire performance of an H4 occupancy, the requirement is stipulated in Paragraph 4.57 of SANS 10400-T (2011). The following requirements are stipulated for a single-storey H4 structure (SANS 10400-T, 2011, p. 67):

- Internal walls shall have a minimum fire resistance of 20 minutes.
- External walls shall have a minimum fire resistance of 30 minutes.
- Safety distance should be a minimum of 500mm.

8.2.4. Fire load, fire load density and heat release rate

In this section, the relationship between the fire load, fire load density and heat release rate is discussed in terms of equations and the definitions.

Fire load is the total amount of energy released by the combustion of all fuels (combustible material) within the compartment. The fire load, q, is measured in mega joules (MJ) and is calculated by the following equation (Buchanan, 2002, p. 37):

$$\boldsymbol{q = \sum M_i \left(\Delta H_{c,n}\right)_i} \quad \textbf{(8.2)}$$

where

M_i = Mass of fuel of item i (kg)

$(\Delta H_{c,n})_i$ = Calorific value or the chemical heat of combustion of item i (MJ/kg). The calorific value is dependent on the moisture content of the item

The fire load density, also known as the fire load energy density (FLED) is measured in mega joules per square meter (MJ/m^2). The FLED is expressed as the net floor area or the total enclosed area. The FLED for the floor area, e_f, is determined by means of (Buchanan, 2002, p. 37):

$$e_f = {}^{q}/_{A_f} \quad \text{..... (8.3)}$$

where,

q = The fire load as calculated in Equation 8.1 (MJ)

A_f = Net floor area of the room or compartment (m^2)

The FLED for the total enclosed area is expressed as (Buchanan, 2002, p. 37):

$$e_t = {}^{q}/_{A_t} \quad \text{..... (8.4)}$$

where,

q = The fire load as calculated in Equation 8.1 (MJ)

A_t = Total enclosed area of room or compartment (m^2), which include the area of the floor, walls and ceiling.

The heat release rate (HRR) is the amount of heat energy released in a certain time and it is measured in megawatts (MW). It depends on whether the fire is fuel controlled or ventilation controlled. For fuel controlled fires, the HRR is calculated by the following equation (Buchanan, 2002, p. 38):

$$HRR = {}^{q}/_{1200} \quad \text{..... (8.5)}$$

where,

q = The fire load as calculated in Equation 8.1 (MJ)

However, for ventilation controlled fires, the HRR is calculated by using:

$$HRR = \sum \dot{m}_i \left(\Delta H_{c,n}\right)_i \quad \text{..... (8.6)}$$

where,

$\dot{m}_i$ = Burning rate (kg/s)

$(\Delta H_{c,n})_i$ = Calorific value or the chemical heat of combustion of item i (MJ/kg). The calorific value is dependent on the moisture content of the item

8.2.5. Post flashover fire time-temperature curves

There are two types of post-flashover fire curves, namely natural and standard fire curves. Natural fire curves are derived for a specific compartment and are based on physical considerations that have an influence on the growth of a fire. In contrast, standard fire curves are prescribed for any compartment (Lennon, 2011, p. 41).

There are numerous methods of determining post-flashover fire curves. Most of these curves are prescribed for concrete and steel structures. However, some of these curves are prescribed for any material structure. These curves are discussed in this section.

Eurocode EN1991 post-flashover parametric temperature–time curve

The parametric fire curve is derived from heat balance equations which consider the thermal properties of the compartment as well as an opening factor. This is a standard fire curve which consists of two phases, a heating and a decay phase. It is independent of the fire load. Thus, a parametric fire curve assumes that the fire load of the compartment is completely combusted at the heating- and cooling down phase. It is dependent on the duration of the fire, i.e. the time of the temperature changes from the heating to the cooling phase (Lennon, 2011, p. 54). The parametric fire curve is a one zone model, which assumes the temperature throughout the compartment is uniform.

The parametric fire curve is valid if the following limitations are met (EN 1991-1-2, 2002):

- The wall height should not be more than 4m.
- The total floor area should be less than 500m^2.

The following equations describe the properties of a parametric fire curve.

Equation for heating phase

The curve describing the heating phase is expressed as (Buchanan, 2002, p. 75):

$$T = T_i + 1325\left(1 - 0.324e^{-0.2t^*} - 0.204e^{-1.7t^*} - 0.472e^{-19t^*}\right) \quad \text{(8.7)}$$

where,

T = Temperature (°C)

T_i = Initial temperature (°C)

t* = Fictitious time (hour)

The fictitious time is calculated using (EN 1991-1-2, 2002):

$$t^* = \Gamma t \quad \text{(8.8)}$$

where,

Γ = Fictitious time factor

t = Time (hour)

The fictitious time factor is calculated by the following equation (EN 1991-1-2, 2002):

$$\Gamma = \frac{(O/b)^2}{(0.04/1160)^2} \quad \text{..... (8.9)}$$

where,

O = Opening factor ($m^{1/2}$)

b = Thermal inertia ($J/m^2°Cs^{1/2}$)

The opening factor, according to the EN 1991-1-2 (2002), have limits of $0.02 \leq O \leq 0.2$ and it is calculated by the following equation:

$$O = \frac{A_v\sqrt{h_{eq}}}{A_T} \quad \text{..... (8.10)}$$

where,

A_v = Total area of vertical openings on all the walls (m^2)

h_{eq} = Weighted average of window heights (m)

A_t = Total enclosed area (m^2)

The thermal inertia has limits of $100 \leq b \leq 2200$ and it is expressed as (EN 1991-1-2, 2002):

$$b = \sqrt{k\rho c} \quad \text{..... (8.11)}$$

where,

k = Thermal conductivity of boundary of enclosure (W/m°C)

ρ = Density of boundary of enclosure (kg/m^3)

c = Specific heat of boundary of enclosure (J/kg°C)

Multiple layers of materials

The parametric fire curve assumes the boundary of the enclosure (walls, ceiling) consists of one layer material. However, if the boundary of the enclosure consists of more than one layer of material the following approach to calculate the thermal inertia should be used (Buchanan, 2002, p. 77).

The material closest to the fire is described as material Layer 1 and the material layer farthest away is denoted as n. The thickness of material Layer *i* is s_i and the thermal inertia of the Layer *i* is b_i. If b_i is smaller than b_{i+1}, the thermal inertia of the enclosed boundary, b, is equal to the thermal inertia of material Layer *i* ($b = b_i$). If b_i is greater than b_{i+1}, the thermal inertia of the boundary of enclosure, b, depends on the limiting

thickness, $s_{lim,1}$, the thickness of material Layer 1, s_1, and the time of the heating phase. Thus, the limiting thickness is calculated by using (Buchanan, 2002, p. 77):

$$s_{lim,1} = \sqrt{tk/\rho c} \quad \text{..... (8.12)}$$

where,

t = time of heating phase of the fire (seconds)

k = Thermal conductivity of material 1 (W/m°C)

ρ = Density of material 1 (kg/m^3)

c = Specific heat of material 1 (J/kg°C)

If $s_1 > s_{lim,1}$, then $b = b_1$, otherwise, the thermal inertia is calculated as follows (Buchanan, 2002, p. 77):

$$b = \left(s_1/s_{lim,1}\right) b_1 + \left(1 - s_1/s_{lim,1}\right) b_2 + \cdots + \left(1 - s_1/s_{lim,1}\right) b_n \quad \text{..... (8.13)}$$

Duration of burning phase

The maximum temperature, T, in the heating phase occurs when t^* equals t^*_{max}. Where the t^*_{max} is calculated by using the following equation (EN 1991-1-2, 2002):

$$t^*_{max} = \Gamma t_{max} \quad \text{..... (8.14)}$$

where,

Γ = Fictitious time factor (Equation 8.7)

t_{max} = time (hour)

t_{max} is calculated by using :

$$t_{max} = \max\begin{cases} 0.2 \times 10^{-3} \cdot \frac{e_t}{O} \\ t_{lim} \end{cases} \quad \text{..... (8.15)}$$

where,

O = Opening factor (m$^{1/2}$) (Equation 8.8)

e_t = Fire load density per total enclosed area (MJ/m^2) (Equation 8.3)

$$t_{lim} = \begin{cases} 25\,\text{min} & slow\ growth\ rate \\ 20\,\text{min} & medium\ growth\ rate \\ 15\,\text{min} & fast\ growth\ rate \end{cases}$$

However, if t_{max} is equal to t_{lim}, the fictitious time t^*, from Equation 8.7, is replaced by the following:

$$t^* = \Gamma_{lim} t \quad \text{..... (8.16)}$$

where,

t^* = Fictitious time (hour)

Γ_{lim} = Fictitious time factor governed by t_{lim}

t = Time (hour)

The fictitious time factor, Equation 8.8, is replaced by the fictitious time factor governed by t_{lim} and it is calculated by the following equation (EN 1991-1-2, 2002):

$$\Gamma_{lim} = \frac{(O_{lim}/b)^2}{(0.04/1160)^2} \quad \text{..... (8.17)}$$

where,

O_{lim} = Opening factor governed by t_{lim} ($m^{1/2}$)

b = Thermal inertia ($J/m^2°Cs^{1/2}$)

The opening factor, Equation 8.9, is substituted by the opening factor which is governed by t_{lim}. It is calculated by using the following equation:

$$O_{lim} = \frac{0.0001\, e_t}{t_{lim}} \quad \text{..... (8.18)}$$

where,

e_t = Fire load density per total enclosed area (MJ/m^2) (Equation 8.3)

$$t_{lim} = \begin{cases} 25\,\text{min} & slow\ growth\ rate \\ 20\,\text{min} & medium\ growth\ rate \\ 15\,\text{min} & fast\ growth\ rate \end{cases}$$

Decay phase

The cooling phase is controlled by the maximum temperature (as calculated in Equation 8.12). Thus, the temperature-time curve for the cooling phase is determined by the following (EN 1991-1-2, 2002):

$$T = T_{max} - 625(t^* - t^*_{max} \cdot x) \quad \text{For } t^*_{max} \leq 0.5 \text{ hours} \quad \text{.....(8.19)}$$

$$T = T_{max} - 250\,(3 - t^*_{max})(t^* - t^*_{max} \cdot x) \quad \text{For } 0.5 \leq t^*_{max} \leq 2 \text{ hours} \quad \text{.....(8.20)}$$

$$T = T_{max} - 250(t^* - t^*_{max} \cdot x) \qquad \text{For } t^*_{max} \geq 2 \text{ hours} \quad \text{.....(8.21)}$$

where,

t* = fictitious time (Equation 8.6)

$$t^*_{max} = \left(0.2\,10^{-3} e_t / O\right) \Gamma$$

$$x = \begin{cases} 1 & if\ t_{max} > t_{lim} \\ t_{lim}\Gamma / t^*_{max} & if\ t_{max} = t_{lim} \end{cases}$$

Ozone

Ozone (version 2.2) is a natural fire curve that was developed in Europe for the investigation of the 'natural fire safety concept' of buildings. This model is based on the Eurocode standard fire curve (EN 1991-1-2, 2002). Ozone is a one zone model, which assumes the compartment to be a well-mixed reactor. Thus, the temperature throughout the compartment is assumed uniform (Buchanan, 2002, pp. 71-73). Ozone requires the following data to calculate a post-flashover fire curve:

- Size of compartment, including the height to the ceiling.
- Type of roof (flat, single pitch or double pitch roof).
- Thickness, unit mass, conductivity, specific heat and size of openings in the walls, floor and ceiling.
- Type of occupancy which results in a fire growth rate (slow, medium or fast), heat release rate (Section 8.2.4) and a fire load density (Section 8.2.4).
- Active firefighting measures if any, such as sprinklers.

ISO834 standard time-temperature curve

The ISO 834 fire curve is a one zone model, which assumes the temperature throughout the compartment is uniform. It is a standard fire curve, which only have a heating phase. It differs from the Ozone and Parametric fire curves, since the ISO 834 fire curve assumes only a heating phase whereas the Ozone and Parametric fire curve has a heating and cooling phase. Ozone takes into account the shape of the compartment as well as the orientation and number of surface area of openings. The temperature of the ISO834 fire curve is calculated by means of the following equation (Engelhardt, 2012):

$$T = T_i + 345\, log_{10}(8t + 1) \quad \text{.....(8.22)}$$

where,

T = Temperature (°C)

T_i = Initial temperature (°C)

t = Time (minute)

8.2.6. Post-flashover time-temperature fire curves

In this section, the post-flashover fire curves, described in Section 8.3.5, for a room within the housing unit is discussed. The fire may spread to the adjacent rooms in the housing unit. However, the maximum fire temperature will occur in the room with the largest fire area containing the largest fire load within the housing unit. Therefore, the kitchen and lounge area was selected. It is assumed that the fire originates in this area of the housing unit. A curve for the room in the housing unit is compiled for modular FFC-, WPC- as well as a block and mortar housing unit.

According to Buchanan (2002, p381) an average fire load density per net floor area for a typical house is 500MJ/m^2 (e_f =500MJ/m^2). The parameters used to determine the fire curves are shown in Table 8.7. The calculations for the fire curves of modular FFC- and WPC housing unit as well as block and mortar housing unit are shown in Appendix F.1, Figure F.1, Figure F.2 and Figure F.3 respectively.

The post-flashover fire curves described in this section indicate the temperatures that will be reached within the compartment, which are assumed uniform throughout the room (one zone model). These fire curves will affect the inner part of the walling system, i.e. the surface of the wall where the fire occurs. A heat transfer analysis is necessary to determine the temperature-time curves across the walls.

Table 8.7: Parameters used to calculated the fire curves

	Modular plastic housing unit	**Block and mortar housing unit**
Net floor area, A_f (m^2)	18.5	16.55
Total enclosed area, A_t (m^2)	45.66	48.96
Fire load density per floor area, e_f (MJ/m^2)	500	500
Fire load, q (MJ)	9 250.00	8 273.80
Fire load density per enclosed area, e_t (MJ/m^2)	202.60	168.99

Eurocode EN1991 post-flashover Parametric temperature–time curve

The comparison of the parametric post-flashover fire curve of these housing units is shown in Figure 8.12. This figure illustrates the heating phase of the post-flashover fire of both the modular housing units is relatively steep when compared to that of the block and mortar housing unit. This might be due to the material used for the walling system, where the FFC and WPC have lower thermal conductivities, densities and higher specific heats. These low thermal conductivities result in a large temperature gradient (refer to Section 4.2.3). However, the FFC and WPC conduct a small amount of heat, which results in the steep heating phase as well as a steep decay phase. The concrete block and mortar, on the other hand, conduct the heat resulting in a less steep heating phase with a decay phase that does not occur within a two hour period of a fire curve. The maximum temperature of the block and mortar housing unit is much less than that of the FFC and WPC housing unit. The fuel is consumed by the fire which causes a steep heating rate. The three fire curves show a portion of the curve that remains approximately steady in temperature before the fire decays. This is due to the fire being fuel controlled and most of the fuel is consumed. Thereafter the fuel controlled fire changes to a ventilation controlled fire, and the fire decays.

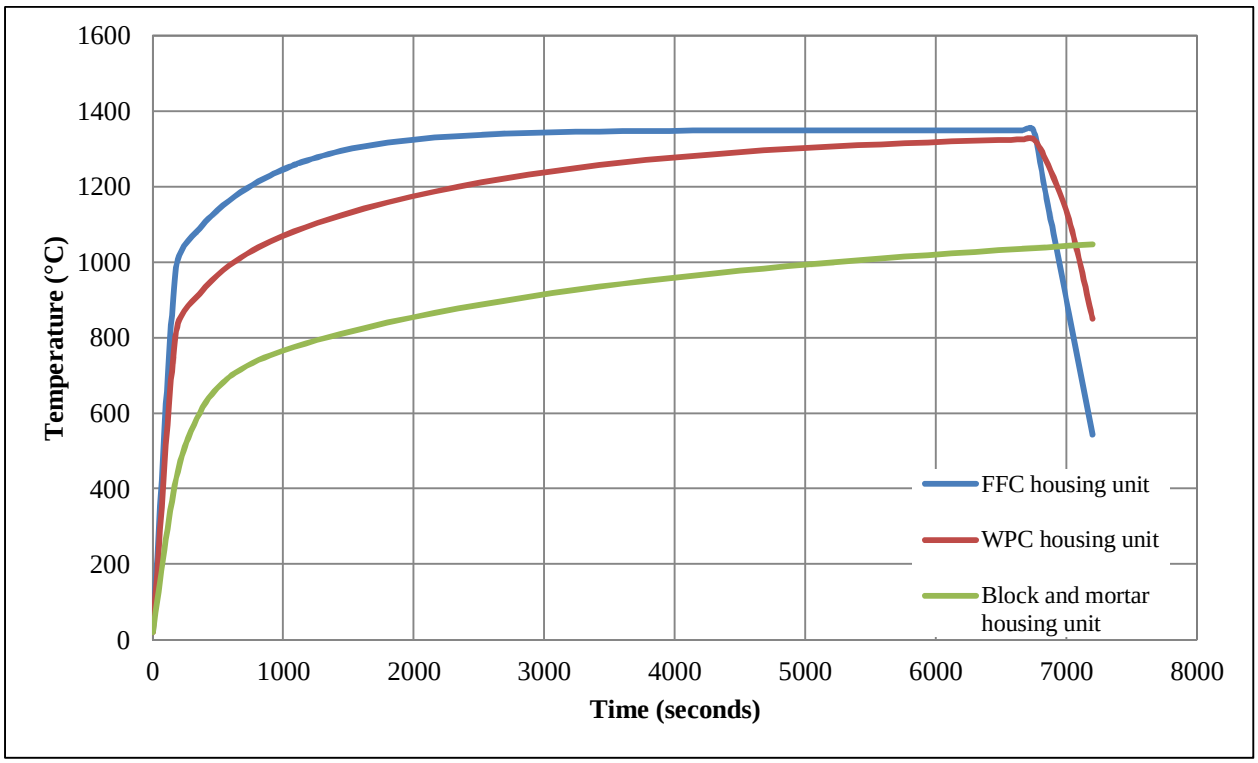

Figure 8.12: Comparison of the EN1991 Parametric fire curve for the FFC housing unit, the WPC housing unit and the block and mortar housing unit

The calculations for the parametric fire curves of the three different housing units are shown in Appendix F.

OZONE (Version 2.2)

As mentioned in Section 8.3.6, Ozone requires input values. The input values, except for the material, layout of compartment and the thicknesses of the material, are shown in Table 8.8. A medium fire growth rate is assumed for dwelling occupancies (Purkiss, 2007). For the HRR the fire is assumed fuel controlled.

Table 8.8: Ozone input values, excluding compartment geometry and material properties.

	Unit	Housing units
Fire growth rate		Medium
Heat release rate (per floor area)	kW/m^2	416.7
80% fractile value of fire load density (per floor area)	MJ/m^2	375
Active firefighting measurements		• Off-site fire brigade • Safe access route
Initial temperature	°C	25
Type of zone model		One zone model

The post-flashover fire curves for the three design types are shown in Figure 8.13. The curves displayed in this figure exhibit relatively high maximum temperatures. This is due to a lack of firefighting measurements (such as sprinklers). The Ozone fire curve shape of the three housing units is the same. This is due to the same fire load density and heat release rate. The maximum temperature reached by the fire is higher for the FFC- and WPC housing unit than that of the block and mortar housing unit. This is due to both being plastic composite materials and the properties being similar. The brick and mortar housing unit, on the other hand, exhibits lower maximum temperatures. This is due to the concrete blocks that have the ability to conduct more heat when compared to the FFC and WPC (lower thermal conductivity). The decay phase for all three housing units is the same. This is due to the amount of fuel available as well as the same amount of ventilation available.

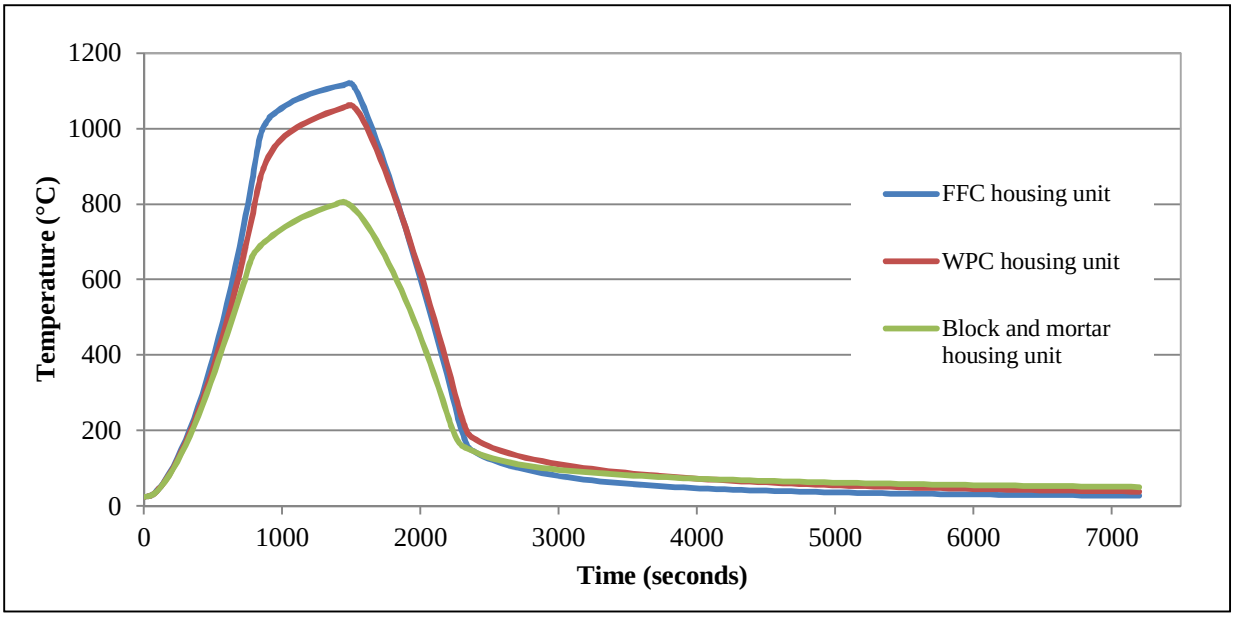

Figure 8.13: Comparison of the Ozone fire curve for the FFC housing unit, the WPC housing unit and the block and mortar housing unit

ISO834 standard time-temperature curve

The ISO834 is a standard post-flashover fire curve and only depends on the initial temperature (assumed 25°C) and the time (in minutes). Therefore, only one curve is described for all three housing units, as shown in Figure 8.14. This curve assumes only a heating phase and is a one zone model.

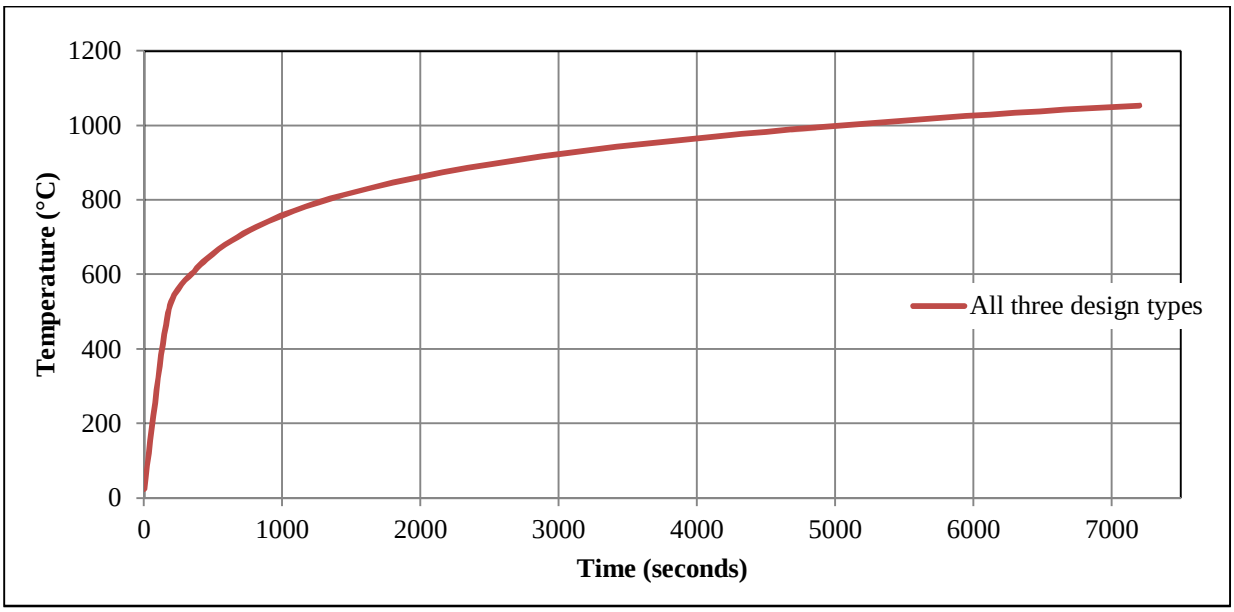

Figure 8.14: The ISO834 fire curve for the FFC housing unit, the WPC housing unit and the block and mortar housing unit

8.2.7. Heat transfer analysis

The fire curves for the housing units, determined in Section 8.3.6, are used as the internal fire temperature for the temperature–time curve within the compartment. ABAQUS™ is used to perform the heat transfer analysis. For each housing unit the three fire curves are used to determine the fire rating of the internal and external walls. The heat transfer analysis is conducted for the selected compartments of the three housing units, namely the modular FFC- , WPC- as well as the block and mortar housing unit. The results of the three analyses are compared in a later section.

The aim of the heat transfer analysis is to determine the fire rating of the housing unit. The serviceability temperatures are shown in Table 8.9. When these temperatures are reached throughout the thickness of the walling system, the plastic materials are considered to be charred and concrete spalling occurs.

Table 8.9: Serviceability temperatures of housing unit materials (Friul Filiere Spa, [S.a]; Fisher, 2013; Rachel, 2013; Buchanan, 2002, p. 228)

	Serviceability temperature (°C)
FFC	120
WPC	230
EPS	70
Block and mortar	400

Plastic materials together with timber material exhibit decomposition as the temperature increases. This decomposition affects the density and mass of the material. For composites, post-fire modelling, generally, assumes a two-layer model, where when decomposition of the material occurs, a charred layer is formed (Mouritz, et al., 2009). This charred layer acts as a protective layer and decreases the thermal degradation of the composite (Fang, et al., 2013). Therefore, it is assumed that the layer that is not charred by the fire, exhibits full strength (Buchanan, 2002, p. 33). This two-layer post-fire modelling, according to Mouritz et al. (2013), correlates well with measured post-fire properties of composite materials. The criteria for which the fire rating is determined, is based on serviceability temperatures. This indicates that if the fire temperature is higher than this serviceability temperature of the material, the material is charred and has lost all strength.

The following parameters were used in ABAQUS™ to determine the heat transfer through the thickness of the walling system:

- For the modular plastic housing units, a meter strip of walling system is used.
- For the block and mortar, a concrete block is used.
- Stefan-Boltzmann constant is equal to $5.67(10^{-8})$ $W/m^{2}°C^{4}$. This constant refers to the radiation emitted by an element or body (Drysdale, 1998, p. 33).
- Absolute zero temperature of -273.15°C.
- Shell elements are used to represent the walling system
- Mesh size of 50mm and a four-noded linear heat transfer quadrilateral mesh type is used.
- The material properties used for the heat transfer is shown in Table 8.10. Refer to Chapter 5 for properties.

Table 8.10: Thermal properties of materials used to conduct heat transfer analysis

Thermal properties	Unit	FFC	WPC	EPS	Concrete block
Density, ρ	kg/m^3	700	1331	15	2250
Thermal conductivity, k	W/m°C	0.13	0.15	0.03	1.1
Specific heat, c	J/kg°C	1300	1860	1500	877.8
Coefficient of thermal expansion, α	/°C x 10^{-6}	100	101	70	10

Heat transfer analysis for modular plastic housing unit

In Table 8.11 and Table 8.12, the fire rating through the thickness of the modular FFC housing unit and modular WPC housing unit is shown respectively. The fire rating was obtained by calculating the time at which the serviceability temperature of the material was reached. An example of time-temperature curves, from which the fire rating is determined, is shown in Figure 8.16. In this figure, the red broken line indicates the serviceability temperature of the WPC, whereas the black broken line refers to the serviceability temperature of the EPS. The other curves in this figure illustrate the temperature-time curves through the thickness of the walling system. For example, at Point b, which is in the middle of the WPC panel (Figure 8.15), the fire rating is equal to that of the time on the x-axis of Figure 8.16. When fire curves, for Point b, intersects the serviceability temperature of the WPC, the fire rating of the material obtained from the time value on the x-axis of the graph. Therefore, if the Eurocode EN1991 Parametric fire curve is considered, Point b has a fire rating of 60 seconds. Figure 8.15 illustrates the thickness through the wall. Note that at the point where the thickness is equal to 61mm, external wall, and 45mm, internal wall, (point d) the serviceability temperature of the EPS is used to obtain the fire rating. For each fire curve, the temperature-time curve through the thickness of the walling system, internal and external, is shown in Appendix F 2.1, for the FFC housing unit and in Appendix F.2.2 for the WPC housing unit.

Table 8.11: Results of fire rating through the thickness of the wall of the FFC housing unit for the three fire curves

	Thickness through the wall (Figure 8.15)		Fire rating (min)		
	Point	**Thickness, t (mm)**	**Eurocode EN1991 Parametric fire curve**	**Ozone fire curve**	**ISO834 standard fire curve**
External walls	a	0	0	4	1
	b	5.5	1	7	1
	c	11	2	8	2
	d	61	10	19	6
	e	111	92	120	68
	f	122	99	120	71
Internal walls	a	0	0	4	1
	b	3.75	1	6	1
	c	7.5	1	6	1
	d	45	5	12	11
	e	82.5	48	120	33
	f	90	51	120	34

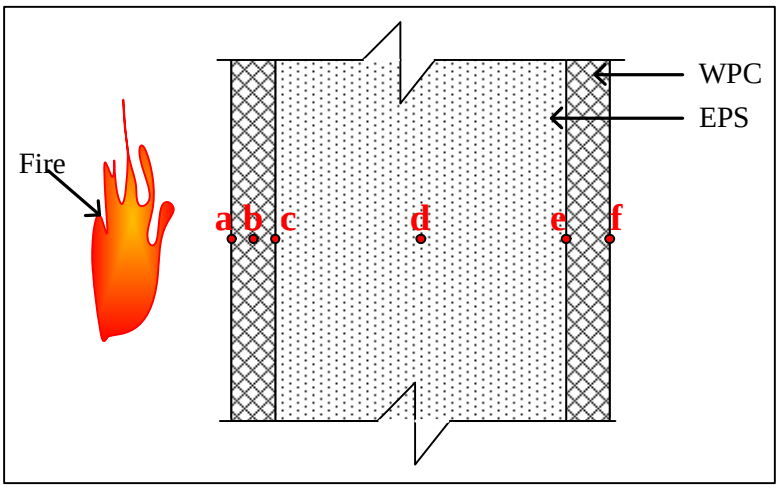

Figure 8.15: Points throughout the thickness of the waling system of the modular plastic housing unit that was considered for the heat transfer analysis

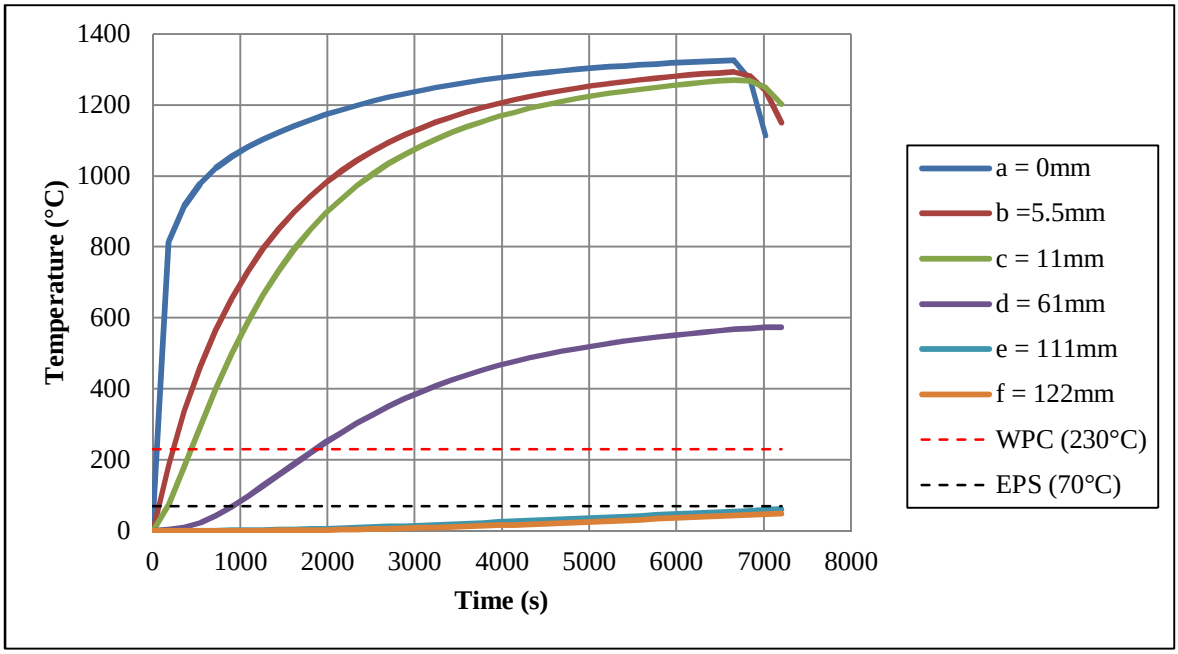

Figure 8.16: Heat transfer through the thickness of the external walls from the EN1991 Parametric fire curve for the WPC housing unit

Table 8.12: Results of fire rating through the thickness of the wall of the WPC housing unit for the three fire curves

	Thickness through the wall (Figure 8.15)		Fire rating (min)		
	Point	**Thickness, t (mm)**	**Eurocode EN1991 Parametric fire curve**	**Ozone fire curve**	**ISO834 standard fire curve**
External walls	a	0	1	6	1
	b	5.5	4	12	6
	c	11	7	15	10
	d	61	15	24	19
	e	111	120	120	120
	f	122	120	120	120
Internal walls	a	0	1	6	1
	b	3.75	2	10	4
	c	7.5	4	10	6
	d	45	6	14	8
	e	82.5	120	120	120
	f	90	120	120	120

From Table 8.11 and Table 8.12, it is shown that the fire rating of the FFC housing unit and the WPC housing unit, respectively, in terms of integrity and insulation, are met for both the internal and external walling systems. According to the SANS 10400-T (2011, p. 67) the external walls and the internal walls have a minimum fire resistance of 30 minutes and 20 minutes respectively. Only the external FFC and WPC panel of the walling system of both internal and external walling, meet the fire rating in terms of stability. When the internal composite plastic panel (the panel subjected to the fire) and the EPS (core panel) are charred, the external composite plastic panel is the only part of the walling system left to serve as a load bearing element. This will result in buckling due to slenderness of this panel (length of 2.7m and thickness of 0.011m). Thus, in terms of stability, the requirement as stipulated in SANS 10400-T (2011, p. 67) are not met.

If the thickness of the internal FFC panel is equal to 40mm, for the Eurocode EN1991 Parametric fire curve the entire thickness is charred. Thus the internal FFC panel should be approximately 51mm to meet the requirements stipulated by SANS 10400-T (2011, p. 67) in terms of stability.

The thickness of the internal WPC panel of the walling system requires to be approximately 31mm, for the Eurocode EN1991 Parametric fire curve (the most stringent fire curve), to meet the requirements in terms of stability. This is since the thickness of the WPC is charred to 20mm and the 11mm WPC panel which is left, which comply with stability requirements of the structure as shown in the numerical analysis (Section 8.1).

From the thicknesses of the internal composite plastic of the walling system and from Table 8.11 and Table 8.12, it is shown that WPC out performs FF under in fire conditions. This is due to the WPC exhibiting a higher thermal conductivity, density and specific heat.

Heat transfer analysis for block and mortar unit

In Table 8.13, the fire rating through the thickness of the walls of the block and mortar housing unit is shown. The fire rating was obtained by calculating the time at which the serviceability temperature of the concrete blocks is reached for each fire curve. Figures illustrated in Appendix F.2.3, are used to determine the fire ratings shown in Table 8.13. Figure 8.17 illustrates the thickness through the wall.

Note that from Table 8.13, the required fire rating according to SANS 10400-T (2011, p. 67) is met in terms of stability, integrity and insulation. The fire rating in terms of stability is reached at a thickness of approximately 30mm for the internal and external walls. Thus, the block and mortar housing unit performs better in terms of fire performance than that of the modular plastic housing units, especially the FFC housing unit.

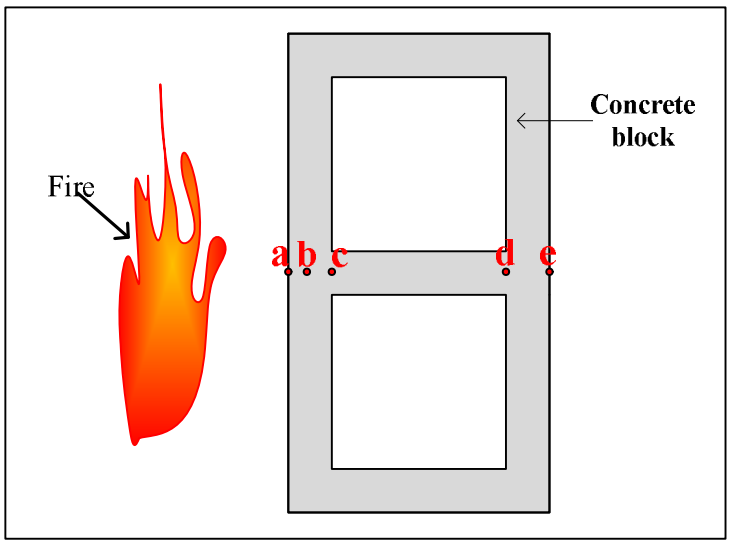

Figure 8.17: Points throughout the thickness of the concrete block of the block and mortar housing unit that was considered for the heat transfer analysis

Table 8.13: Results of fire rating through the thickness of the wall of the block and mortar housing unit for the three fire curves

	Thickness through the wall (Figure 8.17)		Fire rating (min)		
	Point	**Thickness, t (mm)**	**Eurocode EN1991 Parametric fire curve**	**Ozone fire curve**	**ISO834 standard fire curve**
External walls	a	0	3	9	2
	b	30	56	120	55
	c	70	120	120	120
	d	110	120	120	120
	e	140	120	120	120
Internal walls	a	0	3	9	2
	b	30	60	120	58
	c	45	119	120	117
	d	60	120	120	120
	e	90	120	120	120

8.3. Durability and long-term loading

In this section, durability and long-term creep of WPC and FFC are discussed.

8.3.1. Durability

EPS is non-biodegradable in water and soil (Horvath, 1994). However, due to the confinement of the EPS in the design of the modular plastic housing unit (Chapter 6), UV resistance is irrelevant whereas water absorption and the reaction to solvents of EPS are to some extent inevitable. However, EPS is not susceptible to water absorption as shown in Section 5.4.7. EPS can dissolve in certain liquids, which include gasoline, diesel fuels and acetone. However, it is unlikely to be exposed to these liquids due to the design layout and conditions of the modular housing unit.

In this section, the durability of FFC and WPC is discussed. Durability is discussed in terms of the degradation of the material by assessing the factors influencing degradation. Note that FFC is comprised of 50% PVC and 50% vegetal fibres and other materials combined, whereas WPC is comprised of 47% PVC,47% wood-flour and 6% interface materials (coupling agent and lubricant) (Friul Filiere Spa, [S.a]; Rachel, 2013). Thus, only the reinforcing agent differs. Both of these products have a guarantee of ten years according to the manufactures. This does not reflect the life span or durability of the products. According to Garcia, et al. (2009), WPC has a design life of approximately 25 to 30 years with an insignificant amount of maintenance required.

Durability of plastic composites is mainly influenced by the degradation of the material as illustrated in Figure 5.11. The degradation of plastic composites depends on its application. The durability of composite plastic foams will be divided into moisture uptake degradation, degradation due to UV radiation, biodegradation and thermal degradation (refer to Section 5.4.7 for a broader perspective). These degradation types that influence the durability of WPC and FFC are discussed below.

Moisture uptake/ water absorption

The wood/vegetal component of WPC and FFC is hydrophilic and the plastic component is hydrophobic, where water absorption is concerned (Morrel, et al., 2010). Thus, water absorption of the composite material results in swelling, since the wood/vegetal component absorbs water. As the wood component in the composite swells, the following occurs within the composite (Morrel, et al., 2010):

- The bonding between the wood flour/vegetal fibres and the PVC breaks down, due to the swelling of the wood/vegetal component.

- Microcracks in the plastic matrix occurs
- Fracturing of the wood/vegetal particles, due to restrained swelling.

According to Klyosov (2007), if the WPC is submerged into room temperature water, the typical absorption is 0.7 to 2% after 24 hours, 1 to 5% after one week and 18 to 22% after several months. This is mainly due to the wood/vegetal component of the plastic composite (refer to Section 5.4.7 and Section 4.1.7), since the wood/vegetal component is hydrophilic. This is also confirmed by the quantity of water absorption of WPC versus PVC, which is 0.8% (Figure 5.12) and 0.08% (Figure 4.12) respectively. The finishes to the product, such as a laminated plastic cover (as in the case of WPC (Ecowood)) can reduce the quantity of water absorption. According to Defoirdt et al. (2010), the quantity of water absorption of unreinforced polyvinyl chloride (PVC) has no significant effect on the mechanical properties of PVC. According to the manufactures of FFC and WPC (Ecowood), these products have the ability to resist water absorption (Friul Filiere Spa, [S.a]; Rachel, 2013).

Elevation of temperature significantly affects the moisture uptake (water absorption) of WPC and FFC (Azwa, et al., 2013). According to Defoirdt et al., (2010), mass change at ambient temperature and at 70°C after twenty days of WPC is approximately 5% and 18% respectively. This implies a higher water absorption of WPC and FFC at elevated temperature. The water absorption of unreinforced PVC, on the other hand, remains constant up until the glass transition temperature (90°C), Figure 4.17. Temperatures higher than the glass transition temperate results in an increase in water absorption. Therefore, up to 90°C (glass transition temperature) the moisture uptake of unreinforced PVC remains approximately 0.08% (Defoirdt, et al., 2010; Matuana & Kamdem, 2002).

As mentioned in Section 5.4.7, an increase of water absorption leads to a decrease in flexural strength of the composite material. Thus, if the elevated temperature is higher than the glass transition temperature (90°C) of unreinforced PVC, which is the laminated layer of WPC and FFC, the water absorption will increase and the flexural strength of these plastic composites will decrease.

Degradation caused by ultraviolet radiation:

Degradation caused by sunlight (UV radiation), termed photodegradation, mainly results in discoloration of composites. Wood is prone to discoloration caused by sunlight. Photodegradation of plastic composites is influenced by numerous factors, as described in Section 5.4.7.

One year of natural weathering testing is equivalent to approximately 800 hours of accelerated weathering testing. This relationship between accelerated weather and real weathering condition does not give an exact

correlation, due to the irregularity of duration, intensity, cycles and exposure conditions between the two weather tests (Azwa, et al., 2013). Weathering degradation in nature is dependent on the climatic conditions, such as temperature, humidity, air pollution and radiation (Azwa, et al., 2013). According to Azwa, et al., (2013) natural weathering will result in more accurate results, whereas accelerated weathering tests result mostly in exaggerated results. However, accelerated weathering test still provides an adequate indication of natural weathering of a material. Accelerated weathering test is preferred to natural weathering test where time constraints are considered. It is recommended that for both FFC and WPC a natural weathering test should be conducted for the life span of the housing unit.

Accelerated UV weathering test of WPC was reported, where UV radiation/condensation cycles were applied to WPC specimen. Approximately, 1733 hours of UV radiation and 867 hours UV condensation were applied to complete a 2600 hour accelerated UV radiation/condensation test. This testing is equivalent to approximately 3 years and 3 months of natural weathering testing. Degradation due to UV radiation/condensation cycles were assessed in terms of coloration, contact angle, Fourier transform infrared (FTIR) spectroscopy, X-ray photoelectron spectra and tensile properties after exposure (Matuana & Kamdem, 2002). According to Maruana & Kamdem (2002), the results of the test are as follows:

- The color measurement assessment was determined according to ASTM D2244, which resulted in a greater discoloration of WPC than when unreinforced PVC is considered.
- The contact angle relates to the wettability of the surface of a material. This assessment resulted in an increase of the wettability on the surface of the weathered WPC, which suggests that chemical changes occurred on the composite's surface.
- FTIR spectroscopy and X-ray photoelectron spectra were used to determine the chemical changes that occurred on the composite's surface, more accurately than the contact angle assessment. These assessments showed that chemical changes occurred on the composite's surface.
- The elongation and stiffness of a plastic material is greatly effected when exposed to UV radiation/condensation cycles (Jiang & Kamdem, 2004). The tensile test, after 2600 hours, resulted in a decrease in the tensile properties of unreinforced PVC, whereas WPC retained its original properties.

When an accelerated weathering test was conducted for WPC over one year (equivalent to 10 years natural weathering test), it was found that the degradation layer was less than 0.5mm below the exposed surface (Fabiyi, et al., 2008; Azwa, et al., 2013). FFC will have similar results for the accelerated UV weathering test compared to those of WPC, due to similar composition of the products. However, due to the laminated PVC layer of the FFC and WPC products, the discoloration of these composites is less, but the tensile properties of the laminated layer will be influenced significantly. This laminated layer acts as a protective layer and not as a component which increases the mechanical properties.

Biodegradation:

The main consequence of biodegradation is weight loss of the composite material, which results in a decrease in mechanical properties. The wood content of the composite is susceptible to termite and fungi attacks. Thus, a higher plastic to wood-flour/vegetal fibres ratio and minimum wood-flour/vegetal fibres exposure to the surface of the product will result in a higher resistance to biodegradation. An increase in the moisture up take (discussed above) can lead to an increase in fungal attack on the surface of the composite (Azwa, et al., 2013). According to Verhey, et al., (2001), the soil-block test which was conducted according to AWPA E10-91 for 12 weeks with the addition of water, resulted in the conclusion that the wood content of composites is proportional to fungal attack (weight loss), as shown in Figure 8.18. From this figure, it is clear that the brown rot results in a higher average weight loss of the wood content of the WPC. This can be due to the addition of water (moisture) during the test, which results in a higher brown rot attack. The lubricant used in the composite such as, Zinc Stearate (ZnSt) or zinc borate (ZB), enhances the resistance to fungi and termites (Verhey, et al., 2001).

The exact composition, especially of the interface material(s), of FFC and WPC is not fully known. The FFC and WPC products are laminated with a PVC layer and since unreinforced plastic materials are not susceptible to biodegradation, the weight loss of these products will be insignificant. According to the manufactures, these products have an adequate resistance to biodegradation (Friul Filiere Spa, [S.a]; Rachel, 2013).

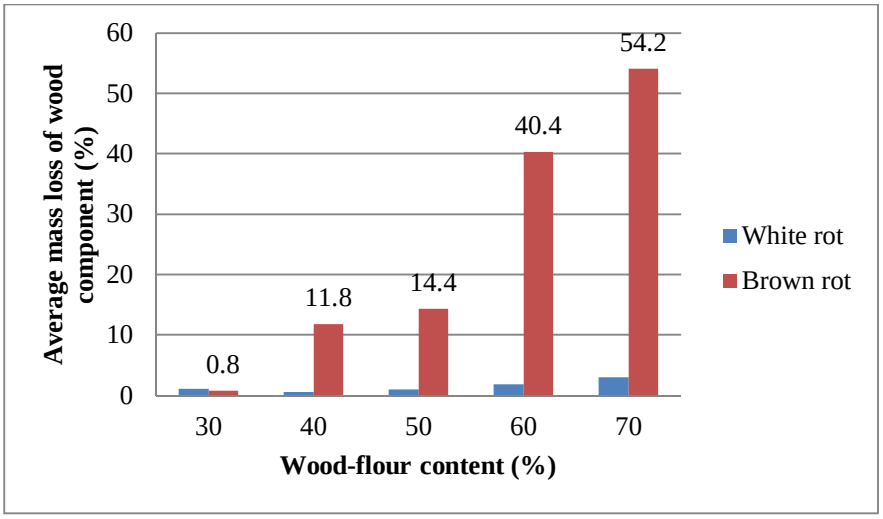

Figure 8.18: Influence of wood-flour content on white and brown rot (Verhey, et al., 2001)

Thermal degradation

When WPC thermally decomposes, it forms a charred layer (as described in Section 8.2.7). This charred layer acts as a thermal barrier, which decreases thermal decomposition and smoke production (Müller, et al., 2012). According to the thermogravimetic analysis (TGA), performed by Müller et al. (2012), at a

temperature range of 20°C to 600°C and a heating rate of 20 degrees Kevin per minute for WPC (50% PVC and 50%wood-flour), the decomposition of the material started at 272°C. This decomposition temperature was significantly influenced by the plastic matrix (Müller, et al., 2012). It was also found that the fabrication process played a significant role in the decomposition of WPC, where a controlled fabrication process increased the decomposition temperature (Müller, et al., 2012).

The effect of interface materials on the thermal degradation and smoke production was experimentally determined by Fang, et al. (2013). A cone calorimetric (CONE) test was used to determine this influence for WPC consisting of 47% PVC, 47% wood flour and 6% interface material (coupling agent and lubricant). According to this experimental work, the addition of lubricant (an interface material) promoted cross-linking of the PVC at low temperatures. This resulted in 56.2% more char formation compared to WPC without lubricant. Thus, an increase in the char formulation results in a decrease of thermal degradation and smoke production of WPC (Müller, et al., 2012).

From these experiments reported, the inclusion of a lubricant as well as a well-controlled fabrication process has a positive influence on the thermal degradation and smoke production of WPC. The thermal decomposition and smoke production of WPC and FFC can further be decreased with the addition of additives, such as heat stabilizers and fire retardant additives (Klyosov, 2007).

The WPC and FFC products are laminated with PVC. PVC releases toxic gases (hydrochloric acid, HCl) when the temperature is above glass transition temperature (90°C), however, PVC is also a self-extinguishing material (Azwa, et al., 2013). This indicates that after the glass transition temperature is reached, the material releases toxic fumes and chars (Section 8.2.7). The amount of toxic gases released, when the temperature exceeds the glass transition temperature of PVC, is approximately 400 part per million (ppm), whereas 1300 to 2000 ppm of HCl is fatal for adults (Pacheco-Torgal, et al., 2012). Thus, human behaviour during a fire is important, since this might prevent the fire to grow (in the pre-flashover phase), thus reducing toxic emissions which can be fatal.

8.3.2. Long term-loading (flexural creep)

Flexural creep of WPC (PVC as plastic component) is mainly influenced by the temperature, applied load and the wood-flour content (Sain, et al., 2000; Jia, et al., 2008). In this section, these influences will be discussed based on experimental work reported. The flexural creep was performed according to the ASTM D2990.

To determine the effect of temperature on the flexural creep of WPC, the wood-flour content and applied flexural strength at 30% were kept constant (Sain, et al., 2000). This resulted in a flexural creep curve as shown in Figure 8.19. From this figure, it can be seen that an increase in temperature results in an increase in creep strain. Although the curve shapes are similar, the spacing between these curves is non-linear (Sain, et al., 2000).

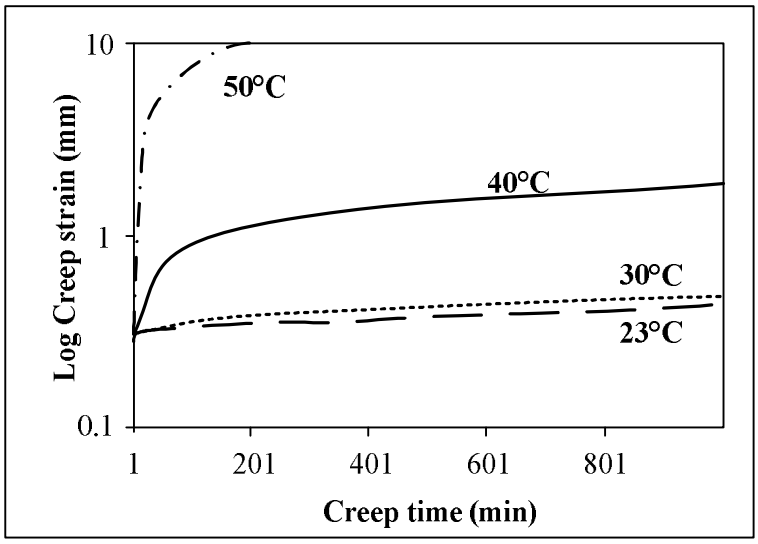

Figure 8.19: Influence of temperature on flexural creep (Sain, et al., 2000, p. 262)

The effect of the applied load was determined by keeping the temperature and wood-flour content at 23°C and 30% respectively (Sain, et al., 2000). This effect on the creep resulted in Figure 8.20 where a higher load results in a higher creep strain. Under higher loading, molecular slippage is the dominant mechanism. However, this effect is reversed if the applied flexural load is 30% or less. Thus, WPC can bear a 30% flexural load without great deformations for long time periods (Sain, et al., 2000).

Lastly, the effect of the wood-flour content on the flexural creep of WPC was determined by maintaining the temperature and applied load constant at 23°C and 50% respectively (Jia, et al., 2008). The results of this experiment conducted by Jia et al., (2008) are shown in Figure 8.21. From this figure, an increase in the wood-flour component of WPC leads to a decrease of creep strain (Jia, et al., 2008). Thus, in terms of flexural strength, the increase in the wood-flour content results in an increase in strength and rigidity of WPC.

Other factors that influence the flexural creep of WPC are the interface materials. When incompatible interface materials are used to produce WPC, surface cracks can form during flexural creep due to the weak

bond strength of the PVC and wood-flour. Thus, compatible interface materials will result in insignificant surface cracks during flexural creep, which can lead to a reduction in creep strain (Jia, et al., 2008).

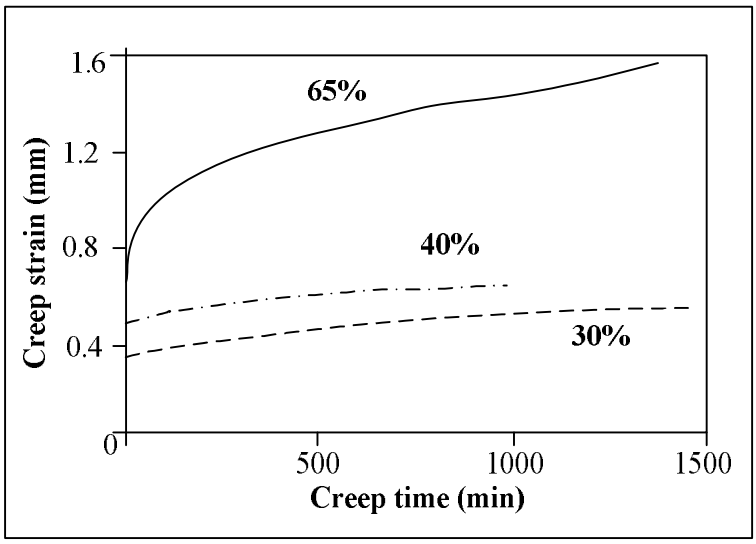

Figure 8.20: Influence of the applied flexural loading on flexural creep (Sain, et al., 2000, p. 264).

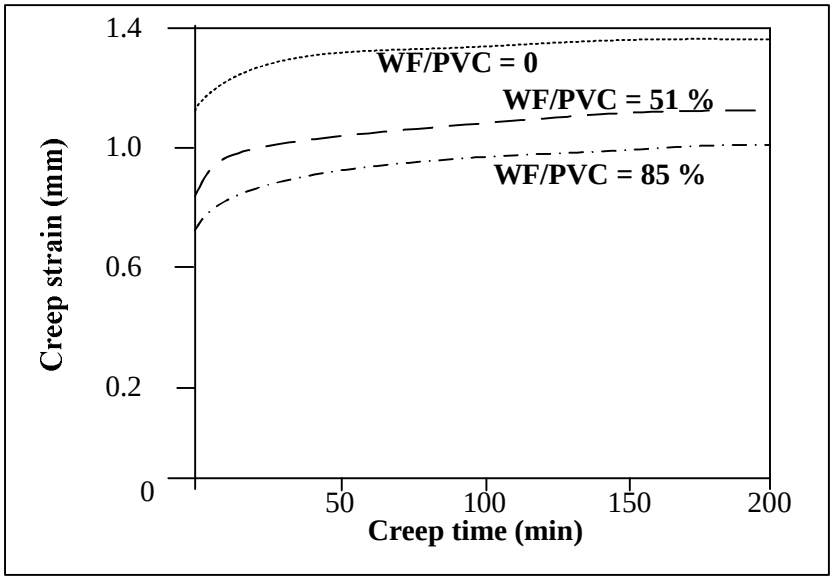

Figure 8.21: Influence of the wood-flour content of WPC on flexural creep (Jia, et al., 2008)

8.4. Summary

In terms of structural stability, the design described in Chapter 6 is satisfactory as the numerical analysis indicates no yielding of any of the materials used. The required stiffness of the soil that supports the WPC flooring system is easily achievable in practice.

When the fire performance of the walling systems is considered, the fire rating in terms of integrity and insulation was met. However, due to the fire rating in terms of stability, the thicknesses of the modular plastic housing unit should be increased to meet the requirements as stipulated in SANS 10400-T (2011). However, fire retardant additives are used in the WPC and FFC, which were not included in the calculation of the fire rating as the effect of these additives are unknown. These fire retardant additives increase the ability of the WPC and FFC to char which increases the fire rating. It should be noted that physical testing (SANS 10177-2) of the fire performance would result in a more accurate fire rating estimation.

Since only structural feasibility of the low-income housing unit was investigated, the human behaviour and smoke control was not considered. Future studies should consider the human behaviour and smoke control burning a fire. The amount of toxic gases release, when temperature exceeds the glass transition temperature of PVC, is approximately 400 part per million (ppm), whereas a 1300 to 2000 ppm of HCl is fatal for adults (Pacheco-Torgal, et al., 2012). Thus, human behaviour during a fire is important since this might prevent fatality or even the fire to develop.

The durability of WPC and FFC is influenced by their degradability (Figure 5.11). Moisture uptake can cause a decrease in flexural strength. However, for PVC, the lamination of FFC and WPC, moisture uptake is insignificant. Temperature elevations above the glass transition temperature of PVC (90°C) can result in moisture uptake, which results in a decrease of flexural strength.

The UV resistance of FFC and WPC can be determined by accelerated weathering test. However, the accuracy of the measurements as well as the extrapolated data cannot be guaranteed. To obtain accurate results a housing unit should be erected and the degradation of the housing unit should be tested over the expected life span of the housing unit. One year of natural weathering test, relate to approximately 800 hours of accelerated weathering testing. When an accelerated weathering test was conducted for WPC over one year, it was found that the degradation layer was less than 0.5mm below the exposed surface (Fabiyi, et al., 2008; Azwa, et al., 2013). The tensile test, after 2600 hours of accelerating weather testing, resulted in decrease in the tensile properties of unreinforced PVC, whereas WPC retain its original properties.

Degradation due to biodegradability of WPC and FFC is irrelevant, since PVC, laminating layer, contains no wood-flour. The wood-flour/vegetal fibre component of WPC/FFC, increase the biodegradability of the products. The increase of moisture uptake can lead to the increase of biodegradability of FFC and WPC. However, as mentioned, due to the lamination, PVC layer, of WPC and FFC moisture uptake is insignificant.

Long term creep (flexural creep), on the other hand, depends on the applied load, temperature and content of wood/flour. An increase in applied load (Figure 8.20) and temperature (Figure 8.19) results in an increase in creep strain, whereas a decrease in the wood-flour component of WPC results in an increase in creep strain (Figure 8.21). Due to WPC and FFC, containing approximately 50% wood-flour and vegetal fibres respectively, only the applied load and temperature elevations plays an important role for these products. For future studies, these factors influencing durability and structural stability of WPC and FFC should be tested.

CHAPTER 9: ECONOMIC FEASIBILITY

In this chapter, the economic feasibility is estimated in terms of relative cost for a conventional block and mortar design housing unit (shown in Appendix C, Figure C.2 and Figure C.3), a modular FFC housing unit and modular WPC housing unit (shown in Appendix C, Figure C.1). The costs of all aspects that are not common in the three designs are compared. It is compared based on the material, labour, transport and maintenance cost.

The following assumptions to quantify the cost are made for the three design types:

- The construction site is the same size. Therefore, the site clearances cost the same.
- The costs for finishes, such as windows, doors, ceiling, thermal insulation for the roofing, services, etc. are the same and therefore are not included in the costs. This however, excludes the cost of paint for the conventional design type.
- All costs exclude contractors profit and 14%VAT.
- The life expectancy of the housing units is assumed as 25 years (SANS 10160-1, 2011, p. 24).
- 3.5 to 7.5 ton trucks are considered for transport.
- A total transport distance of 50km is assumed. This is the distance from the plant to the site.

9.1. Cost estimation of modular FFC housing units

The concept design for a modular plastic housing unit is shown in Appendix C, Figure C.1. A single storey housing unit of 40m^2 is used for the quantification process. The external walls consist of five sandwich panels on each of the four outer surface lengths.

The system boundary used for the quantification process is shown in Figure 9.1. The modular plastic housing units require no surface finishes, as in the case of paint used as surface finishes for the block and mortar housing unit. Therefore, finishes are excluded from the system boundary of the modular plastic housing units, as shown in Figure 9.1. All services are also excluded from the system boundary.

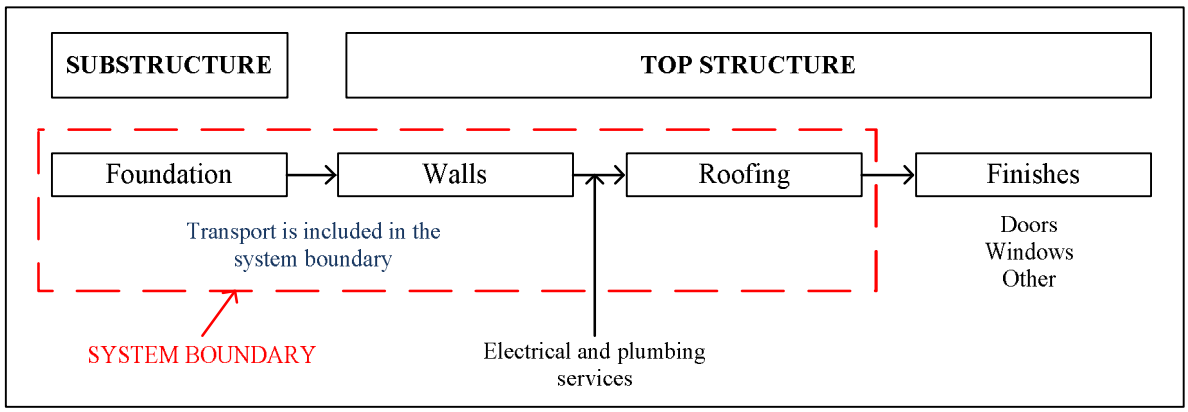

Figure 9.1: System boundary for modular plastic designs

A Bill of Quantities was used for the quantification process. The quantities, rates and prices were used to determine the cost. The cost was calculated for the material, labour, transport and maintenance cost of a FFC housing unit as well as a WPC housing unit. WPC cost estimates are discussed in Section 9.2. The cost calculations are shown in Appendix G.1.

9.1.1. Material cost

The material cost was determined by categorising the cost into foundation, floor slab, external walls, internal walls, ceiling and thermal insulation and roofing. The material cost of the substructure and the top structure for the modular FFC housing unit totals R 57 325.

Each building element is shown as a percentage of the total material cost in Figure 9.2. For Figure 9.2, it is clear that the external walls contribute the most towards the material cost, followed by the roofing. This is due to the large area that needs to be covered as well as the high prices of FFC.

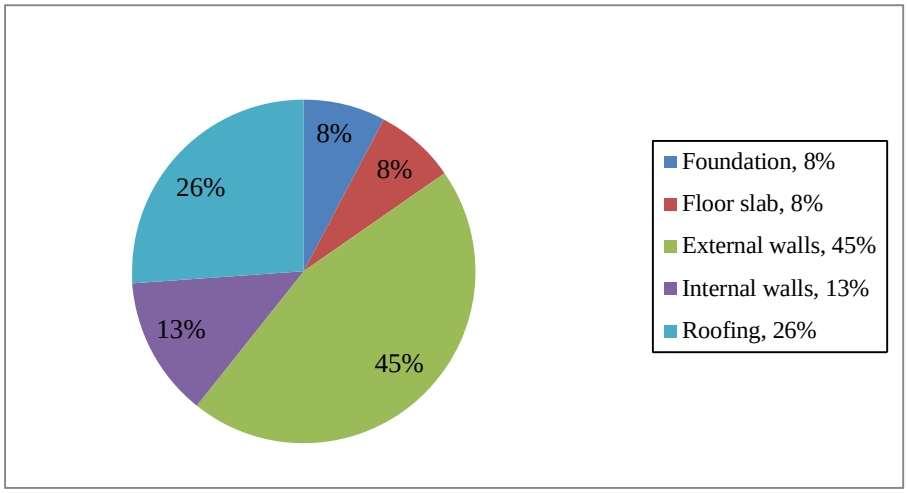

Figure 9.2: Material cost breakdown of modular FFC housing unit

9.1.2. Labour cost

The labour cost was determined by categorising the labour cost into foundation, floor slab, external walls, internal walls, ceiling and thermal insulation and roofing. Human labour will be used to erect the housing unit. A walling sandwich panel weighs approximately 56kg, whereas a roofing panel weighs about 74kg. The labour cost of the substructure and the top structure for the modular plastic housing unit totals R 11 779.

Each building element is shown in Figure 9.3, as a percentage of the labour total. As seen in Figure 9.3, the external walls contribute the most towards the labour cost, followed closely by the roofing. This is due to 20 panels that need to be erected by human labour to construct the external walls.

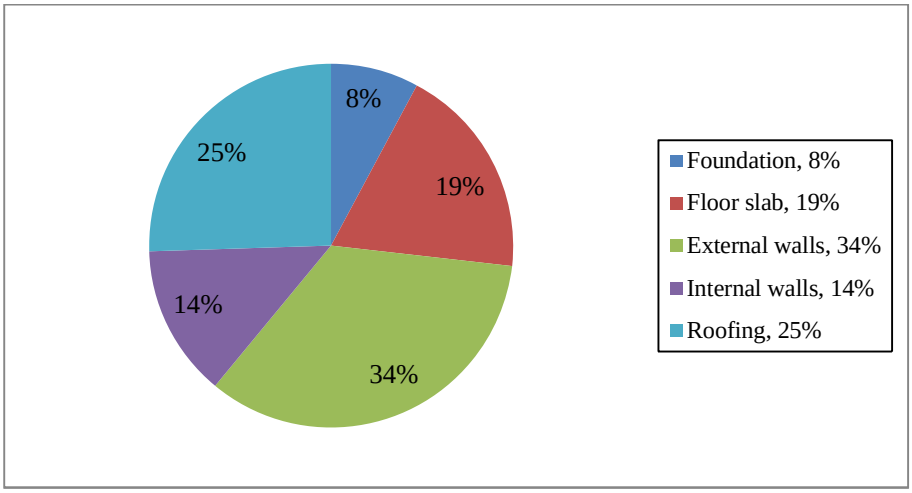

Figure 9.3: Labour cost breakdown of modular plastic housing units

9.1.3. Transport and maintenance cost

The modular plastic housing unit does not require any maintenance since FFC panels include surface finishes and no paint is required. The transport cost calculations are shown in Appendix G, Table G.4, and totals at R462.

9.1.4. Total cost

The total cost of the modular FFC plastic housing unit totals R69 566. The total cost breakdown is shown in Figure 9.4. Note from this figure, that material cost contributes to 82% of the total cost. This is mainly due to cost of the FFC.

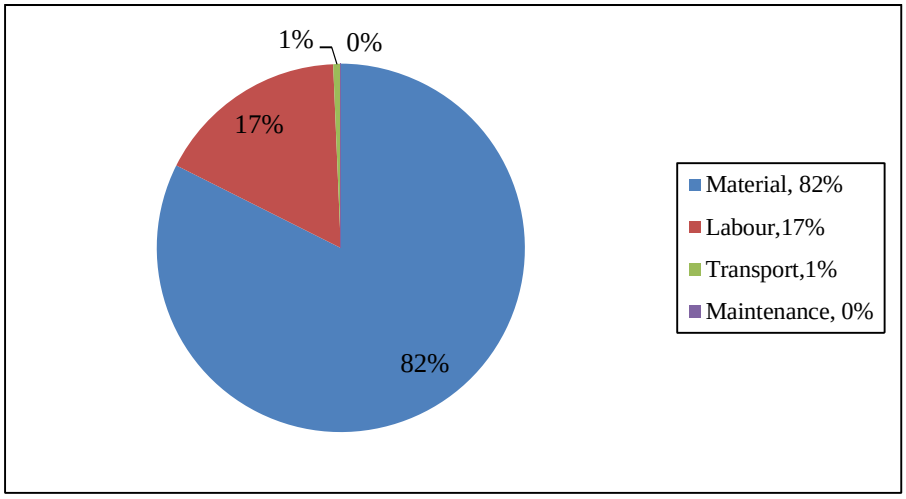

Figure 9.4: Breakdown of total cost of the modular FFC housing unit

9.2. Cost estimation of modular WPC housing units

As mentioned before, WPC is the alternative composite plastic for the structural panels of the modular housing unit that is shown in in Appendix C, Figure C.1. The same housing unit, size of panels, assumptions and system boundary (Figure 9.1) as used in Section 9.1 is used. The only difference is that the WPC is used as the structural panels.

9.2.1. Material cost

The material cost was calculated by categorising the cost into foundation, floor slab, external walls, internal walls, ceiling and thermal insulation and roofing. The material cost of the substructure and the top structure for the modular WPC housing unit totals R 87 038.

The contribution of each building element is shown in Figure 9.5 as a percentage of the total cost. This figure shows that the external walls contribute the most towards the material cost followed by the roofing. This is due to large area that needs to be covered by the WPC.

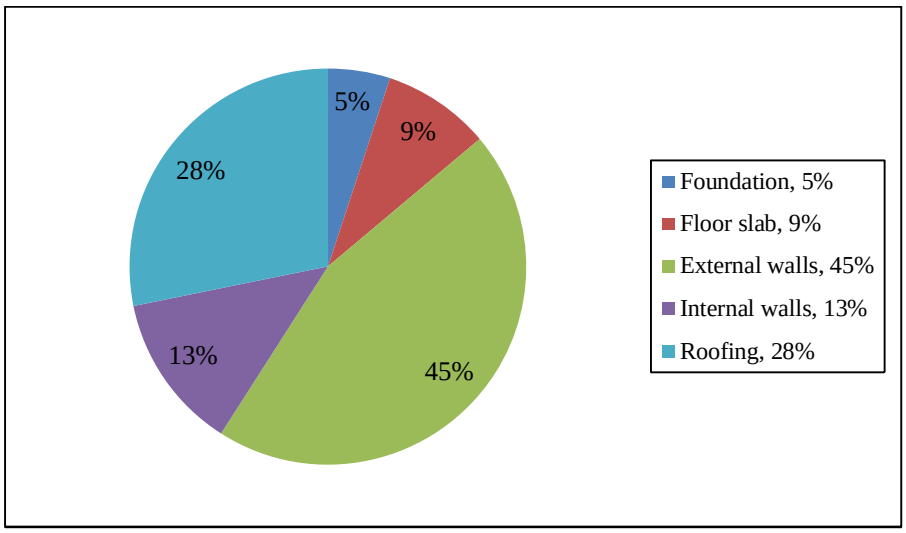

Figure 9.5: Material cost breakdown of modular WPC housing unit

9.2.2. Labour cost

Human labour will again be used to construct the housing unit. An external wall panel and a roof sheeting panel weighs about 102kg and 140kg respectively. The labour cost is the same as for the FFC housing unit and totals R 11 779. Refer to Figure 9.3 for the breakdown of the labour cost.

9.2.3. Transport and maintenance cost

The transport cost for the modular WPC housing unit is R658. The calculations are shown in Appendix G.1, Table G.5. There is no maintenance required for the WPC housing unit, since the panels include surface finishes and require no paint.

9.2.4. Total cost

The total cost of the modular plastic housing unit is R100 059. The total cost breakdown is shown in Figure 9.6. Note from this figure, that material cost of the modular WPC housing unit contributes to 87% of the total cost. This is mainly due to the high cost of WPC.

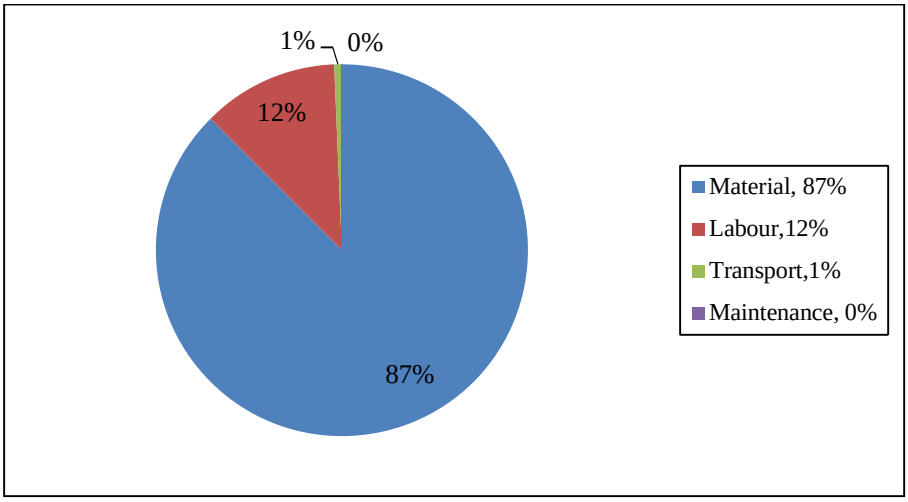

Figure 9.6: Breakdown of total cost of the modular WPC housing unit

9.3. Cost estimation of conventional block and mortar housing unit

An existing housing project, the Kayamandi Watergang Housing Project near Stellenbosch was used for the quantification of the block and mortar housing unit. The plan view, strip foundation and retaining wall detail of this housing unit are shown in Appendix C, Figure C.2 and Figure C.3. The project comprised of several different types of housing units, which include single units, duplex units and semi-detached single or duplex units (Brewis, 2011, p. 37). To ensure consistency, a single storey housing unit of 40m^2 was used for the quantification process, which would be compared with the modular plastic housing units.

The system boundary used for the quantification process is shown in Figure 9.7. Note form this figure, that services and most of the finishes, except paint, are excluded from the system boundary. This is due to the same processes or elements used in all three the designs. However, paint is not used in all the designs, since the modular plastic houses do not require any surface finishes, whereas for the block and mortar design paint is used as a surface finish.

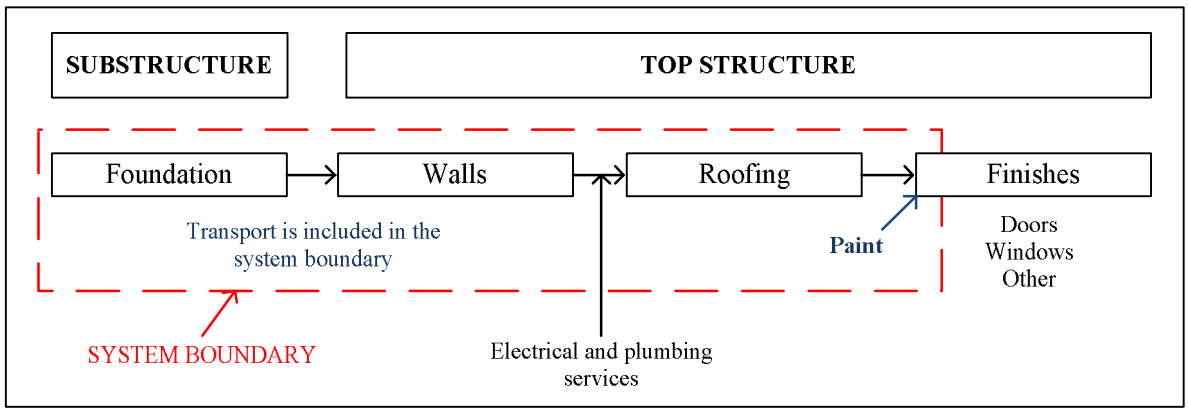

Figure 9.7: System boundary for conventional housing design

A Bill of Quantities was used for the quantification process. The quantities, rates and prices were used to determine the cost. The cost per quantity for 2013 was provided by specialist consultant, Le Roux (2013). The cost was calculated for the material, labour, transport and maintenance cost. The cost calculations are shown in Appendix G.2.

9.3.1. Material cost

The material cost was calculated by determining the cost of the foundation, floor slab, external walls, internal walls, ceiling and thermal insulation, roofing and covering. The material cost of the substructure and the top structure, excluding the paint, for the conventional block and mortar design type material totals R 45 128.

Each building element is shown in Figure 9.8 as a percentage of the total, excluding the paint. For Figure 9.8, it is clear that external walls contribute the most towards the material cost followed by the roofing and covering. This is due to the large area covered as well as the high concrete prices.

Only the outer surface of the external wall is painted. When the paint is included in the price, the material cost totals R45 863. The paint is estimated at R9.80 per m^2, thus the material cost for the paint is R735 for the conventional design type.

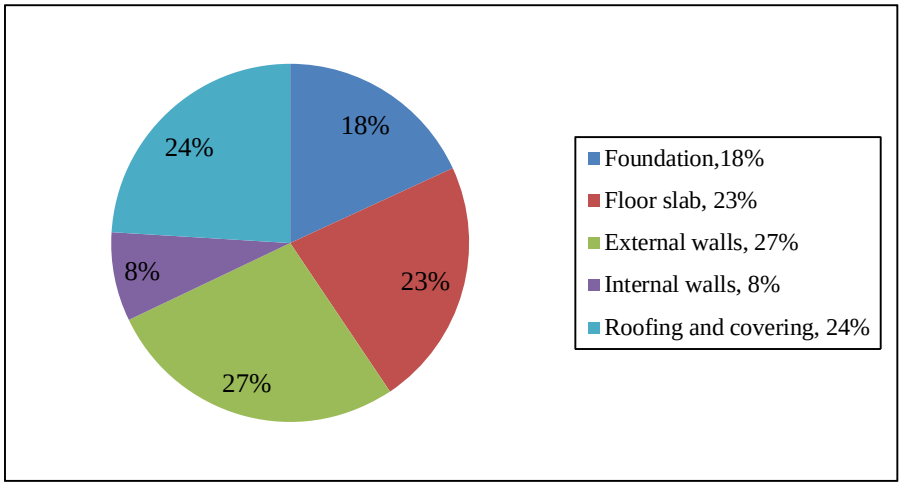

Figure 9.8: Material cost breakdown of conventional block and mortar design type

9.3.2. Labour cost

The labour cost was calculated by determining the labour cost in foundation, floor slab, external walls, internal walls, ceiling and thermal insulation, roofing and covering. A soft soil excavation was assumed for the foundations. The labour cost of the substructure and the top structure, excluding the paint, for the conventional block and mortar design type totals R 12 922. Each building element is shown in Figure 9.9 as a percentage of the labour total, excluding the paint.

As seen in Figure 9.9, the external walls contribute the most towards the labour cost, followed closely by the foundation. Construction of concrete block and mortar walls usually requires skilled labourers. Skilled labourers, as well as the large area covered by the walls, results in high labour costs. The labour intensity process of constructing the foundation, excavation, concrete casting and floating, causes high labour cost.

The cost of labour to paint the outer surface of the external walls is R21.74 per m^2, therefore the total labour cost, including the paint, is R 14 552.

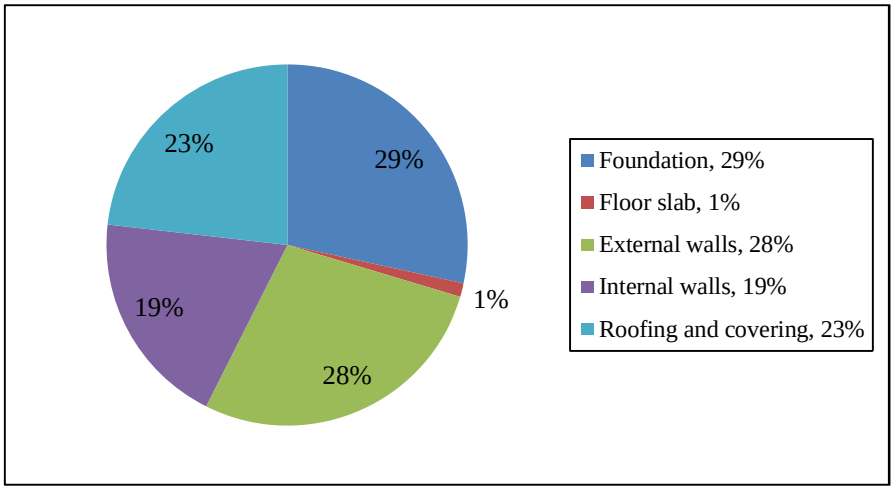

Figure 9.9: Labour cost breakdown of conventional block and mortar design type

9.3.3. Transport and maintenance cost

The calculations of the transport cost of the conventional block and mortar housing unit are shown in Appendix G, Table G.8. Considering all the assumptions made regarding transport, the total transport cost for approximately 48 tons is R 4 418.

The maintenance cost of a low-income house includes painting the outer surface of the external walls and unforeseen restoration work. For the maintenance cost, it is assumed that the housing unit should be painted twice in the expected life span. The maintenance for the conventional block and mortar house is estimated at R4 731. This price includes the material and labour cost of the paint.

9.3.4. Total cost for the conventional design type

The total cost of the conventional design type, including paint as a finish, is R 69 564. The total cost breakdown is shown in Figure 9.10. From this figure, it can be seen that the material cost contributes to more than half of the total cost. Transport and maintenance, on the other hand, contributes the least to the total cost.

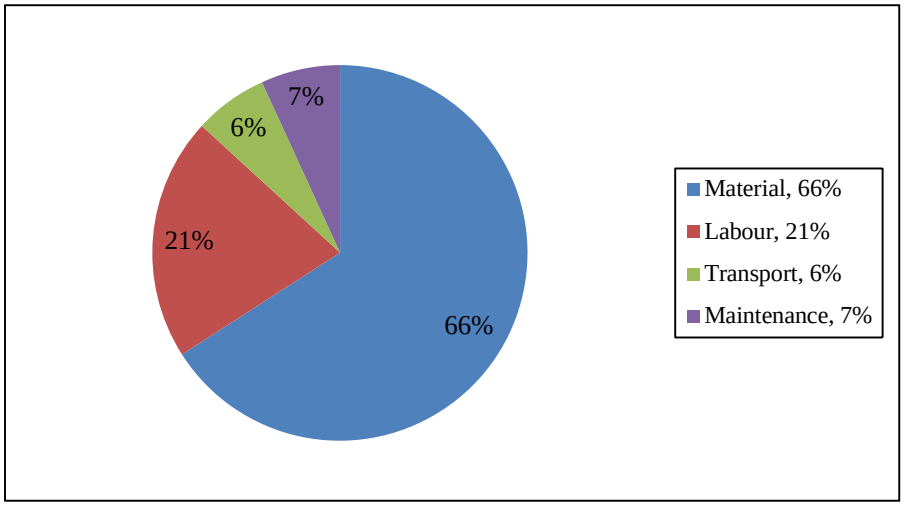

Figure 9.10: Breakdown of total cost of the conventional block and mortar housing unit

9.4. Cost comparison of the three housing units

The cost of the conventional design type, the modular FFC and WPC housing unit is compared in terms of material, labour, transport, maintenance and total cost.

9.4.1. Material cost

Figure 9.11 illustrates the material cost comparison of the three design types. The material cost of the modular FFC housing unit is approximately 25% more than the conventional block and mortar housing unit. This is due to the large difference in the cost of the external and internal walls and the roofing. Whereas, the WPC is approximately 90% more expensive than the conventional block and mortar housing unit and is approximately 52% more expensive than the modular FFC housing unit. This is mainly due to the high cost of WPC. As shown in Figure 9.11, the WPC housing unit is much more expensive, especially the internal and external walls and the roofing system which contributes to the material cost. However, the finishes, the floor slab and the foundation of the WPC housing unit are less expensive than that of the block and mortar housing unit.

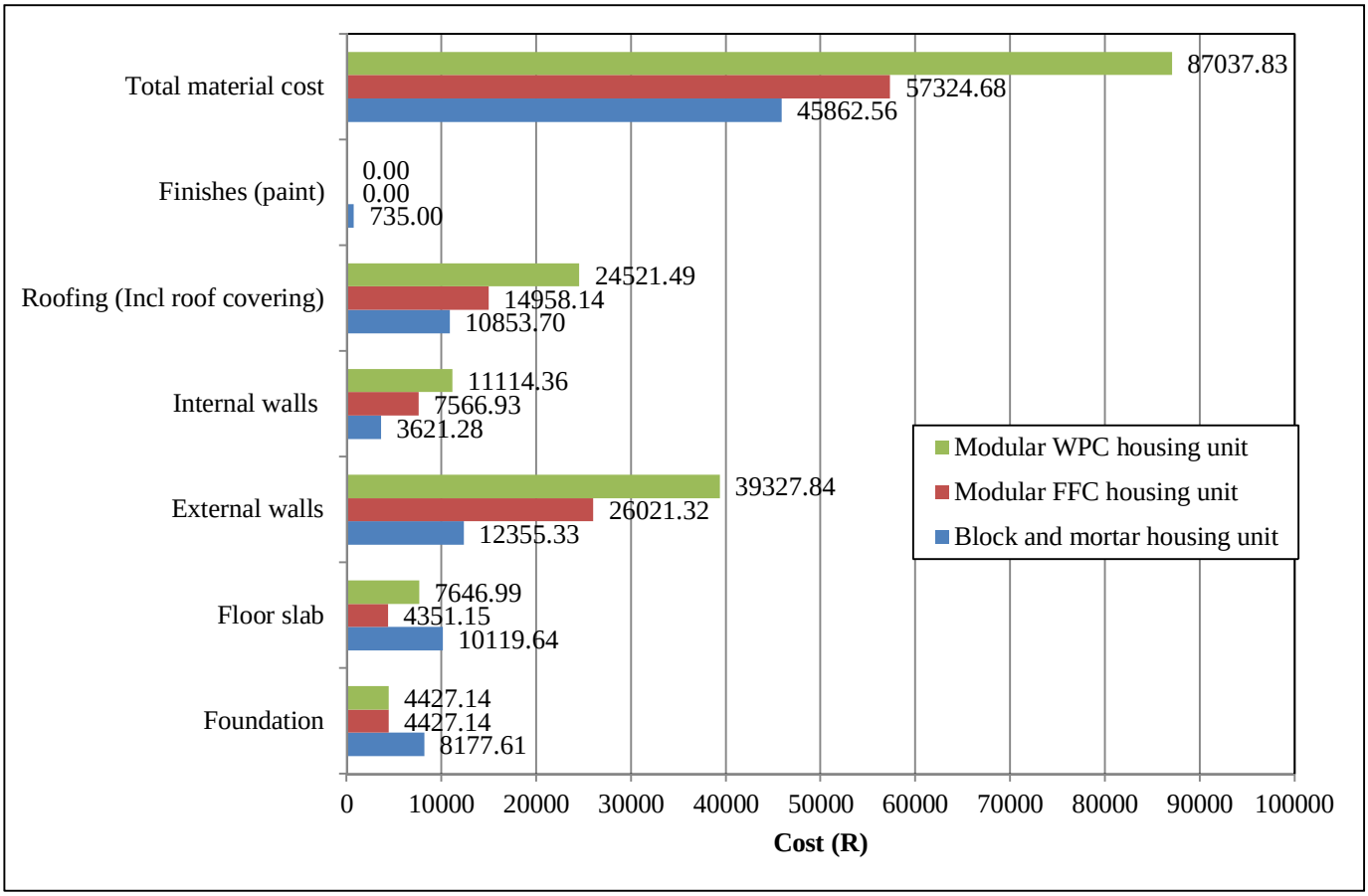

Figure 9.11: Comparison of the material cost of the conventional block and mortar housing unit and the modular plastic housing units

9.4.2. Labour cost

The labour cost of the modular FFC and WPC housing unit is the same (see Section 9.2.2). Therefore, the transport cost is compared for the modular housing units and the conventional block and mortar design type. The comparison is shown in Figure 9.12. This figure illustrates that the floor slab and external walls are the components of the modular plastic housing unit that are more expensive compared to those of the conventional block and mortar housing unit. The labour cost of the conventional design type is approximately 24% more than the modular plastic housing unit. This is the result of the mechanised nature of the production of the WPC and FFC. The labour cost for the manufacturing of the panels is included in the material cost.

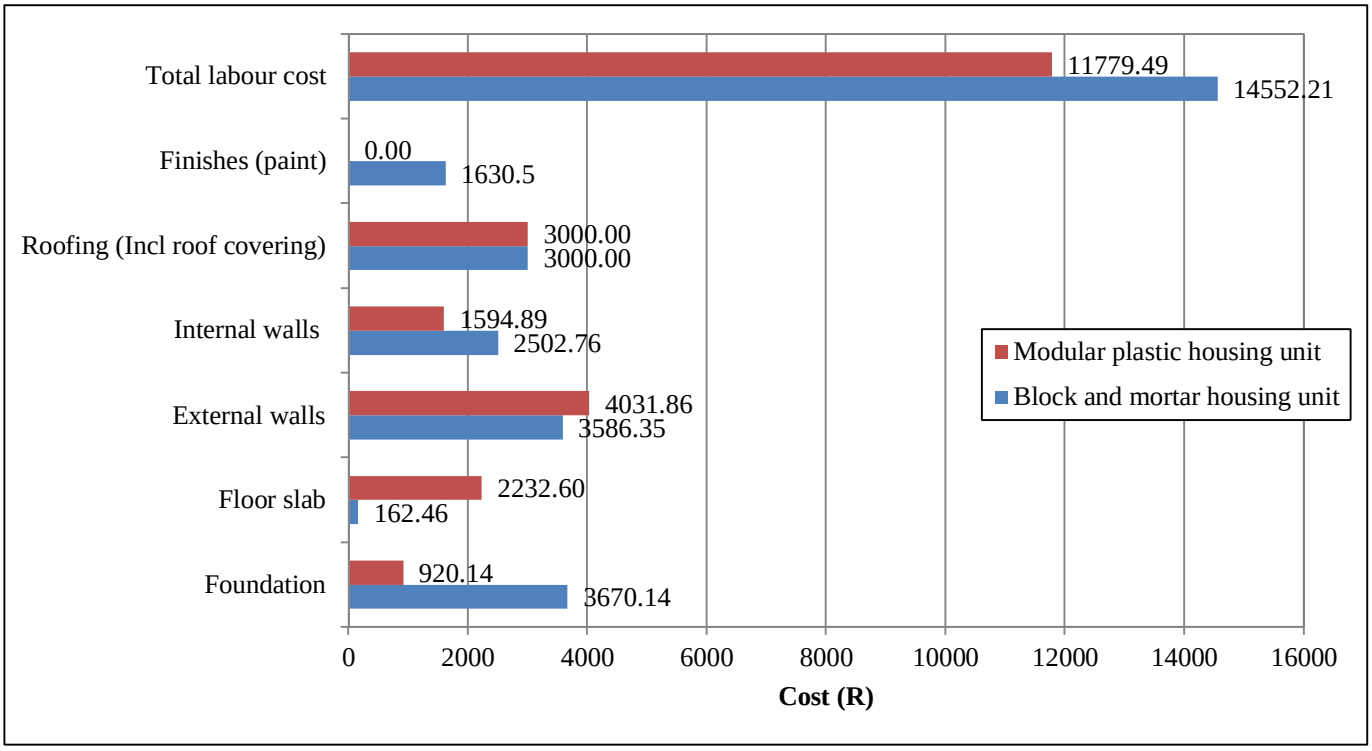

Figure 9.12: Comparison of the labour cost of the conventional block and mortar housing unit and the modular plastic housing units

9.4.3. Transport and maintenance cost

The transport and maintenance cost of the three designs is compared in Figure 9.13. The modular plastic housing units require no maintenance, whereas for the conventional design type the maintenance cost is due to painting of the exterior surface of the external walls.

The transport cost was determined for a distance of 50km. Since, the components of the plastic design type are much lighter, the transport cost of the block and mortar housing unit is approximately 856% more than the transport cost of the FFC housing unit and is about 571% more than that of the transport cost of the WPC housing unit. The transport cost of the WPC housing unit it is approximately 42% more expensive than that of the FFC housing unit. FFC is a lighter plastic material than WPC and therefore the transport cost is less.

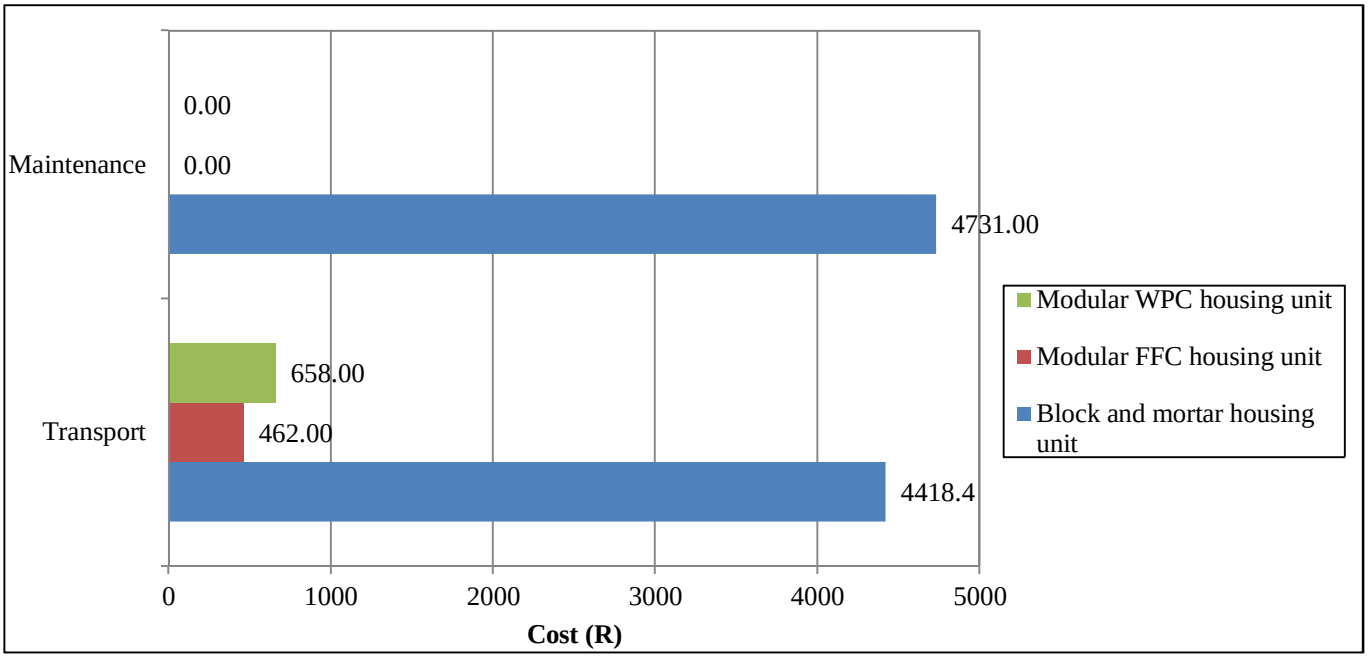

Figure 9.13: Comparison of the transport and maintenance cost of the conventional block and mortar housing unit and the modular plastic housing unit

The transport cost as well as the total cost is relatively sensitive to transport distance, as shown in Figure 9.14. In this figure, transport cost of the modular plastic housing units, FFC and WPC respectively and the conventional block and mortar design type, CD, are compared with changes in the transport distance ranging from 0km to 200km. For the transport cost, as the distance increases, the transport cost of the design types increase. Thus, the transport cost for the design types is sensitive to the transport distance.

Figure 9.14 also illustrates the change in the total cost as the transport distance changes. From this figure, it can be seen that at a transport distance of approximately 50km, the total cost of the FFC housing unit is equal to that of the block and mortar housing design. The total cost for these two design types at a transport distance of approximately 50km is R69 567. Thus, any transport distance greater than 50km will result in the total cost of modular FFC housing unit being more economical than the conventional design type. This is due to the lighter load that is transported for the modular plastic housing unit.

The transport distance of approximately 448km will result in the total cost of the WPC housing unit being equal to the cost of the block and mortar housing unit. This is a large transport distance and the probability of this transport distance is not likely. The total cost is therefore remarkably sensitive to the transport cost.

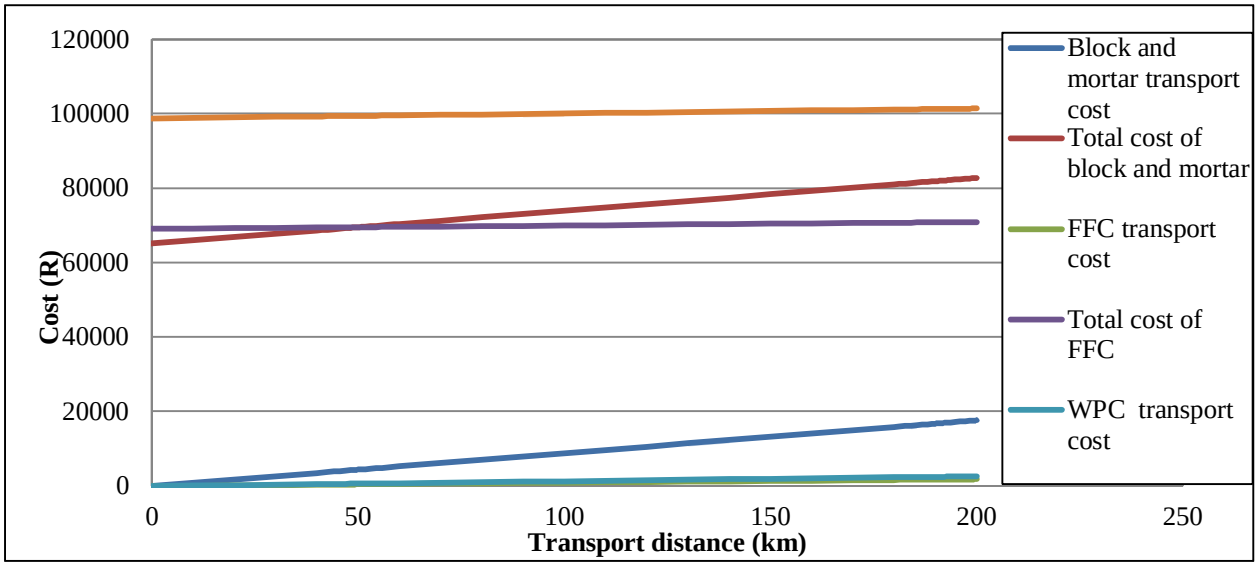

Figure 9.14: Sensitivity of cost as a function of transport distance

9.4.4. Total cost

A summary of all the components of the total relative cost for the three design types is shown in Figure 9.15. This figure illustrates that the material cost of the modular plastic housing units is the only component that is greater when compared to the same component of the conventional block and mortar housing unit. This component causes the total cost of the modular FFC housing unit to be greater by approximately 3% than the total cost of the conventional design type. The modular WPC housing unit, on the other hand, has a total cost of approximately 43% greater than that of the block and mortar housing unit and the FFC housing unit.

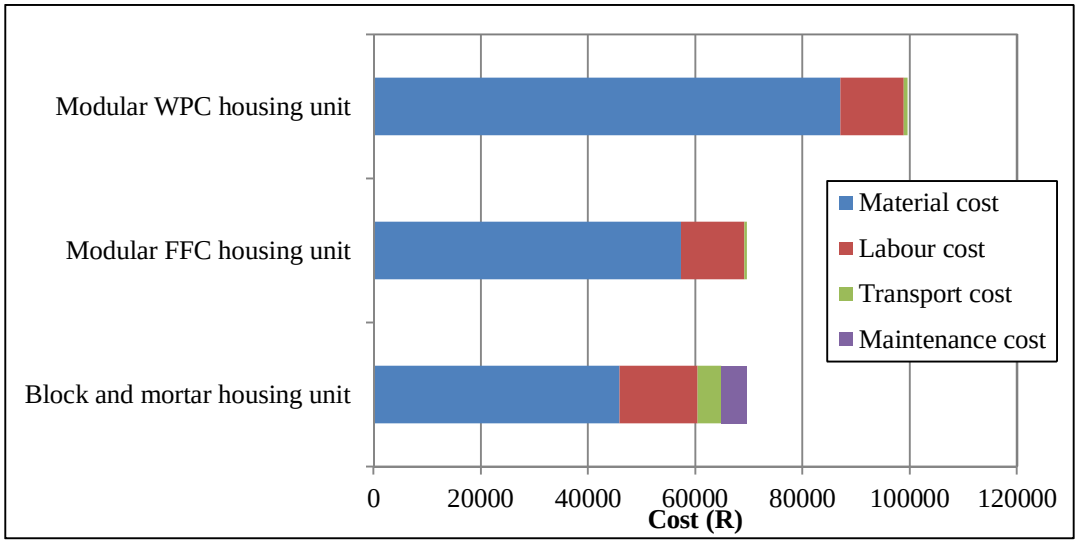

Figure 9.15: Comparison of the total cost of the conventional block and mortar housing unit and the modular plastic housing unit

9.5. Summary

According to cost comparison done by Brewis (2011), the LSFB (light steel frame building) unit was approximately 33% more expensive than the conventional block and mortar housing unit. LSFB is used as an alternative building technology for low-income houses in South Africa (refer to Section 2.2), since it can be erected faster than a conventional design type. Thus in terms of cost, the FFC housing unit is a plausible alternative for low-income housing. Since this housing unit is 3% more expensive than the conventional design type, but can be erected in a maximum of three days.

The WPC housing unit is approximately 43% more expensive than the block and mortar housing unit. Thus, it is about 11% more expensive than the LSFB. In terms of cost, this housing unit is not a plausible alternative as the FFC housing unit.

The modular plastic (FFC or WPC) housing unit typically utilises unskilled human labour to construct a housing unit, whereas the block and mortar alternative requires skilled human labour (brick layers). Furthermore, the socio-economic conditions of a community can be improved by the construction of modular plastic housing units by means of job creation. Due to the relative ease of construction of a modular plastic housing unit, the demand for housing can be reached at a more rapid pace than by using the conventional method.

CHAPTER 10: ENVIRONMENTAL FEASIBILITY

In this chapter, the environmental impact assessment (EIA) and environmental impact index (EII) for the pre-use phase as well as the energy efficiency is determined for the modular FFC-, the WPC- and the block and mortar housing unit. Environmental impact assessment and energy efficiency of these three housing units is also compared. The environmental friendliness of a building envelope is dependent on the environmental impact, in this case for the pre-use phase, as well as its energy efficiency.

10.1. Environmental impact assessment

In this section, the environmental impact assessment is conducted to compare the modular plastic (FFC and WPC) housing units to the block and mortar housing unit (Appendix C). Environmental impact categories are selected and discussed as well as the methodology which was followed to conduct this assessment.

A lifecycle analysis (LCA) of a building is used to determine the environmental impact of this building. Three phases exist for the LCA of a building, namely the pre-use phase, use phase and the end-of-life phase (Brewis, 2011). For the determination of the environmental impact assessment (EIA), the pre-use phase is compared for the housing units since a lack in data available for the plastic modular housing unit the operational phase as well as the end-of-life phase is not included EIA. The pre-use phase of the LCA includes the entire construction period (start to end) as well as the production of material used for the building and the transport of the material from the plant to the site. In this section, the production of the material and the transport are considered for the pre-use phase.

Most plastic materials are produced from by-products of the petroleum and oil industry. To consider the production of plastic materials for the pre-use phase, the process of source to product needs to be considered. This process or overview of the plastic industry from source to product is shown in Figure 10.1. Petroleum (oil) is converted to petrochemicals (feedstock); the feedstock is again converted into monomers. Monomers are polymerised to form polymers, whereas polymers are the basic part of plastics (Chapter 3). The fabrication of plastic materials was discussed in Chapters 4 and 5. PVC is produced mainly from natural resources such as oil and salt (chloride), which lead to a synthetic material (Rosato & Rosato, 2004, p. 195). Note that the examples in red illustrate the process for PVC. Since PVC is one of the main components in WPC and FFC.

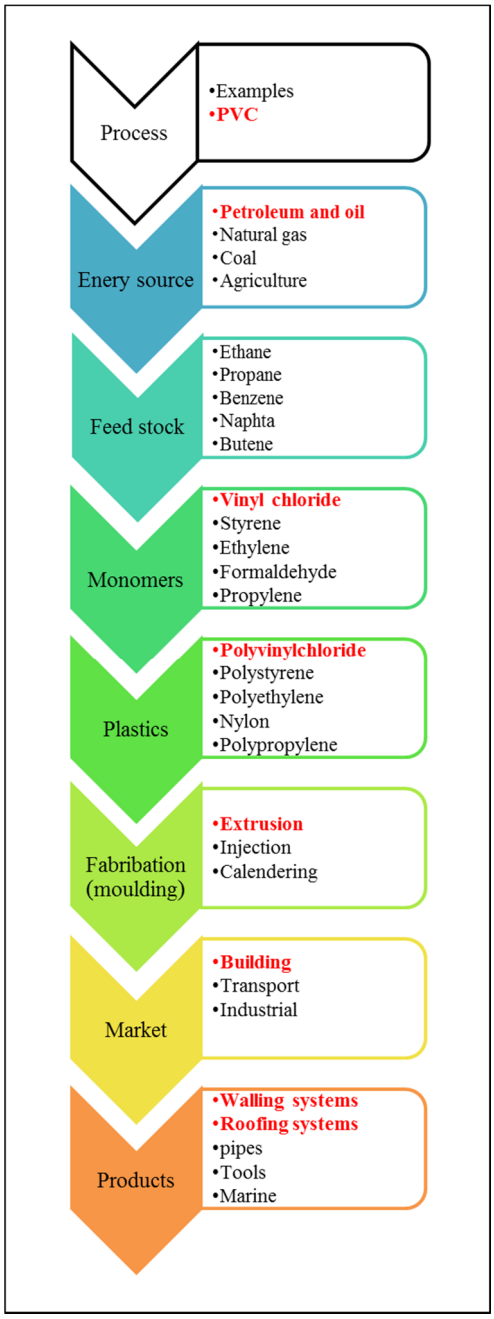

Figure 10.1: Overview of the plastic industry from source to product (Rosato & Rosato, 2004, p. 195)

10.1.1. Proposed method for the quantification process of environmental impact for pre-use phase

The LCA of a building can be performed as stipulated in ISO 14040 (Environmental Management: Life cycle assessment: Principles and framework). The LCA according to ISO 14040, comprises of four phase. These four phases are the goal and scope definition, the inventory analysis, impact assessment and the interpretation of the results.

Phase 1: The goal and scope definition includes the system boundaries of the building, in this case the housing unit (Brewis, 2011, p. 28) . The system boundary for the modular housing unit and the block and mortar housing unit is shown in Figure 9.1 and the Figure 9.7 respectively.

Phase 2: In the inventory analysis phase, the relevant input and output needs to be quantified in order to conduct the impact assessment phase. The Ecoinvent 3 database is used in the inventory phase. The database contains about 4000 thousand datasets for produces, processes and services and it is developed by the Swiss Centre of Life Cycle Inventories. These datasets are often used in case studies and Life Cycle Assessments (LCA) (Ecoinvent, 2013). Ecoinvent 3 lacks emission data for South Africa, therefore global data is used, unless stated otherwise.

Phase 3: Currently, two methods exist to quantify the environmental impact of a structure. These methods are either application-oriented or analysis-oriented (Brewis, 2011, p. 22). An analysis-oriented method is used to conduct the LCA of the pre-use phase. The analysis-oriented method comprises of a variety of Life Cycle Impact Assessment (LCIA) methods, which include CML 2001, Environmental Design of Industrial Products (EDIP) and Eco-indicator 99. These methods are constructed on the same basis, where the method consists of three steps (Brewis, 2011, p. 23):

- Step 1: Determining the environmental impact potential
- Step 2: Normalising the environmental impact potential, to compare the impact with a common reference
- Step 3: Weighting factors are applied, to enable comparison of impacts relative to one another.

The model developed by Brewis (2011) is used to determine the environmental impact of the pre-use phase of the housing unit's lifecycle. Three environmental impact categories are used in this model, which include Emissions, Waste Generation and Resource Depletion. Due to insignificant data available the Waste Generation and Resource Depletion for the modular plastic housing units cannot be quantified. Thus, only the Emissions are included as an environmental impact category in model of Brewis (2011). Ecoinvent 3 is used to determine the environmental impact potential (Step 1).

To quantify the emission environmental impact potential, Brewis (2011) suggests that the emission impact category is quantified by the following expression:

$$E_i = e_i m_i \quad \text{.....} \quad \textbf{(10.1)}$$

where,

E_i = Quantity of emission emitted (kg)

e_i = emission factor of the material

m_i = Mass or flow of the material (kg)

The emission impact category is subdivided into different gasses. The different gasses include Carbon Footprint (CF) referred to as Environmental impact 1 (EI_1), the Acidification Potential (AP) (EI_2) and the Eutrophication Potential (EP) (EI_3) (Brewis, 2011; Brits, 2011). To calculate these environmental impacts the following equations were used (Brewis, 2011; Brits, 2011):

$$\boldsymbol{EI_1 = \sum GWP_i E_i} \quad \textbf{(10.2)}$$

$$\boldsymbol{EI_2 = \sum f_i E_i} \quad \textbf{(10.3)}$$

$$\boldsymbol{EI_3 = \sum g_i E_i} \quad \textbf{(10.4)}$$

where,

EI_1 = Carbon Footprint (CF) ($kgCO_{2e}$)

GWP_i = Global Warming Potential (from literature)

EI_2 = Acidification Potential (AP)

f_i = Acidification Potential factor (from literature)

EI_3 = Eutrophication Potential (EP)

g_i = Eutrophication factor (from literature)

E_i = Quantity of emission emitted (kg), Equation 10.1

After the quantitation of the emission environmental impact potential, normalising and weighting factors are applied to the environmental impact category. Brewis (2011) suggests that the factors of EDIP '97 method are used. These factors as well as the reference origin are shown in Table 10.1.

Table 10.1: Normalisation and Weighting factors of EDIP (Stranddorf, et al., 2005; Goedkoop, et al., 2007; Brewis, 2011; Brits, 2011)

Environmental impact	Normalisation factor		Weighting factor	Reference origin
	Value	Unit		
Carbon Footprint	kg CO_{2e}/capita/year	8700	1.12	Global
Acidification	kg SO_{2e}/capita/year	59	1.27	Europe
Eutrophication	kg NO_{3e}/capita/year	95	1.22	Europe

Finally, to determine the environmental impact index (EII), the normalised and weighted impacts are summed by using the following (Brewis, 2011; Brits, 2011):

$$EII = \sum c_i \frac{EI_i}{EI_{i,ref}} \quad \text{..... (10.5)}$$

where,

EII = Environmental impact index

c_i = Weighting factor related to EI_i

EI_i = Environmental Impact

$EI_{i,\,ref}$ = Normalised reference factor

Phase 4: The interpretation of the results phase of the LCA according to ISO 140140 includes the results, conclusions and recommendations for improvement of the model.

10.1.2. Emissions

As mentioned in the previous section, the impact category, emissions, is investigated for the LCA of the low-income housing unit. In order to quantify emissions, it is essential to determine which gasses should be considered as the most important and relevant gasses to this study. The emissions, as mentioned previously, include the Carbon Footprint (CF), the Acidification Potential (AP) and the Eutrophication Potential (EP). These emissions are selected based on the process by which plastic materials are produced (Figure 10.1). These environmental impacts are described below.

Carbon Footprint

Global warming exists mainly due to the increase of greenhouse gasses (GHG's) in the atmosphere. To quantify the Carbon Footprint of a system applicable to the built environment, the Kyoto Protocol listed contributing GHG's. These GHG's include carbon dioxide (CO_2), nitrous oxide (N_2O) and methane (CH_4) (Hauschild & Wenzel, 1998, p. 7). The emission of these gases into the atmosphere, during the production of a building element, has a negative impact on the environment. The Carbon Footprint (CF) is quantified by Equation 10.2. However, to sum all the components, the components need to be of CO_2-equaivalents (CO_{2e}) form (Brewis, 2011, p. 29). The Global Warming Potential (GWP) factors, Equation 10.2, related to the certain emission are shown in Table 10.2.

Table 10.2: GWP factor (Pachauri & Reisinger, 2007)

Greenhouse gas (GHG)	Chemical formula	GWP for100 years (kg CO_2/kg emission)
Carbon dioxide	CO_2	1
Nitrous oxide	N_2O	310
Methane	CH_4	25

Acidification Potential

Acidification results in a decrease of the acid neutralising capacity of aquatic ecosystems and soil. This occurs mainly due to gasses, for example SO_2 and NO_x, which transform to acidic substances (Hauschild & Wenzel, 1998, p. 161). The two main acidic substances which increase the acidity of the aquatic ecosystems and soil are nitric acid (HNO_3) and sulphuric acid (H_2SO_4), which can result in corrosion of manmade structures (Azapagic, et al., 2004, p. 435).

The Acidification Potential (AP) is quantified by using Equation 10.3 and is measured in sulphur dioxide equivalents (SO_{2e}) (Brewis, 2011, p. 30). The acidification factors of two gasses are shown in Table 10.3.

Table 10.3: Acidification Potential (AP) factor (Azapagic, et al., 2004)

Gas name	Chemical formula	AP factor (kg SO_{2e}/kg emission)
Sulphur dioxide	SO_2	1
Oxides of nitrogen	NO_x	0.7

Eutrophication Potential

Eutrophication is the increase of chemical nutrients, such as nitrogen (N) and phosphorus (P) into a water body (Ertebjerg, et al., 2003, p. 9). Nutrient enrichment results in changes in the ecosystem. These changes include the increase in the algae growth and a reduction in water quality (Rossouw, et al., 2008, p. 1).

The Eutrophication Potential (EP) is quantified by using of Equation 10.4. EP is measured in terms of nitrate equivalents (SO_{2e}) (Brits, 2011, p. 29). The EP factors, for certain substances, are shown in Table 10.4.

Table 10.4: Eutrophication Potential (EP) factor (Hauschild & Wenzel, 1998).

Substance	EP factor, g, (kg NO_{3e}/kg emission)
NO_3-	1
NO_x	1.35
NH_3	3.64
PO_4^{3-}	10.45
$P_2O_7^{2-}$	11.41

Summary of environmental impact categories

Three environmental impact categories were selected to determine and compare the environmental impact of the pre-use phase of the modular plastic housing unit and the block and mortar housing unit. A summary of the categories considered is shown in Table 10.5.

Table 10.5: Summary of considered environmental impact categories

Environmental impact (EI*i*)	Name	Unit
EI_1	Carbon Footprint Potential (GWP)	kg CO_{2e}
EI_2	AP	kg SO_{2e}
EI_3	EP	kg NO_{3e}

10.1.3. Assumptions to quantify the environmental impact

To perform the quantification of the environmental impacts, the following assumptions are made for both the modular plastic housing unit and the block and mortar housing unit:

- The pre-use phase of the project of the housing units was assumed to be for the duration of one year. This is due to the normalisation factor which is measured annually (Table 10.1). Thus, for a year duration, a dimensionless normalised value was obtained, which can be compared.
- The Ecoinvent 3 database does not contain impact potential factors for plaster and mortar. Thus, a sand to cement ratio of 1:14 was used to obtain the impact potential factors.
- 3.5 to 7.5 ton trucks were used for transport (see assumptions made for cost analysis, Chapter 9)
- A total transport distance of 50km is assumed. This is the distance from the plant to the site (see assumptions made for cost analysis, Chapter 9).

Impact factors (described in Sections 10.1.1 and 10.1.2) are necessary to quantify the environmental impact of the housing units. The materials used to construct a housing unit (used in the Bill of Quantities) were closely related to the available materials on the Ecoinvent 3 database. The Bill of Quantities for each housing unit is shown in Appendix H.1. Table 10.6 and Table 10.7 illustrate the materials selected from the Evoinvent 3 database and a description thereof, for the modular plastic housing unit, as well as the block and mortar housing unit, respectively.

Table 10.6: Material selected from Ecoinvent 3 database for the modular plastic housing unit

Item on Bill of Quantities	Ecoinvent name	Unit	Description
Concrete	Concrete production, normal	m^3	Includes the whole manufacturing processes to produce ready-mixed concrete, internal processes (transport, etc.) and infrastructure. Density: 2380 kg/m3. Ingredients: Cement 300 kg, Water 190 kg, Aggregates 1890 kg.
Reinforcing	Reinforcing steel production	kg	Mix of different produced steels
EPS	polystyrene production, expandable	kg	Production by suspension polymerisation out of benzene and ethylene
PVC	Extrusion production, plastic pipes	m^2	1kg of this process equals 0.996kg of extruded PVC plastic pipes
Ceiling	Gypsum plasterboard production	kg	Production of board (incl. drying)
Thermal insulation	Glass wool mat production	kg	Included processes: melting, fibre forming & collecting, hardening & curing and internal processes (workshop, etc.). Additional transportation of raw materials and energy carrier for furnace, packing and infrastructure are included.
Roofing	Planing, softwood, air dried	m^3	Includes planing process. Planing mill is assumed to be located on the sawmill site. No transport is considered. Dust emissions are neglected for a lack of data.
Transport	Transport, freight, lorry 3.5-7.5 metric ton, EURO3	tkm	Operation of vehicle; production, maintenance and disposal of vehicles; construction and maintenance and disposal of road. Diesel and diesel engine. Lorry transport is further differentiated with respect to vehicle weight and emission technology standard (EURO-standard).

Table 10.7: Material selected from Ecoinvent 3 databases for the block and mortar housing unit

Item on Bill of Quantities	Ecoinvent name	Unit	Description
Concrete	Concrete production, normal	m^3	Includes the whole manufacturing processes to produce ready-mixed concrete, internal processes (transport, etc.) and infrastructure. Density: 2380 kg/m3. Ingredients: Cement 300 kg, Water 190 kg, Aggregates 1890 kg.
Reinforcing	Reinforcing steel production	kg	Mix of different produced steels and hot rolling
Blockwork	Concrete block production, normal	kg	Includes the raw material normal concrete which is poured into a mould, air-dried and packed. Some transports and infrastructure are also included.
Brickforce	Steel production, low-alloyed, hot rolled	kg	Mix of differently produced steels and hot rolling.
Galvanising	Zinc coating, coils	m^2	Includes the process steps surface cleaning, heat treatment, immersion in a bath of molten zinc and finishing treatment. Also includes zinc input and transportation to coiling plant.
Damp proof membrane/ course	Polyethylene production, low-density, granulate	kg	Aggregated data for all processes from raw material extraction until delivery at plant.
Plaster	Silica sand production	kg	Includes the raw material sand, a certain additional amount of conveyor belt and the energy for drying the sand. No requirements for administration are included.
Ceiling	Gypsum plasterboard production	kg	Production of board (incl. drying)
Thermal insulation	Glass wool mat production	kg	Included processes: melting, fibre forming & collecting, hardening & curing and internal processes (workshop, etc.). Additionally transportation of raw materials and energy carrier for furnace, packing and infrastructure are included.
Roofing	Planing, softwood, air dried	m^3	Includes planing process. Planing mill is assumed to be located on the sawmill site. No transports are considered. Dust emissions are neglected for a lack of data.

Item on Bill of Quantities	Ecoinvent name	Unit	Description
Roof sheeting	Steel production, low-alloyed, cold rolling	kg	Mix of differently produced steels
Transport	Transport, freight, lorry 3.5-7.5 metric ton, EURO3	tkm	Operation of vehicle; production, maintenance and disposal of vehicles; construction and maintenance and disposal of road. Diesel and diesel engine. Lorry transport is further differentiated with respect to vehicle weight and emission technology standard (EURO-standard).
Paint	Alkyd paint production, white, solvent-based, production in 60% solution state	kg	Alkyd paint can be made of many different resins.

10.1.4. Quantification of environmental impact of the three housing units and the comparison thereof

In this section, the environmental impact, in terms of the emissions (Section 10.1.2) and the environmental impact index (EII), is discussed for each of the housing units as well as the comparison thereof. For each emission, the quantification of environmental impact is divided into the following building elements:

- Foundation
- Flooring system
- External walls
- Internal walls
- Ceiling and insulation
- Roofing system, which includes the roof covering
- Transport
- Finishes, such as paint for the block and mortar housing unit

Appendix H.1, illustrates the calculation sheet used to obtain the environmental impact for the modular plastic (FFC and WPC) housing units as well as the block and mortar housing unit. For the WPC and FFC housing units, the wood-flour and vegetal fibres are not taken into account. These reinforcing agents are

waste materials and are not specially produced for WPC and FFC. Using waste materials has a positive impact on the environment. WPC and FFC are comprised of the same plastic material, PVC, thus only the transport element will differ for these two housing units.

Carbon Footprint

Figure 10.2 illustrates the Carbon Footprint (CF) for each of the building elements of the three 40m^2 housing units, namely the modular FFC, modular WPC and block and mortar housing unit. When the FFC and WPC housing units are considered, it is clear from Figure 10.2 that the foundation contributes the most to the Carbon Footprint. This is due to the large amount of GHG's which is emitted when concrete is produced. For the block and mortar housing unit, the foundation contributes the most to the CF followed by the external walls. Again, this is due to the large amount of GHG's emitted when concrete is produced.

When the CF's of the three housing units are compared, it is clear that for each building element, the block and mortar housing unit has a larger CF. This is due to the amount of concrete used for the block and mortar housing unit. Since PVC (plastic component of WPC and FFC) is produced from a by-product of the petroleum and oil industry, it does not contribute significantly to the CF.

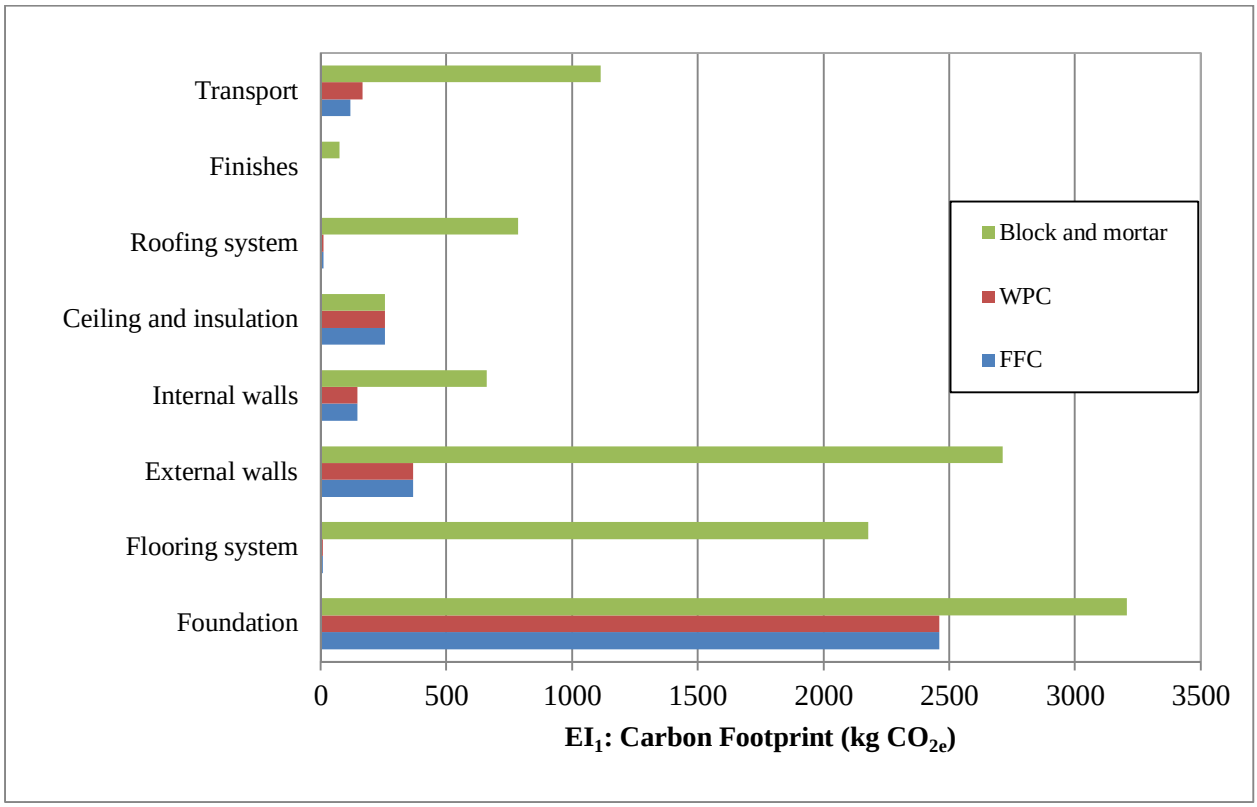

Figure 10.2: Carbon Footprint (EI_1) of the modular FFC and WPC housing unit and block and mortar housing unit

Acidification Potential

The Acidification Potential (AP) for each of the building elements of the modular FFC, modular WPC and block and mortar housing units, are shown in Figure 10.3. The foundation contributes the most to the Acidification Potential impact for the modular FFC and WPC housing units, since the foundation is comprised of concrete. For the block and mortar housing unit, the roofing system contributes the most to the AP, followed by the external walls and foundation. The roofing system of the block and mortar housing unit is mainly comprised of steel sheeting. This roof sheeting leads to the roofing system contributing the most towards the acidification potential.

When the Acidification Potentials (AP's) of the housing units are compared, the block and mortar design has a larger AP for each of its building elements. The AP factor for galvanising is obtained from the Ecoinvent 3 database. The larger galvanised area of the roof sheeting contributes greatly to the AP of the block and mortar housing unit.

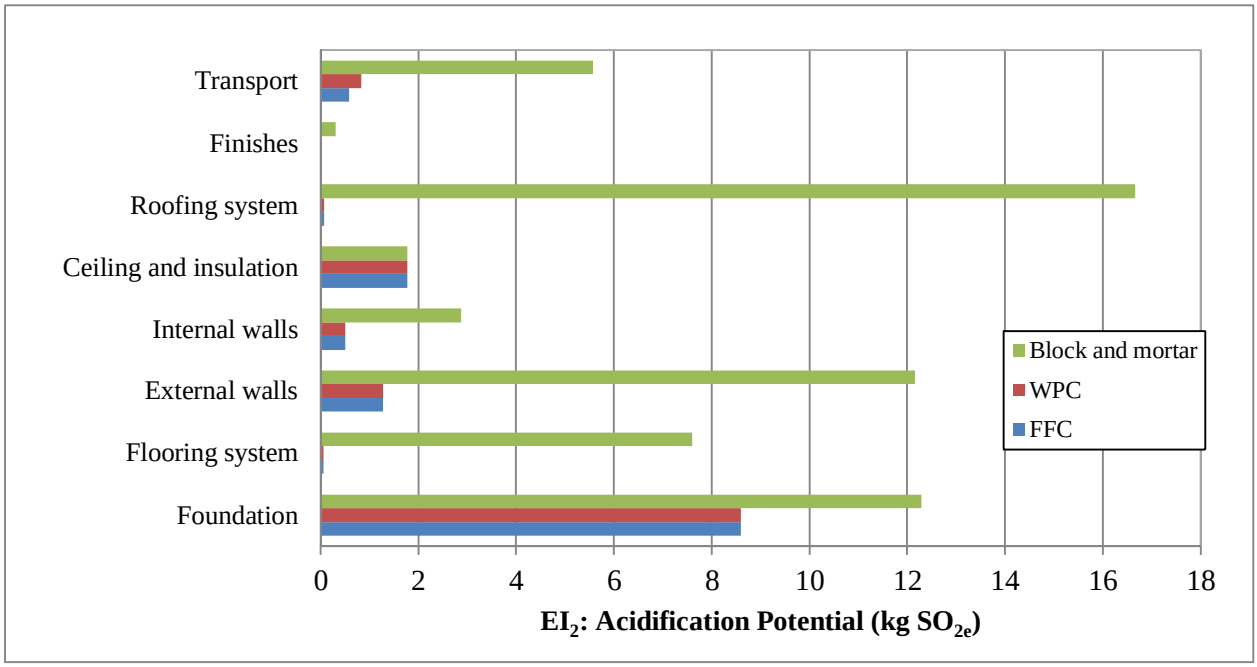

Figure 10.3: Acidification Potential (EI_2) for the modular FFC and WPC housing unit and block and mortar housing unit

Eutrophication Potential

In Figure 10.4, the Eutrophication Potential (EP) for the modular FFC and WPC housing units as well as the block and mortar housing unit are shown. Again, the foundation contributes the most to the EP of the FFC and WPC housing units, whereas the roofing system, followed by the external walls and foundation, contribute the most to the EP of the block and mortar housing unit. The block and mortar housing unit exhibits a greater EP for each of the building element, when compared to that of the FFC and WPC housing

units. This is due to the greater amount of concrete used, as well as the use of steel roof sheeting, to construct the block and mortar housing unit.

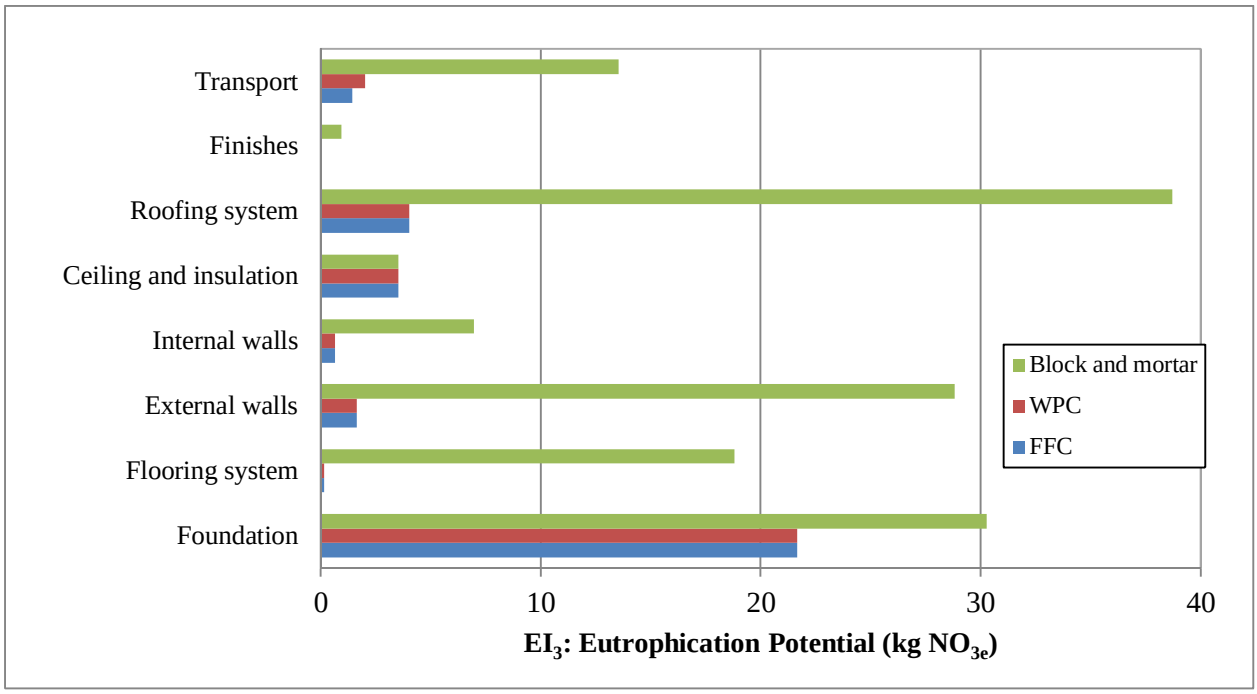

Figure 10.4: Eutrophication Potential (EI_3) for the modular FFC and WPC housing unit and block and mortar housing unit

Weighted and normalised environmental impact for each emission

The weighting factors as well as the normalisation factors, as shown in Table 10.1, were taken into account to compile Table 10.8. The total environmental impact represents the total impact (sum of all the building elements) of each housing unit.

The weighted and normalised environmental impacts of each emission and housing unit (Table 10.8) are shown in Figure 10.5. From this figure, it is clear that the block and mortar unit has the greatest negative environmental impact when the emissions are considered. The Carbon Footprint is the greatest environmental indicator that contributes to the environmental impact of the FFC and the WPC housing units. The Eutrophication Potential contributes the most to the environmental impact of the block and mortar housing unit.

Table 10.8: Environmental impacts, normalised and weighted values for the FFC, WPC and block and mortar housing unit

	CF (kg CO_{2e})			AP (kg SO_{2e})			EP (kg NO_{3e})		
	FFC	**WPC**	**CD**	**FFC**	**WPC**	**CD**	**FFC**	**WPC**	**CD**
Total environmental impact	3361	3410	10979	12	13	59	33	33	141
Normalised	0.39	0.39	1.26	0.22	0.22	1.00	0.35	0.35	1.49
Normalised and weighted	0.43	0.44	1.41	0.28	0.28	1.27	0.42	0.43	1.82

Note:

FFC - modular FFC housing unit

WPC - modular WPC housing unit

CD - Conventional block and mortar housing unit

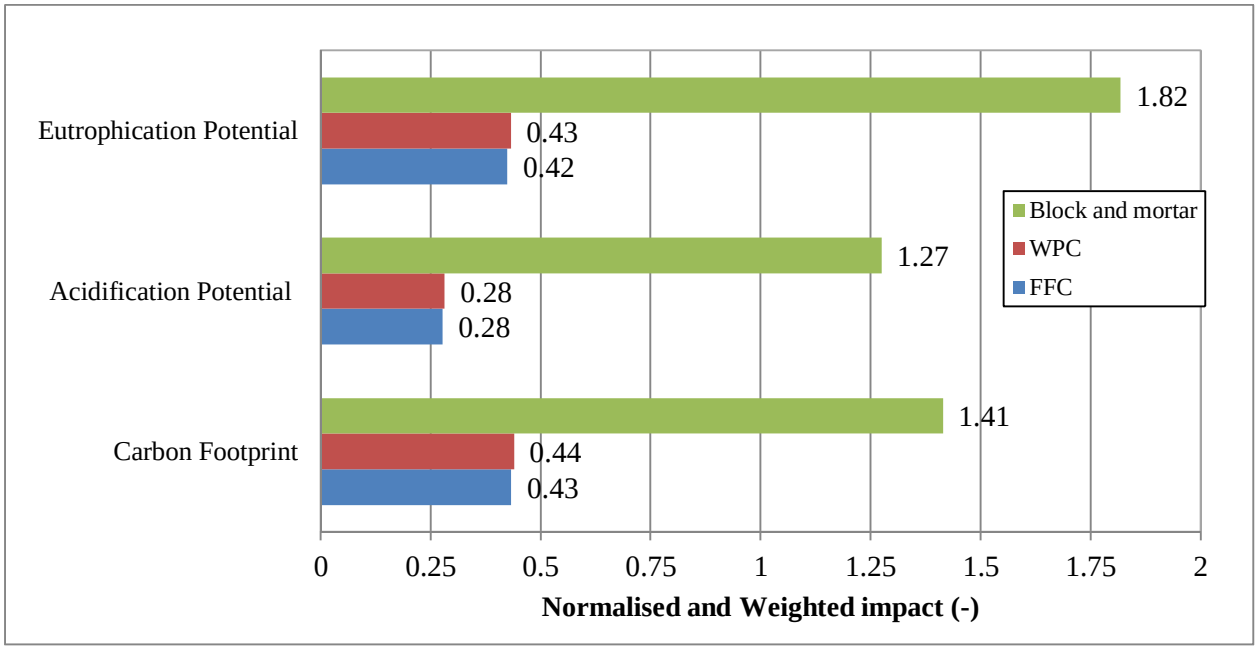

Figure 10.5: Weighted and normalised environmental impact for each emission and housing unit

Environmental Impact Index

The environmental impact index (EII) is calculated by using Equation 10.5 and is shown in Figure 10.6. From this figure, it is clear that the FFC, closely followed by the WPC housing unit, have a lower environmental impact index than that of the block and mortar unit. Therefore, the plastic housing units are more environmentally friendly in terms of pre-use emissions compared to the block and mortar housing unit.

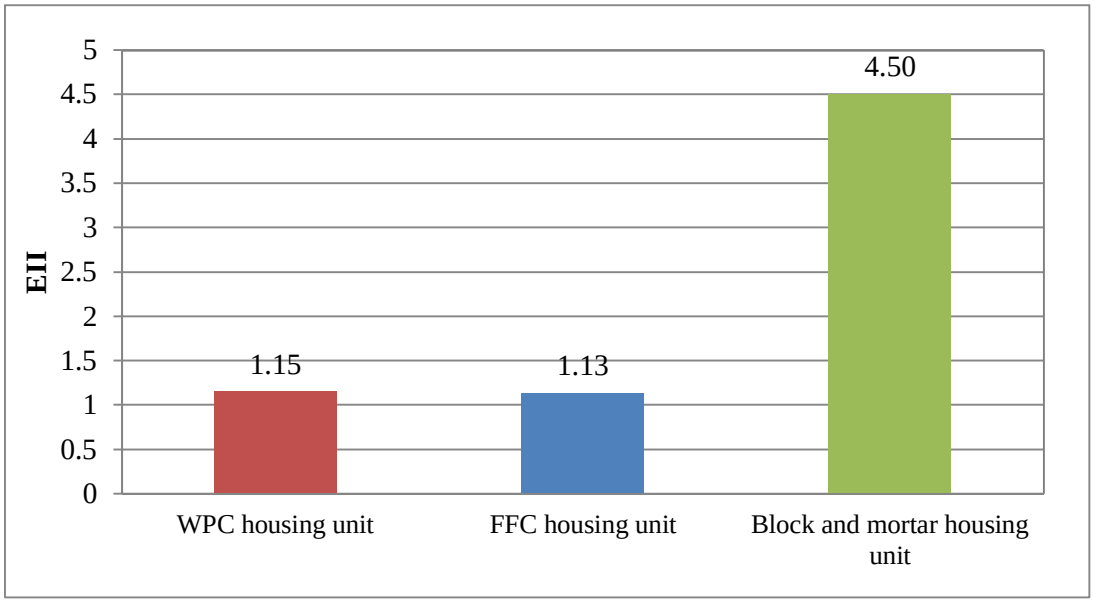

Figure 10.6: Environmental impact index for the FFC, WPC and block and mortar housing unit

10.1.5. Sensitivity analysis

A sensitivity analysis was conducted to estimate the sensitivity of variables which were assumed to have a particular value for the calculations of environmental impacts of the housing units. These variables are transportation distance of the material and the weighting factors used to calculate the EII.

Transport

The transport distance was assumed 50km from the plant to the site. The sensitivity analysis was conducted for a transportation distance of 0 to 200km. The EII was determined for this variation in transport distance, as shown in Figure 10.7. This figure illustrates that the transport distance of the block and mortar housing unit is more sensitive (steeper slope) than that of the modular FFC and WPC housing units. This is due to greater total mass of the block and mortar housing unit. The FFC and WPC have comparable variations in the EII caused by variations in the transport distance. This is due to the similarity in mass that needs to be transported for these housing units.

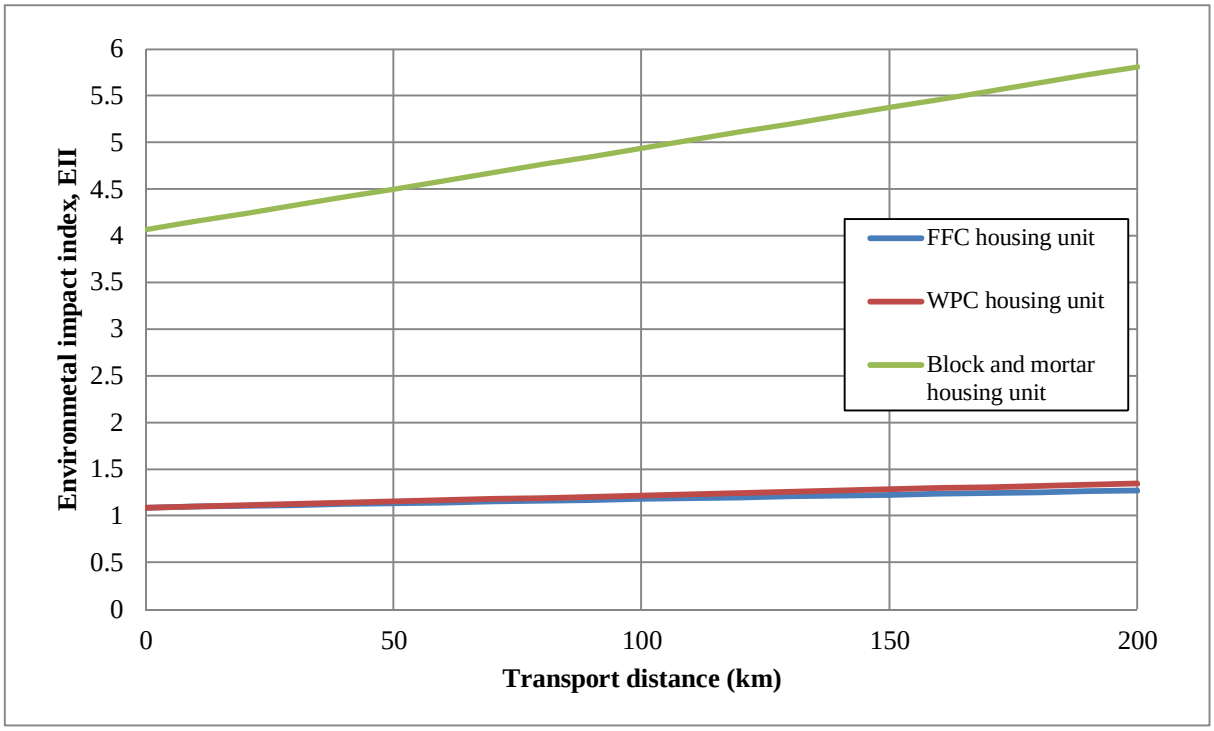

Figure 10.7: Sensitivity of the EII of each housing unit as a function of transport distance

Weighting factors

The weighting factors assumed for each impact category are shown in Table 10.1. The weighting factors were varied alternating between 0.9 and 1.4 per impact, while the other impacts were kept constant. The EII was determined for a variation in weighting factors for each housing unit, as shown in Figure 10.8, Figure 10.9 and Figure 10.10.

In Figure 10.8, the EII of the modular FFC housing unit was determined as a function of the variation in the weighting factors for each emission. From this figure, the slopes of the CF and EP weighting factor variations are 0.38 and 0.35 respectively. The AP weighting factor variation is 0.22. This indicates that the CF weighting factor is the most sensitive, closely followed by the EP weighting factor, of the weighting factors when the FFC housing unit is considered.

The EII of the modular WPC housing unit was determined for a variation in the weighting factors for each emission. This is shown in Figure 10.9. The slopes for each of the weighting factors of the emissions are the same as for the FFC housing unit. This is since the environmental impacts of the FFC and WPC housing units only differ in terms of transport mass. However, the values of the EII reached by the variations in the weighting factors are higher for a WPC unit, than that of a FFC housing unit.

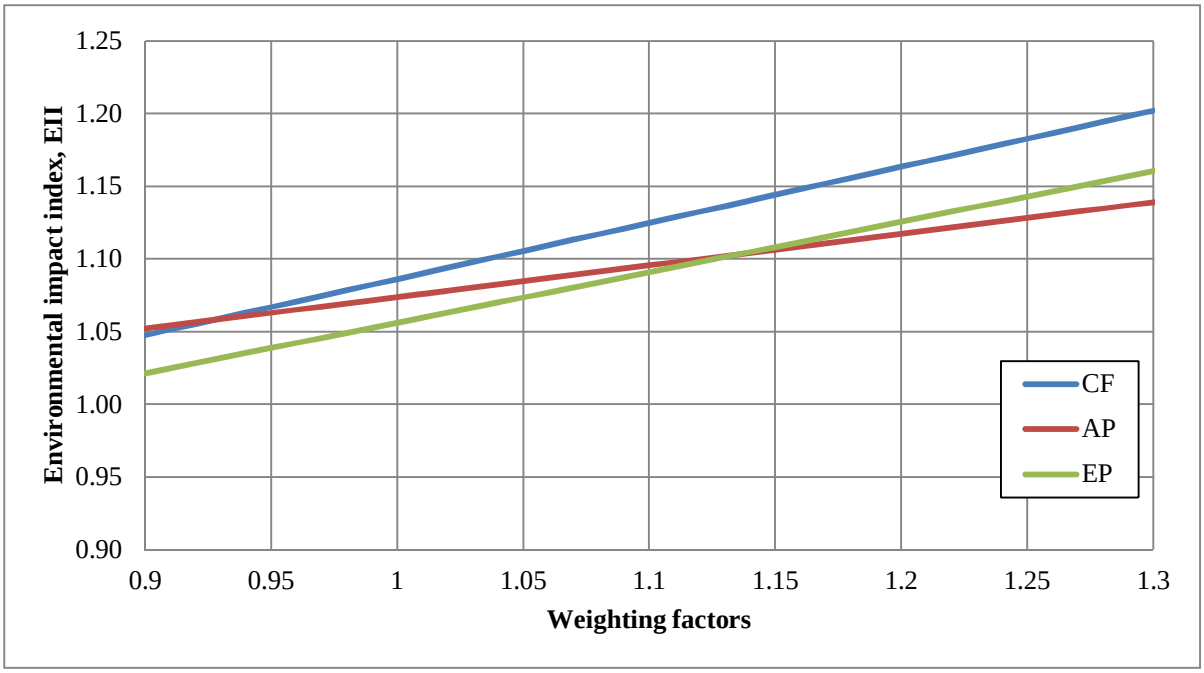

Figure 10.8: Sensitivity of the EII of the FFC housing unit as a function of weighting factors

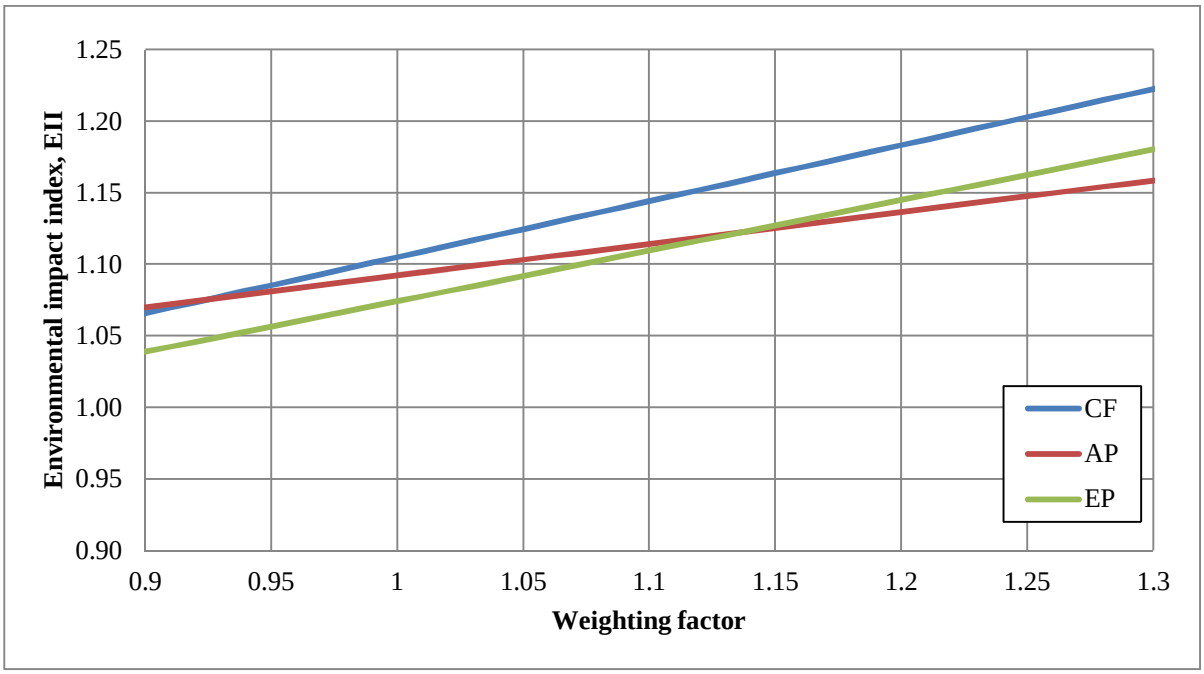

Figure 10.9: Sensitivity of the EII of the WPC housing unit as a function of weighting factors

In Figure 10.10, the EII of the block and mortar housing unit was determined as a function of the variation in the weighting factors for each emission. From this figure, the slope is 1.26 for a variation in the CF, 1.00 for a variation in the AP and 1.49 for the variation in the EP weighting factor. This indicates that the EP

weighting factor is the most sensitive of the three weighting factors, when the block and mortar housing unit is considered.

When all three housing units are considered, the variation in the values of the weighting factors influence the EII of the block and mortar design more than that of the modular plastic housing units.

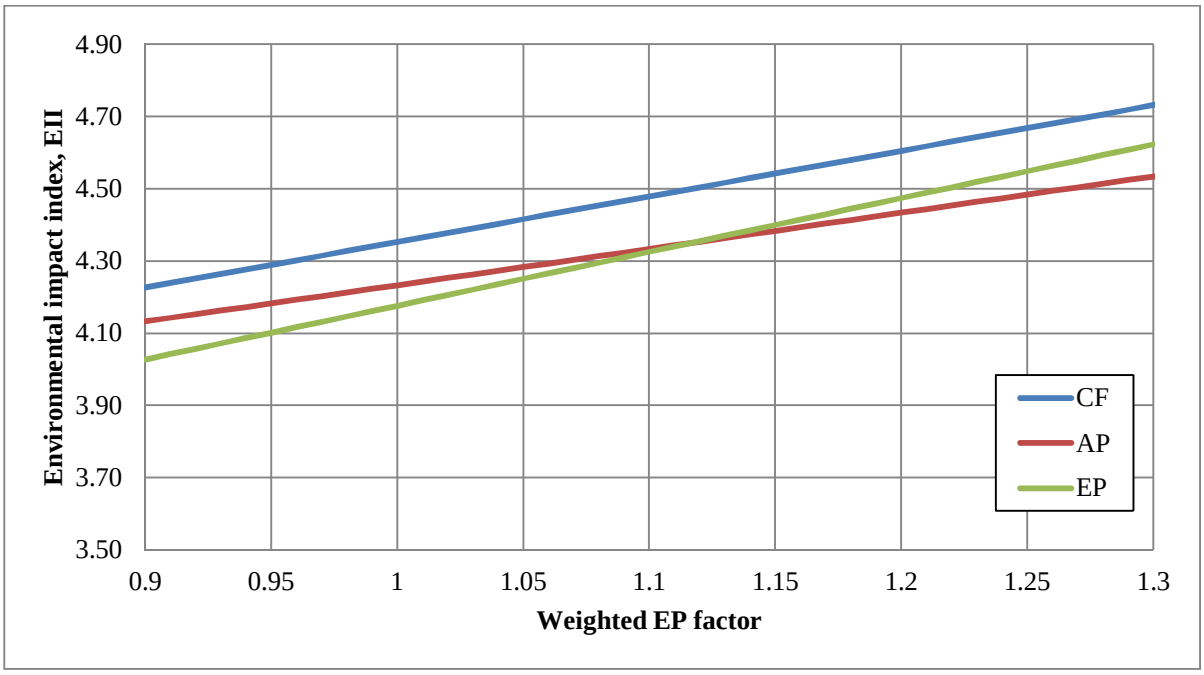

Figure 10.10: Sensitivity of the EII of the block and mortar housing unit as a function of weighting factors

10.2. Energy efficiency of the housing units

South Africa is divided into climate zones, for which the energy efficiency requirements differ (SANS 10400-A, 2010). The South African climate zone map is shown in SANS 10400-XA (2011, Figure A.1).

The three design types, namely the modular FFC housing unit, the modular WPC housing unit and the block and mortar housing unit, are compared based on energy efficiency. The design of the modular plastic housing unit was discussed in Chapter 6, where the block and mortar housing unit is shown in Appendix C. The energy efficiency of these housing units is investigated to determine whether the requirements stipulated in SANS 10400-XA (2011) and SANS 204 (2011) are met. The energy efficiency differs for each building element and for each climate zone. The optimum requirements are investigated in this chapter for the walling

and roofing system. The building orientation, floor, fenestration and shading are assumed the same for both design types and therefore are not included.

10.2.1. Method for calculating the energy efficiency

The method for calculating the energy efficiency of a building envelope depends on the various building elements, such as the flooring system, external walls and the roofing assembly. To estimate the energy efficiency of the building elements the thermal capacity (C_s), thermal resistance (R-value) and the CR-value need to be calculated. Therefore, the methods calculating these terms are discussed.

Thermal capacity

The thermal capacity (C_s) of a material is the ability to store heat energy and it is measured in Joule per square meter per degree Celsius (J/m^2°C). The higher the C_s is, the larger the capacity of the material to store heat. The C_s is calculated by means of the following equation (SANS 204, 2011, p. 6):

$$C_s = V.\rho.c \quad \text{..... (10.6)}$$

where,

V = Volume of building element per square meter or thickness of building element (m)

ρ = Density of material (kg/m^3)

c = Specific heat of material (J/kg°C)

However, the total C_s of a building element is calculated by means of the following equation:

$$Total\ C_s = C_{s1} + \cdots C_{sn} \quad \text{..... (10.7)}$$

where,

C_{s1}, C_{s2}, … C_{sn} = C_s for each component of the composite wall, as calculated in Equation 10.6 (J/m^2°C)

Thermal resistance

The thermal resistance (R-value) of a material is a measurement of the ability of the material to resist heat-flow across the material and is measured in square meter degree Celsius per watt (m^2°C/W). The higher the R-value number is, the greater the ability of the material to resist heat flow. An extremely high R-value can indicate a thermal insolative material. The R-value for each building element is calculated by using the following equation (SANS 204, 2011, p. 6):

$$R = {}^{d}/_{k} \quad \text{..... (10.8)}$$

where,

d = Thickness of the material of the building element (m)

k = Thermal conductivity (W/m°C)

To calculate the total R-value of a building element, the following equation is used (Harris, 2012, p. 76):

$$Total\ R\_value = {}^{1}/_{h_1} + {}^{1}/_{h_0} + \left({}^{1}/_{a_1} + \cdots {}^{1}/_{a_n}\right) + (R_1 + \cdots R_n) \quad \text{..... (10.9)}$$

where,

h_1 = Co-efficient of heat transfer for inner surface wall (W/m^2°C)

h_0 = Co-efficient of heat transfer for outer surface wall (W/m^2°C)

a_1, a_2, ...a_n = The thermal conductances of n separate airspaces incorporated in the structure (W/m^2°C)

R_1, R_2, … R_n = R-value for each component of composite wall, as calculated in Equation 10.8 (m^2°C/W)

CR-value

The CR-value is a time constant (measured in hours) of a composite building element, such as a walling system (SANS 204, 2011). It is defined as the arithmetic product of the total thermal resistance (total R-value) and the total thermal capacity (total C_s-value). The CR-value indicates the ability of the composite building element to minimise and moderate the climatic conditions on the interior of the building, due to the effects of the external climatic conditions. The higher the CR-value, the greater the ability to minimise and moderate the climatic conditions on the interior of the building (SANS 204, 2011). The CR-value of a composite building element is calculated by using the following equation:

$$CR\_value = (Total\ R\_value)x\ (Total\ C_s)x\ (y) \quad \text{..... (10.10)}$$

where,

Total R-value = Total thermal resistance of the composite building element, Equation 10.9(m^2°C/W)

Total C_s = Total thermal capacity of the composite building element, Equation 10.7 (J/m^2°C)

y = conversion factor of 0.2778

Thermal transmittance

The thermal transmittance (U-value) of a material indicates the amount of heat energy that passes through a building element when one degree Kelvin is applied across the element. It is measured in watt per square meter degree Celsius (W/m^2°C). The U-value is calculated by the following expression (Harris, 2012, p. 35):

$$U\_value = {}^{1}/_{R} \quad \text{.....} \quad \textbf{(10.11)}$$

where,

R-value = Thermal resistance of a building element, Equation 10.8 (m^2°C/W)

To calculate all of the above values, the thermal conductivity, k, and the specific heat, c, of the material play an important role. The values used for thermal conductivity and the specific heat are shown in Section 6.5. These values as well as typical ranges of WPC (and FFC) for these parameters are shown in Table 10.9. From this table, it is clear that the thermal conductivity, k, and the specific heat, c, values used for WPC and FFC fall within these ranges (Mikulenok, 2012).

Table 10.9: Thermal conductivity, k, and the specific heat, c, ranges for WPC and FFC (Mikulenok, 2012)

	Thermal conductivity (W/m°C)	Specific heat (J/kg°C)
WPC	0.150	1860.00
FFC	0.130	1300.00
Range	0.12 - 0.19	1100 - 2100

10.2.2. Energy efficiency of external walls

The external walls (Section 6.1) of the modular plastic housing unit, where FFC and WPC are used, and the external walls of the block and mortar housing unit are compared in terms of energy efficiency. The external walls of these design types need to comply with the requirements shown in Table 10.10. According to SANS 10400-A (2010) Table 1, the occupancy classification of a low-income house is H4. Therefore, from Table 10.11 a minimum CR-value of 60 to 100 hours, depending on the climate zone, is required. For the non-masonry walls, the minimum total R-value required is 2.2 m^2°C/W.

Table 10.10: SANS 204 (2011) paragraph 4.3.3.1 and 4.3.3.2: Requirements for external walls

SANS 204 paragraph 4.3.3.1: **Masonry walls (Block and mortar housing unit)**	SANS 204 paragraph 4.3.3.1: **Non-masonry walls (Modular plastic housing unit)**
• A minimum CR-value for a specific climate zone and occupation type shall be achieved as described in Table 10.11.	• A minimum CR-value for a specific climate zone and occupation type shall be achieved as described in Table 10.11. • For a 1 and 6 climate zone a minimum R-value of 2.2 shall be achieved. • For a 1 and 6 climate zone a minimum R-value of 1.9 shall be achieved.

Table 10.11: Table 3 of SANS204 (2011): Minimum CR-value, in hours, for external walling of residential H4 occupancies

Occupancy group	**Climate zone**					
	1	2	3	4	5	6
Residential: H4	100	80	80	100	60	90

To calculate the energy efficiency of the external wall, the total R-value (Equation 10.9), total C_s (Equation 10.7) and the CR-value (Equation 10.10) were determined. For calculating the total R-value (Equation 10.9), there are no airspaces in the walling systems of the modular plastic housing units, therefore the thermal conductances of *n* separate airspaces incorporated in the structure (*a*) equals zero. However, the block and mortar housing unit consists of hollow concrete blocks. Therefore, the thermal conductance of *n* separate airspaces incorporated in the structure (*a*) equals 6.8 according to Harris (2012, p87). The coefficients of surface thermal conductance (h_1 and h_0) are obtained from Harris, (2012, p. 86), where h_1 equals 9.4 W/m^2°C and h_0 equals 20 W/m^2°C. The total R-values as well as the CR-values of the three housing units are shown in Figure 10.11. The calculations for the total R-values, the thermal capacity (C_s) and the CR-values for the external walls of the modular FFC housing, modular WPC housing unit and block and mortar housing unit are shown in Appendix H.2.

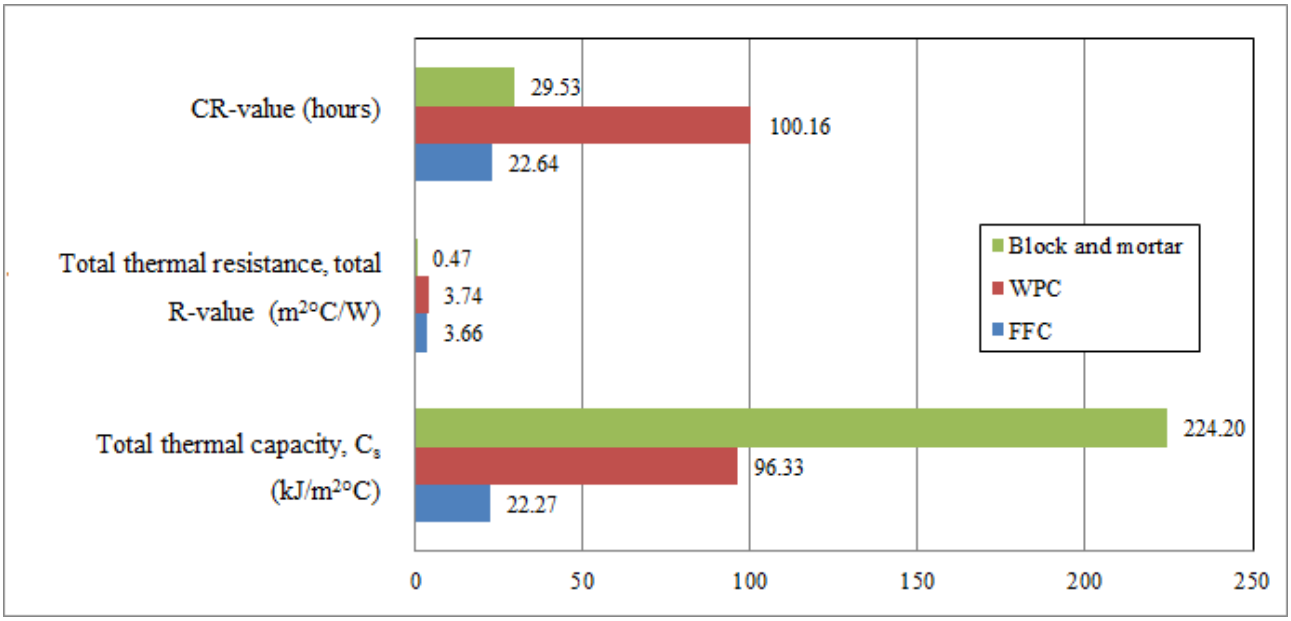

Figure 10.11: The comparison of total R-value, the thermal capacity (C_s) and the CR-value for the external walls of the modular FFC and WPC housing units and block and mortar housing unit

The total R-value of the external walls of both the modular plastic housing units is much greater when compared to the total R-value of the external walls of the block and mortar house, as shown in Figure 10.11. The WPC housing unit has a slightly higher R-value than the FFC housing unit. This implies that the external walls of the plastic housing units, especially the WPC housing unit, can resist more heat-flow than that of the block and mortar. The total R-value of the external walls of both the modular plastic housing units, meet the requirements of a minimum total R-value of 2.2m^2°C/W, as prescribed by SANS 204 (2011). The block and mortar housing unit does not meet these requirements.

When the CR-values of the three design types are compared, the CR-value of the modular WPC housing units is greater than that of the block and mortar housing unit and the modular FFC housing unit, for the external walls. This is due to WPC having a greater density, compared to FFC, and a greater specific heat, compared to block and mortar as well as FFC.
The thermal capacity, on the other hand, of the external walls of the conventional design type is greater when compared to both of the modular plastic design types, which implies that the block and mortar external walls have a greater capacity to store heat.

From Figure 10.11, only the WPC housing unit meets the requirements of a minimum CR-value of 100 hours, as prescribed in Table 10.11. This is due to a large thermal capacity together with a larger R-value. However, to achieve a CR-value of 100 hours for the FFC housing unit as well as the block and mortar

housing unit, the thickness of the panels of the FFC housing unit as well as the thickness of the brickwork of the block and mortar housing unit should increase to the following:

- For the modular FFC housing unit, a panel thickness of 22mm and an EPS core thickness of 230mm are required.
- For the block and mortar housing unit, brickwork thickness of approximately 340mm without cavities is required.

10.2.3. Roofing assembly (including ceiling and thermal insulation)

The roofing assembly of the modular plastic housing units (Section 6.2) as well as the block and mortar design type need to comply with the requirements stipulated in SANS 204 (2011) paragraph 4.3.6.1.1. These requirements are shown in Table 10.12.

Table 10.12: Table 8 of SANS 204 (2011): Minimum total R-values of roof assemblies

	Climate zone					
	1	2	3	4	5	6
Minimum required total R-value (m^2K/W)	3.7	3.2	2.7	3.7	2.7	3.5
Direction of heat-flow	Up	Up	Down and up	Up	Down	Up

To estimate the energy efficiency of the roof assembly, the total R-value (using Equation 10.9) of the two design types is calculated. According to Harris (2012, p87), h_1 equals $11W/m^2°C$, h_0 equals $20W/m^2°C$ and a_1 is equal to $2.6W/m^2°C$. The total R-value for the roof assembly of the three housing units is shown in Figure 10.12. The calculation for the total R-value for the roof assembly of both the modular plastic housing units and block and mortar housing unit are shown in Appendix H.2, respectively.

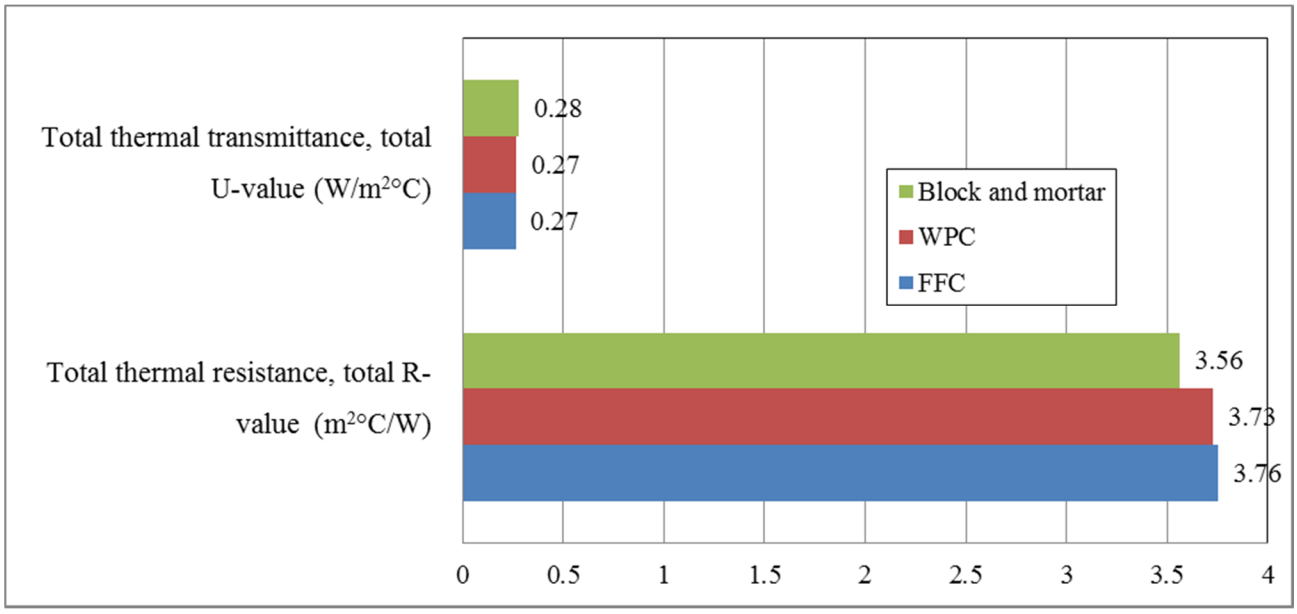

Figure 10.12: The comparison of total R-value, the total U-value for the roof assembly of the modular FFC plastic housing units and block and mortar housing unit

The total R-value of the roof assembly of both the modular plastic houses is greater when compared to that of the block and mortar house, as shown in Figure 10.12. This implies that the roofing of the plastic housing units can resist more heat-flow and that they have better isolative properties compared to the roofing of the block and mortar housing unit. From Figure 10.12, it can be seen that the total R-value of the modular FFC and WPC housing unit is 3.76m^2°C/W and 3.73m^2°C/W respectively. Thus, according to SANS 204 (2011), the modular plastic housing units do meet the requirements of the minimum total R-value for the roof assembly of 3.7m^2°C/W (as shown in Table 10.12). The block and mortar housing unit does not meet this requirements. Insignificant differences are encountered when the U-value of all three housing units is compared. Thus, the amount of energy that passes through the roofing assemblies of these housing units is nearly the same.

10.3. Summary

The environmental impact caused by the pre-use phase of the block and mortar is greater than that of the FFC housing unit and the WPC housing unit. Thus, the modular plastic housing units, especially the FFC housing unit, are more environmentally friendly than the block and mortar housing unit.

From the sensitivity analysis (Section 10.1.5), it is clear that the EII of the FFC and WPC housing unit are not as sensitive to transport distance as the EII of the block and mortar housing unit. By comparing the EII's of the three housing units, only the block and mortar housing unit is sensitive to transport distance. However,

the block and mortar housing unit have a greater negative environmental impact irrespective of the transport distance.

The sensitivity analysis showed that the individual EII's are sensitive to the weighting factors. Therefore, the weighting factors need to be selected carefully. However, the change in weighting factors does not change the ranking of the EII's of the three housing units relative to each other. The weighting factors for EI_2 and EI_3 are factors described for European conditions. These factors should be determined for South Africa, to obtain a more accurate EII. The weighting factor for EI_1 is a global factor and can therefore be applied to South Africa, but is recommended to determine this factor for South African conditions as well.

When the energy efficiency of the housing units is considered, the modular plastic housing units, especially the WPC housing unit, are more energy efficient than the block and mortar housing unit. Thus, in terms of environmental impacts and energy efficiency, the plastic housing units perform better than the block and mortar housing unit.

CHAPTER 11: CONCLUSIONS AND RECOMMENDATIONS

11.1. Conclusions

This study investigated plastic materials as possible alternative building materials to meet the demand for adequate housing in a quicker, yet more sustainable manner. Plastic materials might be a way to address the housing backlog problem in South Africa.

As part of the methodology to reach the aim and the objectives of this study, viable plastic materials needed to be identified. Some properties of unreinforced plastics, which are considered disadvantages of unreinforced plastic materials, can be improved by the addition of a reinforcing agent. Thus, it was found that composite materials exhibit more adequate properties for load bearing applications. Plastic foams were found to be adequate thermal insulators.

For low-income housing, the structure must comply with the requirements of structural stability, but cost efficiency is also important. After investigating various plastic materials for their suitability as structural elements, FFC (foam fibre composite) was considered the most viable, with WPC (wood-plastic composite) as an alternative material. EPS (expanded polystyrene) with a density of 15kg/m^3 was considered the most viable core material.

WPC was used to represent the structural element of the design. It is a homogenous and anisotropic material. After conducting compressive-, tensile-, bending- and creep tests for WPC the following can be concluded:

- The Young's modulus of this material differs for tension and compression loading. The compressive Young's modulus (1.347GPa) is greater than the Young's modulus in tension (0.949GPa), however still relatively small. The compressive yield stress (23.933MPa) of WPC is greater than that of the tensile yield stress (18.152MPa). Thus, the material is stronger, and stiffer in the compression than in tension.
- The bending test performed on WPC resulted in an average deflection to span length ratio of 3.56% which is relatively high. Thus, the material is ductile up until the point of failure.

The average creep strain-time response for 30% of the compressive stress resulted in a displacement of approximately 11mm over the length of the walling system, for a 1000 hour compressive creep test. The

average creep-modulus response proved that the curve stagnates after about 20 hours, after which the modulus remains approximately constant.

Testing conducted on the sandwich panel's materials includes a push-through shear- and bending test. From the combined results of these tests, it can be conclude that the Pekadur A663 polyurethane adhesive is the more suitable adhesive for the specific application for the bond between the WPC and EPS. When the results from the bending tests on the composite beams are compared to that of the WPC beams, it is clear that the EPS causes the composite to fail at significantly lower bending strengths and greater deflections.

A structural building envelope (load-bearing walling, roofing and flooring system) for a low-income housing unit, which addresses the backlog in housing, is determined. The design consists of panels which are assembled on site. The design is shown in Chapter 6. This design results in the erection of housing units at a more rapid pace compared to that of the conventional block and mortar housing unit. The design can accommodate standard services as well as window and door frames, etc. It is a 40m^2 housing unit.

A combination of the most viable plastic materials as well as the building envelope (load-bearing walling, flooring and roofing system) needed to be determined which is structurally stable, cost efficient and environmentally sustainable.

The first objective was to determine the structural feasibility in terms of a numerical analysis, comparison of the fire performance and durability of the viable plastic materials. To validate the design of Chapter 6, a numerical analysis was performed by using the material properties obtained in Chapter 7. From this numerical analysis, the following was found:

- The design described in Chapter 6 is structurally stable.
- The required stiffness of the soil that supports the WPC flooring system is easily achievable in practice.

In terms of the fire performance of FFC, WPC and the block and mortar designs, it was found that the block and mortar design outperformed the plastic materials and met the requirements as stipulated in SANS 10400-T (2011). The fire rating in terms of integrity and insulation was met for all three designs. However, due to the fire rating in terms of stability, the thicknesses of the modular plastic housing units should be increased to meet the requirements. However, fire retardant additives are used in WPC and FFC, which were not included in the calculations of the fire rating. These additives increase the fire rating of the plastic materials. It should be noted that physical testing (SANS 10177-2) of the fire performance would result in a more accurate fire rating estimation.

The minimum norms, according to the Home Building Manual and Agrément, required for an adequate housing unit should be met (Section 2.1.3). According to these requirements, although not mandatory, WPC and FFC do not meet the minimum norms due to their emission of hydrochloride acid (HCl). Thus, these WPC and FFC housing units are not adequate, in terms of emission of harmful gases when burnt. The lamination material should be investigated, to ensure no harmful gas emissions.

In terms of durability of WPC and FFC, degradability has the greatest effect where UV radiation and temperature changes are the most significant contributing factors. When an accelerated weathering test was conducted for WPC over one year, it was found that the degradation layer was less than 0.5mm below the exposed surface (Fabiyi, et al., 2008; Azwa, et al., 2013). Another accelerated weathering test of 2600 hours (equal to over 3 years of natural weathering) resulted in unchanged properties of WPC. Temperature elevation can result in an increase in flexural creep. Temperature dependence of plastic material plays an important role in the mechanical properties of plastics and thus should be tested.

The second objective was to quantify the cost efficiency. A comparative study was conducted between FFC, WPC and a block and mortar housing unit. From this investigation, the following can be concluded:

- The FFC housing unit is a plausible alternative for low-income housing, since this housing unit is only 3% more expensive than the block and mortar housing unit.
- If the transport distance is 50km or more, the FFC housing unit is the most cost efficient option. However, if the transport distance is less than 50km, the block and mortar housing unit is the most cost efficient option.
- The WPC housing unit, on the other hand, is approximately 43% more expensive than the block and mortar design. This housing unit is not the most efficient in terms of cost.
- The material cost of the FFC and WPC is greater than that of the block and mortar design, however the plastic alternatives require no maintenance.
- The modular plastic (FFC as well as WPC) housing units typically utilise unskilled labour to construct a housing unit, whereas the block and mortar alternative requires skilled labour. Furthermore, the socio-economic conditions of a community can be improved by the construction of modular plastic housing units by means of job creation.
- Due to the relative ease of construction and a construction period of approximately three days, the demand for housing can be met at a more rapid pace, depending on the availability of plastic composite materials, than by using the conventional methods. Thus, the modular plastic housing units can provide a possible solution to the backlog in housing, in terms of cost efficiency.

The last objective was determining the environmental feasibility. This was performed in terms of an environmental assessment for the pre-use phase and energy efficiency. In terms of the environmental impact caused by emissions of the pre-use phase, the following can be concluded:

- The modular plastic housing units, especially the FFC housing unit, have less negative environmental impacts than the block and mortar housing unit.
- The environmental impact indices (EII) of the FFC and WPC housing units are not as sensitive to transport distances as that of the block and mortar design.
- EII is sensitive to the weighting factors used and therefore the weighting factors should be selected carefully. However, when a comparative study is done, the change in the values of the weighting factors does not influence the relative EII's.

In terms of the energy efficiency of the housing units, the modular plastic housing units, especially the WPC housing unit, are more energy efficient than the block and mortar housing unit. Thus in terms of environmental impacts and energy efficiency, the plastic housing units perform better than the block and mortar housing unit.

11.2. Recommendations

In terms of the viable materials used for the design in Chapter 6, the following recommendations can be made:

- An extensive study should be conducted to determine the bond strength of various reinforcing agents within the plastic composite as well as the effect of different lubricants and coupling agents to determine an optimum composition.
- Further studies should be done on the use of post-consumer (waste) plastic materials as a main component of plastic composites which can be used as structural elements.
- 15kg/m^3 EPS was used as the core material for the design described in Chapter 6. The effects of recycled EPS should be determined, since it can lead to a more cost- and environmentally efficient material compared to that of the 15kg/m^3 EPS.
- The Pekadur A663 polyurethane adhesive (Adhesive 1) is selected as the most viable adhesive in this study. However, an adhesive with a bond strength as close as possible to that of the EPS, while still lower will result in the best adhesive for this design, since no rupture will occur within the EPS.
- Toxic gases are emitted by PVC, laminating layer of FFC and WPC, when burning. However, the emission of toxic gases can be improved by adding additives to control, and in some cases prevent, smoke production.

For this study, recommendations can be made for the structural, economic and environmental feasibility. In terms of structural feasibility, the following is recommended for further studies:

- The FFC properties should be confirmed with tests. Thereafter, a numerical analysis should be performed to determine the structural stability of the modular FFC housing unit.
- The human behaviour and smoke control during a fire should be investigated, since PVC can emit toxic gasses when burning. Due to this emission of toxic gasses, the housing unit is not adequate. Alternative lamination materials and/or alternative plastic materials should be investigated.
- To accurately determine the durability of WPC and FFC, UV radiation, the main contributing factor, should be tested for the duration of the expected life span of the housing unit. UV resistance can also be determined by accelerated weathering testing, however accuracy of the measurements as well as the extrapolated data cannot be guaranteed.
- Temperature dependent mechanical properties of WPC and FFC should be tested.
- Tensile and flexural creep tests should be conducted with WPC and FFC, since roof sheeting is mainly subjected to flexural creep.
- It should be investigated whether plastic materials can be used for duplex housing units.

In terms of the cost comparison conducted in Chapter 9, the following can be recommended:

- Modular FFC housing units should be constructed for low-income housing in rural areas where the transport distance is more than 50km.
- The composition of FFC and WPC should be optimised in terms of cost, to ensure that the material cost used in the design is as low as possible. This can result in WPC being a plausible structural material for the design described in Chapter 6.
- From an aesthetical point of view, the plastic roof sheeting can be replaced by alternative materials, such as zinc. However, WPC and FFC can be painted to satisfy the aesthetics.

For the environmental feasibility, weighting factors should be determined for South African conditions, to obtain a more accurate EII. It is also recommended that the environmental impact assessment should be extended to include the use- and end-of-life phases.

The use of viable plastic materials, WPC and FFC, as well as the design of the modular housing unit was found to be a viable solution in terms of cost efficiency, environmental sustainability and some cases of structural stability (durability, stability), expect the structural stability in terms of fire and toxic emissions when the burning. However, these excluded aspects could be improved upon.

REFERENCES

Act No. 103, 1977. *National Building Regulation and Standards Act, 1977.* Cape Town: s.n.

Addis, B., 1998. *Fundamentals of concrete.* Midrand: Cement and Concrete Institute.

Agarwal & Gupta, 2011. Plastics in Buildings and Constructions. In: *Applied plastics engineering handbook: processing and materials.* USA: William Andrew Pub, pp. 553-564.

Agrément South Africa, 2009-a. *Imison 3 Building System,* s.l.: Certificate 2008/324.

Agrément South Africa, 2009-b. *Innovida Building System,* s.l.: Mantag Certificate 2009/M55.

Agrément South Africa, 2013. *Agrément South Africa.* [Online] Available at: http://agrement.co.za [Accessed 29 April 2013].

ASTM D5045, 1996. *Standard test method for plan strain fracture and strain energy release rate of plastic materials,* West Conshohocken (USA): ASTM International.

ASTM D5045, 1996. *Standard test method for plane strain fracture and strain energy release rate of plastic materials,* West Conshohocken (USA): ASTM International.

ASTM D6272, 2010. *Standard Test Method for Flexural Properies of Unreinforced and Reinforced Plastics and Electrucak Insulating Materials by Four-point Bending,* West Conshohocken (USA): ASTM International.

ASTM D638, 2010. *Standard Test Method for Tenile Properties of Plastics,* West Conshohocken (USA): ASTM International.

ASTM D695, 2010. *Standard Test Method for Compressive Properties of Rigid Plastics,* West Conshohocken (USA): ASTM International .

Axion, [S.a]. *Axion: Greening tomorrow's infrastructure.* [Online] Available at: http://www.axionintl.com [Accessed 6 May 2013].

Azapagic, A., Perdan, S. & Clift, R., 2004. *Sustainable Development in Practice: Case studies for Engineers and Scientist.* Chichester: John Willey & Sons Ldt.

Azeez, N., 2012. *Seminar Paper: Engineering Seminar Topic.* [Online] Available at: http://www.seminarpaper.com/2012/03/plastic-injection-molding-process.html [Accessed 7 May 2013].

Azwa, Z., Yousif, B., Manalo, A. & Karunasena, W., 2013. A review on the degradability of ploymeric composites based on natural fibres. *Materials and Design,* 47(1), pp. 424-442.

Baker, G., 2002. *Performance of Expanded Polystyrene Insulated Panel Exposed to Radiant Heat,* Christchurch: University of Caterbury (Department of Civil Engineering).

Barito, R. & Eastman, W., 1975. Plastic and Elastomeric Foams. In: *Handbook of Plastics and Elastomers.* New York: McGraw-Hill, Inc, pp. 7.1-7.79.

Beam, R., 1990. Polyethylene, High density HDPE. In: I. Rubin, ed. *Handbook of Plastic Materials and Technology.* New York: John Wiley and Sones, Inc, pp. 339-348.

Benjamin, B., 1969. *Structural Design with Plastics.* Canada: Van Nostrand Reinhold Company.

Bibee, D., 1990. Polythylene, LDPE. In: I. Rubin, ed. *Handbook of Plastic Materials and Technology.* New York: John Wiley and Sones, Inc, pp. 317-327.

Birley, A., Heath, R. & Scott, M., 1988. *Plastics Materials: Properties and Applications.* Second ed. New York: Blackie & Son Ldt.

Birley, A. & Scott, M., 1982. *Plastics Materials: Properties and Applications.* First ed. Glasgow: Leonard Hill.

Bon, E., 2003. *Structural Opportunities for Glass,* Massachusetts: Massachusetts Institute of Technology.

Braun, D., 1999. *Simple Methods for Identification of Plastics.* Canada: Hanser Publishers.

Breslin, V., Senturk, U. & Berndt, C., 1998. Long-term engineering properties of recycled plastic lumber used in pier construction. *Resources, Conservation and Recycling,* 23(4), pp. 243--258.

Brewis, C., 2011. *Quantifing the environmental dimension of sustainability for the built environment: with a focus on low-cost housing in South Africa,* Stellenbosch: University of Stellenbosch: Unpublished master's thesis.

Brits, J., 2011. *Quantifying the sustainability of the built environment: Model for the determination of the environmental impact of the end-of-life phase,* University of Stellenbosch: Unpublished master's thesis.

Brown, W., 1990. Polystrene. In: I. Rubin, ed. *Handbook of Platic Materials and Technology.* New York: Wiley and Sons, Inc, pp. 459-486.

Buchanan, A., 2002. *Structural Design for Fire Safety.* First ed. England: John Wiley & Sons.

Cantor, K. & Watts , P., 2011. Plastic Materials. In: *Applied Plastics Engineering Handbook: Processing and Materials.* USA: Elsevier Inc, pp. 3-5.

Chanda, M. & Roy, S., 2012. *Plastic technology handbook.* s.l.:CRC press.

Chau, V., Bunge, F. & Hood, L., 2011. Advances in Thermal Insulation of Extruded Polystyrene Foams. *Cellular Polymers,* 30(3), pp. 137-154.

Clark, S., 1982. Release Agents. In: *Handbook of Composite.* New York: Van Nostrand Reinhold, pp. 633-638.

Craig, R., 2000. *Mechanics of Materials.* Second ed. United States of America: John Wiley & Sons.

Craig, R., 2004. *Craig's Soil Mechanics.* Seventh edition ed. London: Spon Press.

Crawford, R., 1981. *Plastic Engineering.* Volume 7 ed. Oxford: Oxford Pergamon.

Damm, P. & Matthies, P., 1990. Nylons. In: I. Rubin, ed. *Handbook of Plastic Materials and Technology.* New York: John Wiley and Sons, Inc, pp. 161-180.

Dastin, S., 1982. Joining and Machining Techniques. In: *Handbook of Composites.* New York: Van Nostrand Reinhold Company Inc., pp. 602-632.

Davies, J., 2008. *Lightweight sandwich construction.* s.l.:John Wiley & Sons..

de Villiers, W., 2012. *Building Capacity for Sustainable Delivery: Regulation of Alternative Building Materials and Systems in South Africa.* Cape Town, s.n.

Defoirdt, N., Gardin, S., van den Bulcke, J. & van Acker, J., 2010. Moisture dynamics of WPC and the impact on fungal testin. *International Biodeterioration and Biodegradation,* Volume 64, pp. 65-72.

Department of Human Settlements, 2012. *Annual Report 2011/2012,* South Africa: Department of Human Settlements.

Domone, P. & Illston, J., 2001. *Construction Materials: Their nature and behaviour.* Third ed. New York: Spon Press.

Drysdale, D., 1998. *An Introduction to Fire Dynamics.* Second ed. Engeland: John Willey & Sons.

Ecoinvent, 2013. *Ecoinvent Database, Data version 3.* [Online] Available at: http://www.ecoinvent.org [Accessed July to September 2013].

EN 1991-1-2, 2002. *Eurocode 1: Actions on structures: Part 1-2: General actions-actions on structures exposed to fire,* London: BSI.

Engelhardt, P. M., 2012. *Introduction to Structural Fire Engineering.* Stellenbosch, University of Stellenbosch.

Epstein, G., 1982. Testing of Reinforced Plastics. In: *Handbook of Composites.* New York: Van Nostrand Reinhold Company Inc., pp. 639-664.

Ertebjerg, G., Andersen, J. & Hansen., O., 2003. *Nutrients and Eutrophication in Danish Marine Waters: A Challenge for Science and Managemen.* Denmark: National Environmental Research Institute.

Eva-Last, [S.a]. *Eva-Last: Composite Decking Solutions.* [Online] Available at: http://www.eva-last.co.za [Accessed 29 May 2013].

Fabiyi, J., McDonald, A., Wolcott, M. & Griffiths, P., 2008. Wood plastic composites weathering: Visual apperrance and chemical changes. *Polymer Degradation and Stability,* 93(1), pp. 1405-1414.

Fang, Y. et al., 2013. Effect of zinc borate and wood flour on thermal digradation and fire retardancy of Polyvinyl chloride (PVC) composites. *Journal of Analytical and Applied Pyrolysis,* Volume 100, pp. 230-236.

Fenner, O., 1975. Chemical and Environmental Properties of Plastics and Elastomers. In: C. Harper, ed. *Handbook of Plastics and Elastomers.* New York: McGraw-Hill, Inc, pp. 4.1 - 4.4.

Findley, W. & Davis, F., 2013. *Creep and Relaxation of Nonlinear Viscoelastic Materials.* USA: Courier Dover Publications.

Fisher, B., 2013. *4Everdeck* [Interview] (27 May 2013).

Fisher, G., 2013. *ECOWOOD* [Interview] (3 June 2013).

Friul Filiere Spa, [S.a]. *FFC: Foam Fibre Composite.* [Online] Available at: www.ffcmaterial.com [Accessed 2 May 2013].

Gan, C. & Tan, S., 2003. *Some constuction experience on soft soil using light weigth materials.* Malaysie, Second International conference on Advances in Soft Soil Engineering.

Gannon, J. & Brytus, V., 1990. Reinforced plastics, Epoxy resins. In: I. Rubin, ed. *Handbook of Plastic Materials and Technology.* Canada: Wiley and Sons, Inc, pp. 829-816.

Garcia, M., Hidalgo, J., Garmendia, I. & Garcia-Jaca, J., 2009. Wood-plastic composites with better fire retardancy and durability performance. *Composites: Part A,* 40(1), pp. 1772-1776.

Gobstein, S., 1990. Poly(vinyl chloride), rigid RPVC. In: I. Rubin, ed. *Handbook of Plastic Materials and Technology.* Canada: Wiley and Sons, Inc, pp. 549-566.

Goedkoop, M., Oele, M., de Schryver, A. & Vieira, M., 2007. *SimaPro Database Maual.* , Netherlands: Pre Consultants.

Gordon, M., 1965. Thermal Properties of High Polymers. In: P. Ritchie, ed. *Physics of plastics.* London: The Plastic Institute, pp. 209-247.

Grelle, P., 2006. Injection Molding. In: C. Harper, ed. *Handbook of Plastic Processes.* New Jersey: John Wiley & Sons, Inc., pp. 1-125.

Hanna, R., 1990. Polypropylene. In: I. Rubin, ed. *Handbook of Platic Materials and Technology.* Canada: Wiley and Sons, Inc, pp. 433-458.

Hanson, D., 2006. Sheet Extrusion. In: C. Harper, ed. *Handbook of Plastic Processes.* New Jesey: John Wiley & Sons, inc., pp. 189-290.

Harper, C., 1975. *Handbook of Plastics and Elastomers.* United States of America: McGraw-Hill .

Harris, H., 2012. *Handbook for the application of the amendments to the National Building Regulations for energy usage.* 2012 Edition ed. Cape Town: Trademax Publications.

Hauschild, M. & Wenzel, H., 1998. *Environmental Assessment of Products: Volume 2:Scientific background.* First ed. London: Chapman & Hall.

Hiatt, G. & Winding, C., 1961. *Polymeric Materials.* New York: McGraw-Hill Book Company.

Hollaway, L., 1990. *Polymers and Polymer Composites in Construction.* London: Amer Society of Civil Engineers.

Horvath, J., 1994. Expanded polystyrene (EPS) geofoam: an introduction to material behavior. *Geotextiles and Geomembranes,* 13(4), pp. 263--280.

Hull, J., 2006. Compression and Transfer Molding. In: C. Harper, ed. *Handbook of Plastic Processes.* New Jersey: John Wiley & Sons, Inc., pp. 455-474.

Hulse, G., 1965. Other Mechanical Properties of High Polymers. In: P. Ritchie, ed. *Physics of Plastics.* New Jersey: D. van Nostrand Company, Inc, pp. 163 -185.

ISO 14040, 2006. *Environmental Management: Life cycle assessment: Principles and framework,* Switzerland: International Standards Organisation.

Jia, M., Xue, P., Zhao, Y. & Wang, K., 2008. Creep Behaviour of Wood Flour/ Poly(vinyl chloride) Composites. *Journal of Wuhan University of Technology- Master of Science Edition,* 24(3), pp. 440-447.

Jiang, H. & Kamdem, P., 2004. Development of Poly(vinyl chloride)/ Wood Composites: A literature review. *Journal of vinyl and additive technology,* Volume 1, pp. 59-69.

Kinney, G., 1967. *Engineering Properties and Applications of Plastics.* United States of America: John Wiley & Sons, inc.

Klyosov, A., 2007. *Wood- Plastic Composite.* USA: John Wiley & Sons, Inc.

Knox, C., 1982. Fibreglass reinforcement. In: *Handbook of Composites.* New York: Van Nostrand Reinhold Company Inc., pp. 136-160.

le Roux, A., 2013. *Brick and mortar cost* [Interview] (12 August 2013).

Lee, A. et al., 2006. Affordable, safe housing based on expanded polystyrene (EPS) foam and a cementitious coating. *Journal of Materials Science,* 41(21), pp. 6908-6916.

Lennon, T., 2011. *Structural Fire Engineering.* First ed. USA: ICE .

Leu, S., Yang, T., Lo, S. & Yang, T., 2012. Optimized material composition to improve the physical and mechanical properties of extruded wood-plastic composite (WPC). *Construction and Building Materials,* 29(1), pp. 120-127.

Lubin, G., 1982. *Handbook of Composites.* New York: Van Nostrand Reinhold Company.

MacDonald, S., 2006. Thermoforming. In: C. Harper, ed. *Handbook of Plastic Processes.* New Jersey: John Wiley & Sons, Inc., pp. 291-304.

Manalo, A., 2013. Structural behaviour of a prefabricated composite wall system made from rigid polyurethane foam and Magnesium Oxide board. *Construction and Building Materials,* 41(1), pp. 642-653.

Marais, L. & Ntema, J., 2013. The upgrading of an informal settlement in South Africa: Two decades onwards. *Habitat International,* 39(1), pp. 85-95.

Marshall, A., 1982. Sandwich Construction. In: *Handbook of Composites.* New York: Van Nostrand Reinhold Company Inc., pp. 557-601.

Matuana, L. & Kamdem, D., 2002. Accelerated Ultraviolet Weathering of PVC/Wood-flour Composites. *Polymer Engineering and Science,* 42(8), pp. 1657-1666.

McFarlane, F., 1990. Thermoplastic Polyester (PET). In: I. Rubin, ed. *Handbook of Plastic Materials and Technology.* New York: Wiley and Sons, Inc, pp. 639-648.

Mikulenok, I., 2012. Determining the thermophysical properties of thermoplastic composite materials. *International Polymer Science and Technologu,* 40(2), pp. 9-13.

Moladi, [S.a]. *Moladi: Building communities.* [Online] Available at: http://moladi.net [Accessed 29 April 2013].

Montgonmery, D. & Runger, G., 2007. *Applied Statistics and Probability for Engineers.* Fourth ed. USA: John Wiley & Sons, Inc..

Morrel, J., Stark, N., Pendleton, D. & McDonald, A., 2010. *Durability of wood-plastic composites: Tenth Interlational Conference on wood and biofibre plastic composites and cellulose nanocomposites Symposium.* Madison, Forest Products Society.

Mouritz, A. et al., 2009. Review of fire structural modelling of polymer composites. *Composites: Part A,* Volume 40, pp. 1800-1814.

Müller, M., Militz, H. & Krause, A., 2012. Thermal degradation of ethonalmine treated poly(vinyl cloride)/wood flour composites. *Polymer Degradation and Stability,* Volume 97, pp. 166-169.

Murphy, J., 1998. *The Reinforced Plastics Handbook.* UK: Elsevier Science Publishers ltd..

New Housing Policy and Strategy for South Africa, 1994. *White Paper,* South Africa: s.n.

NHBRC, 1999. *Home Building Manual Part 1 & 2, Revision 1.* South Africa: s.n.

Ogorkiewicz, R., 1970. *Engineering Properties of Thermoplastics.* England: Imperical Chemical Industries, Plastics Division.

Ogorkiewicz, R., 1977. *The Engineering Properties of Plastics.* Hampshire: Oxford University Press for the Design Council, the British Standards Institution, and the Council of Engineering Institutions.

Olukoya, S., 2011. *Nigeria's plastic bottle house.* [Online] Available at: http://www.bbc.co.za/news/world-africa-14722179 [Accessed 29 May 2013].

Onyon, P., 1965. Introduction. In: P. Ritchie, ed. *Physics of Plastics.* London: The Plastics Institute, pp. 1-23.

Pachauri, R. & Reisinger, A., 2007. *Climate Change 2007: Synthesis Report. Contribution of Working GroupsI,II and III to the Fourth Assessment Report of the Intergovernmental Panel on Climate Change,* IPCC: Geneva.

Pacheco-Torgal, F., Jalali, S. & Fucic, A., 2012. *Toxicity of building materials.* s.l.:Elsevier.

Palin, G., 1967. *Plastics for Engineers: An Introductory Course.* Oxford: Pergamin Press.

Petrie, E., 1975. Plastic and Elastomers as Adhesives. In: *Handbook of Plastics and Elastomers.* USA: McGraw - Hill , Inc., pp. 10.1 -10.134.

Pilarski, J. & Matuana, L., 2005. Durability of Wood Flour-Plastic Composites Exposed to Accelerated Freeze-Thaw Cycling: Rigid PVC Matrix. *Journal of Vinyl & Additive Technology,* Volume 1, pp. 1-8.

Pillichody, C. & Kelley , P., 1990. Acrylonitrile-Butadiene-Styrene (ABS). In: I. Rubin, ed. *Handbook of Plastic Materials and Technology.* Canada: John Wiley and Sones, Inc, pp. 25-43.

Purkiss, J., 2007. *Fire Safety Engineering Design of Structures.* Second ed. United Kingdom: Elsevier.

Rachel, 2013. *ISOLITE CAPE (PTY) LTD (Email)* [Interview] (17 September 2013).

Richardson, M., 1977. *Polymer Engineering Composites.* London: Applied Science Publishers Ltd.

Riddell, M. & O'Toole, J., 1969. Significant Properties of Plastics for Design. In: McCormick, ed. *Structural Plastics Properties and Possibilities.* Kentucky: s.n., pp. 37-40.

Rosato, D., 1982. An Overview of Composites. In: *Handbook of Composites.* New York: Van Nostrand Reinhold Company Inc., pp. 1-19.

Rosato, D., 1997. *Plastics Processing Data Handbook.* Second Edition ed. New York: Chapman & Hall.

Rosato, D. & Rosato, D., 2004. *Reinforced Plastics Handbook.* Third Edition ed. USA: Elsevier.

Rossouw, J., Harding, W. & Fatoki, O., 2008. *A Guide to Catchment-Scale Eutrophication Assessment for Rivers, Reservoirs and Lacustrine Wetlands,* South Africa: WRC Report No TT 352/08.

Rubin, I., 1990. *Handbook of Plastic Materials and Technology.* New York: John Wiley & Sons, Inc.

Rudd, B. & Sampson, P., 1975. Mechanical Properties and Testing of Plastics and Elastomers. In: C. Harper, ed. *Handbook of Plastics and Elastomers.* New York: McGraw-Hill Book Company, pp. 3-8.

Sain, M., Balatinecz, J. & Law, S., 2000. Creep Fatigue in Engineered Woof Fibre and Plastic Composition. *Journal of Applied Polymers,* Volume 77, pp. 260-268.

Sampson, R., 1975. Laminated, Reinforced Plastic and Composites. In: *Handbook of Plastics and Elastomers.* New York: McGraw- Hill, Inc., pp. 5.1- 5.111.

SANS 10160-1, 2011. *Basis of structural design and actions for buildings and industrial structures: Part 1: Basis of structural design,* Pretoria: SABS Standard Division.

SANS 10160-2, 2011. *Basis of structural design and actions for buildings and industrial structures: Part 2: Self-weight and imposed loads,* Pretoria: SABS Standard Division.

SANS 10160-3, 2011. *Basis of structural design and actions for buildings and industrial structures: : Part 3: Wind actions,* Pretoria: SABS Standard Division.

SANS 10400-A, 2010. *Application of National Building Regulations: PART A: General principles and requirements,* Pretoria: SABS Standard Division.

SANS 10400-L, 2011. *The application of the National Building Regulations: Part L: Roofs,* Pretoria: SABS Standards Division.

SANS 10400-T, 2011. *The application of the National Building Regulations: Part T: Fire protection,* Pretoria: SABS Standards Division.

SANS 10400-XA, 2011. *The application of the National Building: Part XA: Energy usage in buildings,* Pretoria: SABS Standard Division.

SANS 204, 2011. *Energy efficiency in buildings,* Pretoria: SABS Standard Division.

SANS 5863, 2006. *Concrete tests: Compressive strength of hardened concrete.* 2.1 ed. Pretoria: Standards of South Africa.

SASFA, [S.a]. *South African Light Steel Frame Building Association.* [Online] Available at: http://www.sasfa.co.za [Accessed 29 April 2013].

Sexwhale, T., 2010. *Innovators urged with alternative building technology (Home page of the Department of Human Settlements).* [Online] Available at: http://www.info.gov.za/speech/DynamicAction [Accessed 7 November 2012].

Sham Prasad, M., Venkatesha, C. & Jayaraju, T., 2011. Experimental Methods of Determining Fracture Toughness of Fiber Reinforced Polymer Composites under various loading conditions. *Journal of Minerals and Materials Characterization and Engineering,* 10(13), pp. 1263-1275.

Shibley, A., 1982. Glass-filled Thermoplastics. In: *Handbook of Composites.* New York: Van Nostrand Reinhold Company Inc., pp. 115-136.

Simonsen, J., Freitag, C., Silva, A. & Morrell, J., 2004. Wood/plastic ratio: Effect on performance of borate biocides against a brown rot fungus. *Holzforschung,* Volume 58, pp. 205-208.

South African Yearbook, 2012. *Human Settlements, South Africa Yearbook,* South Africa: Department of Human Settlements.

Southern Africa Steel Construction, 2010. *The Red Book.* Seven ed. Johannesburg: Southern Africa Steel Construction.

Sperati, C., 1990. Fluoropolymers. In: I. Rubin, ed. *Handbook of Plastic Materials and Technology.* New York: Wiley and Sons, Inc, pp. 101-136.

Stark, N. & Rowlands, R., 2003. Effects of wood fibre characteristics on mechanical properties of wood/polypropylene composites. *Wood and Fibre Science,* 35(2), pp. 167-174.

Staunton, R., 1982. Environmental Effects on Properties of Composites. In: *Handbook of COmposites.* New York: Van Nostrand Reinhold Company, Inc., pp. 513-532.

Stec, A. & Hull, T., 2011. Assessment of the fire toxicity of building inslation materials. *Energy and Buildings,* 43(2-3), pp. 498-506.

Stewart, R., 2010. Building on the advantages of composites in construction. *Reinforced Plastics,* 54(5), pp. 20-27.

Stranddorf, H., Hoffman, L. & Schmidt, A., 2005. *Impact categories, normalisation and weighting in LCA,* Danish ministry of the environment: Environmental news No. 78.

Tangent, 2009. *Tangent Technologies, LLC.* [Online] Available at: http://www.tangentusa.com [Accessed 29 May 2013].

Technical report No 34, 2003. *Concrete Industrial Ground Floors.* Third ed. UK: The Concrete Society.

Tech-Wood, [S.a]. *Tech-Wood: Wood that Never Rots.* [Online] Available at: http://www.techwood-cladding.com [Accessed 1 May 2013].

Tesser, L. & Scotta, R., 2012. Flexural and shear capacity of composite steel truss and concrete structure with inferior precast concrete base. *Engineering Structures,* Volume 49, pp. 135-145.

Tonkin, A., 2008. *Sustainable medium density housing: A resource book.* Cape Town: Development Action Group (GAP).

United Nations, 2010. *Millennium Development Goals,* South Africa: United Nations Development Programme.

Verhey, S., Laks, P. & Richter, D., 2001. Laboratory decay resistance of woodfibre/thermoplastic composites. *Forestry Products Society,* 51(9), pp. 44-49.

Vertech, [S.a]. *Vertech: Infinite uses without compromise.* [Online] Available at: http://vertechcomposites.co.uk [Accessed 1 May 2013].

Vo, C., Bunge, F., Duffy, J. & Hood, L., 2011. Advances in Thermal Insulation of Extruded Polystyrene Foams. *Cellular Polymers,* 30(3), pp. 137-155.

Warby, M. et al., 2003. Finite element simulation of thermoforming processes for polymer sheets. *Mathematics and Computers in Simulation,* 61(3), pp. 209-218.

Young, P., 1982. Thermoset Matched Die Molding. In: *Handbook of Composites.* New York: Van Nostrand Reinhold Company, Inc, pp. 390-447.

APPENDIX A: PLASTIC PROPERTIES

Table A. 1: Mechanical properties of unreinforced plastics

Materials	Abbreviation	Specific gravity	Average Tensile Yield Strength	Average Young's Modulus	Average Compressive Strength	Average Flexure Strength	Average elonagation at rupture	Average Impact Resistance Strength
		Average	MPa	GPa	MPa	MPa	%	J/m
Thermoplastics								
Acrylonitrile butadiene styrene	ABS	1.07	40	2.3	50	67	77	289
High density Polyethylene	HDPE	0.95	28	0.9	19	17	700	91
Low density Polyethylene	LDPE	0.93	12	0.2	-	(4)	380	(7)
Nylon 6.6	Nylon 6.6	1.13	90	2.9	91	84	40	59
Nylon 6	Nylon 6	1.14	81	2.3	81	75	83	53
Polycarbonates	PC	1.21	61	2.3	83	88	110	406
Polyester	PET	1.40	124	3.1	80	99	7	27
Polyethylene	PE	0.94	17	0.5	17 (2)	41	400	53
Polypropylene	PP	0.89	34	1.3	55	48	500	32
Polystyrene	PS	1.07	85	3.4	95	78	2	14
Polytetrafluoroethylene	PTFE	2.18	24	0.4	11	(4)	95	200
Polytrifluorochloroethylene	PTFCE	2.12	41	1.5	379	58	100	240
Polyvinyl chloride	PVC	1.69	42	0.5	16	36	25	36
PVC (rigid)	PVC (rigid)	1.40	50	3	64	90	10	373
Thermosets								
Epoxy	EP	1.26	59	3.2	153	103	5	32
Melamine formaldehyde	MF	1.50	69	9	221	90	0.7	16
Phenol formaldehyde	PH	1.30	49	6	155	93	1	13
Polyester(unsaturated)	UP	1.28	54	4.4	163	86	5	14
Other building materials								
Aluminium	Aluminium	2.80	275	73	275	103	17	1065
Concrete	Concrete	2.25	(1)	30	30 (3)	4,5 (5)	(6)	-
Glass	Glass	2.60	7000	60	600	0.7	(6)	-
Steel (S355JR)	Steel (S355JR)	7.85	355	200	355	340	20	-
Wood	Wood	0.68	24	12	37	57	60	-

Note:

(1) Concrete are for loading in compression only
(2) PE do not rupture; only compression yield strength (no ultimate strength)
(3) Depending on the cement-water-ratio and time dependent (7days after casting)
(4) No rupture
(5) Usaually bewteen 10-20% of compresive strength
(6) Insignificant elongation at rupture
(7) No rupture, thus though material

Table A. 2: Thermal properties of unreinforced plastics

Materials	Abbreviation	Specific heat	Thermal conductivity	Average Coefficient of thermal expansion
		J/kg°C	W/m°C	/°C x 10^{-6}
Thermoplastics				
Acrylonitrile butadiene styrene	ABS	1546.6	0.17	95
High density Polyethylene	HDPE	2382.6	0.49	135
Low density Polyethylene	LDPE	2299	0.29	190
Polyamide (Nylon 6.6)	Nylon 6.6	1672	0.25	103
Polyamide (Nylon 6)	Nylon 6	1672	0.29	100
Polycarbonates	PC	1212.2	0.22	66
Polyester	PET	2340.8	0.2	60
Polyethylene	PE	2299	0.4	180
Polypropylene	PP	2048.2	0.17	110
Polystyrene	PS	1337.6	0.15	125
Polytetrafluoroethylene	PTFE	1045	0.25	101
Polytrifluorochloroethylene	PTFCE	919.6	0.17	54
Polyvinyl chloride	PVC	1337.6	0.13	190
PVC (rigid)	PVC (rigid)	1254	0.15	38
Thermosets				
Epoxy	EP	1672	0.19	70
Melamine formaldehyde	MF	1672	0.28	43
Phenol formaldehyde	PH	1672	0.19	49
Polyester(unsaturated)	UP	1254	0.18	123
Other building materials				
Aluminium	Aluminium	877.8	217.57	22
Concrete	Concrete	877.8	1.1	10
Glass	Glass	794.2	0.04	8
Steel (S355JR)	Steel (S355JR)	480	50	12
Wood	Wood	2382.6	0.17	10.6

Table A. 3: Thermal properties of plastic composites and plastic foams

	Abbreviation	Thermal conductivity	Average Coefficient of thermal expansion	Heat distortion temperature
		W/m°C	/°C x 10^{-6}	°C
Plastics				
Thermoplastics		0.24	110.5	98.6
Thermosets		0.21	71.3	164.5
Glass fibre reinforced plastic	GFRP	1.4	26.8	190.5
Foam fibre composite	FFC	0.13	100	65
Wood-plastic composite	WPC	0.15	101	100.6
Plastic Foams		0.03	73	90
Other building materials				
Aluminium	Aluminium	217.57	22	
Concrete	Concrete	1.1	10	
Glass	Glass	0.04	8	
Steel (S355JR)	Steel (S355JR)	50	12	
Wood	Wood	0.17	10.6	

Table A. 4: Mechanical properties of plastic composites and plastic foams

Materials	Abbreviation	Specific gravity	Average Tensile Yield Strength	Average Young's Modulus	Average Compressive Strength	Average Flexure Strength	Average elongation at rupture	Water absorption
		Average	MPa	GPa	MPa	MPa	%	%
Plastics								
Thermoplastics		1.29	52	1.8	85.3	65	181	0.1
Thermosets		1.33	58	5.7	173	93	3	0.3
Glass fibre reinforced plastic	GFRP	1.50	163.4	9.7	170.3	225.7	3.87	0.4
Foam fibre composite	FFC	0.70	15	(2)	15	35	9.5	0.8
Wood-plastic composite	WPC	1.30	14.2	2.9	31.3	30.7	1.4	0.8
Plastic Foams		0.03	0.13	3.3	0.43	0.18		0.2
Other building materials								
Aluminium	Aluminium	2.80	275	73	275	103	17	
Concrete	Concrete	2.25	(1)	30	30 (3)	4.5 (5)	(6)	
Glass	Glass	2.60	7000	60	600	0.7	(6)	
Steel (S355JR)	Steel (S355JR)	7.85	355	200	355	340	20	
Wood	Wood	0.68	24	12	37	57	60	

Note:

(1) Concrete are for loading in compression only
(2) Unknown
(3) Depending on the cement-water-ratio and time dependent (7days after casting)
(4) No rupture
(5) Usually between 10-20% of compressive strength
(6) Insignificant elongation at rupture
(7) No rupture, thus though material

APPENDIX B: COST ESTIMATIONS FOR VIABLE MATERIALS

FFC			
Panel [mm] (b,h,w) :	1220	2700	11
Density =	700 kg/m^3		
Price of material =	1.3 euro/kg		
Euro to rand	R 12.85 /euro		
Price :	**R 128.63 /m^2**		
ECOWOOD			
Panel [mm] (b,h,w) :	1220	2700	11
Size of decking plank[mm] (b, h,w):	110	4000	22
Price of plank=	R 214.91		
Price :	**R 244.22 /m2**		
4EVERDECK			
Panel [mm] (b,h,w) :	1220	2700	11
Price of material=	R 633.00 /m^2		
Plank thickness =	25 mm		
Price :	**R 278.52 /m^2**		
EVERJADE			
Panel [mm] (b,h,w) :	1220	2700	11
Size of decking plank[mm] (b, h,w):	140	5500	23
Price of material=	29 USD/m^2		
USD to rand	R 9.88 /USD		
Price :	**R 137.03 /m^2**		
EVA-LAST			
Panel (mm) (b,h,w) :	1220	2700	11
Panel volume =	0.036234 m^3		
Size of decking plank (mm)	146	5800	24
Price of plank=	R 515.75 /plank		
Price :	**R 279.15 /m^2**		

Glassfibre reinforce plastic										
	UP 30% GF	EP 80%GF	Nylon 6.6 30%GF	Nylon 6 30%GF	PET 30%GF	PC 10% GF	PP 40% GF	ABS 20% GF
Panel (mm) (b,h,w) : 1220 2700 1								
Panel volume = 0.003294 m^3								
Density of glassfibre= 1400 kg/m^3								
%volume glassfibre :	30.000	80.000	30.000	30.000	30.000	10.000	40.000	20.000
Volume glassfibre per panel (m^3) :	0.001	0.003	0.001	0.001	0.001	0.000	0.001	0.001
Weight of glassfibre required (kg):	1.383	3.689	1.383	1.383	1.383	0.461	1.845	0.922
bags required of 1.6kg?	0.865	2.306	0.865	0.865	0.865	0.288	1.153	0.576
Price per 1.6kg bag = R 220								
Require 5l of resin per 1.6kg bag								
Glassfibre resin per 1l = R 140								
Total price of glassfibre -=	795.50	2121.34	795.50	795.50	795.50	265.17	1060.67	530.33
Density of plastic material (kg/m^3)=	1280.00	1260.00	1130.00	1140.00	1400.00	1210.00	890.00	1070.00
Volume plastic per panel (m^3) : ($x\ 10^{-3}$)	2.306	0.659	2.306	2.306	2.306	2.965	1.976	2.635
Weight of plastic required (kg):	2.951	0.830	2.606	2.629	3.228	3.587	1.759	2.820
Price of plastic (R/kg) _estimation	143.40	143.40	336.12	336.12	304.75	336.12	94.11	125.48
Total Price of plastic =	423.23	119.03	875.78	883.53	983.77	1205.72	165.54	353.81
TOTAL PRICE OF PANEL =	1218.74	2240.37	1671.28	1679.03	1779.27	1470.89	1226.21	884.15
Price (R/m2) :	**369.99**	**680.14**	**507.37**	**509.72**	**540.16**	**446.53**	**372.25**	**268.41**

Abbreviation	Material
ABS	Acrylonitrile butadiene styrene
UP	Polyester (unsateurated)
PP	Polypropolene
PC	Polycarbonates
PET	Polyester (thermoplastic)
EP	Epoxy
GF	Glass fibre

APPENDIX C: CONCEPT DESIGN OF MODULAR PLASTIC HOUSING UNIT AND CONVENTIONAL DESIGN HOUSING UNIT

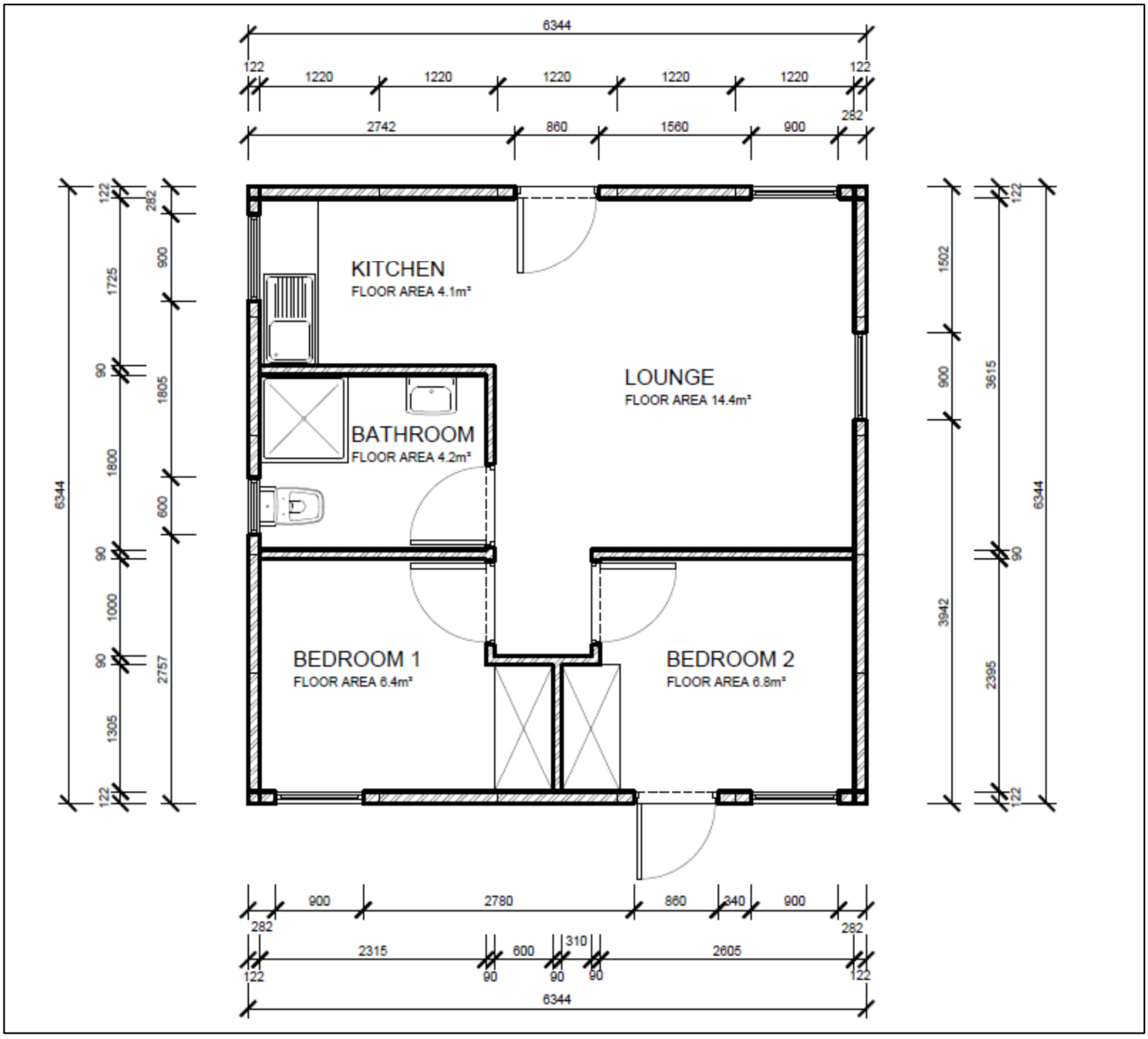

Figure C.1: Plan view of low-income modular plastic housing unit

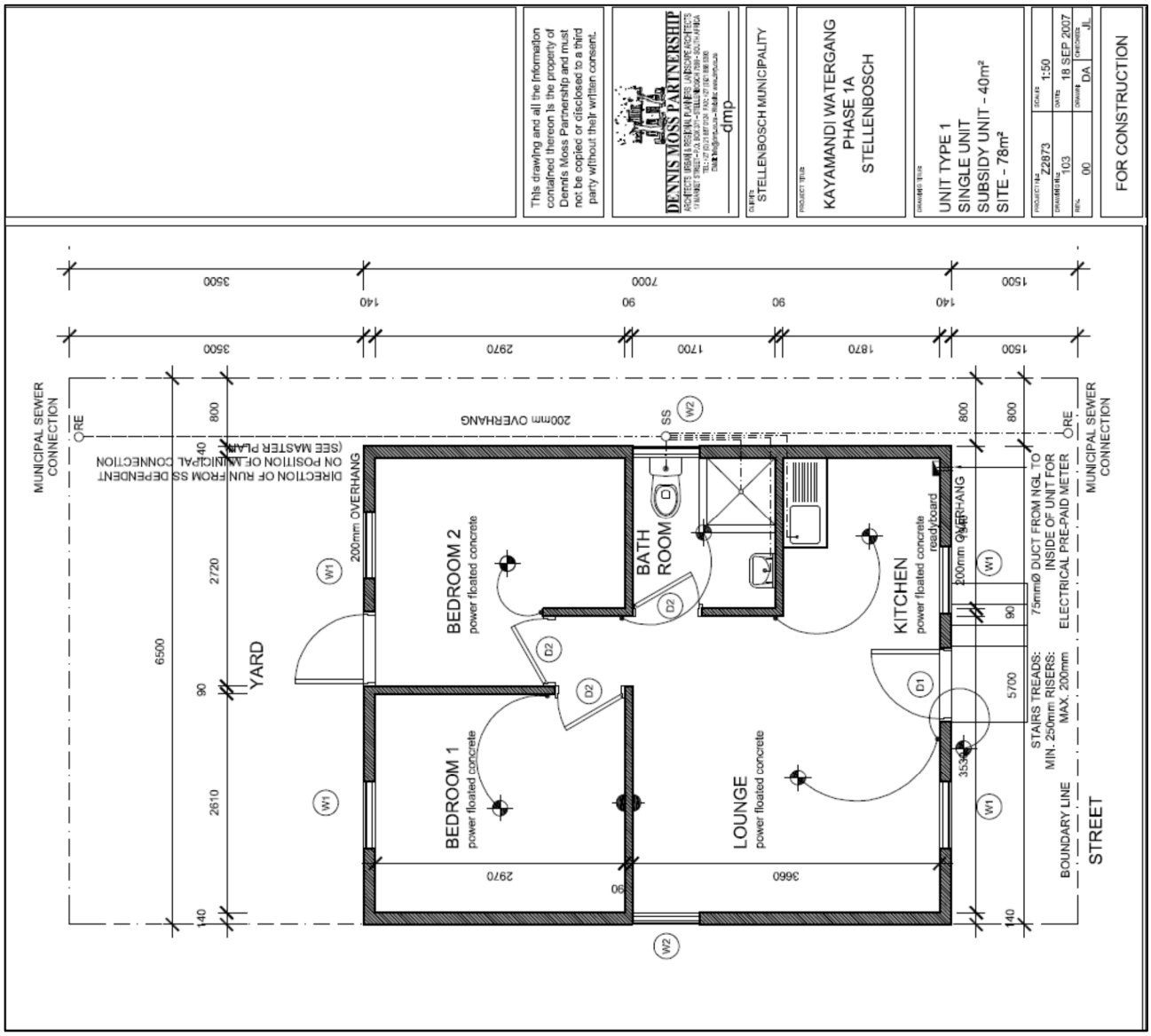

Figure C.2: Plan view of conventional block and mortar housing unit (Brewis, 2011)

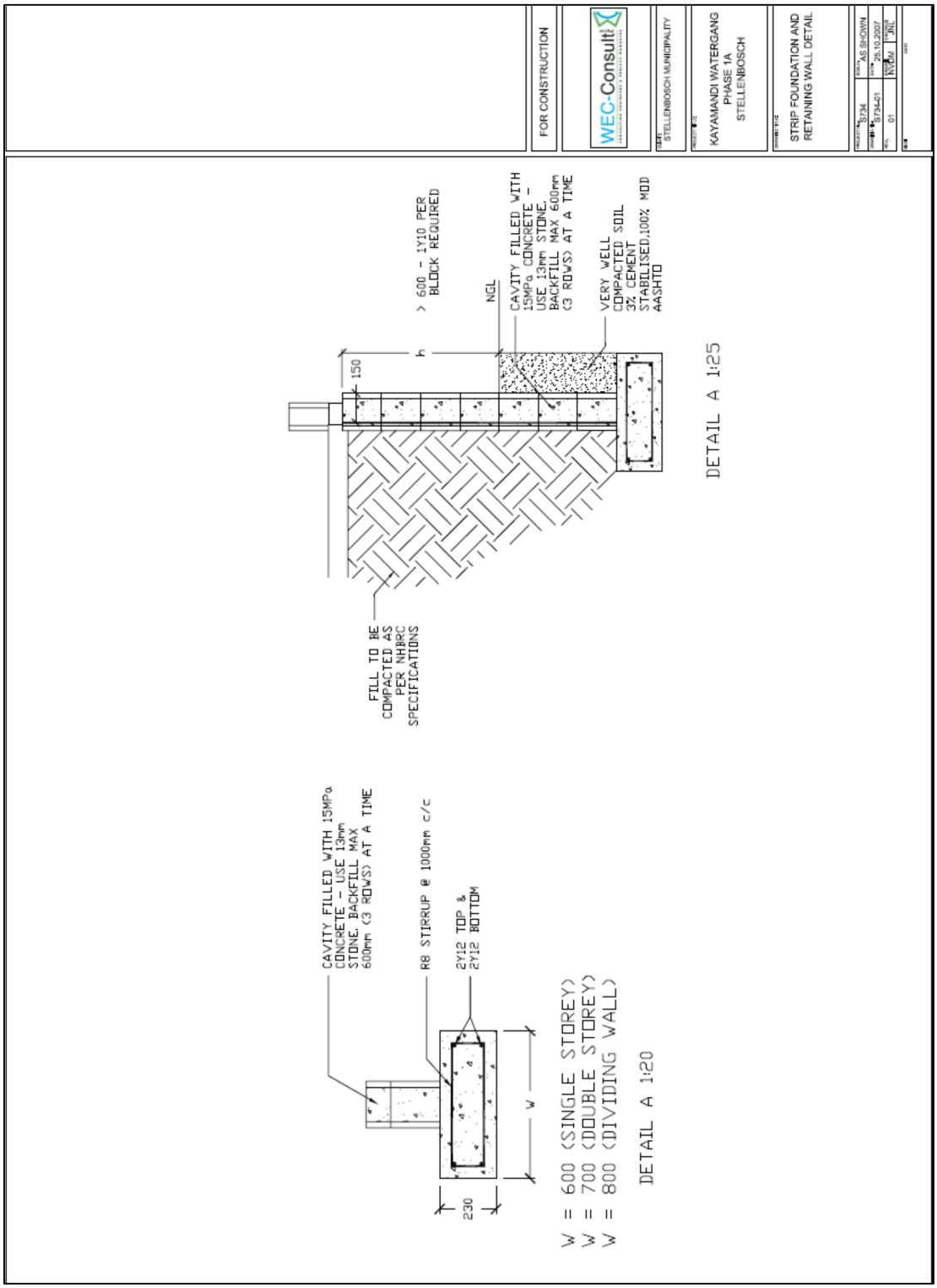

Figure C.3: Detailed foundation drawings of the conventional block and mortar housing unit (Brewis, 2011)

APPENDIX D: EXPERIMENTAL CALCULATIONS

Composite panel bending

The Pekadur A663 polyurethane adhesive

Bending stress of the outer fibres

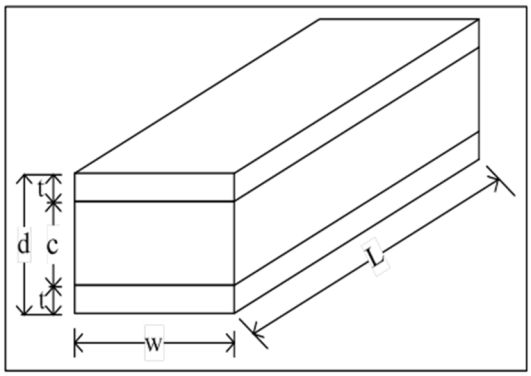

Experimentally determined

Bending moment, M =	209.590	Nm
Maximum applied load, P =	2794.537	N
Span length, L =	0.450	m

Specimen parameters

WPC thickness, t =	0.011	m
EPS thickness, c =	0.100	m
Depth of specimen, d =	0.122	m
Width of specimen, w =	0.095	m

EPS Young's modulus, E_{EPS} =	2.000E+06	Pa	(Table 6.6)
WPC Compressive Young's modulus, $E_{c,WPC}$ =	1.348E+09	Pa	(Experimentally determined)
WPC Tensile Young's modulus, $E_{t,WPC}$ =	9.494E+08	Pa	(Experimentally determined)
Moment of inertia of EPS, I_{EPS} =	7.917E-06	m^4	
Moment of inertia of WPC, I_{WPC} =	6.459E-06	m^4	

Bending stress of outer fibres:

$$\sigma = \frac{PLE_{t,WPC}\, d}{12(EI)_{eq}}$$

(Davies, 2008)
(Craig, 2000, p. 362)

$$(EI)_{eq} = E_{t,WPC}.w.t.(c+t)^2/2$$

For $E_{EPS}/E_{t,WPC} \leq 0.01$ (lightweight core sandwich panel)

$$(EI)_{eq} = \sum E_i I_i$$

For $E_{EPS}/E_{t,WPC} > 0.01$ (Sandwich panel)

$E_{EPS}/E_{t,WPC}$ = 0.0021 (<0.01)

$(EI)_{eq}$ = 6111.944 $N.m^2$

Bending stress at outer fibre (Bottom WPC panel):

Calculated bending stress, σ = 1985952 Pa

σ = 1.986 MPa

Experimently determined tensile strength of WPC = 18.152 MPa (Section 7.3)

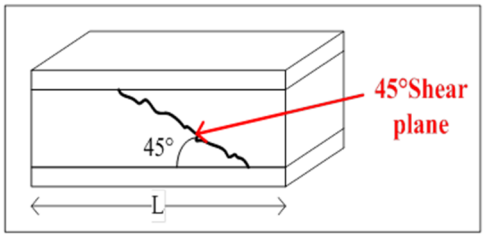

Shear stress (due to shear failure of EPS):

Shear area (45°): 95 mm

141 mm

Shear area, A = 13435 mm^2

Shear force at EPS shear failure, V = 1129.472 N

$$\tau = \frac{V sin45°}{A}$$

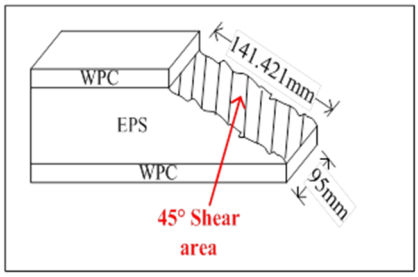

Calculated shear stress of EPS,

τ = 0.059 MPa

τ = 59.446 kPa

Expeimently determined shear stress of EPS = 46.662 kPa (Section 7.7)

The GB685 spray grade rubber adhesive

Bending stress of the outer fibres

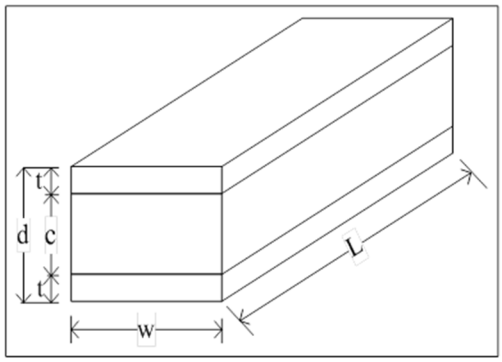

Experimentally determined

Bending moment, M = 106.058 Nm

Maximum applied load, P = 1414.104 N

Span length, L = 0.450 m

Specimen parameters

WPC thickness, t = 0.011 m

EPS thickness, c = 0.100 m

Depth of specimen, d = 0.122 m

Width of specimen, w = 0.095 m

EPS Young's modulus, E_{EPS} = 2.000E+06 Pa
WPC Compressive Young's modulus, $E_{c,WPC}$ = 1.348E+09 Pa
WPC Tensile Young's modulus, $E_{t,WPC}$ = 9.494E+08 Pa

Moment of inertia of EPS, I_{EPS} = 7.917E-06 m^4
Moment of inertia of WPC, I_{WPC} = 6.459E-06 m^4

Bending stress of outer fibres:

$$\sigma = \frac{PLE_{t,WPC}\, d}{12(EI)_{eq}}$$

(Davies, 2008)
(Craig, 2000, p. 362)

$$(EI)_{eq} = E_{t,WPC} . w . t . (c + t)^2 / 2$$

For $E_{EPS}/E_{t,WPC} \leq 0.01$ (lightweight core sandwich panel)

$$(EI)_{eq} = \sum E_i I_i$$

For $E_{EPS}/E_{t,WPC} > 0.01$ (Sandwich panel)

$E_{EPS}/E_{t,WPC}$ = 0.0021 (<0.01)

$(EI)_{eq}$ = 6111.944 Nm^2

Bending stress at outer fibre (Bottom WPC panel):

Calculated bending stress, σ = 1004940 Pa
σ = 1.005 MPa

Experimentaly determined tensile strength of WPC = 18.152 MPa (Section 7.3)

Shear stress (due to shear failure of EPS):

Transformed section method:

$$\tau = n\frac{VA^*\bar{y}^*}{t\, I_z}$$

(Craig, 2000, p. 362)

$n_1 = E_{c,\,WPC}/E_{EPS}$ = 673.890
$n_2 = E_{t,\,WPC}/E_{EPS}$ = 474.698

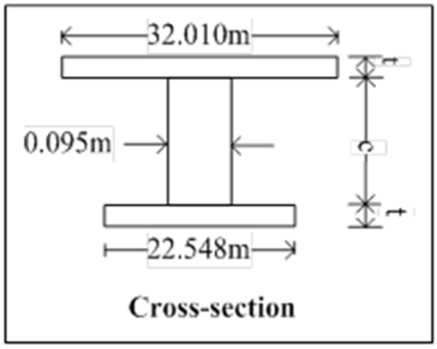

WPC thickness, t =	0.011	m
EPS thickness, c =	0.100	m

Change in length (as stated by transformed section method):

$$l^* = n\,l$$

l* = new length
$n_1 = E_{c,\,WPC}/E_{EPS}$
$n_2 = E_{t,\,WPC}/E_{EPS}$
l = original length

New widths:

WPC (Bottom) width =	22.548	m	(use n_2)
EPS width =	0.095	m	
WPC (Top) width =	32.010	m	(use n_1)

Neutral axis:

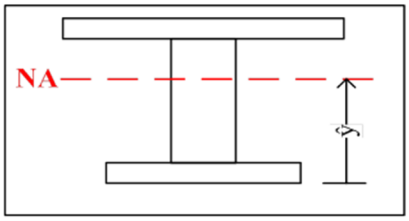

$$\bar{y} = \frac{\sum A\bar{y}}{\sum A}$$

$\sum A\bar{y}$ =	0.424	m^3
$\sum A$ =	6.011	m^2
$\bar{y}$ =	0.071	m

Shear stress parameters:

A* =	0.352	m^2	(WPC (top) length* WPC thickness)
$\bar{y}$* =	0.040	m	(0.122 -$\bar{y}$ - t)
t =	32.010	m	

Moment of inertia:

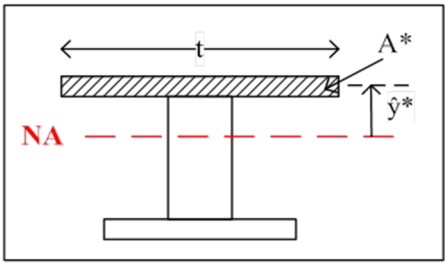

$$I_z = \sum\left(\frac{bh^3}{12} + Ad^2\right)$$

$I_{top,\,WPC}$ =	1.05E-02	m^4
I_{EPS} =	8.79E-06	m^4
$I_{bottom,\,WPC}$	7.45E-03	m^4

I_z =
$I_1+I_2+I_3$ I_z = 1.80E-02 m^4

Shear forces at EPS shear failure, V =	707.052	N	

Shear stress:

$$\tau = n_1 \frac{V A^* \bar{y}^*}{t I_z}$$

Calculated shear stress of adhesive, τ =	11761	Pa	
τ =	**11.761**	**kPa**	
Experimentaly determiend shear stress of adhesive, τ =	7.593	kPa	(Section 7.7)

Figure D. 1: WPC flexural test calculations

APPENDIX E: NUMERICAL ANALYSIS

E.1 Wind calculations

Fundamental value for basic wind speed:

$v_{b,0}$ = 36 m/s (Figure1) (SANS 10160-3, 2011)

Probability factor:

$$C_{prob} = \left[\frac{1 - K.\ln(-\ln(1-p))}{1 - K.\ln(-ln0.98)}\right]^{n}$$

K = 0.2
n = 0.5
Design life = 25 years (SANS 10160-1, 2011, p. 24)
p= 0.04

C_{prob} = 0.960

Basic wind speed:

$$v_b = C_{prob} \cdot v_{b,0}$$

v_b = 34.548 m/s

Terrain Roughness:

Terrain category = B (Table 2) (SANS 10160-3, 2011)

z_g = 350
z_0 = 3 (Table 1) (SANS 10160-3, 2011)
z_c = 5
α = 0.12

$$C_r(z) = 1.36\left[\frac{z - z_0}{z_g - z_c}\right]^{\alpha}$$

z = 3.39 m
$C_r(z)$ = 0.602

Peak wind speed

$$V_p(z) = 1.4\, C_r(z).\, C_0(z)\, .\, v_b$$

$V_p(z)$ = 29.140 m/s

Peak wind speed pressure:

$$q_p(z) = 0.5\, \rho.\, {v_p}^2\ (z)$$

ρ = 1.2 kg/m3 (Table 4) (SANS 10160-3, 2011)

$q_p(z)$ = 509.47 Pa

Internal wind coefficients

0°

μ = 0.692 (Figure16) (SANS 10160-3, 2011)

Cpi = -0.05

90°

μ = 1.000 (Figure16) (SANS 10160-3, 2011)

Cpi = -0.4

External wind coefficients

0°

Walls:

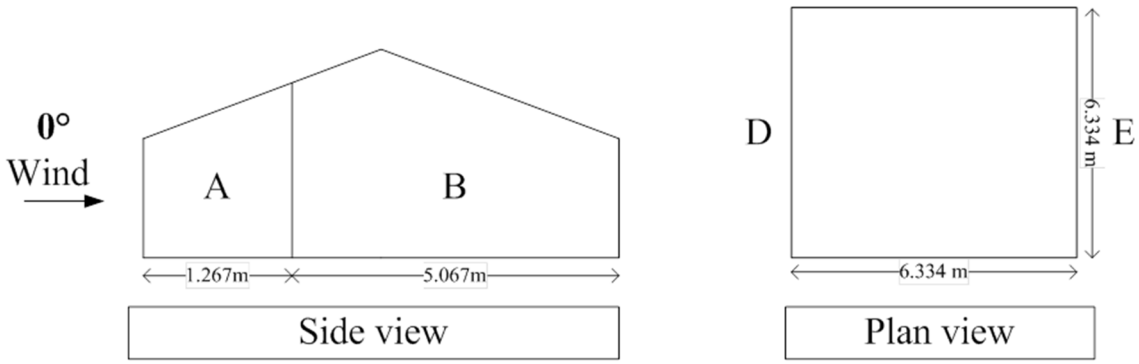

-

-

h/d = 0.556

b= 6.334 m

h = 3.39 m

e = 6.334 m

	Cpe
A	-1.2
B	-0.8
D	0.7
E	-0.3

(Table 6) (SANS 10160-3, 2011)

Roof:

0°

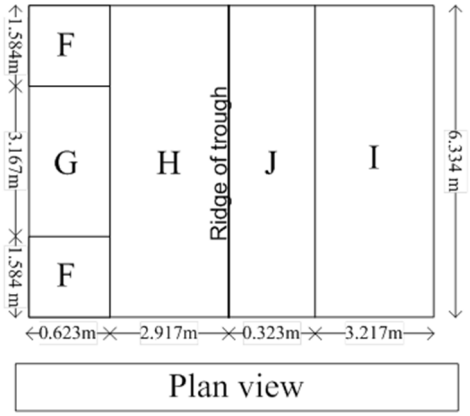

	Cpe1	Cpe2	Cpe3	Cpe4
F	-1.22	0.12	-0.56	-0.54
G	-0.96	0.12	-0.36	-0.48
H	-0.42	0.12	-0.12	-0.18
I	-0.48	-0.24	-0.24	-0.48
J	-0.52	-0.24	0.08	-0.48

(Table 10) (SANS 10160-3, 2011)

90°

Walls:

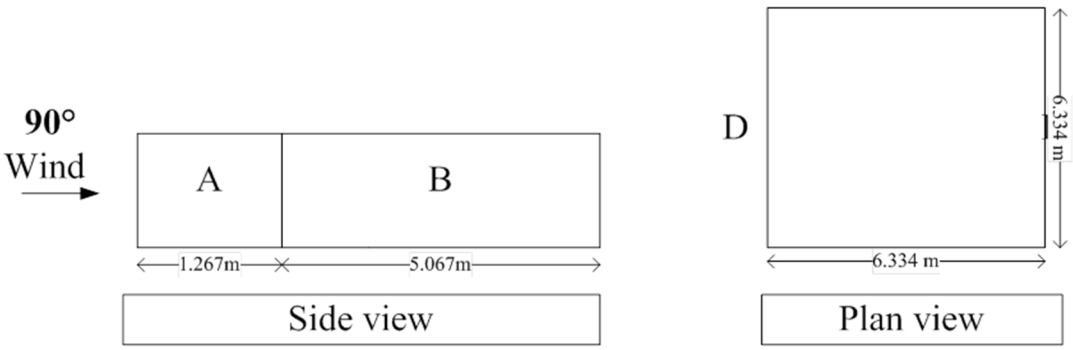

h/d = 0.556

b= 6.334 m
h = 3.39 m
e = 6.334 m

	Cpe
A	-1.2
B	-0.8
D	0.7
E	-0.3

(Table 6) (SANS 10160-3, 2011)

Roof:

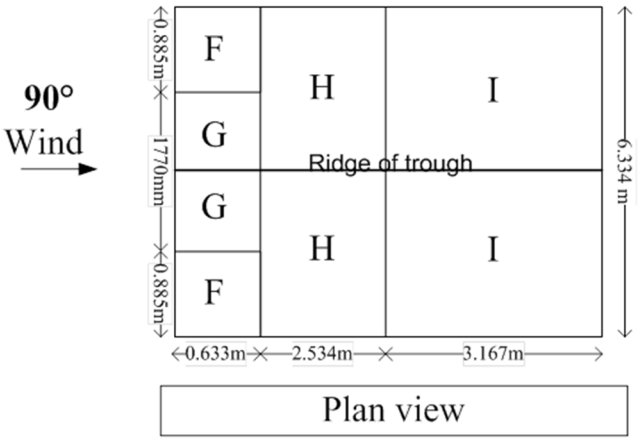

α = 11.2°

	Cpe1
F	-1.42
G	-1.3
H	-0.64
I	-0.54

(Table 11) (SANS 10160-3, 2011)

Wind pressures (Open doors)

0°

Walls:

	Cpe	Cpt	**Wind pressure (Pa)**
A	-1.2	-1.15	-586
B	-0.8	-0.75	-382
D	0.7	0.75	382
E	-0.3	-0.25	-127

Roof:

	Ct1	Ct2	Ct3	Ct4
F	-1.17	0.17	-0.51	-0.49
G	-0.91	0.17	-0.31	-0.43
H	-0.37	0.17	-0.07	-0.13
I	-0.43	-0.19	-0.19	-0.43
J	-0.47	-0.19	0.13	-0.43

	Wind pressures (Pa)			
	WP1	WP2	WP3	WP4
F	-596	87	-260	-250
G	-464	87	-158	-219
H	-189	87	-36	-66
I	-219	-97	-97	-219
J	-239	-97	66	-219

90°

Walls:

	Cpe	Cpt	**Wind pressure (Pa)**
A	-1.2	-0.8	-408
B	-0.8	-0.4	-204
D	0.7	1.1	560
E	-0.3	0.1	51

Roof:

	Cpe1	Cpt	**Wind pressure (Pa)**
F	-1.42	-1.02	-520
G	-1.3	-0.9	-459
H	-0.64	-0.24	-122
I	-0.54	-0.14	-71

Wind pressures (Close doors)

0°

Walls:

	Cpe	**Wind pressure (Pa)**
A	-1.2	-611
B	-0.8	-408
D	0.7	357
E	-0.3	-153

Roof:

	Ct1	Ct2	Ct3	Ct4
F	-1.22	0.12	-0.56	-0.54
G	-0.96	0.12	-0.36	-0.48
H	-0.42	0.12	-0.12	-0.18
I	-0.48	-0.24	-0.24	-0.48
J	-0.52	-0.24	0.08	-0.48

	Wind pressures (Pa)			
	LC1	LC2	LC3	LC4
F	-622	61	-285	-275
G	-489	61	-183	-245
H	-214	61	-61	-92
I	-245	-122	-122	-245
J	-265	-122	41	-245

90°

Walls:

	Cpe	**Wind pressure (Pa)**
A	-1.2	-611
B	-0.8	-408
D	0.7	357
E	-0.3	-153

Roof:

	Cpe1	**Wind pressure (Pa)**
F	-1.42	-723
G	-1.3	-662
H	-0.64	-326
I	-0.54	-275

Factorised load (1.3WL)

Wind pressures (Open doors)

0°

Walls:

	WL	1.3WL
A	-586	-762
B	-382	-497
D	382	497
E	-127	-166

Roof:

	1.3WL	
	LC1	LC2
F	-775	113
G	-603	113
H	-245	113
I	-285	-126
J	-311	-126

90°

Walls:

	WL	1.3WL
A	-408	-530
B	-204	-265
D	560	729
E	51	66

Roof:

	WL	1.3WL
F	-520	-676
G	-459	-596
H	-122	-159
I	-71	-93

Wind pressures (Closed doors)

0°

Walls:

	WL	1.3WL
A	-611	-795
B	-408	-530
D	357	464
E	-153	-199

Roof:

	1.3WL	
	LC1	LC2
F	-808	79
G	-636	79
H	-278	79
I	-318	-159
J	-344	-159

90°

Walls:

	WL	1.3WL
A	-611	-795
B	-408	-530
D	357	464
E	-153	-199

Roof:

	WL	1.3WL
F	-723	-940
G	-662	-861
H	-326	-424
I	-275	-358

E.2 ABAQUS™ results for each loading scenario

Scenario 1	
Maximum Stresses (Pa)	**Maximum resultant deflection (m)**
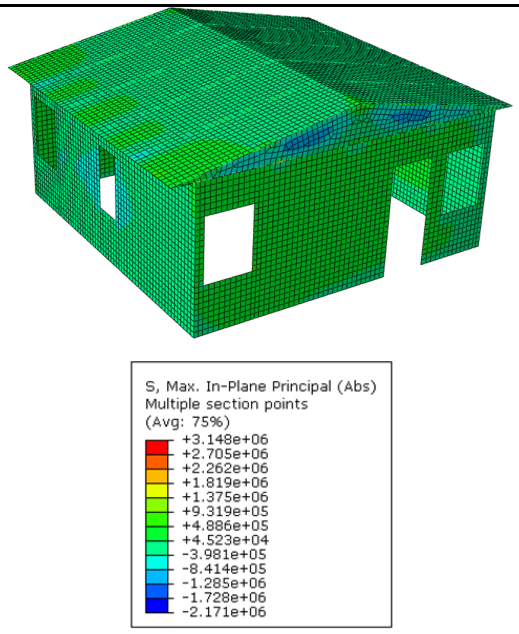	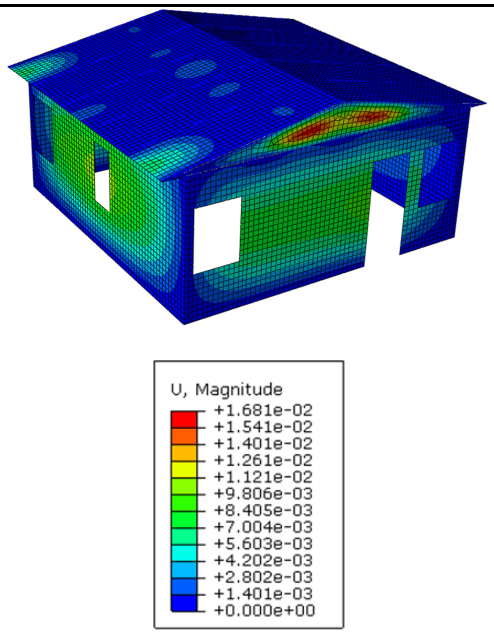

Scenario 2	
Maximum Stresses (Pa)	**Maximum resultant deflection (m)**
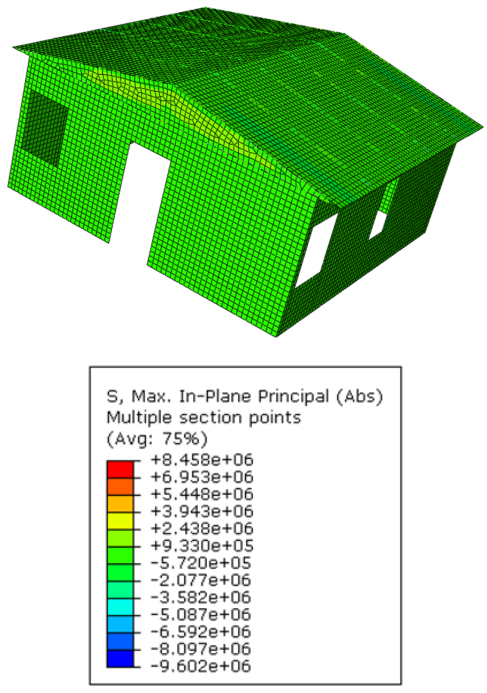	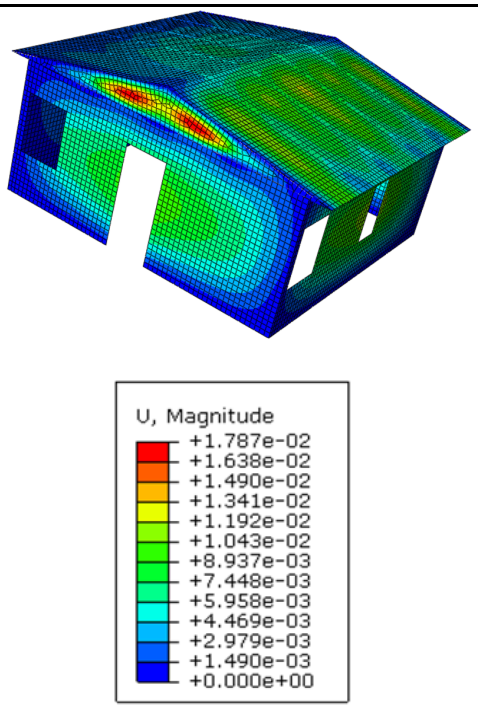

Scenario 3	
Maximum Stresses (Pa)	**Maximum resultant deflection (m)**
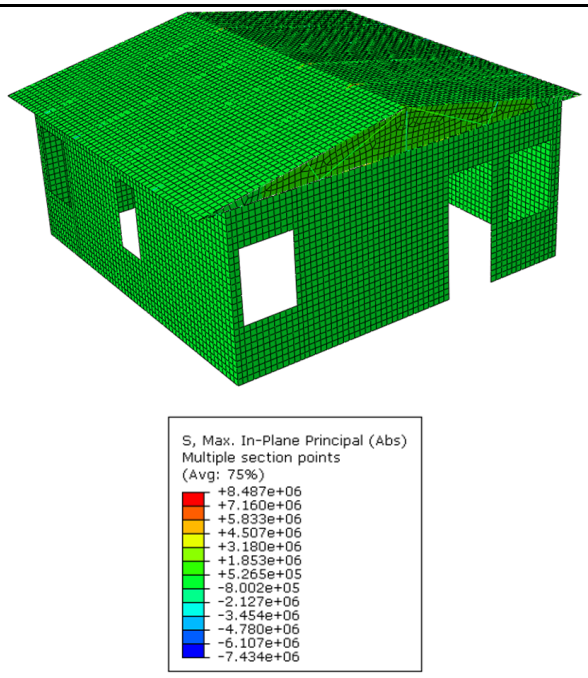	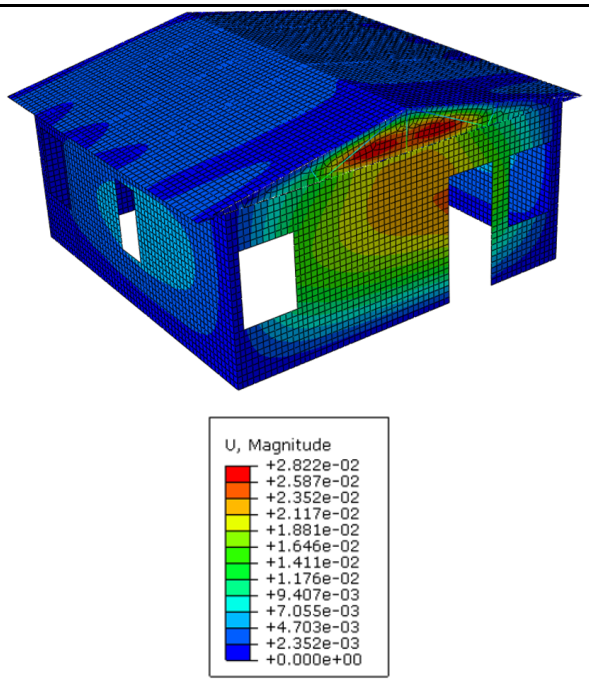

Scenario 4	
Maximum Stresses (Pa)	**Maximum resultant deflection (m)**
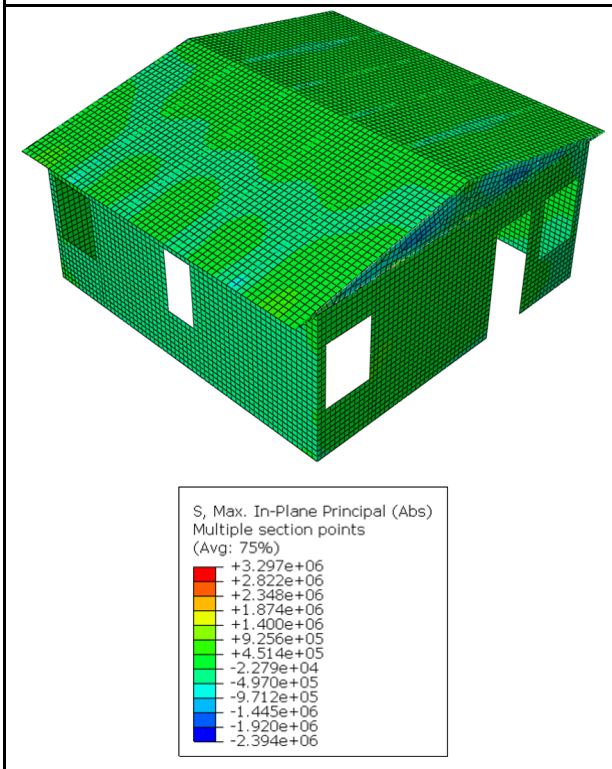	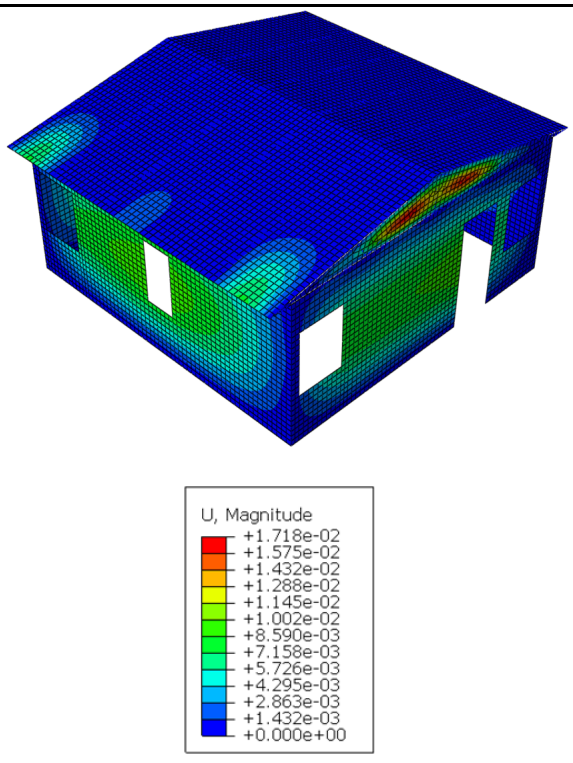

Scenario 5	
Maximum Stresses (Pa)	**Maximum resultant deflection (m)**
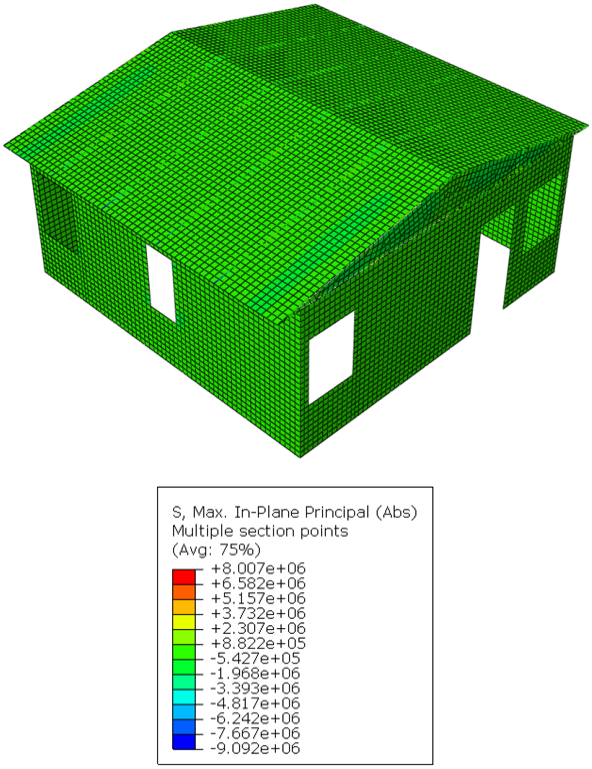	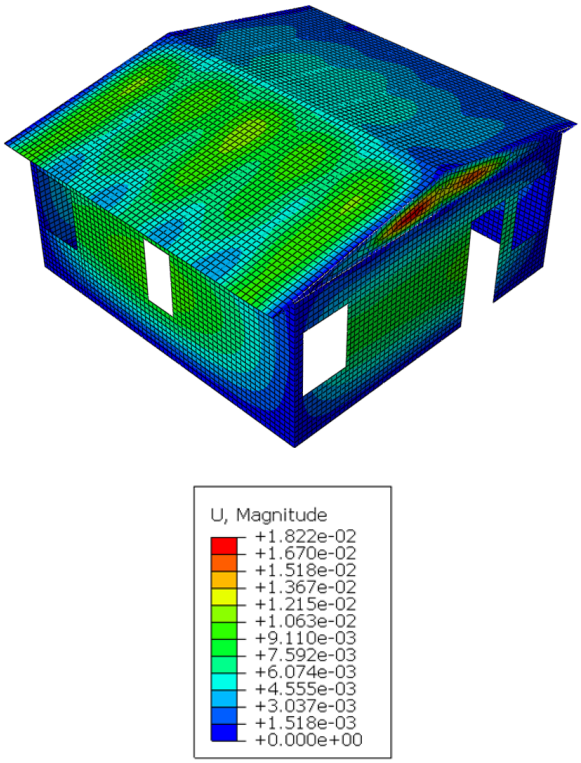

Scenario 6	
Maximum Stresses (Pa)	**Maximum resultant deflection (m)**
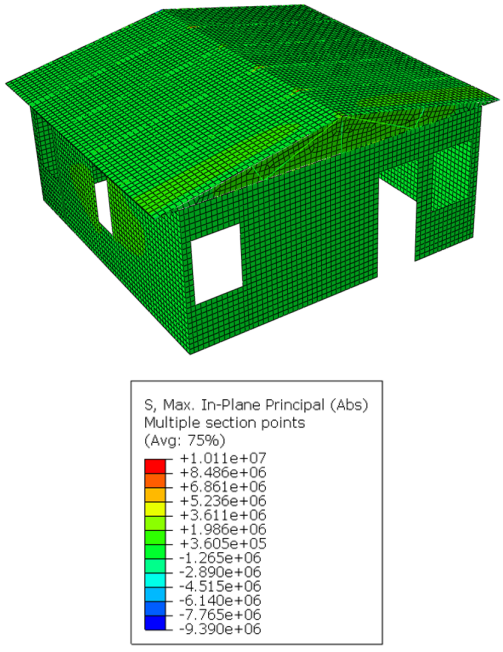	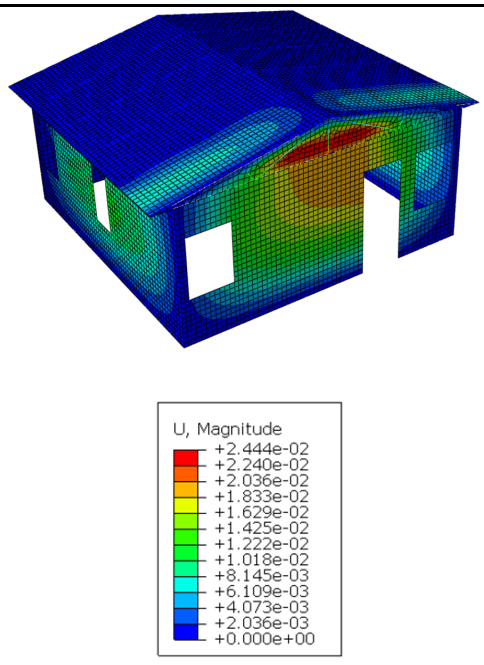

E.3 Flooring load calculations

Size of floor:

Floor area =	37.21	m^2
Floor volume =	372100000	mm^3
	0.3721	m^3

WPC properties:

ρ =	1331	kg/m^3

Own weight:

G_k =	13057.11	N/m^2

Imposed load:

Q_k =	1.5	kN/m^2	(Table 1, SANS 10160-1)

Load combination:

LC = 1.0(Own weight) x 1.1Q_k

LC =	14707.11	N/m^2

Deflection of soil (as well as floor slab)

$$s = \frac{q\,B}{E}(1-\nu^2)I_s$$ (Craig, 2004)

Load combination, q =	14707.11	N/m^2
Length of slab, B =	6.1	m
(soil modulus of elasticity 100 - 200 N/mm^2)		
Soil modulus of elasticity , E =	100	N/mm^2
Soil Poisson ratio, ν =	0.025	
Influence factor (flexible), I_s =	0.95	

Soil deflection, s =	0.00085	m
	0.852	mm

Stiffness of soil required:

$$k = \frac{q}{s}$$

(Craig, 2004)

Soil stiffness, k = 17267047.297 N/m^3

0.017 N/mm^3

Stiffness of compacted soil (ranges):

Slightly compacted =	0.015 - 0.03	N/mm^3
Well compacted =	0.05 - 0.1	N/mm^3
Extremely well compacted =	0.1 - 0.15	N/mm^3

Thus, 0.017 N/mm^3 is slightly compacted

APPENDIX F: FIRE PERFORMANCE

F.1 Calculations of fire curves for each housing unit

Table F. 3: The EN1991 post-flashover fire curve for the FFC housing unit

EUROCODE EN1991 POST-FLASHOVER PARAMETRIC TEMPERATURE –TIME CURVE (FOR FFC)					
Room:					
Wall height:	2.7	m		**OK**	(Wall height <4 m)
A_f =	18.50	m^2		**OK**	(A_f <500 m^2)
A_T =	45.66	m^2			
e_f =	500.00	MJ/m^2	Assume		
q =	9250.00	MJ			
e_t =	202.60	MJ/m^2			
Openings:					
A_v =	6.936	m^2			
h_{eq}=	0.9	m			
Opening factor (O):					
			(Equation 8.8)	**OK**	(0.02<O<0.2)
O =	0.14	$m^{1/2}$			
Multiple layers of materials:					
Layer 1 (FFC):					
s_1 =	11	mm			
k_1 =	0.13	W/m°C			
ρ_1 =	700	kg/m^3			
c_1 =	1300	J/kg°C			
b_1 =	343.95	$J/m^2°Cs^{1/2}$	(Equation 8.9)		
Layer 2 (EPS):					
s_2 =	100	mm			
k_2 =	0.03	W/m°C			
ρ_2 =	15	kg/m^3			

c_2 =	1500	J/kg°C		
b_2 =	25.98	$J/m^2°Cs^{1/2}$	(Equation 8.9)	
Layer 3 (FFC):				
s_3 =	11	mm		
k_3 =	0.13	W/m°C		
ρ_3 =	700	kg/m^3		
c_3 =	1300	J/kg°C		
b_3 =	343.95	$J/m^2°Cs^{1/2}$	(Equation 8.9)	
t =	172986.68	seconds		
$s_{lim,1}$ =	0.01	m	(Equation 8.11)	
$s_1/s_{lim,1}$ =	0.840139			
b =	348.10	$J/m^2°Cs^{1/2}$	**OK**	(100<b<2200)

Room boundaries:

Γ = 144.16

Determine t*:

Equation 8.6

Compute t_{max} (temp at which Θ_g occurs):

Γ = 144.16

$0.2x10^{-3}e_t/O$ = 0.28 hours

t_{lim} =

25 min	slow growth rate
20 min	medium growth rate
15 min	fast growth rate

t_{max} =	**0.33**	**hours**	**Fuel controlled**
t^*_{max} =	**48.05**	**hours**	
x=	**1.00**		

Burning phase:

O_{lim} =	0.060779	**OK**	(0.02<O<0.2)
Γ_{lim} =	25.64		

Table F. 2: The EN1991 post-flashover fire curve for the WPC housing unit

EUROCODE EN1991 POST-FLASHOVER PARAMETRIC TEMPERATURE –TIME CURVE (FOR WPC)					
Room:					
Wall height:	2.7	m		**OK**	(Wall height <4m)
A_f =	18.50	m^2		**OK**	(A_f <500 m^2)
A_T =	45.66	m^2			
e_f =	500.00	MJ/m^2	Assume		
q =	9250.00	MJ			
e_t =	202.60	MJ/m^2			
Openings:					
A_v =	6.936	m^2			
h_{eq}=	0.9	m			
Opening factor (O):					
			(Equation 8.8)	**OK**	(0.02<O<0.2)
O =	0.14	$m^{1/2}$			
Multiple layers of materials:					
Layer 1 (WPC):					
s_1 =	11	mm			
k_1 =	0.15	W/m°C			
ρ_1 =	1331	kg/m^3			
c_1 =	1860	J/kg°C	$b_1>b_2$		
b_1 =	609.38	$J/m^2°Cs^{1/2}$	(Equation 8.9)		
Layer 2 (EPS):					
s_2 =	100	mm			
k_2 =	0.03	W/m°C			
ρ_2 =	15	kg/m^3			
c_2 =	1500	J/kg°C			
b_2 =	25.98	$J/m^2°Cs^{1/2}$	(Equation 8.9)		
Layer 3 (WPC):					
s_3 =	11	mm			
k_3 =	0.15	W/m°C			
ρ_3 =	1331	kg/m^3			
c_3 =	1860	J/kg°C			
b_3 =	609.38	$J/m^2°Cs^{1/2}$	(Equation 8.9)		

t =	56447.01	seconds		
$s_{lim,1}$ =	0.01	m	(Equation 8.11)	
$s_1/s_{lim,1}$ =	1.290036			
b =	609.38	$J/m^2°Cs^{1/2}$	**OK**	(100<b<2200)

Room boundaries:

Γ = 47.04

Determine t*:

Equation 8.6

Compute t_{max} (temp at which Θ_g occurs):

Γ = 47.04

$0.2x10^{-3}e_t/O$ = 0.28 hours

t_{lim} =

25 min	slow growth rate
20 min	medium growth rate
15 min	fast growth rate

t_{max} =	**0.33**	**hours**	**Fuel controlled**
t^*_{max} =	**15.68**	**hours**	
x=	**1.00**		

Burning phase:

O=	0.06	$m^{1/2}$	**OK**	(0.02<O<0.2)
Γ =	8.37			

Table F. 3: The EN1991 post-flashover fire curve for the block and mortar housing unit

EUROCODE EN1991 POST-FLASHOVER PARAMETRIC TEMPERATURE –TIME CURVE (FOR BLOCK AND MORTAR)

Room:

Wall height:	3	m	**OK**	(Wall height <4 m)
A_f =	16.55	m^2	**OK**	(A_f <500 m^2)
A_T =	48.96	m^2		
e_f =	500.00	MJ/m^2		

q =	8273.80	MJ		
e_t =	168.99	MJ/m^2		

Openings:

A_v =	6.936	m^2		
h_{eq}=	0.9	m		

Opening factor (O):

(Equation 8.8) **OK** (0.02<O<0.2)

O =	0.13	$m^{1/2}$

Block and mortar (Room boundaries):

s_1 =	140	mm		
k_1 =	1.1	W/m°C		
ρ_1 =	2250	kg/m^3		
c_1 =	877.8	J/kg°C		
b_1 =	1473.96	$J/m^2°Cs^{1/2}$	(Equation 8.9)	
			OK	(100<b<2200)
Γ =	6.99		(Equation 8.7)	

Determine t*:

Equation 8.6

Compute t_{max} (temp at which Θ_g occurs):

$0.2x10^{-3}e_t/O$ = 0.251481 hours

t_{lim} =

25 min	slow growth rate
20 min	medium growth rate
15 min	fast growth rate

t_{max} =	**0.33**	**hours**	**Fuel controlled**
t^*_{max} =	**2.33**	**hours**	
x =	**1**		

Burning phase:

O=	0.05	$m^{1/2}$	**OK**	(0.02<O<0.2)
Γ =	0.99			

F.2 The temperature-time curves through the thickness of the walling systems of the FFC, WPC and block and mortar housing unit

F.2.1. Modular FFC housing unit

Heats transfer through the thickness of the external walls:

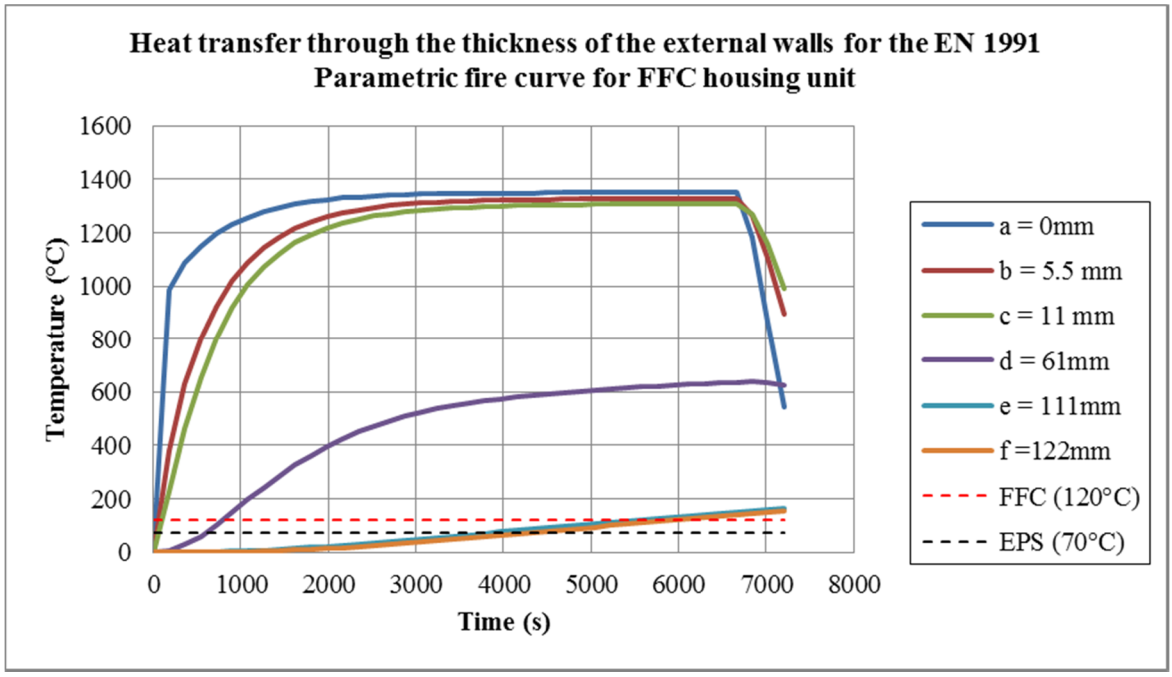

Figure F. 1: Heat transfer through the thickness of the external walls for the EN1991 Parametric fire curve for the FFC housing unit

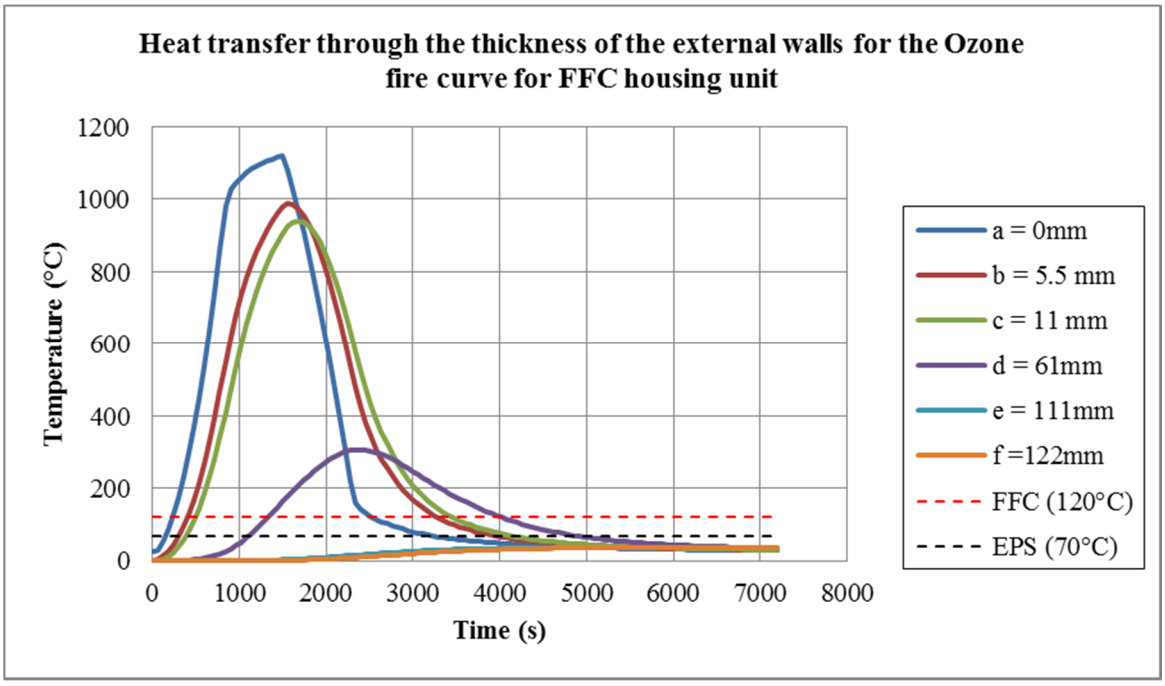

Figure F. 2: Heat transfer through the thickness of the external walls for the Ozone fire curve for the FFC housing unit

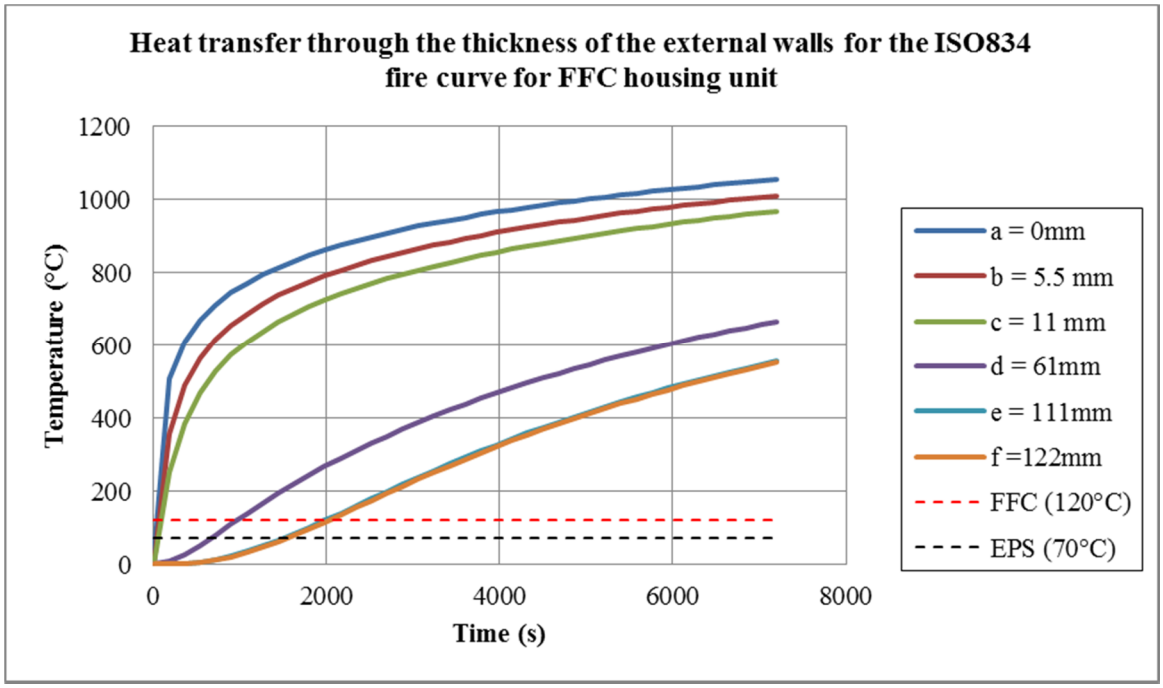

Figure F. 3: Heat transfer through the thickness of the external walls for the ISO834 fire curve for the FFC housing unit

Heats transfer through the thickness of the internal walls:

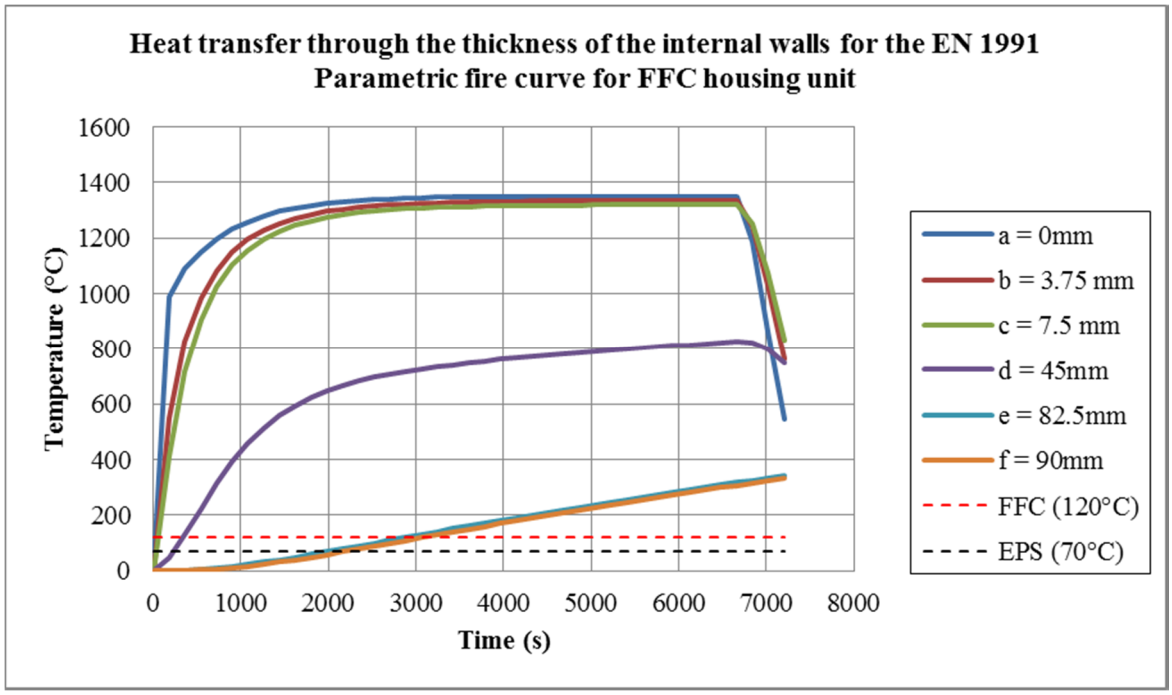

Figure F. 4: Heat transfer through the thickness of the internal walls for the EN1991 Parametric fire curve for the FFC housing unit

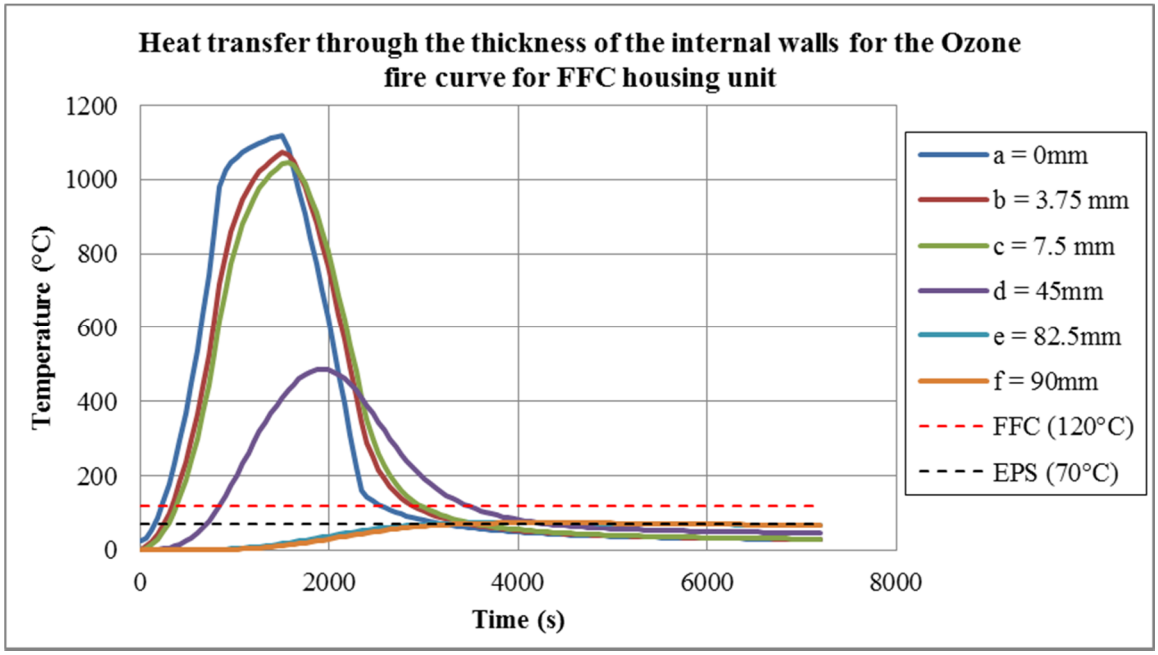

Figure F. 5: Heat transfer through the thickness of the internal walls for the Ozone fire curve for the FFC housing unit

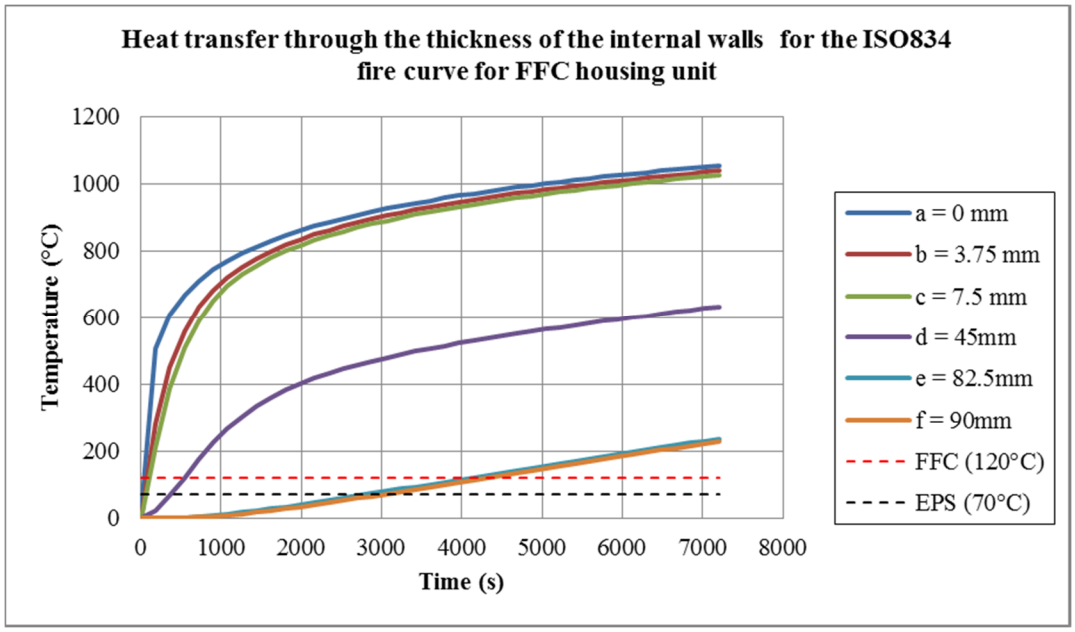

Figure F. 6: Heat transfer through the thickness of the internal walls for the ISO 834 fire curve for the FFC housing unit

F.2.2. Modular WPC housing unit

Heats transfer through the thickness of the external walls:

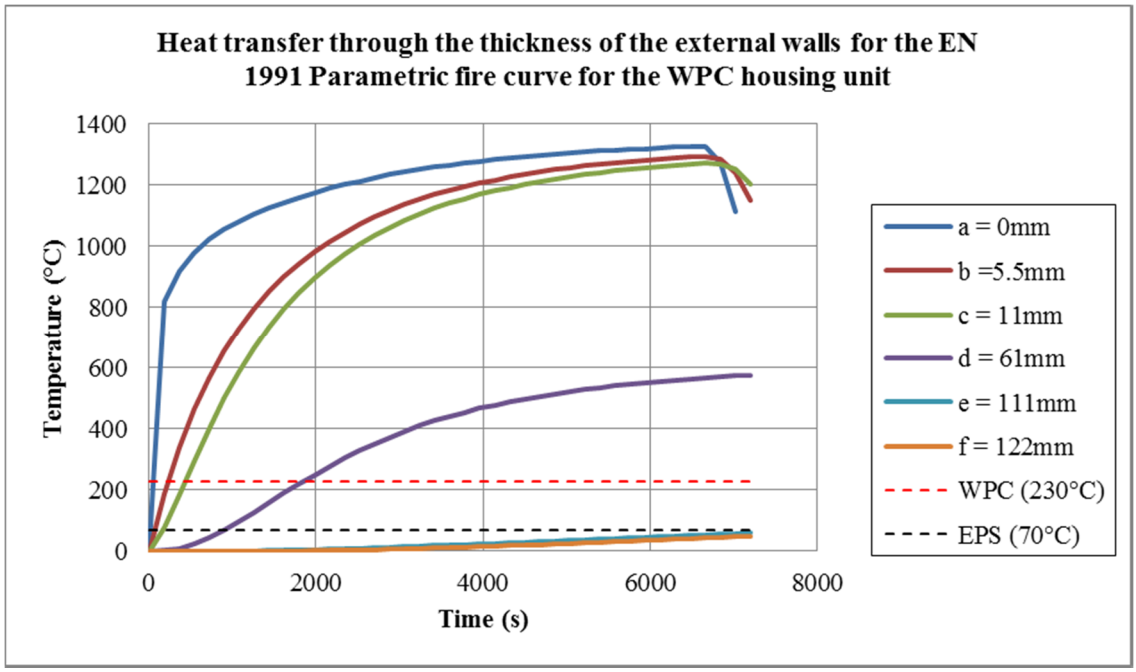

Figure F. 7: Heat transfer through the thickness of the external walls for the EN1991 Parametric fire curve for the WPC housing unit

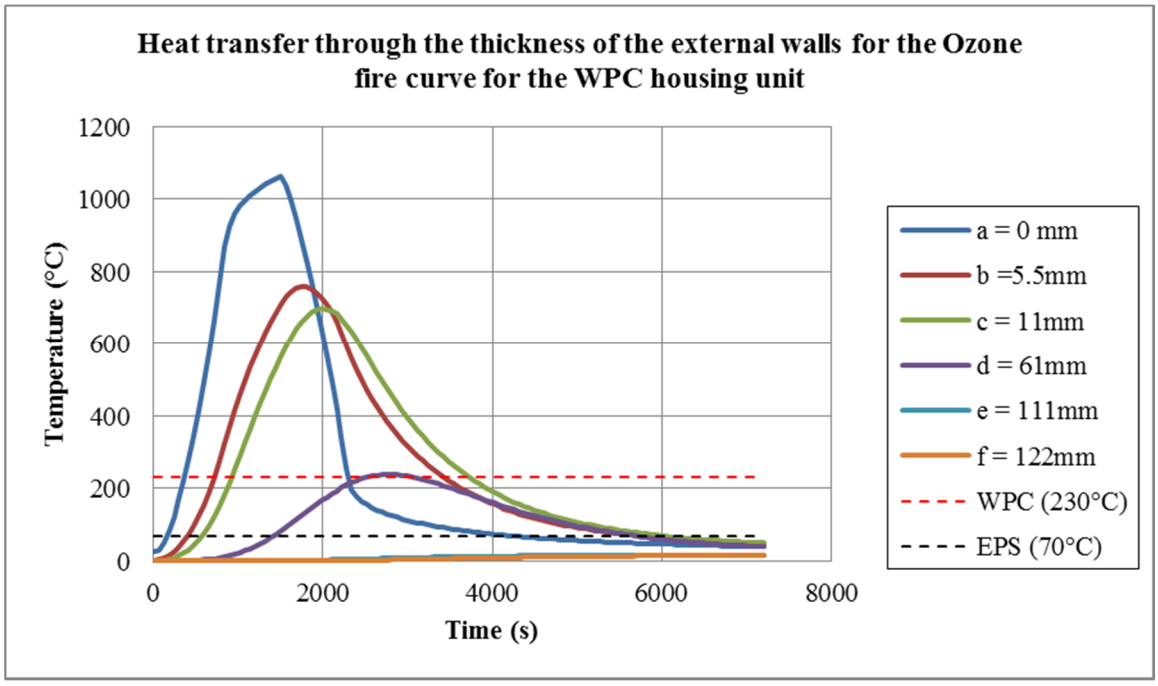

Figure F. 8: Heat transfer through the thickness of the external walls for the Ozone fire curve for the WPC housing unit

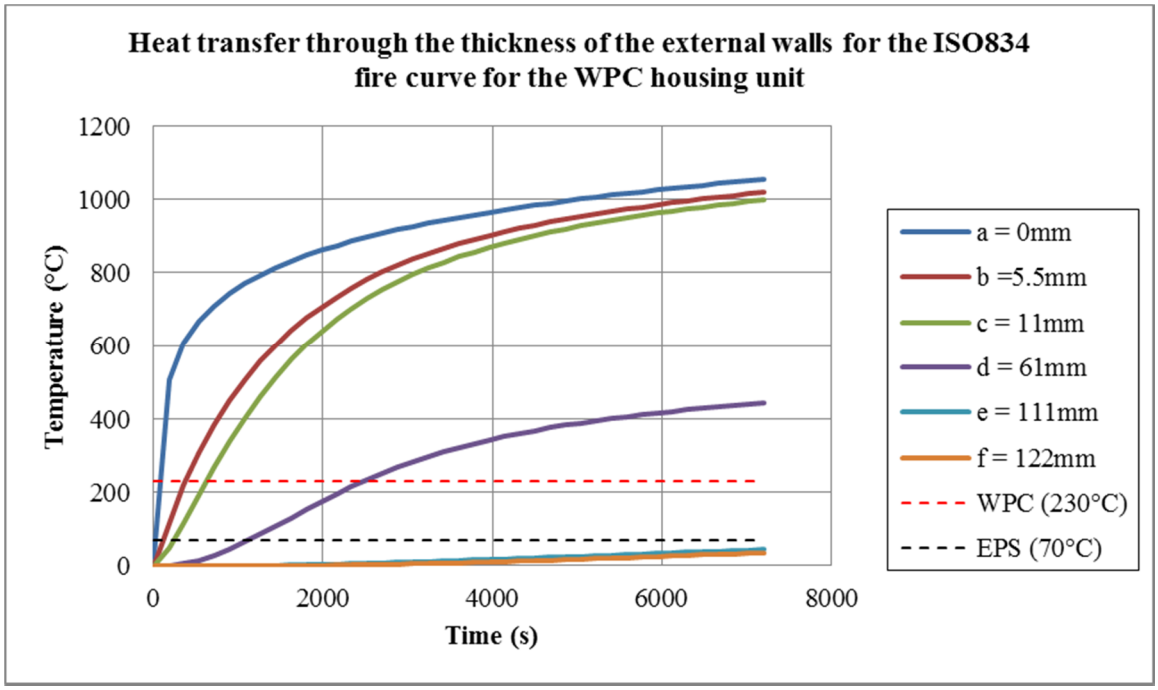

Figure F. 9: Heat transfer through the thickness of the external walls for the ISO834 fire curve for the WPC housing unit

Heats transfer through the thickness of the internal walls:

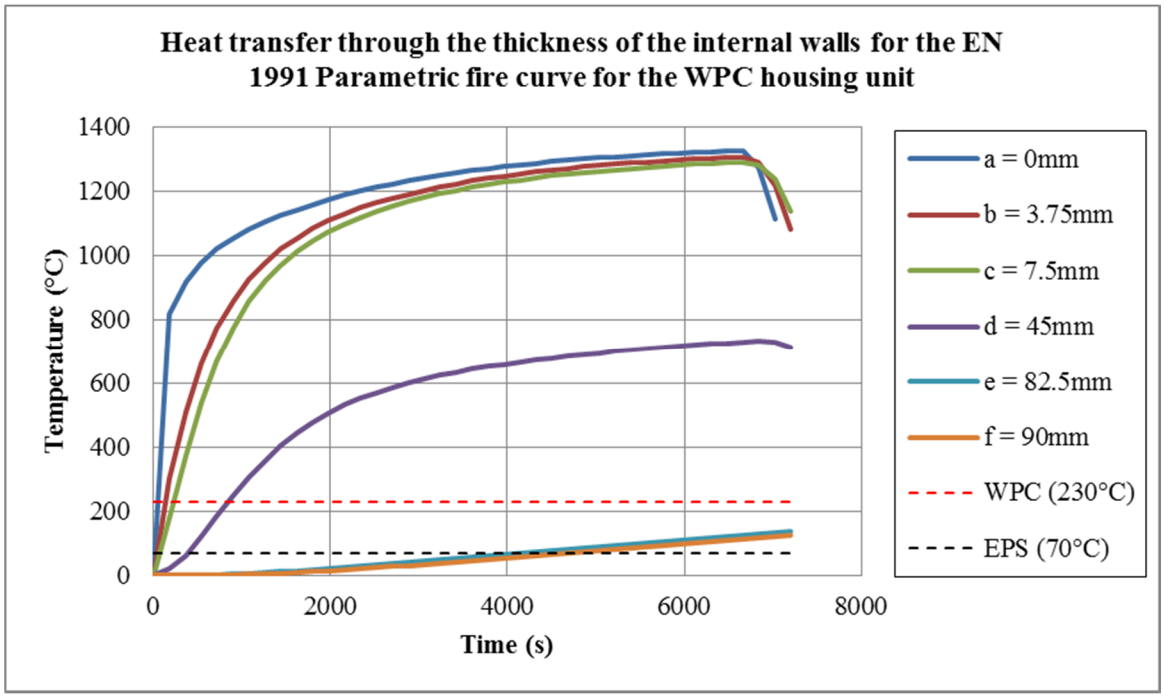

Figure F. 10: Heat transfer through the thickness of the internal walls for the EN1991 Parametric fire curve for the WPC housing unit

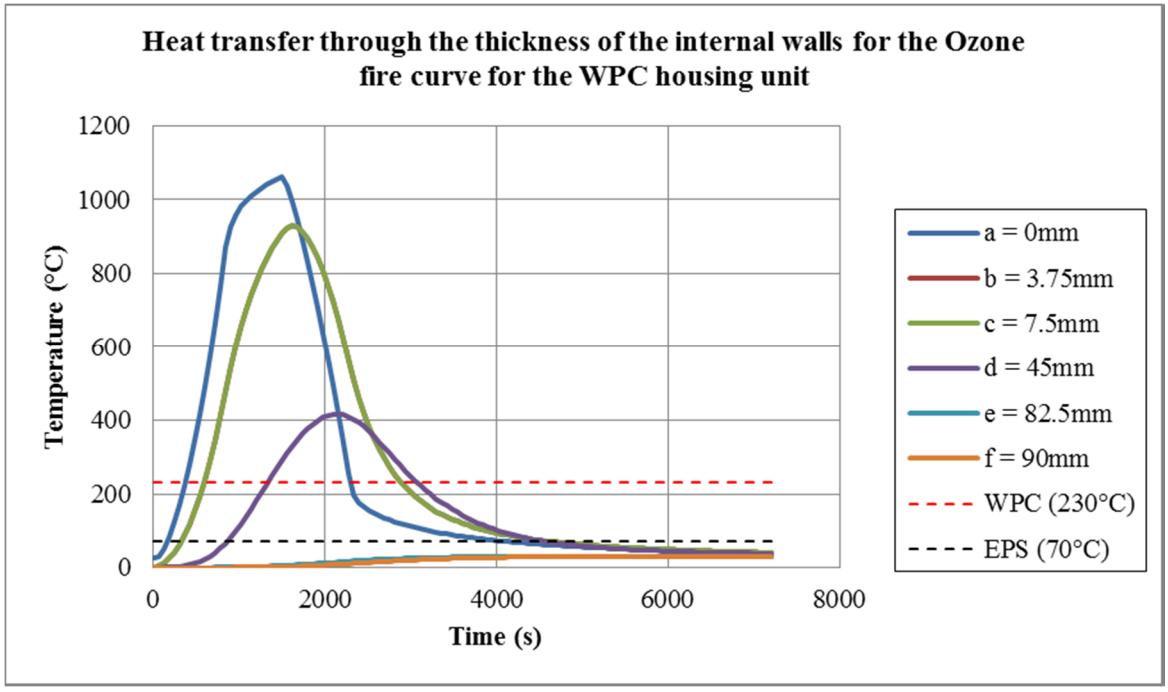

Figure F. 11: Heat transfer through the thickness of the internal walls for the Ozone fire curve for the WPC housing unit

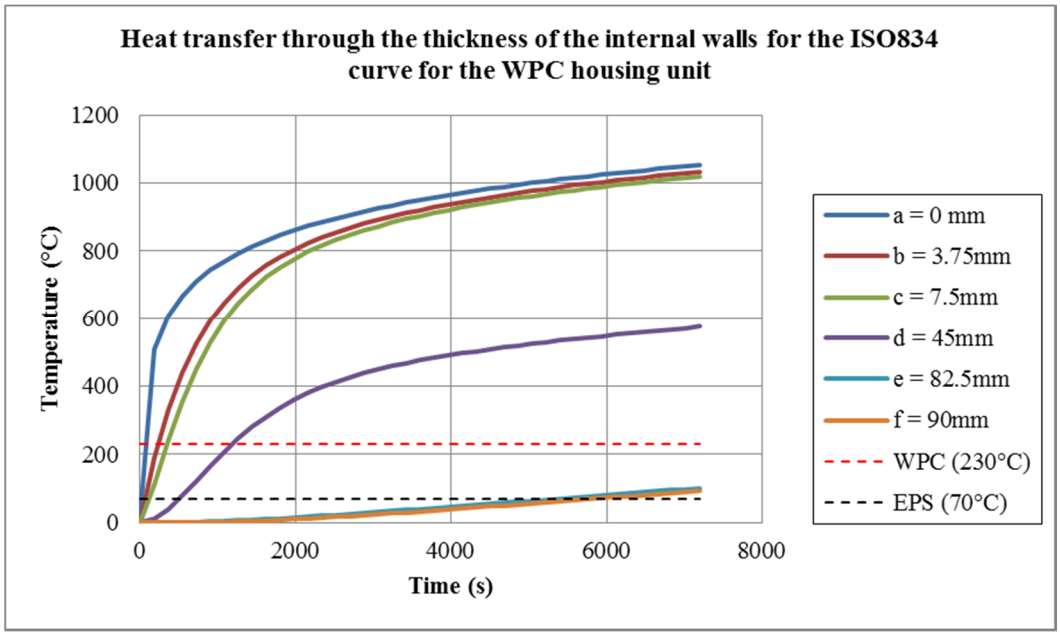

Figure F. 12: Heat transfer through the thickness of the internal walls for the ISO 834 fire curve for the WPC housing unit

F.2.3. Conventional block and mortar housing unit

Heats transfer through the thickness of the external walls:

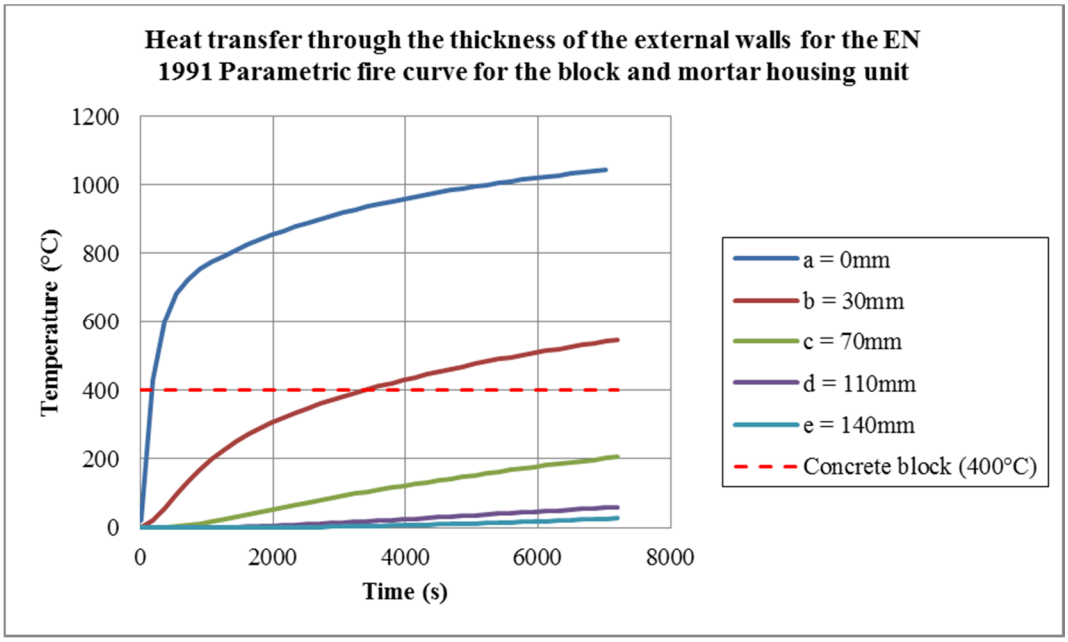

Figure F. 13: Heat transfer through the thickness of the external walls for the EN1991 Parametric fire curve for the block and mortar housing unit

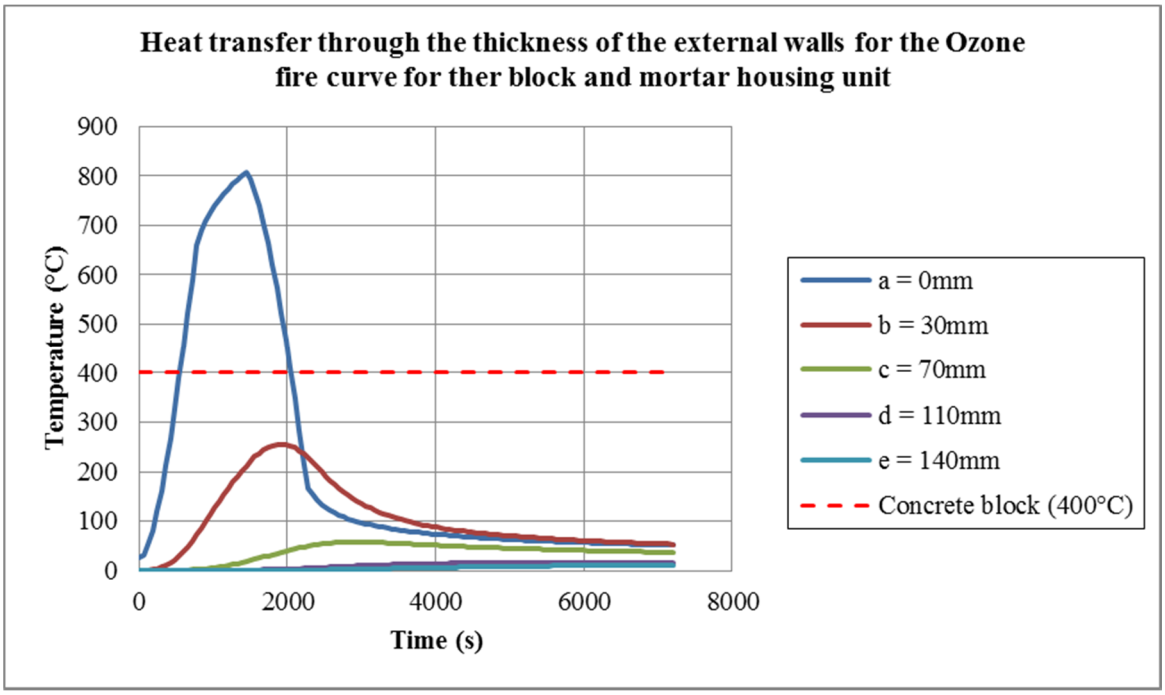

Figure F. 14: Heat transfer through the thickness of the external walls for the Ozone fire curve for the block and mortar housing unit

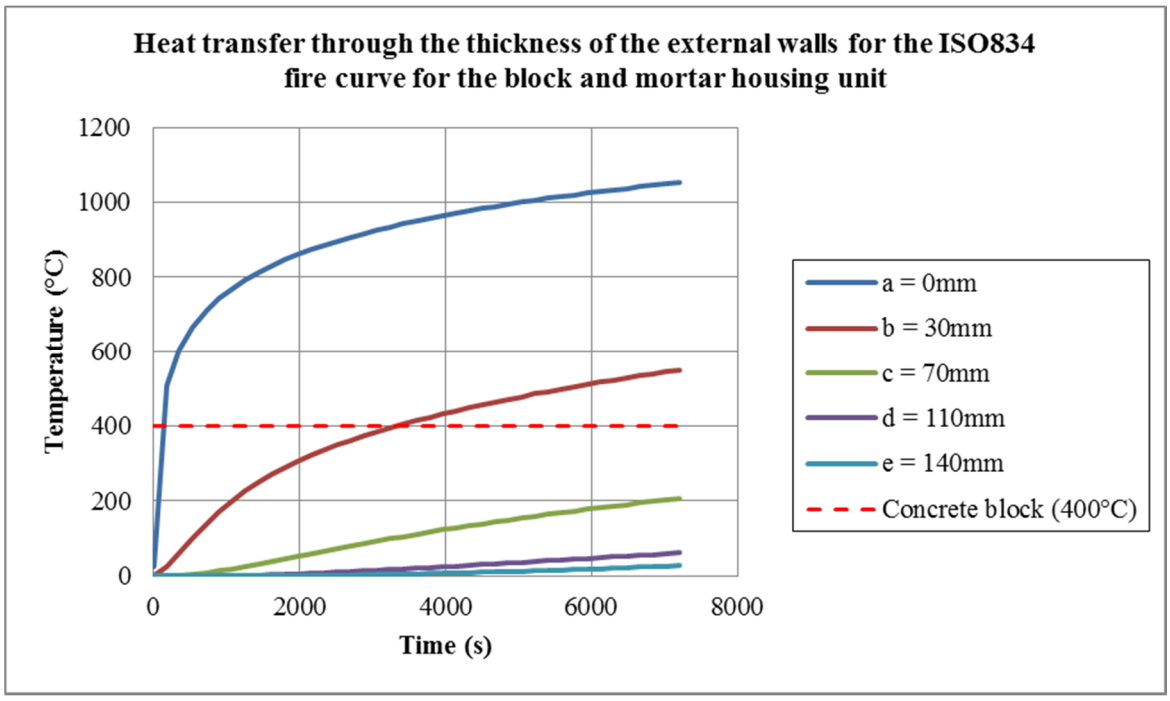

Figure F. 15: Heat transfer through the thickness of the external walls for the ISO834 fire curve for the block and mortar housing unit

Heats transfer through the thickness of the internal walls:

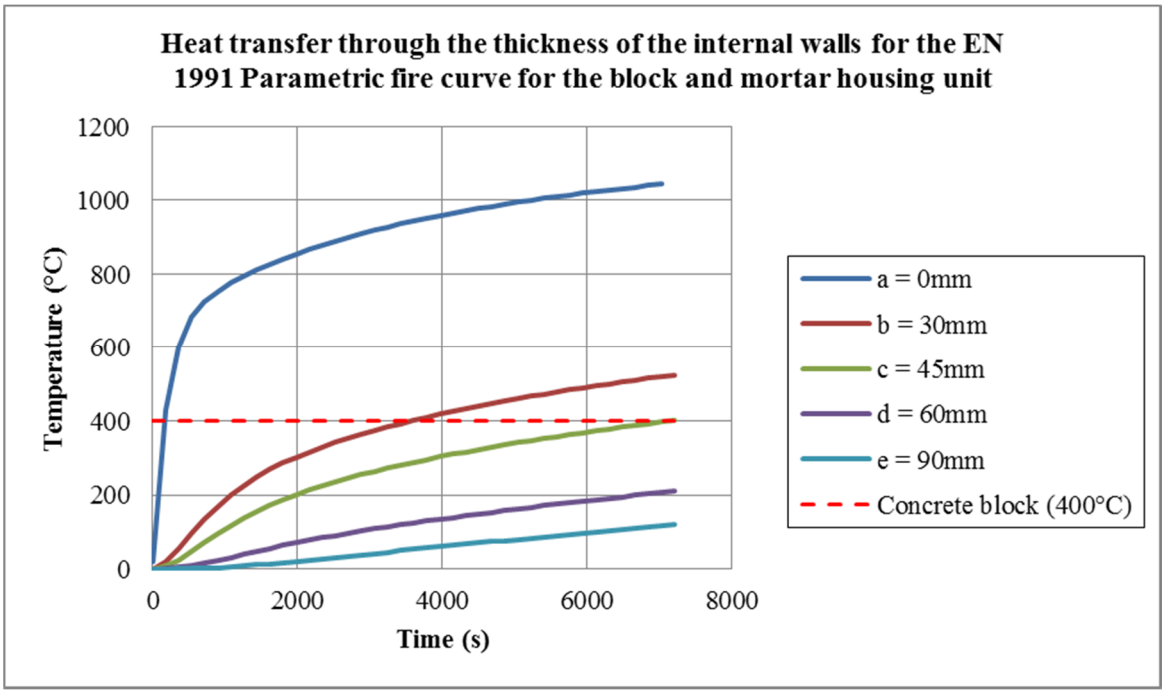

Figure F. 16: Heat transfer through the thickness of the internal walls for the EN1991 Parametric fire curve for the block and mortar housing unit

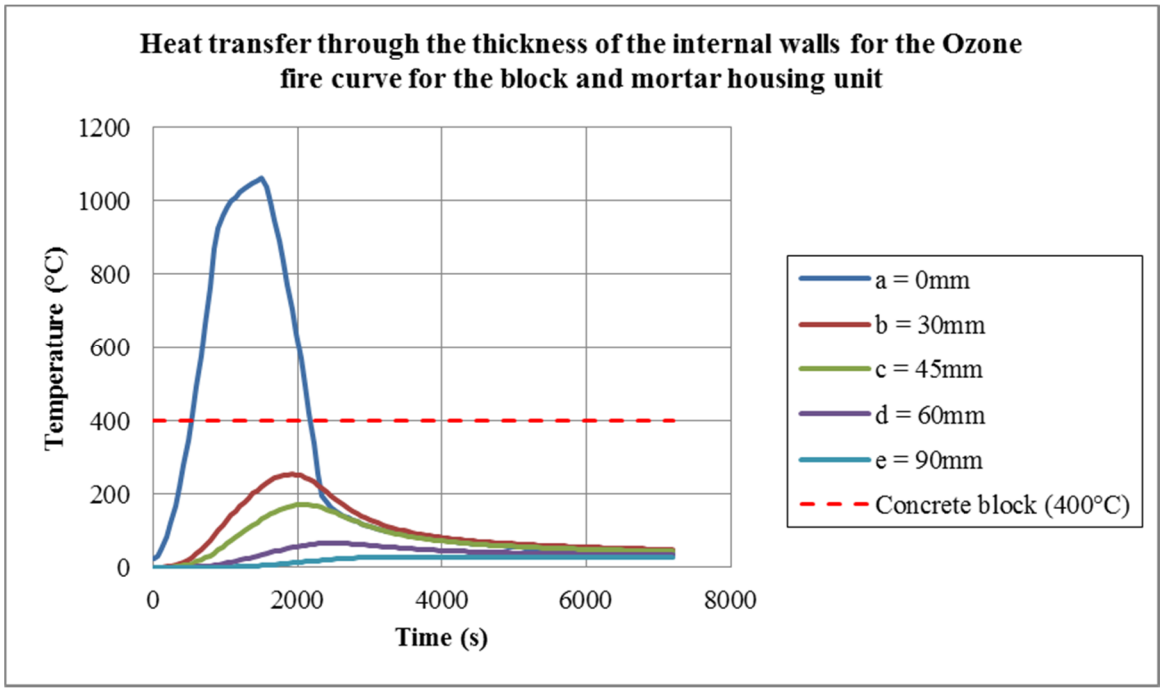

Figure F. 17: Heat transfer through the thickness of the internal walls for the Ozone fire curve for the block and mortar housing unit

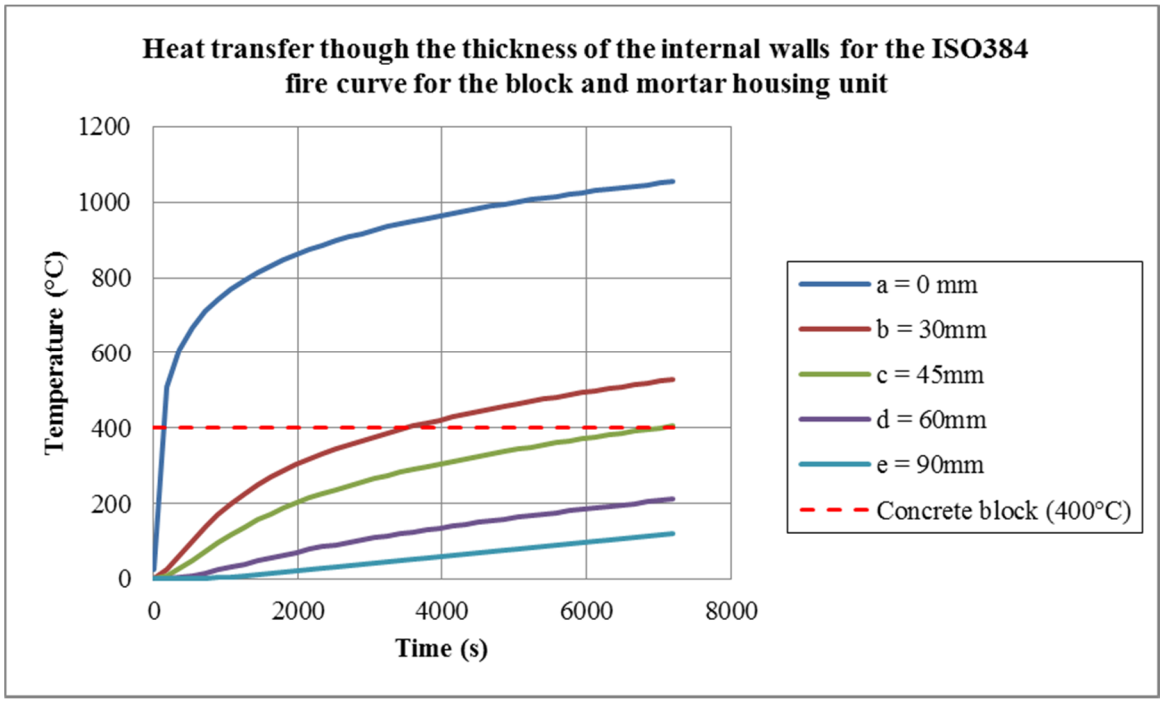

Figure F. 18: Heat transfer through the thickness of the internal walls for the ISO 834 fire curve for the block and mortar housing unit

APPENDIX G: COST ESTIMATION

G.1 Cost calculations for the modular plastic housing unit

Table G. 1: Material cost estimation calculations for the modular FFC housing unit

Modular FFC plastic house: Cost estimation				
Materials			**MATERIAL Cost estimation**	
Items	Unit	Quantity	Rate [R/unit]	Cost [R]
Connections and foundation				
Concrete strip footing	m^3	5.50	923.00	5077.74
Floor slab				
FFC Floor panel	m^3	0.37	11693.50	4351.15
External walls 122mm				
FFC wall panel	m^3	1.48	11693.50	17287.05
EPS (t=100mm)	m^2	67.20	71.23	4786.49
Adhesive	ℓ	134.40	27.29	3667.65
FFC gable (t=5mm)	m^3	0.02	11693.50	280.14
Internal walls 90mm				
FFC wall panel	m^3	0.40	11693.50	4683.30
EPS (t =75mm)	m^2	26.70	53.42	1426.33
Adhesive	ℓ	53.40	27.29	1457.30
Roofing				
Roof trusses (Gr 5 Pine)	m	99.05	19.76	1957.23
Rafter (Gr 5Pine)	m	19.00	19.76	375.44
Roof sheeting (25mm)	m^3	1.08	11693.50	12625.47
TOTAL MATERIAL COST ESTIMATION				**R 57 975.28**

Table G. 2: Material cost estimation calculations for the modular WPC housing unit

Modular WPC plastic house: Cost estimation				
Materials			**MATERIAL Cost estimation**	
Items	Unit	Quantity	Rate [R/unit]	Cost [R]
Foundation				
Concrete strip footing	m^3	5.50	923.00	5077.74
Floor slab				
WPC Floor panel	m^3	0.37	20550.91	7646.99
External walls 122mm				
WPC wall panel	m^3	1.48	20550.91	30381.38
EPS (t=100mm)	m^2	67.20	71.23	4786.49
Adhesive	ℓ	134.40	27.29	3667.65
WPC gable (t=5mm)	m^3	0.02	20550.91	492.33
Internal walls 90mm				
WPC wall panel	m^3	0.40	20550.91	8230.73
EPS (t =75mm)	m^2	26.70	53.42	1426.33
Adhesive	ℓ	53.40	27.29	1457.30
Roofing				
Roof trusses (Gr 5 Pine)	m	99.05	19.76	1957.23
Rafter (Gr 5Pine)	m	19.00	19.76	375.44
Roof sheeting (25mm)	m3	1.08	20550.91	22188.82
TOTAL MATERIAL COST ESTIMATION				**R 87 688.42**

Table G. 3: Labour cost of modular housing units

Modular plastic house: Cost estimation				
Labour			**LABOUR cost estimation**	
Items	**Unit**	**Quantity**	**Rate [R/unit]**	**Cost [R]**
Connections and foundation				
Excavation and earth by hand (external walls)	m^3	5.50	103.34	568.5084756
Concrete and strip foundation	m^2	3.43	83.02	284.5859184

Floor slab FFC Floor panels	m^2	37.21	60.00	2232.60
External walls 122mm Sandwich panel	m^2	67.20	60.00	4031.86
Internal walls 90mm Sandwich panels	m^2	26.58	60.00	1594.89
Roofing Labour	m^2	40.00	75	3000
TOTAL MATERIAL COST ESTIMATION				**R 11 712.44**

Table G. 4: Transport cost estimation of FFC housing unit

Modular FFC house: Cost estimation					
Transport				**Cost estimation**	**Cost [R]**
Items	**Unit**	**Distance of transport**	**Quantity [ton]**	**Rate [R/unit]**	
Transport	7.5t/km	50 km	4.95	14	462.00
TOTAL TRANSPORT COST ESTIMATION					**R 462.00**

Table G. 5: Transport cost estimation of WPC housing unit

Modular WPC house: Cost estimation					
Transport				**Cost estimation**	**Cost [R]**
Items	**Unit**	**Distance of transport**	**Quantity [ton]**	**Rate [R/unit]**	
Transport	7.5t/km	50 km	7.05	14	658.00
TOTAL TRANSPORT COST ESTIMATION					**R 658.00**

G.2 Cost calculations for the block and mortar housing unit

Table G. 6: Material cost estimation calculations for the block and mortar housing unit

Conventional design: Cost estimation				
Materials			**MATERIAL Cost estimation**	
Items	Unit	Quantity	Rate [R/unit]	Cost [R]
Foundation:				
10 MPa concrete foundation (600x230mm)	m^3	3.43	923.00	3163.97
Reinforcing (4 x Y12)	kg	103.00	8.80	906.40
190mm blockwork including	m^2	14.90	114.80	1710.52
brickforce (75 x 2.8mm)	m	125.00		0.00
galvanised	m^2	2.45		0.00
filled with concrete	m^3	0.97		0.00
Floor slab				
Damp proof membrane 250 micron	m^2	41.00	3.57	146.37
25 MPa concrete	m^3	4.92	1032.00	5077.44
Steel mesh ref 193	m^2	41.00	111.81	4584.21
Screed	m^2	39.90	7.81	311.62
External walls 140mm				
Two top courses of brickwork to be filled with 10 MPa concrete	m^3	0.65	923.00	599.95
Brickwork, mortar &	m^2	75.00	114.80	8610.00
brickforce as NHBRC standard	m	125.00		0.00
galvanised	m^2	2.45		0.00
Plaster externally (12mm thick)	m^2	75.00	28.84	2163.00
Bagged internally	m^2	75.00	12.24	918.00
DPC (110mm width) -375 micron	m	29.00	2.22	64.38
Internal walls 90mm				
Blockwork, mortar	m^2	26.00	114.80	2984.80
Bagged	m^2	52.00	12.24	636.48

Roofing				
Howe type truss to be designed by supplier for 7.62m span	sum	1.00	4653.14	4653.14
114x38 wall plate including beam filling	m	12.00	30.27	363.24
50x76mm purlins on edge at maximum 1.2m spacing	sum	1.00	454.38	454.38
Roof Covering				
0.54mm Fielders corrugated Colour bond G550 AZ150 anti-corrosive	m^2	46.00	103.39	4755.94
"Zincalume"based steel sheeting	m^2	46.00		0.00
Ridge cappings 450mm girth	m^2	6.00	104.50	627.00
galvanised	m^2	2.70		
TOTAL MATERIAL COST ESTIMATION (excluding finishes):				**R 42 730.84**

Conventional design: Cost estimation				
Materials			**Cost estimation**	
Items	**Unit**	**Quantity**	**Rate [R/unit]**	**Cost [R]**
Total material cost excluding finished				42730.84
Finishes				
Paint (twice per expected life time)	m^2	150.00	9.80	1470.00
TOTAL MATERIAL COST INCLUDING PAINT =				**R 44 200.84**

Table G. 7: Labour cost estimation calculations for the block and mortar housing unit

Conventional design: Cost estimation				
Labour			**LABOUR Cost estimation**	
Items	**Unit**	**Quantity**	**Rate [R/unit]**	**Cost [R]**
Foundations				
Excavation and earth by hand (external walls)	m^3	8.94	103.34	924.11
Excavation and earth by hand (internal walls)	m^3	1.66	103.34	171.54
Concrete and strip foundation	m^2	3.43	83.02	284.59
Blockwork	m^2	14.90	84	1251.60

Floor slab				
Concrete cast, float and screed	m^2	4.92	33.02	162.46
External walls				
Plaster	m^2	75.00	25	1875.00
Blockwork	m^2	14.90	84	1251.60
Bagged internally	m^2	75.00	6.13	459.75
Internal walls				
Blockwork	m^2	26.00	84	2184.00
Bagged	m^2	52.00	6.13	318.76
Roofing + covering				
Labour	m^2	40.00	75	3000.00
TOTAL LABOUR COST ESTIMATION (excluding finishes):				**R 11 883.41**

Labour			**Cost estimation**	
Items	**Unit**	**Quantity**	**Rate [R/unit]**	**Cost [R]**
Total labour cost estimation (excluding finishes)				11883.41
Finishes				
Paint	m^2	150.00	21.74	3261.00
TOTAL LABOUR COST ESTIMATION (INCLUDING FINISHES)				**R 15 144.41**

Table G. 8: Transport cost estimation calculations for the block and mortar housing unit

Conventional design: Cost estimation					
Transport				**TRANSPORT cost estimation**	
Items	**Unit**	**Distance of transport**	**Quantity [ton]**	**Rate [R/unit]**	**Cost [R]**
Transport	7.5t/km	50 km	47.34	14	4418.4
TOTAL TRANSPORT COST ESTIMATION					**R 4 418.40**

APPENDIX H: ENVIRONMENTAL FEASIBILITY

H.1. Calculations for environmental impact assessment

FFC housing unit : Environmental Impact													
Materials				Conversion			Carbon Footprint EI_1		Acidification Potential EI_2		Eutrophication Potential EI_3		
Items		Unit	Quantity	Ecoinvent unit	Conversion factor	New amount	factor[kg CO_{2e}]	per item	[kg So_{2e}/ unit]	per item	[kg NO_{3e}/unit]	per item	
Connections and foundation													
Concrete strip footing		m^3	5.50	m^3		5.50	385.40	2120.22	1.3324	7.33	3.0475	16.77	
Reinforcing (4 x Y12)		kg	103.00			103.00	3.2999	339.89	0.012278	1.26	0.047424	4.88	
Floor slab													
FFC Floor panel	50% PVC	m^3	0.19	m^2	100.00	18.61	0.44	8.16	0.0030	0.06	0.0083	0.15	
External walls 122mm													
FFC wall panel	50% PVC	m^3	0.74	m^2	90.91	67.20	0.44	29.46	0.0030	0.20	0.0083	0.56	
EPS (t=100mm)		m^2	67.20	kg	1.50	100.80	3.34	336.61	0.0105	1.06	0.0104	1.04	
FFC gable (t=5mm)	50% PVC	m^3	0.01	m^2	200.00	2.40	0.44	1.05	0.0030	0.01	0.0083	0.02	
Internal walls 90mm													
FFC wall panel	50% PVC	m^3	0.20	m^2	133.33	26.70	0.44	11.71	0.0030	0.08	0.0083	0.22	
EPS (t =75mm)		m^2	26.70	kg	1.50	40.05	3.34	133.75	0.0105	0.42	0.0104	0.41	
Ceiling and Thermal Insulation													
6.4mm gypsum plaster boards		m^2	40.00	kg	5.70	228.00	0.16	36.92	0.0010	0.22	0.0011	0.25	
50mm glass wool laid to manufacturers specifications, finished with cover strips (incl cornices)		m^2	40.00	kg	2.00	80.00	2.72	217.61	0.0193	1.54	0.0407	3.26	
Roofing													
Roof trusses (Gr 5 Pine)		m	99.05	m^3	0.35	34.71	0.00	0.00	0.0000	0.00	0.0928	3.22	
Rafter (Gr 5Pine)		m	19.00	m^3	0.35	6.66	0.00	0.00	0.0000	0.00	0.0928	0.62	
Roof sheeting (25mm)	50% PVC	m^3	0.54	m^2	40.00	21.59	0.44	9.47	0.0030	0.07	0.0083	0.18	
Transport (50km)		tkm	247.50	tkm		247.50	0.47	116.22	0.0024	0.58	0.0057	1.41	
TOTAL IMPACT:								**3361.05**		**12.83**		**33.00**	

WPC housing unit : Environmental Impact												
Materials				**Conversion**			**Carbon Footprint EI_1**		**Acidification Potential EI_2**		**Eutrophication Potential EI_3**	
Items		Unit	Quantity	Ecoinvent unit	Conversion factor	New amount	factor[kg CO_{2e}]	per item	[kg So_{2e}/ unit]	per item	[kg NO_{3e}/unit]	per item
Connections and foundation												
Concrete strip footing		m^3	5.50	m^3		5.50	385.40	2120.22	1.3324	7.33	3.0475	16.77
Reinforcing (4 x Y12)		kg	103.00			103.00	3.2999	339.89	0.012278	1.26	0.047424	4.88
Floor slab												
FFC Floor panel	50% PVC	m^3	0.19	m^2	100.00	18.61	0.44	8.16	0.0030	0.06	0.0083	0.15
External walls 122mm												
FFC wall panel	50% PVC	m^3	0.74	m^2	90.91	67.20	0.44	29.46	0.0030	0.20	0.0083	0.56
EPS (t=100mm)		m^2	67.20	kg	1.50	100.80	3.34	336.61	0.0105	1.06	0.0104	1.04
FFC gable (t=5mm)	50% PVC	m^3	0.01	m^2	200.00	2.40	0.44	1.05	0.0030	0.01	0.0083	0.02
Internal walls 90mm												
FFC wall panel	50% PVC	m^3	0.20	m^2	133.33	26.70	0.44	11.71	0.0030	0.08	0.0083	0.22
EPS (t =75mm)		m^2	26.70	kg	1.50	40.05	3.34	133.75	0.0105	0.42	0.0104	0.41
Ceiling and Thermal Insulation												
6.4mm gypsum plaster boards		m^2	40.00	kg	5.70 [10.00]	228.00	0.16	36.92	0.0010	0.22	0.0011	0.25
50mm glass wool laid to manufacturers specifications, finished with cover strips (incl cornices)		m^2	40.00	kg	2.00	80.00	2.72	217.61	0.0193	1.54	0.0407	3.26
Roofing												
Roof trusses (Gr 5 Pine)		m	99.05	m^3	0.35	34.71	0.00	0.00	0.0000	0.00	0.0928	3.22
Rafter (Gr 5Pine)		m	19.00	m^3	0.35	6.66	0.00	0.00	0.0000	0.00	0.0928	0.62
Roof sheeting (25mm)	50% PVC	m^3	0.54	m^2	40.00	21.59	0.44	9.47	0.0030	0.07	0.0083	0.18
Transport (50km)		tkm	352.50	tkm		352.50	0.47	165.52	0.0024	0.83	0.0057	2.01
TOTAL IMPACT:								**3410.36**		**13.08**		**33.60**

Conventional design (brick and mortar) : Environmental Impact											
Materials			**Conversion**			**Carbon Footprint EI_1**		**Acidification Potential EI_2**		**Eutrophication Potential EI_3**	
Items	Unit	Quantity	Ecoinvent unit	Conversion factor	New amount	factor[kg CO_{2e}]	per item	[kg SO_{2e}/ unit]	per item	[kg NO_{3e}/unit]	per item
Foundation:											
10 MPa concrete foundation (600x230mm)	m^3	5.11	m^3		5.11	385.4	1970.51	1.3324	6.81	3.0475	15.58
Reinforcing (4 x Y12)	kg	103.00			103.00	3.2999	339.89	0.012278	1.26	0.047424	4.88
190mm blockwork including	m^2	14.90	kg	160.00	2384	0.19538	465.79	0.00084748	2.02	0.0020572	4.90
brickforce (75 x 2.8mm)	m	125.00	kg	0.11	13.75	3.2979	45.35	0.012698	0.17	0.046682	0.64
galvanised	m^2	2.45	m^2		2.45	3.8236	9.37	0.29047	0.71	0.52817	1.29
filled with concrete	m^3	0.97	m^3		0.97	385.4	373.84	1.3324	1.29	3.0475	2.96
Floor slab											
Damp proof membrane 250 micron	m^2	41.00	kg	0.23	9.43	2.0878	19.69	0.0077913	0.07	0.0063249	0.06
25 Mpa concrete (power floated)	m^3	4.92	m^3		4.92	385.4	1896.17	1.3324	6.56	3.0475	14.99
Steel mesh ref 193	m^2	41.00	kg	1.93	79.13	3.2999	261.12	0.012278	0.97	0.047424	3.75
External walls 140mm											
Two top courses of brickwork to be filled with 10 Mpa concrete	m^3	0.65	m^3		0.65	385.4	250.51	1.3324	0.87	3.0475	1.98
Brickwork, mortar &	m^2	75.00	kg	160.00	12000	0.19538	2344.56	0.00084748	10.17	0.0020572	24.69
brickforce as NHBRC standard	m	125.00	kg	0.11	13.75	3.2979	45.35	0.012698	0.17	0.046682	0.64
galvanised	m^2	2.45	m^2		2.45	3.8236	9.37	0.29047	0.71	0.52817	1.29
Plaster externally (12mm thick)	m^2	75.00	kg	27.60	75.00	0.013426	1.01	0.0001095	0.01	0.00020699	0.02
DPC (110mm width) -375 micron	m	29.00	kg	0.03	29.00	2.0878	60.55	0.0077913	0.23	0.0063249	0.18
Internal walls 90mm											
Blockwork, mortar	m^2	26.00	kg	130.00	3380	0.1954	660.38	0.0008	2.86	0.0020572	6.95
Ceiling and Thermal Insulation											
6.4mm gypsum plaster boards	m^2	40.00	kg	5.70	228	0.1619	36.92	0.0010	0.22	0.0011011	0.25
50mm glass wool laid to manufacturers specifications, finished with cover strips (incl cornices)	m^2	40.00	kg	2.00	80	2.7201	217.61	0.0193	1.54	0.04072	3.26
Roofing											
Howe type truss to be designed by supplier for 7.62m span	sum	1.00	m^3		0.63	88.8730	55.99	0.5546	0.35	1.5194	0.96
114x38 wall plate including beam filling	m	12.00	m^3		0.05	88.8730	4.44	0.5546	0.03	1.5194	0.08
50x76mm purlins on edge at maximum 1.2m spacing	sum	1.00	m^3		0.22	88.8730	19.55	0.5546	0.12	1.5194	0.33
Roof Covering											
0.54mm Fielders corrugated Color bond G550 AZ150 anti-corrosive	m^2	46.00	kg	5.03	231.38	2.1191	490.32	0.0082	1.90	0.047424	10.97
"Zincalume"based steel sheeting	m^2	46.00	m^2		46.00	3.8236	175.89	0.2905	13.36	0.52817	24.30
Ridge cappings 450mm girth	m2	6.00	kg	2.26	13.56	2.1191	28.73	0.0082	0.11	0.047424	0.64
galvanised	m^2	2.70	m^2		2.70	3.8236	10.32	0.2905	0.78	0.52817	1.43
Finishes											
Paint	m^2	75.00	kg	0.20	15	5.0016	75.02	0.0205	0.31	0.062467	0.94
Transport (50km)	tkm	2367.00	tkm		2367.00	0.4696	1111.47	0.0024	5.56	0.0057115	13.52
TOTAL IMPACT:							**10979.71**		**59.18**		**141.49**

H.2. Calculations for energy efficiency

Modular FFC housing unit : Energy efficiency								
Material	**Thickness (m)**	**Density (kg/m^3)**	**Specific heat (J/kg°C)**	**Thermal conductivity (W/m°C)**	**Thermal capacity ($kJ/m^2°C$)**	**Thermal resistance ($m^2°C/W$)**	**Thermal transmittance (W/m2°C)**	**CR-value (hours)**
		ρ	**c**	**k**	**Cs**	**R-value**	**U-value**	
Floor slab (40mm)								
FFC	0.040	700.000	1300.000	0.130		**0.455**	**2.199**	
External walls (122mm)								
Layer 1: FFC	0.011	700.000	1300.000	0.130	10.010	0.085		
Layer 2: EPS	0.100	15.000	1500.000	0.030	2.250	3.333		
Layer 3: FFC	0.011	700.000	1300.000	0.130	10.010	0.085		
					22.270	**3.659**	**0.273**	**22.6365**
Roof, ceiling and thermal insolation								
FFC roof sheeting	0.025	700.000	1300.000	0.130		0.192		
6.4mm gypsum plaster boards	0.006	993.000		0.170		0.038		
120mm glass wool laid to manufacturers specifications	0.120	24.000		0.040		3.000		
						3.755	**0.266**	

Modular WPC housing unit : Energy efficiency								
Material	**Thickness (m)**	**Density (kg/m^3)**	**Specific heat (J/kg°C)**	**Thermal conductivity (W/m°C)**	**Thermal capacity ($kJ/m^2°C$)**	**Thermal resistance ($m^2°C/W$)**	**Thermal transmittance (W/m2°C)**	**CR-value (hours)**
		ρ	**c**	**k**	**Cs**	**R-value**	**U-value**	
Floor slab (40mm)								
WPC	0.040	1331	1860.000	0.150		**0.414**	**2.417**	
External walls (122mm)								
Layer 1: WPC	0.019	1331	1860.000	0.150	47.038	0.127		
Layer 2: EPS	0.100	15	1500.000	0.030	2.250	3.333		
Layer 3: WPC	0.019	1331	1860.000	0.150	47.038	0.127		
					96.325	**3.743**	**0.267**	**100.161**
Roof, ceiling and thermal insolation								
WPC roof sheeting	0.025	1331	1860.000	0.150		0.167		
6.4mm gypsum plaster boards	0.006	993		0.170		0.038		
120mm glass wool laid to manufacturers specifications	0.120	24		0.040		3.000		
						3.730	**0.268**	

Block and mortar housing unit : Energy efficiency								
Material	**Thickness (m)**	**Density (kg/m^3)**	**Specific heat (J/kg°C)**	**Thermal conductivity (W/m°C)**	**Thermal capacity ($kJ/m^2°C$)**	**Thermal resistance ($m^2°C/W$)**	**Thermal transmittance (W/m2°C)**	**CR-value (hours)**
		ρ	**c**	**k**	**Cs**	**R-value**	**U-value**	
External walls (140mm)								
Brickwork	0.14	1826.00	877.00	0.820	224.196	0.171		
					224.196	**0.474**	**2.109**	**29.53**
Roofing								
"Zincalume"based steel sheeting	0.001	700.000	0.000	53		0.000		
6.4mm gypsum plaster boards	0.006	993.000		0.170		0.038		
120mm glass wool laid to manufacturers specifications	0.120	24.000		0.040		3.000		
					0.000	**3.563**	**0.281**	